

A dissertation submitted to the
FACULTY OF BIOLOGY, CHEMISTRY AND
GEOSCIENCES
UNIVERSITY OF BAYREUTH

to attain the academic degree of
DR. RER. NAT.

**High-Resolution Modelling of Surface-Atmosphere
Interactions and Convection Development at Nam
Co Lake, Tibetan Plateau**

TOBIAS GERKEN
Diplom Geoökologe

born 26 January, 1983
in Malsch, Germany

Bayreuth, November 2013

supervised by

PROF. DR. THOMAS FOKEN
PROF. DR. HANS-F. GRAF

High-Resolution Modelling of Surface-Atmosphere
Interactions and Convection Development at Nam Co Lake,
Tibetan Plateau

supervised by
PROF. DR. THOMAS FOKEN and PROF. DR. HANS-F. GRAF

Die vorliegende Arbeit wurde in der Zeit von März 2009 bis Juli 2013 in Bayreuth an der Abteilung Mikrometeorologie und an der University of Cambridge unter Betreuung von Herrn Prof. Dr. Thomas Foken und Herrn Prof. Dr. Hans-F. Graf angefertigt.

Vollständiger Abdruck der von der Fakultät für Biologie, Chemie und Geowissenschaften der Universität Bayreuth genehmigten Dissertation zur Erlangung des akademischen Grades eines Doktor der Naturwissenschaften (Dr. rer. nat.).

This work was executed between March 2009 and July 2013 in Bayreuth at the Department of Micrometeorology and at the University of Cambridge. It was supervised by Prof. Dr. Thomas Foken and Prof. Dr. Hans-F. Graf.

This is a full reprint of the dissertation accepted by the Faculty of Biology, Chemistry and Geosciences, University of Bayreuth to attain the academic degree of Doktor der Naturwissenschaften (Dr. rer. nat.).

Dissertation eingereicht am/*Submitted*: 31. Juli 2013 (Poststempel)
Zulassung durch die Prüfungskommission/*Accepted by the faculty*: 8. August 2013
Wissenschaftliches Kolloquium/*Defended*: 25. November 2013

Amtierender Dekan/*Acting Dean*:
Prof. Dr. Rhett Kempe

Prüfungsausschuss/*Degree Committee*:
Prof. Dr. Michael Hauhs (Erstgutachter/*First reviewer*)
Prof. Dr. Hans-F. Graf (Zweitgutachter/*Second reviewer*)
Prof. Dr. Andreas Held (Vorsitz/*Chair*)
Prof. Dr. Thomas Foken
Prof. Dr. Walter Zimmermann

Contents

List of manuscripts	v
Summary	vii
Zusammenfassung	ix
Acknowledgements	xi
1. Introduction	1
1.1. Framework of this thesis	5
1.2. Objectives of this thesis	5
2. Methods	11
2.1. ATHAM and Hybrid	11
2.1.1. Model development	12
2.2. Data from field experiments	21
2.2.1. Site description of Nam Co Lake	21
2.2.2. Eddy-covariance measurements	22
2.2.3. Radiosonde measurements	23
3. Results	27
3.1. Improved model performance and stability for simulations of atmo- spheric convection	27
3.2. An improved surface temperature formulation in Hybrid	30
3.3. Cloud development and mesoscale circulations at Nam Co Lake	34
3.3.1. Boundary-Layer development	34
3.3.2. Interactions of mesoscale circulations and background wind	37
3.3.3. Influence of temperature, relative humidity and uncertainty in profiles	40
3.3.4. Precipitation at Nam Co Lake	45
4. Conclusions	49
References	53

A. Individual contributions to the joint publications	67
B. Gerken et al. (2012)	71
C. Gerken et al. (2013a)	89
D. Gerken et al. (2013b)	109
Erklärung	125

List of manuscripts

This dissertation is presented in a cumulative form. It is based on publications and submitted manuscripts as listed below.

Peer-reviewed publications

Gerken, T., Babel, W., Hoffmann, A., Biermann, T., Herzog, M., Friend, A. D., Li, M., Ma, Y., Foken, T., and Graf, H.-F.: *Turbulent flux modelling with a simple 2-layer soil model and extrapolated surface temperature applied at Nam Co Lake basin on the Tibetan Plateau*, Hydrol. Earth Syst. Sci., 16, 1095–1110, doi:10.5194/hess-16-1095-2012, 2012.

Previously published as: Gerken, T., Babel, W., Hoffmann, A., Biermann, T., Herzog, M., Friend, A. D., Li, M., Ma, Y., Foken, T., and Graf, H.-F.: *Turbulent flux modelling with a simple 2-layer soil model and extrapolated surface temperature applied at Nam Co Lake basin on the Tibetan Plateau*, Hydrol. Earth Syst. Sci. Discussions, 8, 10275–10309, 2011.

Gerken, T., Biermann, T., Babel, W., Herzog, M., Ma, Y., Foken, T., Graf, H.-F.: *A modelling investigation into lake-breeze development and convection triggering in the Nam Co Lake basin, Tibetan Plateau*, Theor. Appl. Climatol., online first, doi:10.1007/s00704-013-0987-9, 2013a

This publication was accepted at the time of submission of this thesis and was published online in final form on 25 August 2013.

Gerken, T., Babel, W., Sun, F., Herzog, M., Ma, Y., Foken, T., Graf, H.-F.: *Uncertainty in atmospheric profiles and the impact on modeled convection development at Nam Co Lake, Tibetan Plateau*, J. Geophys. Res., 118, early view, doi:10.1002/2013JD020647, 2013b

This publication was submitted at the time of submission of this thesis and was published online in final form on 19 November 2013.

Publications not included in this thesis

Peer-reviewed

Foken, T., Meixner, F. X., Falge, E., Zetzsch, C., Serafimovich, A., Bargsten, A., Behrendt, T., Biermann, T., Breuninger, C., Dix, S., Gerken, T., Hunner, M., Lehmann-Pape, L., Hens, K., Jocher, G., Kesselmeier, J., Lüers, J., Mayer, J. C., Moravek, A., Plake, D., Riederer, M., Rütz, F., Scheibe, M., Siebicke, L., Sörgel, M., Staudt, K., Trebs, I., Tsokankunku, A., Welling,

M., Wolff, V., and Zhu, Z.: *Coupling processes and exchange of energy and reactive and non-reactive trace gases at a forest site — results of the EGER experiment*, *Atmos. Chem. Phys.*, 12, 1923–1950, doi:10.5194/acp-12-1923-2012, 2012

Not peer-reviewed

Gerken, T., Fuchs, K., and Babel W.: *Documentation of the Atmospheric Boundary Layer Experiment, Nam Tso, Tibet 08th of July – 08th of August 2012*, *Arbeitsergebnisse* 53, University of Bayreuth, Bayreuth, ISSN 1614–8916, p. 48, 2013

Summary

The Tibetan Plateau has recently become an area of increased interest for the atmospheric and environmental sciences. Surface-atmosphere interactions and specifically the exchange of momentum, turbulent energy and water vapour as well as the development of convection are not only important for the surface energy balance and local water resources, but also have influence on the evolution of the monsoon system and climate. High-resolution, numerical atmospheric models with a fully coupled surface model are a valuable tool for the systematic investigation of surface-atmosphere interactions. Nam Co Lake, located at the northern extent of the monsoon's influence, was selected as a complex system in order to study the interaction of the land and the lake in the generation of mesoscale circulations and the development from boundary-layer clouds to moist convection.

Turbulent fluxes estimated by eddy-covariance and atmospheric profiles measured by radiosondes are used in this work in conjunction with the ATHAM (Active Tracer High-resolution Atmospheric Model) and Hybrid models. Substantial model development is undertaken for both ATHAM and Hybrid. This means a more consistent formulation of tracer and heat transport in ATHAM and improved model stability. Hybrid has been modified with an extrapolated surface temperature, to be used for the calculation of turbulent fluxes. A quadratic temperature profile based on the layer mean and surface model base temperature is assumed in each layer and extended to the surface. Compared to eddy-covariance measurements and a Surface-Vegetation-Atmosphere Transport (SVAT) Model there is an overall reasonable model performance, when tested on four days for two sites with variable environmental conditions during the 2009 summer monsoon season. At the same time, errors are reduced by 40–60% compared to the unmodified Hybrid.

Subsequently, the coupled modelling system is used for 2-dimensional cross-sections through the Nam Co Lake basin with horizontal resolutions of 200 m and at least 150 vertical layers between the surface and the model top located in the lower stratosphere. The 2-dimensional modelling approach has a tendency to overestimate convective strength due to the underestimation of dry air entrainment and cannot reproduce fully realistic flow fields. Nevertheless, it provides a valuable tool for systematic investigations of environmental factors, where 3D simulations are prohibitively expensive.

In simulations with several background wind speeds it is found that the model adequately simulates the mesoscale circulation system between the lake and the surrounding mountain chains. Dependent on the geostrophic wind direction there are two different mechanisms for the triggering of convection: Convective triggering, when overflowing topography, and triggering due to convergence between the lake-breeze front and the background wind. It is concluded that coupled modelling setup is capable of reproducing the system's most important dynamics, such as

realistic turbulent surface fluxes, mesoscale circulations and cloud evolution.

Thereafter, the influence of the atmospheric profiles of temperature and relative humidity and the uncertainty that arises from them is discussed. Simulations are initialised with profiles based on direct measurements (radiosondes), NCEP-I and ERA-INT reanalysis and GFS-FNL analysis data on two days during the summer of 2012. The simulated convection from radiosondes compares reasonably well with weather observations for the first day, but less well for the second day, when large-scale synoptic effects, which are not included in the model, gain importance. The choice of vertical profile information leads to strongly differing convection development, causing modifications of the surface energy balance and thus of the energy and water cycle for Nam Co Lake.

With respect to precipitation it is found that a large fraction of the precipitation that is generated in the simulations is deposited within the basin and on the slopes of the surrounding mountain chains and thus locally recycled. This also means that a weather station in the centre of the basin is not representative of the system. Furthermore, Nam Co Lake may be of importance as a water supply for the region. Additionally, the choice of profile and the initial water vapour contents determine the amount of precipitation so that there are strong differences spanning one order of magnitude in the generated precipitation between the model simulations driven by different vertical profiles.

The findings from the thesis provide an example of the impacts of surface-atmosphere interactions, mesoscale circulations and convective evolution on the Tibetan Plateau. Scaled to the entire plateau these processes are highly relevant to ecosystems, climate and the water cycle.

Zusammenfassung

In den letzten Jahren hat das Interesse für das Tibetische Plateau in den Atmosphären- und Umweltwissenschaften zugenommen. Wechselwirkungen zwischen der Oberfläche und der Atmosphäre, v.a. der Austausch von Impuls, turbulenter Energie und Feuchtigkeit sowie die Entwicklung von Konvektion sind nicht nur für die Energiebilanz der Oberfläche und die lokale Verfügbarkeit von Wasser wichtig, sondern haben auch einen Einfluss auf den Monsun und das Klima. Hochauflösende, numerische Zirkulations-Modelle, die vollständig mit der Oberfläche gekoppelt sind, sind ein wichtiges Werkzeug für die systematische Erforschung von Oberflächen-Atmosphären Wechselwirkungen. Der Nam Co See, am nördlichen Rand des Monsun-Systems gelegen, wurde als ein komplexes System ausgewählt, um die Interaktion zwischen See, Land und Atmosphäre bei der Bildung mesoskaliger Zirkulationen sowie der Entwicklung von Grenzschicht-Wolken zu freier Konvektion untersuchen.

Mit der Eddy-Kovarianz Methode gemessene Flüsse und Profile der Atmosphäre aus Radiosondierungen werden in dieser Arbeit zusammen mit den Modellen ATHAM (Active Tracer High-resolution Atmospheric Model) und Hybrid verwendet. Beiden Modelle wurden signifikant weiterentwickelt, so dass ATHAM nun über eine konsistentere Behandlung des Transports von Tracern und Temperatur verfügt und numerisch stabiler läuft. Die Berechnung der turbulenten Flüsse in Hybrid ist auf eine extrapolierte Oberflächentemperatur umgestellt. Hierbei wird ein quadratisches Temperatur-Profil in beiden Schichten angenommen und zur Oberfläche erweitert, während die Temperatur am Unterrand des Bodenmodells konstant ist. Im Vergleich zu Eddy-Kovarianz Messungen und einem SVAT Modell werden für vier Tage an zwei Orten mit wechselnden Umweltbedingungen während des 2009 Sommer-Monsuns zufriedenstellende Ergebnisse erzielt. Darüber hinaus werden die Fehler im Vergleich zum nicht modifizierten Hybrid um 40–60% reduziert.

Anschließend wurde das Modellsystem in 2D am Nam Co verwendet. Dabei wurde ein Querschnitt des Tals mit einer horizontalen Auflösung von 200 m und mindestens 150 Schichten zwischen der Oberfläche und dem Modellrand in der unteren Stratosphäre verwendet. Dieses 2D-setup hat die Tendenz, die Stärke der Konvektionsentwicklung zu überschätzen, da die Einmischung von trockener Luft unterschätzt wird. Außerdem ist das Strömungsfeld nicht vollständig realistisch. Trotzdem können so systematische Untersuchungen von Einflussfaktoren auf das System durchgeführt werden, wenn 3D Simulationen zu rechenintensiv sind.

Durch Simulationen mit verschiedenen geostrophischen Windgeschwindigkeiten wurde herausgefunden, dass das Modell die Mesoskalige Zirkulation zwischen See und Bergen realistisch nachbildet. Je nach Windrichtung existieren zwei Mechanismen für das Triggern von Konvektion: Beim Überströmen der Topographie und bei Konvergenz zwischen Hintergrund-Wind und der Front der Seebrise. Das ge-

koppelte Modell ist in der Lage die wichtigsten Eigenschaften des Systems, wie Oberflächenflüsse, mesoskalige Zirkulationen und Wolkenbildung zu simulieren.

Anschließend wird der Einfluss von atmosphärischen Temperatur- und Feuchteprofilen sowie die sich daraus ergebenden Unsicherheiten diskutiert. Es werden Profile für zwei Tage im Sommer 2012 verwendet, die direkt durch Radiosondierung gemessen wurden, von den NCEP-I und ERA-INT Reanalysen sowie der GFS-FNL Analyse stammen. Die mit den Radiosonden modellierte Konvektion ist in guter Übereinstimmung mit Wetterbeobachtungen für den ersten Tag. Am 2. Tag treten großräumige synoptische Effekte auf, die in der Simulation nicht enthalten sind, so dass die Ergebnisse weniger gut mit den Beobachtungen übereinstimmen. Die Wahl des vertikalen Profils hat einen großen Einfluss auf die Entwicklung von Konvektion, mit großen Folgen für die Energiebilanz an der Oberfläche und damit für den Energie- und Wasserkreislauf.

Ein großer Teil der in dem Modell-Läufen generierten Niederschläge fällt innerhalb des Tals und auf den Berghängen, so dass von lokalem Recycling gesprochen werden muss. Dies hat zur Folge, dass eine Wetterstation im Zentrum des Tals nicht repräsentativ für das System ist. Darüber hinaus ist der Nam Co wahrscheinlich für den regionalen Wasserkreislauf wichtig. Die Wahl des Profils und sein initialer Wassergehalt bestimmen die Menge des Niederschlags mit Unterschieden die eine komplette Größenordnung ausmachen.

Die Ergebnisse dieser Arbeit sind ein Beispiel für die Auswirkungen von Oberflächen-Atmosphären Wechselwirkungen, der Entwicklung mesoskaliger Zirkulationen und der Konvektionsentwicklung auf dem Tibetischen Plateau. Auf der Plateau-Skala sind diese Prozesse hochgradig relevant für Ökosysteme, Klima und den Wasserkreislauf.

Acknowledgements

I am deeply grateful for the support I received while completing this thesis. I would like to thank each and every person involved and in particular:

- Prof. Thomas Foken and Prof. Hans-F. Graf for their guidance during all stages of this work, for their helpful comments and the fruitful discussion of scientific issues and for assisting me on the journey of becoming a better scientist.
- Michael Herzog for the incredible amount of both practical support I received in developing an understanding of the model ATHAM and the discussion of the scientific experiments conducted with it.
- All the people involved in the experiments at Nam Co Lake and especially Wolfgang Babel and Tobias Biermann.
- (A)lex Hoffman and Paul Griffiths for continuous support in the long hours of working on this thesis.
- The staff and PhD students of the Geography Department at the University of Cambridge for their support and helpful discussions.
- Fanglin Sun (Cold and Arid Regions Environmental and Engineering Research Institute, Chinese Academy of Sciences, Lanzhou) and Kathrin Fuchs for their help, support and shared time during the 2012 radiosonde measurements at Nam Co Lake and all the researchers and staff of ITP Nam Co Monitoring and Research Station for their work on the Tibetan Plateau and help during the field trips, and Prof. Ma Yaoming (Institute of Tibetan Plateau Research, Chinese Academy of Sciences, Beijing) as project partner and leader of the Chinese working group.
- My family, my friends and Caitlin.

This work has been financed through the Deutsche Forschungsgemeinschaft Priority Programme 1372 (DFG Fo 226/18-1.2) “Tibetan Plateau: Formation, Climate, Ecosystems” (TiP). The role of CEOP-AEGIS, a Collaborative Project/Small or medium-scale focused research project – Specific International Co-operation Action coordinated by the University of Strasbourg, France and funded by the European Commission under FP7 topic ENV.2007.4.1.4.2 “Improving observing systems for water resource management” is also acknowledged.

1. Introduction

With an average elevation of more than 4500 m above sea level (a.s.l.) and an extension of more than $2.5 \times 10^6 \text{ km}^2$, the Tibetan Plateau constitutes the largest mountain highland in the world. Located north of the Himalayan Mountains, it contains the largest glaciated area outside the polar regions and has increasingly become an area of interest in environmental sciences (Qui, 2008; Yao et al., 2012). The effects of increasing population, associated land-use change and global climate change will have an effect on ecosystems and regional water resources. The impact and extent of land-use change such as permafrost degradation (Cheng and Wu, 2007), grassland degradation and deforestation have been presented in Cui and Graf (2009) and Cui et al. (2006). The water supply of more than 1.4 billion people in South-East Asia is dependent on rivers that originate on the Tibetan Plateau (Immerzeel et al., 2010). At the same time the hydrological resources of the Tibetan Plateau and especially the cryosphere are undergoing rapid changes (i.e. Yao et al., 2007; Ni, 2011; Kang et al., 2010; Yang et al., 2011). Climate change and its impacts in mountain regions are reviewed in Beniston et al. (1997) and Beniston (2003) addressing changes to ecosystems, to the cryosphere and to water resources.

While the narrow Himalayan Mountain chain and the associated release of latent heat by air travelling across are now believed to be the Indian monsoon's major forcing (Molnar et al., 2010; Boos and Kuang, 2010, 2013), the elevated heat source of the Tibetan Plateau (i.e. Flohn, 1952; Gao et al., 1981; Yanai et al., 1992) is still thought to influence regional circulation and precipitation patterns in south-east Asia through the modification of westerly air transport (Boos and Kuang, 2010; Xu et al., 2008; Chen et al., 2012).

As a consequence, there have been several coordinated efforts to improve the understanding of the Tibetan Plateau's role in the global energy and water cycles: TIPEX (Tibetan Plateau EXperiment), GAME/Tibet (GEWEX - Asian Monsoon Experiment, with GEWEX as Global Energy and Water cycle Experiment, <http://monsoon.t.u-tokyo.ac.jp/tibet/>), CAMP (Coordinated enhanced observing period Asia-Australia Monsoon Project, Ma et al., 2003, 2005), TORP (Tibetan Observation and Research Platform, Ma et al., 2009b) and CEOP-AEGIS (www.ceop-aegis.org).

Regardless, the Tibetan Plateau is a remote and inaccessible region, so that despite these efforts observations and data remain both sparse and inhomogeneous

with respect to quality and coverage (Frauenfeld et al., 2005; Kang et al., 2010; Maussion et al., 2011). The choice of measurement locations is often determined by accessibility and historic factors rather than by objective criteria, often causing the collected data to not be representative for the region. This is illustrated by the fact that there are no permanent weather stations on the Tibetan Plateau located above 4800 m (Maussion et al., 2011), while the mean elevation of the Tibetan Plateau is commonly cited at more than 4500 m. These uncertainties also extend to the gridded data sets such as TRMM (Tropical Rainfall Measuring Mission) or reanalysis data (Frauenfeld et al., 2005; Yin et al., 2008; Ma et al., 2008), which depend on data-assimilation of measurements or ground truthing for quality control of automatic data post-processing. Differences in terrain height between meteorological stations and reanalysis data sets, which can reach up to 2000 m on the plateau (Wang and Zeng, 2012), affect the quality of surface data products.

While most comparison studies focus on surface level data (Frauenfeld et al., 2005; Ma et al., 2008, 2009a; Wang and Zeng, 2012), where systematic biases in elevation can with some effort be accounted for, there is to our knowledge only a single study addressing errors in vertical atmospheric profiles (Bao and Zhang, 2013): This study uses radiosondes collected during GAME Tibet (1998), which were not assimilated into gridded products, and compares the mean profiles for temperature, humidity and wind with commonly used reanalysis data. They concluded that there were small biases with regard to temperature and wind speeds, but considerably larger biases for relative-humidity (RH): Below 200 hPa ERA-Int (European Centre for Medium-Range Weather Forecasts Interim reanalysis – Dee et al., 2011) shows a positive bias of approx. 10% RH . The bias in NCEP/NCAR RA-I (National Centers for Environmental Prediction/ National Center for Atmospheric Research ReAnalysis-I – Kalnay et al., 1996) decreases from +10% close to the surface to -5% at 300 hPa. Both products have a negative temperature bias below 200 hPa, corresponding to -0.5°C increasing to -2°C with height for ERA-Int and -1.5°C close to the surface decreasing to -0.5°C . Biases follow a temporal pattern with the smallest values during the daytime. These biases are likely caused by the complex terrain of the Tibetan Plateau, the sparseness of meteorological measurements that are assimilated into the gridded products and the surface’s forcing to the lower troposphere. It is presently unclear how to correct these biases that are likely to be larger on the Tibetan Plateau than in more developed and less mountainous regions. While the mean profile has some importance for climate, convection development is dependent on the actual profiles, whose quality is not addressed in this study. Due to the complex topography, one would expect profiles to be highly variable in space, while reanalysis-data is available on the degree-scale. With regard to vertical resolution, such profiles are relatively coarse

and are thus smoothed compared to directly measured profiles.

The large elevation of the Tibetan Plateau is located at a subtropical latitude and receives strong solar radiation input during summer, which leads to large diurnal surface flux and temperature cycles (i.e. Gao et al., 1981; Tanaka et al., 2001; Ma et al., 2009b). Due to the clear atmosphere (Cong et al., 2009), only a small fraction of the total radiation is diffuse, so that clouds blocking direct radiation have a profound impact on the available energy and thus “skin” temperature. Turbulent fluxes of latent and sensible heat as well as the complex topography have great influence on the state of the atmosphere. However, these surface-atmosphere interactions, such as surface energy partitioning, and their temporal dynamics lack quantitative understanding (e.g. Ma et al., 2009b; Tanaka et al., 2003). The development of convection on the Tibetan Plateau is dependent on the vertical state of the atmosphere. According to Taniguchi and Koike (2008) there are three different atmospheric regimes found on the plateau over the course of a year: (1) In the early pre-monsoon phase the atmospheric profile is dry, relatively unstable and has a high mixed layer due to large sensible and latent heat fluxes; convection occurs frequently. (2) Before the onset of the monsoon the profile stabilizes and a lack of atmospheric moisture impedes convections. (3) With the onset of the monsoon the profile moistens and becomes conditionally unstable, thus allowing the development of convection. This development illustrates the complex interactions of atmospheric state, surface fluxes and convection and the importance of atmospheric moisture exerting control over convective developments. In the monsoon season the total precipitable water in the atmospheric column increases from approx. 5 mm to >15 mm (Taniguchi and Koike, 2008). In the early pre-monsoon phase very high boundary-layer heights of up to 5 km agl are reported by Chen et al. (2013), whereas boundary layers in the monsoon phase are substantially lower.

In general, convection triggered by topography is a major source of precipitation in semi-arid mountainous environments (e.g Banta and Barker Schaaf, 1987; Gochis et al., 2004). On the Tibetan Plateau, diurnal cloud and convection development is organized through thermal valley-circulation systems that form in the major valleys with widths between 100 and 300 km (Yatagai, 2001; Kuwagata et al., 2001; Kurosaki and Kimura, 2002; Ueno, 1998; Ueno et al., 2009). This organisation works in both ways with daytime precipitations organised along mountain ridges and night-time precipitation occurring through convergence in the centre of valleys (Ueno et al., 2009). Modelling investigations have found valley scales of 160 to 240 km to be most efficient for this process (Kuwagata et al., 2001), which is in the range of typical large Tibetan valleys (valley width: 100–300 km). Yang et al. (2004) have highlighted the influence of mesoscale hills in this process and found secondary convection triggering in valleys caused by cold-pool fronts that

form from convective downdrafts and re-evaporation of precipitation associated convection over Tibetan mountains. These processes have been described more generally in modelling studies (Chu and Lin, 2000; Chen and Lin, 2005; Reeves and Lin, 2007; Miglietta and Rotunno, 2009). Stable isotope analysis demonstrates the importance of the ocean as a water source for summer precipitation on the southern Tibetan Plateau, while the influence of the monsoon declines to the north (Tian et al., 2001a, 2003, 2007). Kurita and Yamada (2008) concluded that local moisture recycling on the central Tibetan Plateau was an essential part in keeping the regional water cycle active. They found that the majority of water that fell as precipitation originated from the boundary layer and that especially during precipitation events termed NL-type (No Low pressure) the fraction of locally recycled water increased from 30 to 80%. Such rains occurred mainly at night and in the centre of valleys due to the mesoscale thermal-circulations discussed above. Additionally, a second type of precipitation recycling local moisture was identified in locally generated convection during high pressure episodes. Precipitation with a non-local source of water was associated with the occurrence of a trough in the dry north-westerlies over the Tibetan Plateau, which leads to convergence ahead of the trough and allows for the transport of moist monsoonal air onto the Tibetan Plateau, while upper high pressure cases prevent transport of moisture across the Himalayas (Sugimoto et al., 2008). Such events tend to form in the south-central plateau and also appear to be of importance in the Nam Co basin. While the primary origin of water on the Tibetan Plateau are the Arabian Sea and the Bay of Bengal (Chen et al., 2012), the system seems to be kept active through local moisture recycling, making these processes an important part of the surface-atmosphere system; yet they remain poorly understood.

High-resolution modelling of local circulation and cloud development over a plateau with hills in China (Nishikawa et al., 2009), showed that topography induced circulations dominate the cloud development process with cloud formation on the up-slopes. While the model with realistic terrain produces more clouds in both a wet and a dry surface case, the cellular, polygonal structure of convection is less apparent and boundary-layer heights are smaller for wet surfaces (Nishikawa et al., 2009). Simulations with the WRF (Weather Research and Forecast) mesoscale model for the Tibetan Plateau at horizontal resolutions between 28 and 3.5 km showed that coarse simulations had a substantial delay in the development of moist summer convection. Resolutions smaller than 7.5 km in contrast were able to adequately simulate daytime convective events reaching the tropopause, which develop their maximum strength between 12:00 and 18:00 local time (UTC+6) as the convective depth of 5–6 km corresponds to the horizontal resolution (Sato et al., 2008). Similar timings were found by Fujinami et al. (2005), who diagnosed a maximum cloud cover frequency at 30° N between 12:00 and 20:00

local time. Localized convection on the Tibetan Plateau is frequently initiated before solar noon (Uyeda et al., 2001) and is associated with and organized by major mountain ridges (i.e. Ueno, 1998; Ueno et al., 2009; Kurosaki and Kimura, 2002). Uyeda et al. (2001) measured maximum cloud top heights of 17 km a.s.l. in the Naqu basin occurring between 12:00 and 15:00 local time.

These complex surface-atmosphere interactions need to be integrated into both modelling and remote sensing approaches that aim to satisfy the need of spatially and temporally comparable datasets. Consequently, experimental approaches and modelling approaches need to be integrated, so that models are developed that work on appropriate temporal and spatial resolutions to represent the system's dynamics (Gerken et al., 2012, Appendix B).

Developing such an approach for the Nam Co Lake basin, integrating experimental data derived from two field campaigns, and adequately representing the complex interactions between land and lake surfaces, the complex topography and the atmosphere and how they influence the development of convection have been the main motivation of this thesis.

1.1. Framework of this thesis

As part of DFG (Deutsche Forschungs-Gemeinschaft) Priority Programme 1372: Tibetan Plateau Formation – Climate – Ecosystems, this work was conducted in collaboration between the Universities of Bayreuth and Cambridge as well as the Institute of Tibetan Plateau Research, Chinese Academy of Sciences, as part of the sub-project: Mesoscale Circulations and Energy and Gas Exchange Over the Tibetan Plateau (MESOTIP). Within this project, I worked to adapt the ATHAM model to the Nam Co Lake region using data gathered at Nam Co Lake, Tibet (Biermann et al., 2013, 2009; Gerken et al., 2013c). In related research, surface-flux modelling with SEWAB (Surface Energy and Water Balance model Mengelkamp et al., 1999) was conducted for both the Nam Co and Kema area (?) and large-scale atmospheric products were downscaled to regional conditions for use in glaciological applications (Maussion et al., 2011).

1.2. Objectives of this thesis

The overall aim of this thesis is the investigation of surface-atmosphere interactions and convection development within the Nam Co Lake basin on the Tibetan Plateau. In order to improve our understanding of atmospheric processes within a changing climate it is necessary to develop methodologies that allow for the studying of a system's sensitivities. Due to the Tibetan Plateau's complex topography

and surface cover, it is at present neither practical nor possible to resolve the mesoscale circulations, cloud development and the triggering of moist convection to a realistic detail for the entire plateau. These processes, however, will affect the surface energy balance, the water cycle and thus may have an effect on large-scale circulations such as the monsoon system.

High-resolution, cloud-resolving models that are coupled to surface models give the possibility to simulate processes and investigate the sensitivities of complex systems. While large-eddy-simulation (LES) models have been used to investigate the development of boundary-layers and shallow convection (i.e. Albertson et al., 2001; Letzel and Raasch, 2003), a conceptual framework of LES fully coupled to surface models was developed by Patton et al. (2005). Similar frameworks have so far mainly been used to study the sensitivity of shallow convection to surface moisture. (i.e. Courault et al., 2007; Huang and Margulis, 2010). These studies are usually limited to small 3-dimensional domains, which do not include the free troposphere. Additionally, high-resolution models with prescribed fluxes have been used for 2D process studies of deep convective triggering (i.e. Petch, 2004, 2006; Wu et al., 2009; Kirshbaum, 2011). Due to the high computational cost, 3D high-resolution studies of deep convection (i.e. Kuang and Bretherton, 2006; Khairoutdinov and Randall, 2006; Derbyshire et al., 2004) are usually limited to very small idealised domains and/ or very few runs and serve for the study of processes.

As stated in Gerken et al. (2012), Appendix B, the study of surface-atmosphere interactions on the Tibetan Plateau requires both atmospheric models with a high enough resolution to directly resolve thermals, clouds and mesoscale circulations as well as surface models that are capable of simulating the system's dynamics. Additionally, a modelling approach is needed that enables the testing of scientific hypotheses and the exploration of system sensitivities with regard to components that are deemed important. Subsequently, this modelling approach can be used for a systematic investigation of the system's dynamics with respect to individual processes and variables of interest.

The first objectives of the present work are the further development of the Active Tracer High-resolution Model (ATHAM, Oberhuber et al., 1998; Herzog, 1998) and of the ecosystem model Hybrid (Friend et al., 1997; Friend and Kiang, 2005), so that they can be used for the simulation of surface-atmosphere interactions on the Tibetan Plateau. While this model development work is described in Section 2.1.1 of this thesis, the feasibility of a surface-flux modelling approach and its adaptation to the Nam Co Lake basin was tested and evaluated with Hybrid (Gerken et al., 2012, Appendix B). This work serves a basis for the incorporation of data gathered in field experiments such as MESOTIP into the atmospheric modelling framework documented in this thesis.



Figure 1.1. Photo sequence taken from the roof of Nam Co station on 17 July 2012 during weather observations for 8, 10 and 12 Local Solar Time (10, 12 and 14 BST). The direction of the photos is towards the North-West and Nam Co Lake.

Subsequently, the modelling framework that has been developed is used for the investigation of surface-atmosphere interactions and convection development at Nam Co Lake. This is done with respect to the complex topography, thermal circulations, the evolution of boundary-layer clouds and convection as well as the role of atmospheric profiles with regard to uncertainties in cloud development. These factors are thought to be of importance for the Nam Co Lake system.

A first test case, which combines several important aspects of the surface-atmosphere interactions at Nam Co Lake, was the investigation into lake breeze development and convection triggering with respect to background wind speed (Gerken et al., 2013a, Appendix C), providing both information about the validity of the modelling approach as well as the interactions between surface and atmosphere through surface fluxes, locally generated circulation systems and geostrophic wind. Regularly developing and theoretically well understood systems such as lake-breezes are a valuable test-bed for the ATHAM modelling system, especially as there is little model validation data available and the complexity of the lake system as a whole has not been fully investigated through observational or modelling studies. Additionally, the focus on a subset of environmental conditions, such as varying geostrophic wind speeds and wind direction in a 2-dimensional setting allowed for the investigation of the triggering mechanism of convection in the Nam Co Lake basin. The diurnal development from shallow cumulus to precipitating convection at Nam Co Lake as illustrated in Figures 1.1 and 1.2 is one of the major variables in the regional water cycle. On the Tibetan Plateau there is a North-South gradient in precipitation and the role of the Indian Summer Monsoon as the primary source of moisture in contrast to regional recycling of water (Tian et al., 2001a,b; Kurita and Yamada, 2008). Thus understanding the triggering mechanisms of locally generated convection may be one of the keys to a better understanding of the regional water cycle.



Figure 1.2. As Figure 1.1, but with photos taken towards the South-East and Nyenchen Thangla Mountains.

Another aspect regulating cloud development and convection at Nam Co Lake, are vertical atmospheric profiles. There is considerable uncertainty associated with these profiles. Due to the remoteness of the Tibetan Plateau, direct, regular observations by radiosondes are sparse, which not only leads to a lack of available measured profiles, but also affects the quality of gridded atmosphere products that rely on the assimilation of atmospheric data. Additionally, the complex topography and surface heterogeneity of the Tibetan Plateau mean that one expects considerable spatial variation of atmospheric profiles. This is a source of uncertainty, when modelling convection and thus on surface energy and water balance estimations on the Tibetan Plateau. Therefore, the quality and representativity of atmospheric profiles has been a major concern for this work. As a consequence, it was decided to directly measure atmospheric profiles at Nam Co Lake with radiosondes for the work described in Gerken et al. (2013b) and Appendix D compared to the previously used downscaled profile information (Maussion et al., 2011).

While there have been some recent studies addressing the quality of reanalysis data on the plateau (Frauenfeld et al., 2005; Ma et al., 2008, 2009a; Wang et al., 2009), all but Bao and Zhang (2013) have focused on surface data, which are relatively easily compared to ground based measurements. Such comparisons are obviously limited by the horizontal and vertical resolutions of the gridded data, which is typically in the order of 1° in the horizontal and standard pressure levels in the vertical. Radiosondes on the other hand are launched at locations often selected due to historic reasons and have a much higher vertical resolution. This makes the comparison of radiosonde data and gridded products difficult. Additionally, there is considerable variation in the profiles on a day to day scale, which was not addressed by Bao and Zhang (2013). There is no study looking at the influence of uncertainties in atmospheric profiles on convection development on the Tibetan Plateau.

Based on radiosondes, launched during the summer of 2012, and on profile data from NCEP/NCAR, ERA-Int reanalysis and GFS-FNL analysis data, the influ-

ence of different atmospheric profiles on convection development is analysed with ATHAM (Gerken et al., 2013b, Appendix D). This work demonstrates the influence of atmospheric profiles and their uncertainty on surface processes and links convection to vertical stability and atmospheric moisture contents. It is shown that vertical profiles govern the evolution of clouds and convection and thus impact the surface energy and water balance. This constitutes a feedback system. It is therefore important to reduce uncertainties in the initial atmospheric profiles. Additionally, this work contributes to the overarching goal of this thesis, by investigating the cloud development's role on surface fluxes, the surface energy-balance and the generation of precipitation. It contributes to a better understanding of surface-atmosphere interactions in the Nam Co basin and investigates processes that are important for the Tibetan Plateau as a whole.

2. Methods

This chapter is divided into two parts. The former part (Sec. 2.1) introduces the models and the setup used within the framework of this thesis and illustrates some of the model development that was undertaken. The latter (Sec. 2.2) discusses the data used for the modelling experiments.

2.1. ATHAM and Hybrid

These investigations use the non-hydrostatic, cloud resolving Active Tracer High-resolution Atmospheric Model (ATHAM – Oberhuber et al., 1998; Herzog, 1998; Herzog et al., 1998, 2003), which was first developed for the investigation of volcanic plumes (Graf et al., 1999). It was then extended for biomass-burning plumes (e.g. Trentmann et al., 2006) and cloud studies (Guo et al., 2004). Its dynamic core solves the Navier-Stokes equation on a two or three dimensional Arakawa-C staggered grid, where scalar quantities are located at the centre of a grid cell and vector variables on the cell boundaries (Mesinger and Arakawa, 1976), with a z -vertical coordinate through an implicit, second-order time stepping scheme. The maximum Courant-Friedrich-Lewy-number (CFL) in order to assure numeric stability for advective transport is $CFL \leq 0.8$. All hydrometeors are treated as active tracers, meaning that they influence heat capacity and density of the mixture for each grid point (Oberhuber et al., 1998). ATHAM’s turbulence scheme predicts both horizontal and vertical turbulent kinetic energy as well as turbulent length scale and is based on 1.5-order turbulence closure (Herzog et al., 2003). ATHAM’s modular structure allows for the incorporation of several physical processes. In this work short- and longwave radiation (Langmann et al., 1998; Mlawer et al., 1997), bulk-microphysics (treating the conversion between water vapour, cloud water, cloud ice, graupel and rain, Herzog et al., 1998) are used. Surface fluxes are estimated through bulk-transfer relationships. For water surfaces the Coupled Ocean-Atmosphere Response Experiment (COARE) - algorithm v2 (Fairall et al., 1996a,b) based on the framework of Liu et al. (1979) is used, whereas fluxes over land are generated by the Hybrid v6 (Friend et al., 1997; Friend and Kiang, 2005). Hybrid is a process-based terrestrial ecosystem and surface model with a simple two-layer representation of the soil, using surface parameterisations from the GISS GCM II (Goddard Institute for Space Studies General Circulation Model

II – Hansen et al., 1983). The upper layer has a depth of 10 cm, whereas the lower layer has a thickness of 4 m. Conceptionally, the “thin” upper layer is supposed follow the diurnal temperature cycle, while the lower layer acts as energy storage for longer timescales (Hansen et al., 1983). There is an approximate two-hour delay in the diurnal surface temperature cycle of the two-layer model presented in Hansen et al. (1983). Bare soil parameterisation follows the approach of SSiB (Xue et al., 1996) that is based on Camillo and Gurney (1986) and Sellers et al. (1986). Turbulent fluxes are calculated through a bulk approach. The sensible heat flux (Q_H , [W m^{-2}]) is calculated with (Friend and Kiang, 2005):

$$Q_H = c_p \rho C_H u(z) (T_0 - T(z)) \quad (2.1)$$

with the air’s specific heat capacity (c_p , [$\text{J kg}^{-3} \text{K}^{-1}$]), the dimensionless Stanton number (C_H) as a function of roughness length (z_0 , [m]) and Bulk Richardson Number, air density (ρ , [kg m^{-3}]), wind speed of the first model layer ($u(z)$, [m s^{-1}]), air temperature ($T(z)$, [K]) at height of the first model level (z , [m]) and surface temperature (T_0 , [K]). The latent heat flux (Q_E , [W m^{-2}]) is derived from bulk soil evaporation (EV, [mm s^{-1}]), a canopy resistance approach estimating plant transpiration (TR, [mms^{-1}]) and the latent heat of evaporation (L_v , [J kg^{-1}]), with $Q_E = (\text{EV} + \text{TR}) \cdot L_v$:

$$\text{EV} = \left(\rho \frac{f_h q_s - q_a}{r_s + r_a} \right) \times \exp(-0.7\text{LAI}) \quad (2.2)$$

$$\text{TR} = \frac{\rho \Delta q_a}{r_c + r_a}, \quad (2.3)$$

with the relative humidity of soil air (f_h) from Camillo and Gurney (1986), saturation water mixing ratio at surface temperature (q_s , [kg kg^{-1}]), atmospheric water vapour mixing ratio (q_a , [kg kg^{-1}]), soil and aerodynamic resistance (r_s , r_a , [s m^{-1}]), leaf area index (LAI, [$\text{m}^2 \text{m}^{-2}$]) and canopy resistance (r_c , [s m^{-1}]) as calculated by the vegetation model component. These stability dependent transfer coefficients are implemented from Hansen et al. (1983) following Deardorff (1968). The plant physiology and stomatal conductance are included through a generalised plant type (GPT) approach.

2.1.1. Model development

Significant model development efforts were undertaken during the work on this thesis. The investigation of surface-atmosphere interaction with the ATHAM model required changes to the model as it had previously been mainly used for highly

idealised “Large-Eddy-Simulation-like” setups or for the investigation of strongly forced systems, such as biomass burning plumes or volcanic eruptions. In contrast atmospheric convection is weakly forced, increasing the importance of a realistic treatment of radiative forcing, topography, and diffusion of atmospheric variables. Furthermore, the Hybrid model, which was coupled to ATHAM, is substantially modified in order to improve its performance at Nam Co Lake.

Radiative transfer

The Rapid Radiative Transfer Model Global version Long-Wave (RRTMG_LW, Mlawer et al., 1997) is a widely used longwave radiation code for 3-dimensional models. While the radiative transfer is solved individually for all vertical columns the code layout is designed to be coupled to dynamical models. The radiation code of ATHAM was redesigned, writing an interface to RRTMG_LW and allowing for a choice between RRTMG_LW and the previous longwave radiation parameterisation based on Chou et al. (2001). As most radiative transfer codes are written for models with a terrain following Sigma-vertical coordinate, it was also necessary to modify the interface between ATHAM and the radiation codes in order to allow for a changing number of atmospheric vertical layers that result from the block vertical coordinate approach in ATHAM.

Water tracers and cyclic boundary conditions

ATHAM allows for the choice between open and cyclic lateral boundary conditions. While the solution of the dynamic equations is mass conserving, when fully converged, for cyclic boundary conditions, this is not true for open lateral boundaries. The interaction between topography and the lateral boundaries led to a positive feedback in mass change, resulting in large increases or decreases of mass and a subsequent destabilisation of the model. It was hence decided to use cyclic boundary conditions. In order to achieve more realistic results in the simulation of the Nam Co Basin, clouds and positive water vapour anomalies are not transported across the lateral boundaries and are removed through nudging. The active tracer formulation of ATHAM, where tracers contribute to the total density of the mixture, made it necessary to achieve this without the introduction of density perturbations that would lead to vertical motion and thus adversely impact the modelling results. Thus the reduction of moisture is compensated for by the introduction of additional active tracers that have the same density as the removed species, but do not take part in the model microphysics.

Improvements to the dynamical core

As described in section 2.2 of Herzog (1998) ATHAM's dynamical core is build on a closed system of four prognostic equations: the Navier-Stokes equations for momentum transport, the pressure equation, tracer-equations and the temperature transport equation. The system is furthermore closed through three 1.5-order turbulence closure equations (Herzog et al., 2003). The prognostic transport equations are given as (reproduced from Herzog, 1998):

- The Navier-Stokes-Equations for momentum (ρu , [$\text{kg m}^{-2} \text{s}^{-1}$]):

$$\begin{aligned}
 \frac{\partial}{\partial t} \rho u_i &= - \frac{\partial}{\partial x_j} \rho u_i u_j && \text{advection} \\
 &+ \frac{\partial}{\partial x_j} \left(\rho K_j \frac{\partial}{\partial x_j} u_i \right) && \text{turbulent diffusion} \\
 &- \frac{\partial}{\partial x_i} P && \text{pressure gradient force} \\
 &- \rho g \delta_{i3} && \text{gravity force} \\
 &+ 2 \rho \epsilon_{ijk} \omega_j (u_k - u_k^*) && \text{Coriolis force} \\
 &+ \rho Q_i && \text{source term}
 \end{aligned} \tag{2.4}$$

for $i = 1,2,3$ in Einstein's summation notation and with the density of the mixture (ρ , [kg m^3]), a turbulent diffusion coefficient (K), the gas pressure (P , [Pa]), the gravitational acceleration (g , [m s^{-2}]), the angular velocity of the Earth's rotation (ω_j , [s^{-1}]), the geostrophic wind speed (u_i^* , [m s^{-1}]) and a momentum source (Q , [$\text{kg m}^{-2} \text{s}^{-1}$]).

- Similarly the active tracer equation is formulated:

$$\begin{aligned}
 \frac{\partial}{\partial t} \rho q &= - \frac{\partial}{\partial x_i} \rho q u_{i,q} && \text{advection} \\
 &+ \frac{\partial}{\partial x_j} \left(K_{j,q} \frac{\partial}{\partial x_j} \rho q \right) && \text{turbulent diffusion} \\
 &+ \rho Q_q && \text{sources and sinks}
 \end{aligned} \tag{2.5}$$

- and the potential temperature equation:

$$\begin{aligned}
 \frac{\partial}{\partial t} \theta &= - u_{i,\theta} \frac{\partial}{\partial x_i} \theta && \text{advection} \\
 &+ \frac{1}{\rho c_p} \frac{\partial}{\partial x_j} \left(\rho c_p K_{j,\theta} \frac{\partial}{\partial x_j} \theta \right) && \text{turbulent diffusion} \\
 &+ Q_\theta && \text{sources and sinks}
 \end{aligned} \tag{2.6}$$

with θ [K] as potential temperature and c_p [$\text{J kg}^{-1} \text{K}^{-1}$] as the heat capacity of the mixture.

To increase the stability of volcanic plume simulations the diffusion term in the momentum eq. 2.4 was implemented as

$$\frac{\partial}{\partial x_j} \left(K_j \frac{\partial}{\partial x_j} \rho u_i \right). \quad (2.7)$$

This leads to a systematic bias in the diffusion of momentum: Due to the decrease of density with altitude, a vertically constant wind speed would lead to upward diffusion of momentum. This is now corrected in the dynamical core. A similar correction was applied to the potential temperature equation changing the diffusion term from its implementation

$$\frac{1}{\rho c_p} \frac{\partial}{\partial x_j} \left(K_{j,\theta} \frac{\partial}{\partial x_j} \rho c_p \theta \right) \quad (2.8)$$

to the form in eq. 2.6.

The diffusion term in the tracer equations was similarly changed from the formulation of eq. 2.5 to the physically correct form of:

$$\frac{\partial}{\partial x_j} \left(\rho K_{j,q} \frac{\partial}{\partial x_j} q \right) \quad (2.9)$$

These corrections required substantial changes in the coding of ATHAM's dynamical routines.

Improvement to the upper boundary condition

Running convective simulations with ATHAM required changes to the rigid-lid upper boundary condition. It was observed that during atmospheric simulations that were not capped with a strongly stable layer (e.g. the stratosphere) the unmodified ATHAM has a tendency to become unstable and would eventually abort. This was investigated to be an error in the upper-boundary formulation. Small inconsistencies at the upper boundary led to model drifts that went unnoticed in previous short and strongly forced volcanic simulations. As a consequence the upper boundary-condition for pressure was modified in order to include one additional layer with temporally constant density and pressure in hydrostatic equilibrium at the model top. This modification enforced hydrostatic balance down to machine precision at the model top. In addition, it was discovered that the spatial discretisation of temperature in advective form was inconsistent with the flux form used in the pressure and momentum equations at the model top. Because temperature,

pressure and momentum are inherently linked through the dynamic core, changes in pressure develop near the top boundary and grow over time in amplitude.

This numerical mode was suppressed almost completely by replacing the original two sided vertical temperature gradient calculation with a one sided gradient at the upper boundary.

Hybrid

It was found out that the first of the original Hybrid's two soil layers, with a thickness of 10 cm, imposes a substantial delay in the diurnal temperature cycle and acts as a low-pass filter for short duration events such as cloud shading, considered to be of special importance on the Tibetan Plateau (Gerken et al., 2012, Appendix B). This becomes apparent in Figure 12 of Hansen et al. (1983), where the GISS II model exhibits a time delay of approx. 2 hours for surface temperatures. A similar behaviour is found in the unmodified Hybrid.

In order to improve the representation of the diurnal surface temperature cycle and subsequently the generated turbulent surface fluxes, a quadratic subgrid soil temperature profile with extrapolated surface temperature (T_0 , [K]) was introduced into Hybrid (Figure 2.1). The approach, fully described in Gerken et al. (2012) and Appendix B, is outlined below: For both layers denoted with the subscripts 1 and 2 from the model top, a quadratic temperature profile ($T(z)$, [K]) is assumed:

$$T_{1,2}(z_{\text{rel}}) = a_{1,2} (z_{\text{rel}} - d_{1,2})^2 + T_{\text{base}_{1,2}} \quad (2.10)$$

with a constant (a , [K m^{-2}]), the depth below the top of the layer (z_{rel} , [m]), the layer thickness (d , [m]) and the temperature at the lower boundary of the respective layer (T_{base} , [K]). There is assumed to be no transfer of heat through the lower model boundary i.e. T_{base_2} is constant and equal to the annual mean temperature of 0°C (You et al., 2006, recited from Keil et al. (2010)), which is a simplification. However, the annual temperature cycle at 4 m is expected to be small and the rate of change in bottom temperature is negligible on the day-scale. For future research a sinusoidal lower boundary temperature could be introduced. The relationship between layer heat content E [J] and temperature profile is given by:

$$E = c_{\text{ps}} \int_{z_{\text{L}}}^{z_{\text{U}}} T(z) dz \quad (2.11)$$

where z_{L} and z_{U} are the lower and upper boundaries of the layer and c_{ps} [$\text{J m}^{-3} \text{K}^{-1}$] is the total soil heat capacity. Hence, with a known heat content for each layer it is possible to solve for

$$a_2 = \frac{\frac{E_2}{c_{\text{ps},2}} - d_2 T_{\text{base}_2}}{\frac{d_2^3}{3}}, \quad (2.12)$$

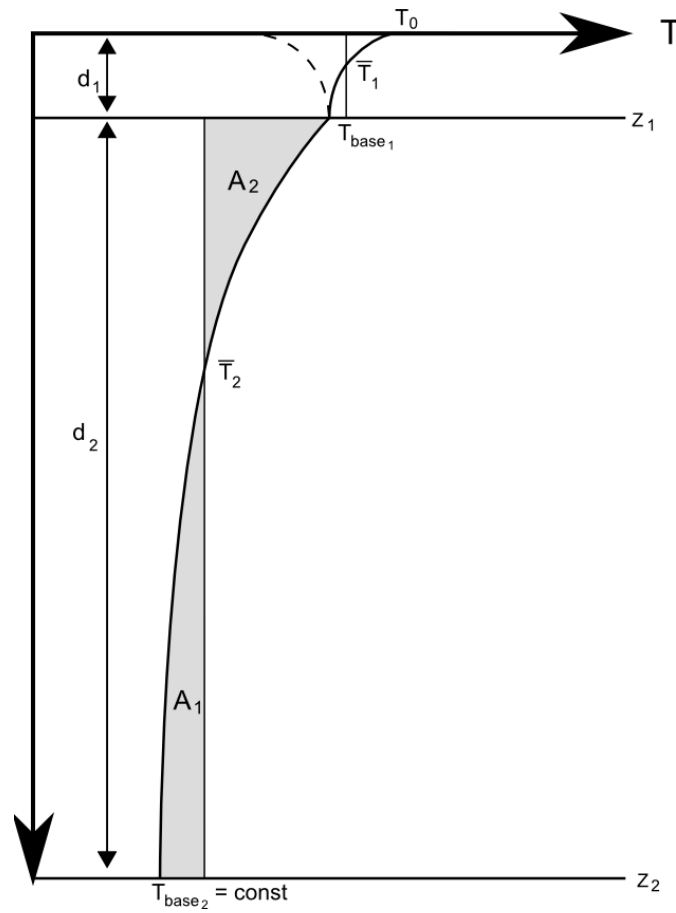


Figure 2.1. Conceptual drawing of the assumed quadratic subgrid soil temperature profile and the associated parameters. In order to derive \bar{T}_1 and \bar{T}_2 geometrically the areas A_1 and A_2 must be equal. Figure from Gerken et al. (2012), Appendix B.

by integrating Eq. (2.11) with Eq. (2.10) from $z_L = 0$ to $z_U = d_2$ and solving for a_2 . The base temperature of the first layer is related to T_{base_2} through

$$T_{\text{base}_1} = T_{\text{base}_2} + a_2 d_2^2. \quad (2.13)$$

In a similar fashion a_1 and T_0 can be approximated:

$$a_1 = \frac{\frac{E_1}{c_{\text{ps},1}} - d_1 T_{\text{base}_1}}{\frac{-z_1^3}{3}} \quad (2.14)$$

and

$$T_0 = T_{\text{base}_1} + a_1 d_1^2. \quad (2.15)$$

Sec. 3.2 discusses the results that were obtained from the modified Hybrid tested at Nam Co Lake.

It was also found that Hybrid's soil heat diffusion algorithm based on Hansen et al. (1983) leads to unrealistic modelled soil heat fluxes ($F(z)$) as they are largely dominated by the residual of turbulent and radiation fluxes ($F(0)$), which is positive during night-time and negative during daytime, thus leading to a net transfer of heat from cold to warm in Hybrid's original parameterisation:

$$F(z) = \frac{3\bar{T}_1 - 3\bar{T}_2 - 0.5F(0)r_1}{r_1 + r_2} \times \Delta t, \quad (2.16)$$

where $F(z)$ depends on the temperature difference between the mean layer layer temperatures (\bar{T}), the residual of Hybrid's integrated energy fluxes, layer thickness, thermal resistances (r) and the model time step (Δt). The ground heat flux is derived from the residual of the surface energy balance. Assuming the above subgrid temperature profile the heat flux between the two layers Eq. (2.16) was modified with a heat diffusion approach using the subgrid temperature profile, integrating

$$\frac{\partial T}{\partial t} = D \frac{\partial^2 T}{\partial z^2} \approx D \Delta t \frac{T(z_1 + \Delta z) - 2T(z_1) + T(z_1 - \Delta z)}{2\Delta z}, \quad (2.17)$$

D being a soil moisture dependent diffusion constant for heat. ∂z is approximated by the diffusion length $L = 2\sqrt{\Delta t D} = \Delta z$. This approach is valid using time-steps with $L \ll d_1$, which would correspond to $\Delta t \ll 30$ min and is much larger than the typical ATHAM time-step in the order of seconds.

Modelling approach and setup

The objective of this thesis is to investigate the atmospheric processes and surface-atmosphere interactions at Nam Co Lake. Therefore, it is important to have a modelling system that is capable of simulating the relevant surface-atmosphere interaction processes with an appropriate temporal and spatial resolution. While a 3-dimensional simulation of the entire Nam Co basin would have been desirable, it has proven to be prohibitively expensive in terms of computational cost. Additionally, there is the question of sparse input data both with respect to atmospheric profiles as well as surface measurements. The high computational cost and associated simulation times would have considerably extended the duration of the project. At the same time, the analysis would have been limited to a very small number of simulations which may have shown very complex behaviour, but would also have been based on very limited and likely not representative data. It was therefore decided that it was more desirable to have a larger number of idealised simulations, which allow for the investigation of several aspects, such as wind speed and atmospheric profiles, within the lake-land-atmosphere system. Ideally, one can thus obtain an estimate of the sensitivities of the system.

ATHAM is consequently used in a 2D-setup, with the horizontal coordinate oriented perpendicular to the lake-land boundary, cutting through Nam Co station and the Nyenchen Thangla chain (Figure 2.2).

The horizontal resolution within the basin is set uniformly to 200 m and the vertical resolution is 25 to 50 m close to the surface and then increasing with altitude from the mid-troposphere to maximum vertical resolutions of approx. 300 and 200 m at the model top (Gerken et al., 2013a,b, Appendices C and D). The initial time step was set to 2.5 s. Such resolutions are sufficient to resolve the mesoscale circulation systems and convection, without the need for special parameterisations. Petch (2004) has called for resolutions in the order of 100 m to do so. We use in excess of 150 layers with a model top above the tropopause.

The model topography is taken from the ASTER-GDEM (Advanced Spaceborne Thermal Emission and Reflection Radiometer – Global Digital Elevation Model) with 90 m resolution smoothed with a 2 km moving window. This approach removes large vertical cliffs, which lead to strong vertical flow in 2D and single grid point depressions, which cannot be dealt with by the numerical solver. Additionally, topography outside the Nam Co basin is reduced to lake level and turbulent surface fluxes are gradually reduced to zero near the lateral boundary. Simulations are integrated from 06:00 BST (04:00 LST), which is approximately 1 hour before sunrise, to 18:00 BST (16:00 LST).

The surface model is initialised with data measured during two field experiments at Nam Co Lake in 2009 and 2012. The atmosphere for 2009 is initialized with profiles that were downscaled from the GFS (Global Forecasting System –

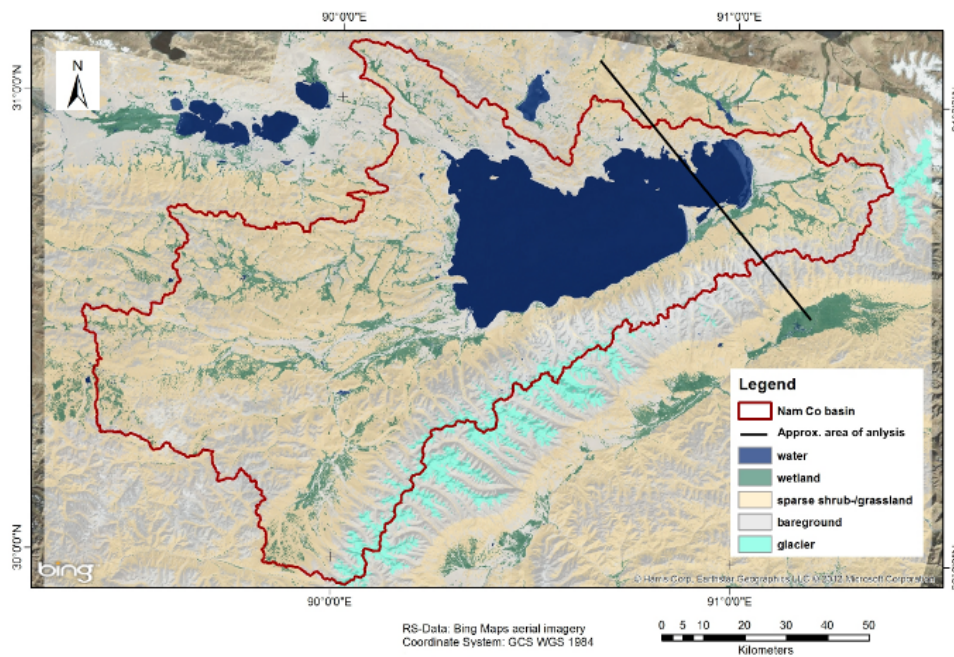


Figure 2.2. Land-use map of Nam Co Lake created from Landsat data. The black line indicates the central 80 km of the model domain. © 2012 the Microsoft Corporation © Harris Corp, Earthstar Geographics LLC. Figure modified from Gerken et al. (2013a), Appendix C.

Kanamitsu et al., 1991; Caplan et al., 1997) product to Nam Co Lake with WRF following the approach of Maussion et al. (2011) or with directly measured profiles and gridded data products are used for the 2012 simulations.

2.2. Data from field experiments

The high-resolution modelling approach as outlined in Section 1.2 is strongly dependent on the availability of data for model initialisation and validation purposes. Freely available, gridded datasets, while being very useful for lower resolution largescale approaches, are generally coarse and will not reflect the local conditions. Additionally, some types of data, such as soil data or vegetation height are almost impossible to determine through remote sensing approaches. Therefore it was necessary to use data gathered in field experiments.

Two field experiments were conducted at Nam Co Lake in cooperation with Institute of Tibetan Plateau Research (ITP), Chinese Academy of Sciences. The 2009 experiment was carried out within the summer monsoon season from 26 June to 8 August, measuring turbulent surface fluxes with the eddy-covariance technique and other atmospheric measurements. A second experiment was executed between 8 July to 8 August 2012, when atmospheric profiles of pressure, temperature, relative humidity and wind speeds were measured with radiosondes. Additionally, turbulent flux data and other atmospheric data were obtained.

2.2.1. Site description of Nam Co Lake

Nam Co Lake (altitude 4730 m a.s.l.) is located on the Tibetan Plateau approximately 150 km north-east of Lhasa. The south of the lake basin is delineated by the Nyenchen Thangla mountain chain, with up to 7270 m altitude. The mean elevation of the basin is 5230 m (Liu et al., 2010). To the north of the lake several hills with elevations of up to several hundred meters are situated. Measurements were carried out near the Nam Co Monitoring and Research Station for Multi-sphere Interactions operated by ITP near a small lake, which is separated by an approx. 500 m wide land bridge from Nam Co Lake, placing the station about 1 km to the south-east of Nam Co Lake's shore. The vegetation around the lake is typical for arid high-altitude vegetation with alpine steppe and meadow grasses (Mügler et al., 2010). Near Nam Co station the vegetation encountered is highly dependent on the availability of soil moisture. Close to the lake and in topographic depressions, wet areas are densely covered alpine meadows dominated by *Kobresia spp.* (grass+, Figure 2.3), while drier areas correspond to alpine steppe with 60 % soil cover (grass-). According to Mieke et al. (2011), Biermann et al. (2009) and ? alpine grasses like *Stipa*, *Carex*, *Helictotrichon*, *Elymus*, *Festuca*, *Kobresia*,

Poa are found in the drier areas. In 2012 the vegetation in the footprint of the eddy-covariance station was comprised of (personal communication: K. Hopping, Colorado State University, from Gerken et al., 2013c): *Adrocaea* and *Arenaria biophyta* as cushion plants, *Leontopodium pusillum*, *Potentilla bifurca*, *Potentilla sauderriana*, *Astragalus sp*, *Oxytropis bifurca*, *Oxytropis glacialis*, *Dacoccephallum*, *Incarvillea younghusbandii*, *Sibaldia adpressa* and sagebrush as forbs, *Potentilla sp* as scrub, *Stipa purpurea*, *Poa sp*, *Poa litwanii* as grasses and a few *Carex* as sedges.

The Lake itself has a maximum depth of more than 95 m at its centre. While most of the lake is more than 50 m deep, the maximum depth in the eastern part close to Nam Co station is approximately 35 m (Wang et al., 2009). Satellite derived lake surface energy fluxes by Haginoya et al. (2009) at Nam Co Lake (Jul 2006–2008: $\overline{Q_H} = 0 \text{ W m}^{-2}$; $\overline{Q_E} = 21 \text{ W m}^{-2}$) are substantially lower than the eddy-covariance measurements conducted during the 2009 experiment. They determined a mean lake surface temperature of 9.4°C and 10.4°C for July and August, respectively, with a negligible diurnal surface temperature cycle.

2.2.2. Eddy-covariance measurements

During the 2009 campaign two energy balance stations that measured turbulent surface fluxes were operated. The eddy-covariance complex consisted of CSAT3 sonic anemometers (Campbell Scientific Ltd) and Li-7500 infrared gas analysers (Li-COR Biosciences). The first measurement complex was located at the lake shore, next to the small lake (denoted as NamUBT, Figure 2.3). Depending on the wind direction, fluxes at NamUBT reflect conditions over the small lake, over the moist surface (grass+) or a mixture of both. The terrain is terraced and land-use showed little change since the first inventory by Metzger et al. (2006). The second complex, operated by ITP (NamITP) is located approximately 300 m away from the lake and at Nam Co station. The surface is flat and dry representing alpine steppe (grass-). The measurements of both eddy-covariance stations were post-processed using the TK2/3 software package (Mauder and Foken, 2004, 2011), applying all necessary flux corrections and post-processing steps for turbulence measurements as recommended in Foken et al. (2012) and Rebmann et al. (2012). When turbulent fluxes are used for quantitative comparisons (i.e. Gerken et al., 2012, Appendix B) data not meeting quality flags of 1–3 of the 9 classes according to Foken et al. (2004) are excluded from the analysis. For qualitative or illustrative purposes data of quality classes 4–6 is also used. Additionally, site-specific footprint climatologies (Göckede et al., 2004, 2008) were created, applying a Lagrangian forward stochastic model by Rannik et al. (2000). More comprehensive documentation of the 2009 experiment and the data post-processing can be found in Biermann et al. (2009) and Biermann et al. (2013). For the 2012

measurement campaign flux data are only available from the NamITP complex. While the location and most of the setup has not changed, it should be noted that the humidity sensor was replaced with a KH2O Krypton hygrometer (Campbell Scientific Ltd), which was calibrated at the site on 13 July 2012 according to Foken and Falke (2012).

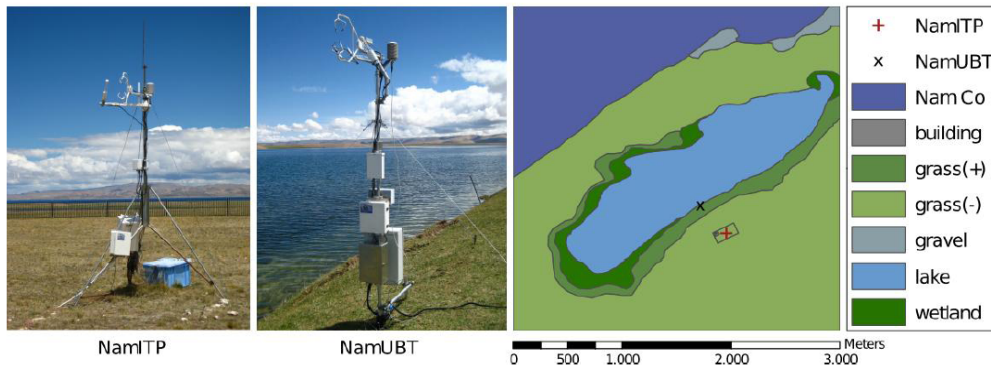


Figure 2.3. Measurement setup near Nam Co station during the 2009 campaign. The position of the eddy-covariance Stations NamITP (left Photo, red +) and NamUBT (right Photo, black x) is indicated in the schematic drawing. Additionally, the land-use classification is given: wetland (dark green), moist (+, medium green), dry (-, light green) grassland, partly flooded gravel (grey), the small lake (light blue) and Nam Co (dark blue). Figure from Biermann et al. (2013).

2.2.3. Radiosonde measurements

Preliminary studies with ATHAM highlighted the need for direct measurements of atmospheric profiles. Hence, radiosonde measurements were conducted between 8 July and 8 August 2012. During selected days, radiosondes were launched for 00, 06 and 12 UTC from Nam Co Station. For 17 July sunrise, noon and sunset were at 23:05, 6:02 and 15:00 UTC according to the National Oceanic and Atmospheric Administration Sunrise/Sunset Calculator. Therefore, these standard times roughly correspond to early morning, solar noon and late afternoon and should give information about diurnal changes of the boundary-layer and the atmospheric profiles. Local solar time (LST) is used in this thesis as UTC+6. Sondes were released approx. 30 minutes prior to the designated observation time, which is within the 45-minute window commonly used (OFCM, 1997). A shorter than usual window was applied due to the high elevation and the resulting shorter

ascent time of the sounding. The *Vaisala RS-95-SGP* radiosondes were used in conjunction with a *TOTEX-TA600* balloon and parachute (when available). Free lift was approximately 1050 g. Data was processed with *SPS 220* and the *DigicORA III MW21 (v. 3.2.1)* software. A total of 25 sondes were launched, giving 8 days with atmospheric profiles of temperature, relative humidity and horizontal wind speeds. Figure 2.4 displays the vertical profiles of temperature and moisture measured during the campaign. It is apparent that the day to day and intra-day variability of atmospheric moisture is much larger than changes in temperature. Nevertheless, profiles frequently show 1–3 distinct temperature inversion layers, which change heights between days. Sondes stayed mostly within the Nam Co basin and should therefore reflect local conditions. The full documentation of the 2012 experiment, which includes flux measurements and radiosoundings, can be found in Gerken et al. (2013c).

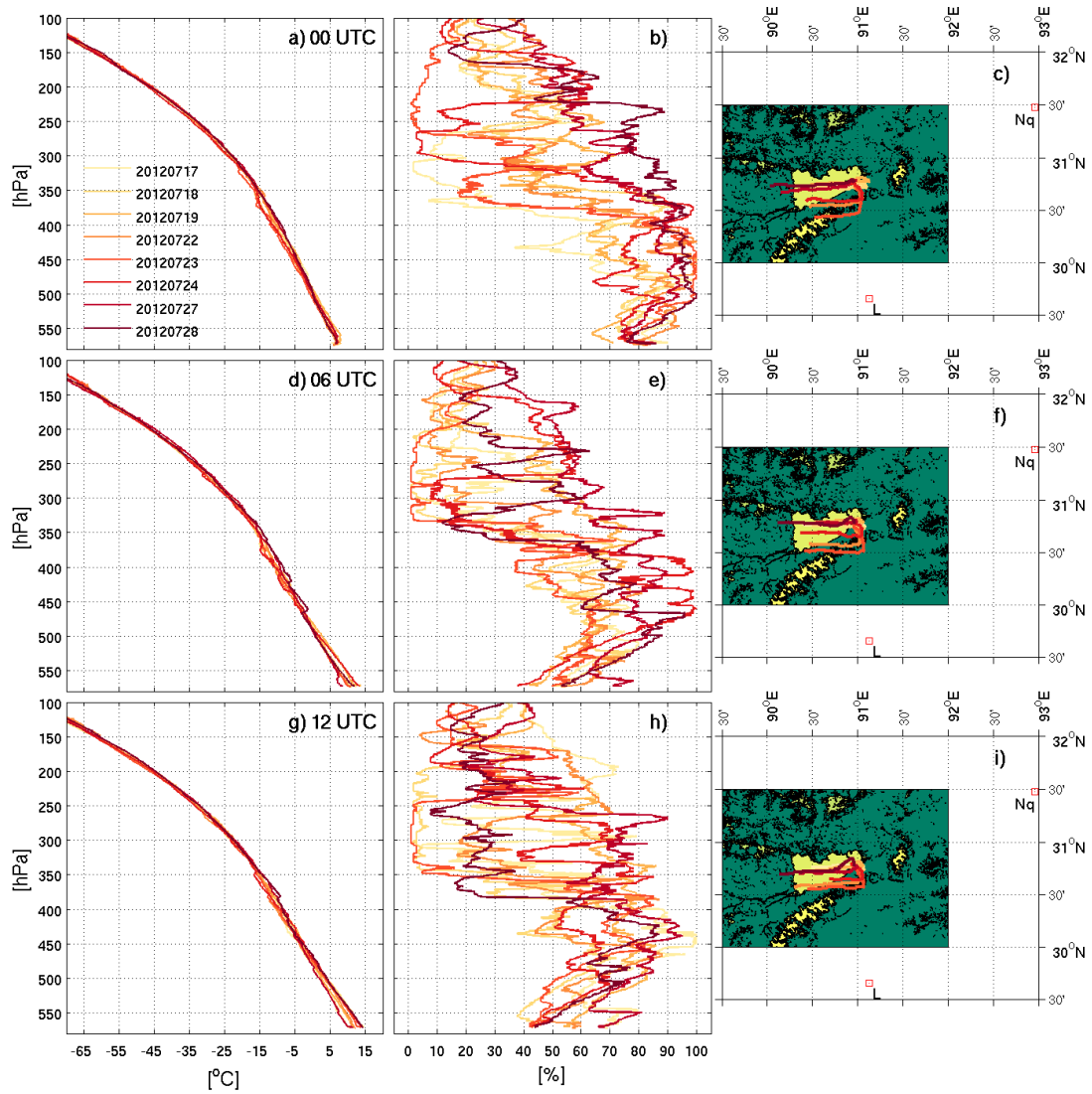


Figure 2.4. Measured radiosonde profiles at Nam Co Lake during summer 2012: Temperature (left column, [°C]), Relative humidity (central column, [%]) and flight path (right column) for sondes launches at 00, 06 and 12 UTC (rows 1–3, respectively). *L* and *Nq* in the right column show the location of the next World Meteorological Organisation radiosounding stations: Lhasa and Naqu.

3. Results

In order to improve the understanding of atmospheric processes in the Nam Co basin, a two step approach has been taken. The model system and its components are validated before investigating the system sensitivities at Nam Co Lake with additional numerical simulations. Sections 3.1 and 3.2 summarise the results that were achieved through model development of ATHAM and Hybrid. The improved surface formulation of Hybrid was published in Gerken et al. (2012) and is attached in Appendix B. The remaining sections show the application of the developed modelling framework and the results with respect to surface-atmosphere interactions and influence of vertical atmospheric profiles at Nam Co Lake published in Gerken et al. (2013a) and Gerken et al. (2013b); Appendices C and D.

3.1. Improved model performance and stability for simulations of atmospheric convection

Over the course of this work several substantial changes have been made to the ATHAM dynamical core as outlined in Sections 2.1.1 and 2.1.1, which have addressed some of the problems encountered during the work on this thesis. The ATHAM model is version-controlled, so that each change to the model's source code is versioned with a unique increasing revision number. The changes to the dynamic core have been performed between revisions 701 and 937. Figure 3.1 displays the development of pressure, temperature and wind speed over a 16 h, 2D model run without surface forcing and with a 500 m high Gaussian mountain in the centre of the domain. It becomes apparent that the revised ATHAM (r937) has far smaller change in pressure throughout the domain and less cooling at the model top, which may be explained by radiative processes. This simulation was initialised with a surface pressure corresponding to the Tibetan Plateau ($P_s = 572$ hPa) and has a constant vertical temperature gradient of $dT/dz = -8$ K, which is capped with an isothermal layer between 10 and 14 km above ground (model top). With the model behaviour shown of revision 937, it can be assumed that the changes in pressure and temperature have a negligible influence on the flow field of the simulation.

However, there are still significant limitations. In the absence of a stable layer at the model top, there remain problems with the stability of the ATHAM model

3. Results

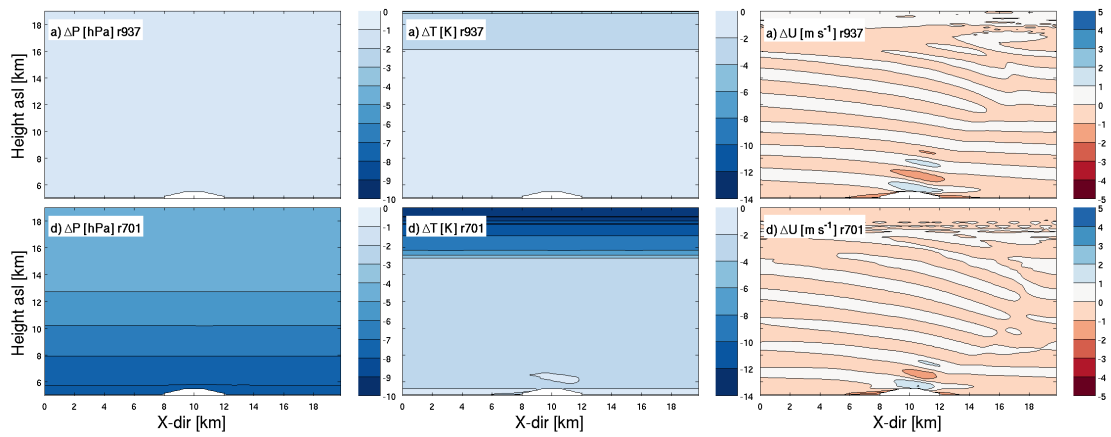


Figure 3.1. Development of **(a+d)** pressure (ΔP , [hPa]), **(b+e)** temperature (ΔT , [K]) and **(c+f)** wind speed (ΔU , [m s^{-1}]) compared to initial conditions for a 16h ATHAM model run with only radiative forcing for current version (r937, upper row) and version before dynamic core modifications (r701, lower row). The initial surface pressure is set to 572 hPa, temperature decreases with $dT/dz = -8 \text{ K}$ for the first 10 km above ground and then remains constant for the last 4 km below model top simulating a tropopause. The wind speed is initialised uniformly at 2 m s^{-1} .

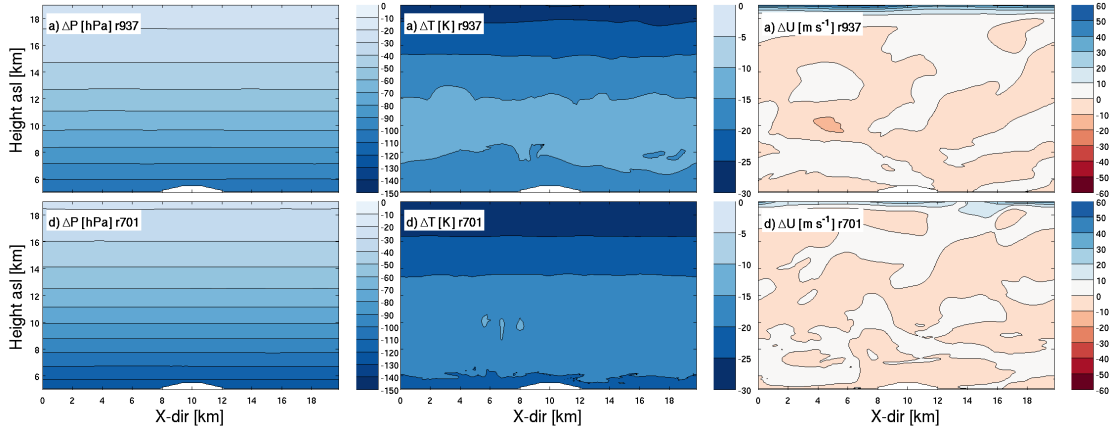


Figure 3.2. As Figure 3.1, but with $dT/dz = -8$ K throughout the domain, simulating the absence of a tropopause.

(Figure 3.2). A pressure loss in the order of 25% of the total pressure is accompanied by excessive cooling and changes in the flow field, which cannot be explained by physical processes.

Investigations into this issue have determined that the growing numerical mode is mainly associated with the total number of model integrations. Therefore, it is useful to investigate the relative change of pressure and potential temperature (θ) with respect to the number of model timesteps (Figure 3.3). From the figure it becomes apparent that the current version of ATHAM remains stable and without significant pressure change up to at least 5×10^4 timesteps as long as the model is capped with a stable layer. Without such a layer the current version of ATHAM performs better than the previous versions, but still exhibits unrealistic changes of pressure and potential temperature that are caused by numerical instabilities. The fact that the radiation code influences the stability of simulations is likely due to the implementation of temperature forcing as an added perturbation and the not strictly energy conserving advective formulation of the heat equation. There was no discernible influence on model stability found for the presence of topography or a change of surface pressure to sea level (1013 hPa).

It should be noted, however, that the simulations of the Nam Co Lake system are typically executed for 12 h or approximately 2×10^4 timesteps. Additionally, as deep convection at Nam Co Lake is frequently observed, all ATHAM simulations of the basin extend to the stratosphere so that results presented in the following sections correspond to simulations within a similar regime as *r701 trY rY* and *r937 trY rY*, where pressure and temperature changes are not dominated by the model

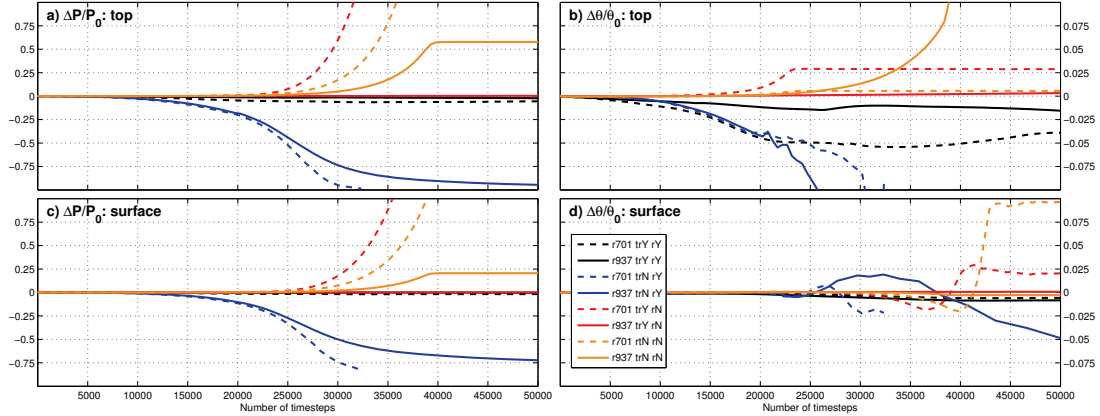


Figure 3.3. Relative change of layer mean (a+c) pressure (P) and (b+d) potential temperature (θ) at model top (top row) and near the surface (bottom row) with respect to the total number of model timesteps. $r701$ identifies the model before dynamic core modifications and $r937$ is the current model version. trY and trN refer to the presence or absence of a stable tropopause at the model top, while rY and rN indicate whether the radiation code is switched on or off.

dynamic core. It was also ensured that the pressure change throughout the model domain and duration of the simulation was limited below 3 hPa. However, as the ATHAM setup does include sources and sinks of mass such as evaporation and precipitation as well as diabatic processes, which have an effect on pressure and temperature, it is impossible to establish the reason for small pressure changes.

3.2. An improved surface temperature formulation in Hybrid

The unmodified Hybrid was observed to have a delay of several hours in the diurnal cycle of surface fluxes compared to observations. This was especially true for the ITP station where on several occasions during the 2009 measurement campaign surface temperatures dropped below the point of freezing in the early morning hours, leading to a 10 cm thick frozen layer as a sink for incoming solar energy. While this problem is avoided with the modified version (introduced in Sec. 2.1.1) Hybrid remains strongly dependent on the initialisation of the layer temperatures and thus of the soil heat contents. Due to the quadratic nature of the assumed subgrid temperature profile, relatively small changes in the layer mean temperature

can have large effects on the surface temperature and thus the turbulent fluxes. This is illustrated in Figure 3.4: Panels (a) + (b) show the individual dependence of temperature variables on each other as expressed in the respective Eqs. (2.13) and (2.15). The third panel (c) gives the parameter space for the surface temperatures, dependent on the initialised layer temperatures \overline{T}_1 and \overline{T}_2 . A random combination of the layer temperatures used to initialize the model runs in Gerken et al. (2012) see Appendix B, would give skin temperatures in an unrealistic range (-10°C to 30°C). In reality T_0 is clustered much more closely. This highlights the importance of a careful initialisation of the surface model and the need to obtain measurements of soil temperatures.

However, when properly initialised, the performance of the modified surface model is greatly improved over the original Hybrid. While the original Hybrid fails to capture the dynamics of turbulent fluxes of sensible and latent heat as well as surface temperature, the modified Hybrid agrees much better for both the UBT (not shown) and ITP (Figure 3.5) sites. For UBT a lake-breeze develops for most days so that there are few eddy-covariance fluxes available for daytime periods. Nevertheless, for days without a lake-breeze there is a greatly improved match between the fluxes derived from the modified Hybrid, eddy-covariance measurements and fluxes generated by SEWAB (Surface Energy and Water Balance model – Mengelkamp et al., 1999). The SEWAB modelling approach taken at Nam Co Lake is documented in ?. While the UBT site is influenced by the lake water table and thus moist, the ITP site has a more complex soil-moisture dynamic, varying between dry conditions with Bowen ratios of approx. 3 (as on 27 July 2009) to moist conditions with Bowen ratios of 1/2 as are commonly encountered at the UBT site. In general there is good agreement between the Hybrid fluxes and the eddy-covariance and SEWAB fluxes used as reference. It should be noted that both the fluxes estimated by Hybrid and the “reference” fluxes have errors, so that true error of the Hybrid model cannot be quantified. The difference in behaviour of Q_H and Q_E on 10 July 2009 after 12:00 BST (10:00 LST) when the cloud cover lifts shows that Hybrid’s sensible heat flux reacts faster than the latent heat flux. There is a rather big spread of results for ITP on 6 August 2009, when $Q_{E,\text{Hybrid}} > Q_{E,\text{EC}} > Q_{E,\text{SEWAB}}$. For Q_H this effect is reversed. The difference between EC and Hybrid may potentially still be explained by daytime measurement errors in the order of 5% for Q_H and 10% for Q_E and by the simple energy balance closure according to Bowen-ratio (Twine et al., 2000), while the SEWAB surface was too dry in comparison with measured soil moistures. An alternative energy balance closure method, which uses the buoyancy flux and thus takes into account the influence of secondary circulations, was recently proposed by Charuchittipan et al. (2013) and ?. For the range of Bowen-ratios of 0.5 to 3 encountered at Nam Co, this means approx. 90% of the flux residual would be added to Q_H instead

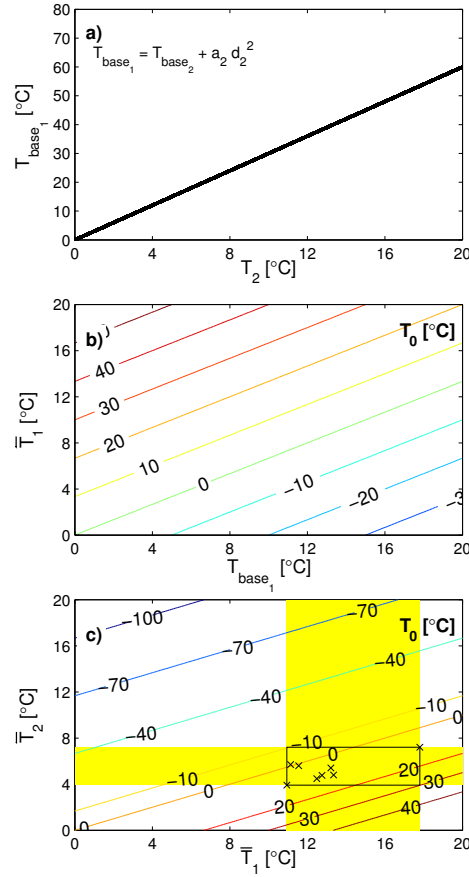


Figure 3.4. Dependency of soil temperature parameters: **(a)** relationship between mean temperature of layer 2 (\bar{T}_2) and bottom temperature of layer 1 [T_{base_1} , Eq. (2.13)] – a_2 is calculated according to Eq. (2.12); **(b)** surface temperature (T_0) contour plot as function of T_{base_1} and layer 1 mean temperature (\bar{T}_1) and **(c)** contours of (T_0) as function of \bar{T}_2 and \bar{T}_1 . The black rectangle at the intersection of the layer temperature ranges (yellow) indicates the theoretical parameter space given by the temperature values used in this study and the black crosses mark the actual configurations. Figure modified from Gerken et al. (2012), Appendix B.

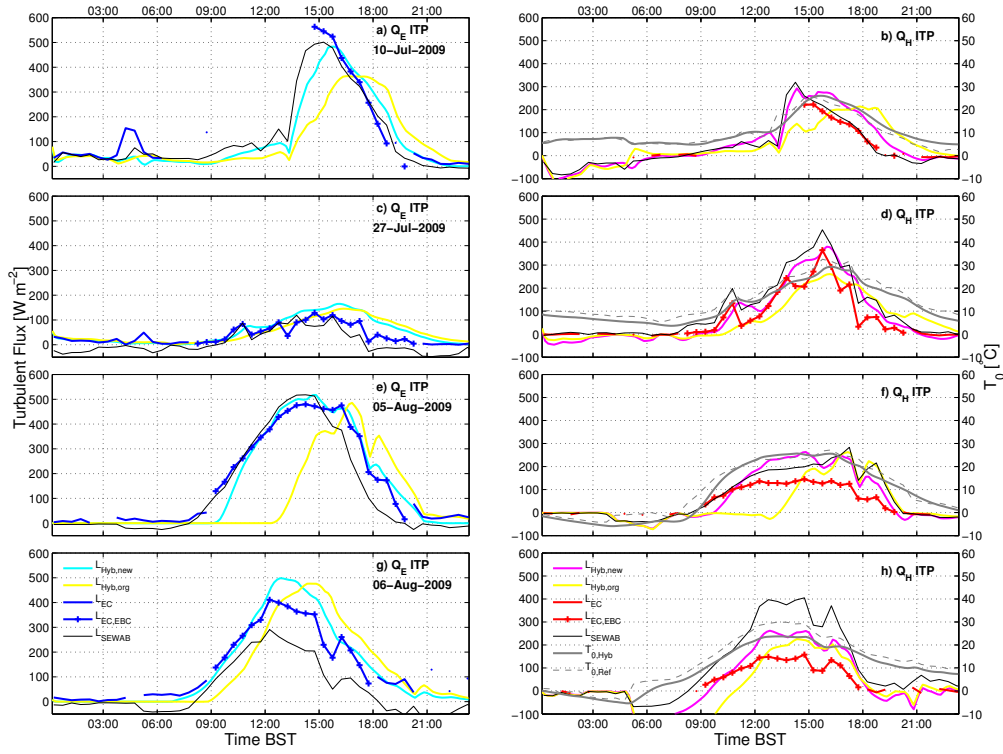


Figure 3.5. Model results for the modified Hybrid at ITP for (a–b) 10 July 2009, (c–d) 27 July 2009, (e–f) 5 August 2009 and (g–h) 6 August 2009. Left column: latent heat flux (Q_E); right column: sensible heat flux (Q_H) and surface temperature T_0 [$^{\circ}\text{C}$]. L refers to “land” as origin of the fluxes. The subscripts Hyb,mod and Hyb,org refer to fluxes from the modified and original Hybrid, whereas $SEWAB$ is a SVAT model. EC and EC,EBC refer to measurements by eddy covariance method where in the latter the energy balance has been closed by distributing the residual according to Bowen-ratio. Figure from Gerken et al. (2012), Appendix B.

of between 33% and 75% as for the Bowen-ratio method. This increases Q_H determined by the eddy-covariance method and thus reduces the difference between modelled and measured sensible heat fluxes.

Even with the old energy balance closure, it can be seen from Table 3.1 that the root mean square deviation (RMSD) is reduced between 40–60 % for the modified surface model. At UBT the number of data points is much lower than for ITP, due to the occurrence of the lake-breeze making a sensible comparison more difficult and being reflected in smaller scores of improvement. Additionally, the time-lag of fluxes was much reduced as reflected by an improvement of cross correlations (Figure 8 in Gerken et al. (2012), Appendix B). In general the fluxes produced by the modified Hybrid and their dynamics seem to agree reasonably well with the observed flux dynamics at the Nam Co Lake stations, so that the modified Hybrid is consequently used for the investigation of surface-atmosphere interactions at the Nam Co Basin.

3.3. Cloud development and mesoscale circulations at Nam Co Lake

It was found that the coupled ATHAM-Hybrid model was able to reasonably reproduce surface and atmospheric processes at Nam Co Lake, giving a realistic land-lake circulation system. Subsequently, the sensitivities of the system were investigated with respect to different components of the system.

3.3.1. Boundary-Layer development

These results were obtained through a MSc thesis by Kathrin Fuchs (2013) co-supervised by me:

Based on surface-flux measurements and radiosonde profiles obtained in summer 2012, boundary-layer development in the Nam Co Lake basin was investigated. Figure 3.6 displays the development of boundary-layer heights for the 17 + 18 July 2009 as determined from radiosondes, a slab model and ATHAM simulations. It was found that the slab model after Batchvarova and Gryning (1991) overestimated boundary-layer heights compared to the radiosonde reference. It is well known that different methods yield large variations in the estimated boundary-layer height even when applied to the same profile (i.e. Seibert et al., 2000). Notwithstanding, the boundary-layer heights determined by the simple parcel method on both days at 13:30 BST (11:30 LST) coincide with a notable reduction in water vapour mixing ratios. This jump from a layer of constant mixing ratio below and a considerably drier atmosphere above is in accordance with the definition of a mixed layer. The determined boundary-layer height at 19:30 BST

Table 3.1. Root mean square deviation (RMSD) between the modelled quantities of the original and modified Hybrid and reference values. The reference quantities used are either measured by the eddy-covariance method and corrected for energy balance closure (EC,EBC) or modelled with SEWAB for fluxes or taken from longwave outgoing radiation for T_0 . The values in parenthesis (N) correspond to the number of elements used for calculation of RMSD. Table from Gerken et al. (2012), Appendix B.

Site	Date	Run	RMSD				
			Q_E EC,EBC	Q_H [W m ⁻²]	Q_E SEWAB	Q_H [W m ⁻²]	T_0 [°C]
UBT	10 July	orig	318	117 (8)	94	74 (94)	4.3 (139)
	27 July		97	58 (19)	60	59 (139)	4.5 (143)
	05 August		168	139 (11)	90	64 (110)	4.3 (143)
	06 August		159	84 (52)	87	71 (128)	3.7 (143)
ITP	10 July	orig	182	93 (25)	97	69 (143)	3.7 (143)
	27 July		43	64 (72)	58	75 (143)	3.8 (143)
	05 August		224	103 (64)	179	68 (143)	8.3 (143)
	06 August		118	80 (52)	130	119 (143)	5.1 (143)
UBT	10 July	mod	214	43 (8)	51	36 (94)	2.3 (139)
	27 July		79	44 (19)	32	28 (139)	2.9 (143)
	05 August		93	62 (11)	36	26 (110)	3.4 (143)
	06 August		78	57 (52)	39	32 (128)	3.2 (143)
ITP	10 July	mod	74	73 (25)	42	32 (143)	1.6 (143)
	27 July		42	58 (72)	55	36 (143)	2.6 (143)
	05 August		44	80 (64)	64	30 (143)	2.6 (143)
	06 August		68	82 (52)	113	77 (143)	3.5 (143)
UBT	all	orig	170	92 (90)	83	67 (471)	4.2 (568)
		mod	100	54 (90)	39	31 (471)	3.0 (568)
ITP	all	orig	152	84 (213)	125	86 (572)	5.6 (572)
		mod	54	73 (213)	74	48 (572)	2.7 (572)

3. Results

(17:30 LST) on 18 July likely results from a detection of a residual boundary layer. Visual inspection of the profile shows that the maximum boundary-layer height for this day was in the order of 1500 m.

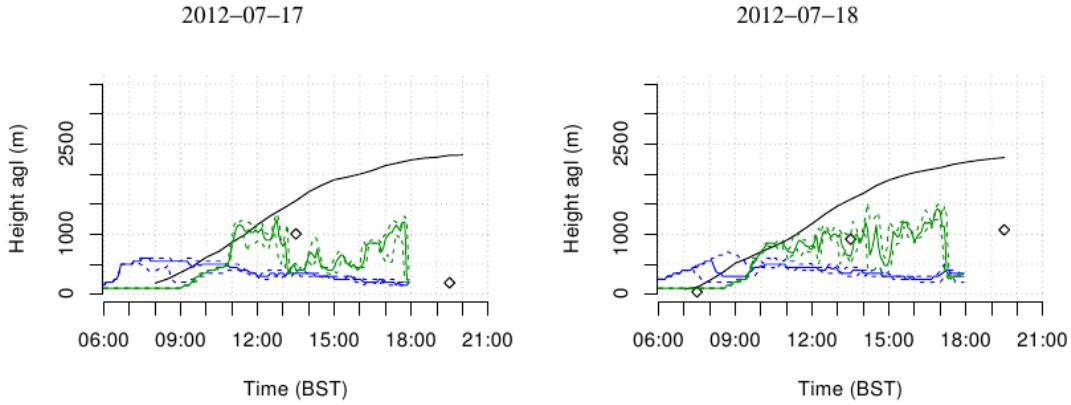


Figure 3.6. Comparison of atmospheric boundary-layer heights estimated by a slab model (after Batchvarova and Gryning, 1991) from measurements (black line), estimated from ATHAM with the simple parcel method above the lake (blue line) and above the plain (green line) and from radiosonde profiles with simple parcel method (black diamonds) for the 17 + 18 July 2012. Figure modified from Fuchs (2013).

ATHAM simulates boundary layers of approx. 500 m depth, as detected by the simple parcel method, over Nam Co Lake, which corresponds to the mean boundary-layer height over oceans (Foken, 2008a). The boundary-layer over the plain starts to grow from approx. 1 h after sunrise until a maximum depth of 1000 to 1500 m is reached. The depth is comparable to the values determined from the soundings by the simple parcel method, which was evaluated as relatively reliable for convective boundary-layer height detection by Seibert et al. (2000). In the afternoons, ATHAM shows strong temporal variation in the simulated boundary-layer depths. This is caused by rising thermals and convective plumes penetrating the top of the boundary layer and compensating downward motion. As the 2D-model is likely to overestimate convection due to the unresolved y-dimension, this temporal change in boundary-layer heights is also likely to be overestimated. In the late afternoon, boundary-layer heights determined for ATHAM collapse due to a strong reduction in surface temperature and sensible heat fluxes. While one would expect to see this happen in the late afternoon, when the surface starts to cool, there are unfortunately no measurements available to investigate whether the

timing of this process is well represented in ATHAM. Overall, the daytime convective boundary layer at Nam Co Lake develops to similar heights as determined for the Tibetan Plateau during the summer monsoon season (Chen et al., 2013). The maximum boundary-layer depth on the Tibetan Plateau is often given as 3 km in the dry season (Ma et al., 2009b; Yang et al., 2004; Taniguchi and Koike, 2008) and significantly lower during the wet season, when sensible heat fluxes are greatly reduced. ATHAM is capable of simulating realistic boundary layers, thus indicating a reasonable representation of the relevant surface-atmosphere interactions.

3.3.2. Interactions of mesoscale circulations and background wind

First of all, the development of a sea breeze is not independent from the background wind. Without a background wind and without topography a symmetric lake breeze is expected to develop, while onshore geostrophic winds (U_g) shift the lake breeze further onto the land. The reverse effect is expected for offshore flow. According to Crosman and Horel (2010) oceanic sea breezes with offshore $U_g > 4\text{--}8\text{ m s}^{-1}$ are expected to stall at the land-lake boundary, while onshore $U_g > 3\text{--}5\text{ m s}^{-1}$ cause sea breezes to become indistinguishable from the background flow. These values are thought to be smaller for lakes, due to their limited size. For the setup used in Gerken et al. (2013a), Appendix C, a unified thermal circulation between the lake and the Nyenchen Thangla mountains developed in the no-wind case and no discernible sea breeze was found to form for an offshore wind speed of $U_g > 6\text{ m s}^{-1}$, which is comparable to the conditions on 6 August, when no lake breeze was found to develop. The lake breeze regime was observed to develop between 9:00 and 12:00 BST (7:00 and 10:00 LST), while lake breezes in ATHAM became clearly observable around 11:00 BST (9:00 LST).

For small wind speeds there is a fast transition between the occurrence of shallow, boundary-layer clouds (t_{cl}) and the triggering of deep and moist convection as indicated by both t_* and t_{13} in Table 3.2. Stronger winds cause triggering of convection later during the day. Additionally and due to a non-symmetric basin, the wind direction is also responsible for the development of boundary-layer clouds. Ascending air over the plain at the footsteps of the Nyenchen Thangla mountains causes adiabatic cooling and promotes cloud development, while adiabatic descent causes suppression of cloud development.

Both the development of a lake breeze and the development of convection are linked to the energy exchange at the surface. When comparing modelled surface fluxes to fluxes measured with the eddy-covariance method, there are two main problems that have to be taken into account. Firstly, the footprint of the eddy-covariance measurements is approximately on the same spatial scale as a single

Table 3.2. Timing of convection in hours BST (LST+2). t_{cl} is the time when first boundary layer clouds appear in the model; t_* corresponds to the triggering of moist convection after Wu et al. (2009) and t_{13} is the time when convection reaches 13 km a.s.l. t_* for U-6.00 was not calculated due to the occurrence of a high cloud over the mountain chain, rendering the calculation of the centre of the cloud mass Z_c inapplicable. Table from Gerken et al. (2013a), Appendix C.

Run	t_{cl}	t_*	t_{13}
U-3.00	09:20	11:40	14:20
U-1.50	11:10	11:40	13:20
U+0.00	11:10	11:50	12:30
U+1.50	11:20	12:00	13:20
U+3.00	11:20	12:50	14:00
U+6.00	11:40	N/A	N/A

grid-cell of the high-resolution model. Therefore, one has to compare a quasi-point measurement with a representative flux from the model. This work uses the median flux and the lower and upper quartile. Secondly, the surface model closes the surface energy balance, distributing all available solar energy between latent, sensible and ground heat-flux, while eddy-covariance fluxes are inherently not closed (i.e. Foken, 2008b; Foken et al., 2011). The observed energy balance closure at Nam Co Lake was close to 70% of the net radiation R_{net} (Biermann et al., 2013). Especially stationary secondary circulations such as sea breezes are thought to transport a substantial amount of energy. Hence, the energy balance of the measured fluxes was closed according to the Bowen-ratio (Twine et al., 2000).

As long as clouds are absent, there is little spatial variation of turbulent fluxes (Figure 3.7). Q_E and Q_H rise until the early evening, when clouds start to reduce the incoming shortwave radiation. As a consequence median turbulent fluxes start to decrease and spatial variation becomes larger. This effect is strongest after the triggering of deep convection. When modelled fluxes are compared to measurements, case U-3.00 m s^{-1} shows triggering of convection at a realistic time and has reasonable agreement between observed and measured fluxes.

In the triggering of convection at Nam Co Lake with respect to the wind direction two main mechanisms are identified and depicted in Figures 3.8 and 3.9. In the first case the background wind and the developing lake-breeze circulation have the same direction and transport moist air towards the south and over the mountain chain. The mountain chain then repeatedly triggers thermals in similar locations, leading to a sequence of convective events downstream of the Nyenchen

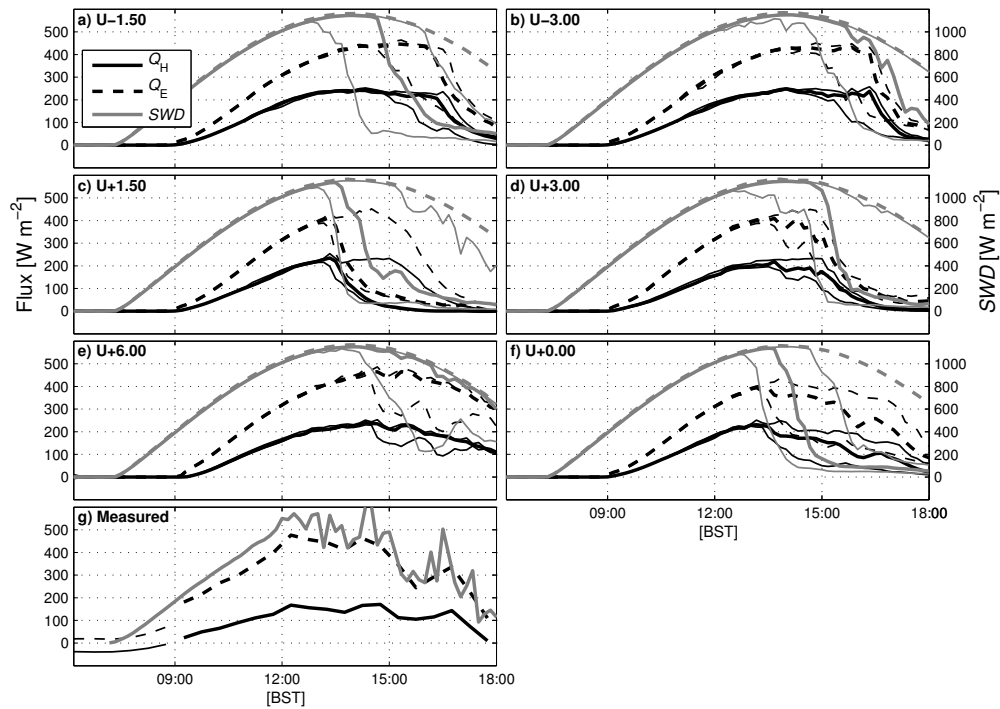


Figure 3.7. Development of turbulent surface fluxes in the Nam Co Lake basin for model runs with initial wind of 1.50, 3.00, -1.50, -3.00 and 0.00 ms^{-1} , (a–f) respectively (Q_H — ; Q_E --; downwelling shortwave radiation (SWD) grey). Thick black lines correspond to median flux over land. Thin lines are upper and lower quartiles of fluxes. The dashed grey line is clear sky SWD; (g) measured turbulent fluxes near Nam Co research station. Thin lines correspond to directly measured eddy-covariance fluxes on 6 Aug 2009. Thick lines are energy-balance corrected fluxes according to Twine et al. (2000). Figure from Gerken et al. (2013a), Appendix C.

Thangla mountains. In the second case, the lake-breeze circulation pushes into the basin and against the background wind thus displacing the moist basin air upwards. This results in convective thermals and eventually deep convection being triggered. A similar mechanism of frontal collision and convergence for Tibetan valleys was described by Yang et al. (2004): Convection triggered by topography leads to secondary convection within valley basins through gust fronts and cold pools associated with downdrafts. In a more theoretical framework, this was studied by several authors (Chu and Lin, 2000; Chen and Lin, 2005; Reeves and Lin, 2007; Miglietta and Rotunno, 2009). Low wind speeds ($U < 10 \text{ m s}^{-1}$) allow for the development of strong cold pools, which cause a blocked state, where a density current travels against the flow and causes precipitation upstream of the topography. For these “low” flow speeds the system was found to be in a blocked state, with a density current travelling against the flow causing precipitation upstream of the topography. At higher wind speeds the advection of heat reduces the strength of the cold pool. While the modelling setup used in the work focuses on low flow speeds, there are several differences: A thermal circulation is caused by the lake and the heated mountain, so that near surface wind speeds are larger than the initialised U_g . Also, surface heat fluxes over the mountain reduce cold pool development. Despite these differences, we see evidence for similar processes in the modelling simulations at later stages, when the overall flow field is dominated by convection.

3.3.3. Influence of temperature, relative humidity and uncertainty in profiles

In addition to wind speed and wind direction, which have a direct impact on the generation of mesoscale circulations as discussed above, convective development is controlled by both atmospheric stability and moisture contents (i.e. Wu et al., 2009). Even more so than surface measurements, accurate profile information is difficult to obtain, thus representing a major source of uncertainty in modelling studies. This is of special importance for high-resolution models such as ATHAM, which have more than 100 tropospheric layers, and therefore resolve the vertical profiles much better than typically achieved with mesoscale or global circulation models, which have typically less than 60 layers over the entire atmospheric column. Hence, the atmospheric profiles’ influence on convection development is analysed in this section.

ATHAM is used to simulate convection in the Nam Co basin on two days during the summer of 2012 (17 and 18 July) using vertical profiles from different sources: Directly measured radiosonde observations (case RS), standard level information extracted from the sounding (StdLev), NCEP/NCAR (NCEP) and ERA-

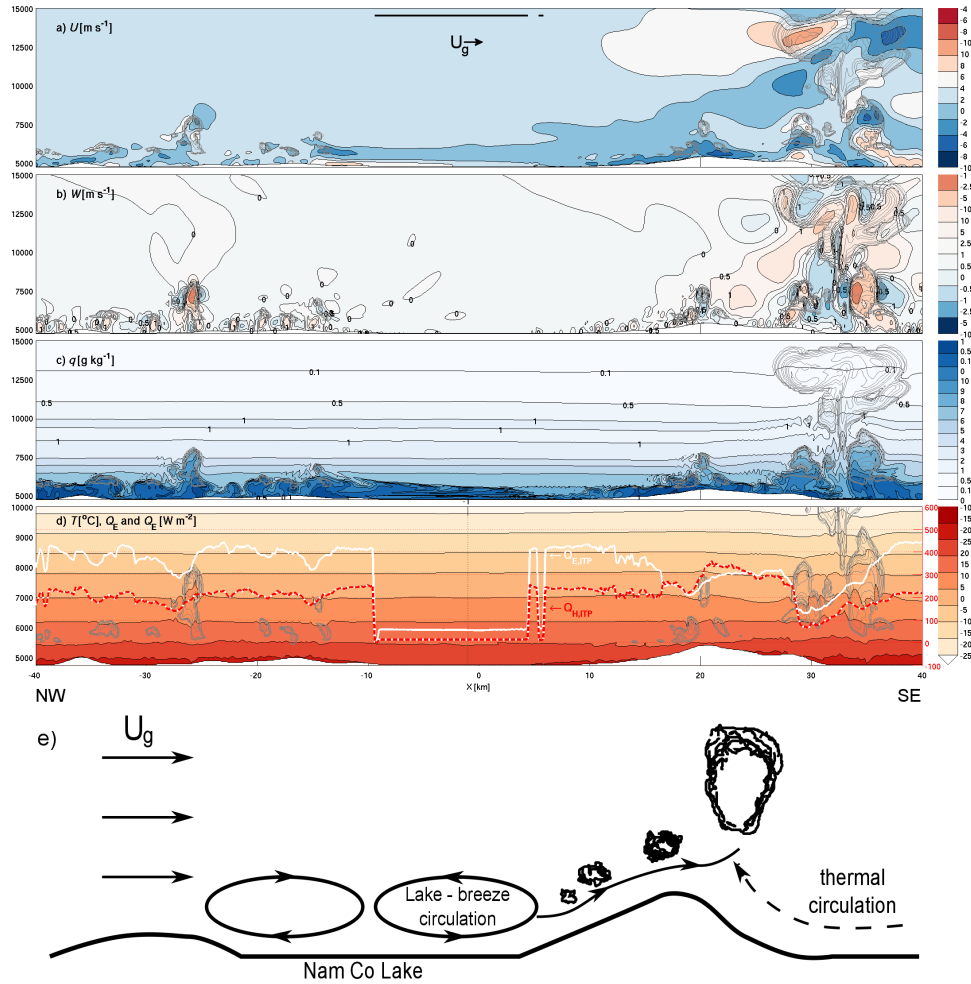


Figure 3.8. Modelled (a) U [m s⁻¹]; (b) W [m s⁻¹]; (c) q [g kg⁻¹] and (d) T [°C] in the Nam Co Lake basin for case U-1.50 at 13:30 h BST (11:30 LST). Grey contours indicate clouds. The red and white lines indicate Q_H and Q_E with the arrows indicating the magnitude of the measured eddy-covariance fluxes. The position of the lake is indicated by the black line. Plot (e) is a sketch of the mechanism. Figure from (Gerken et al., 2013a), Appendix C.

3. Results

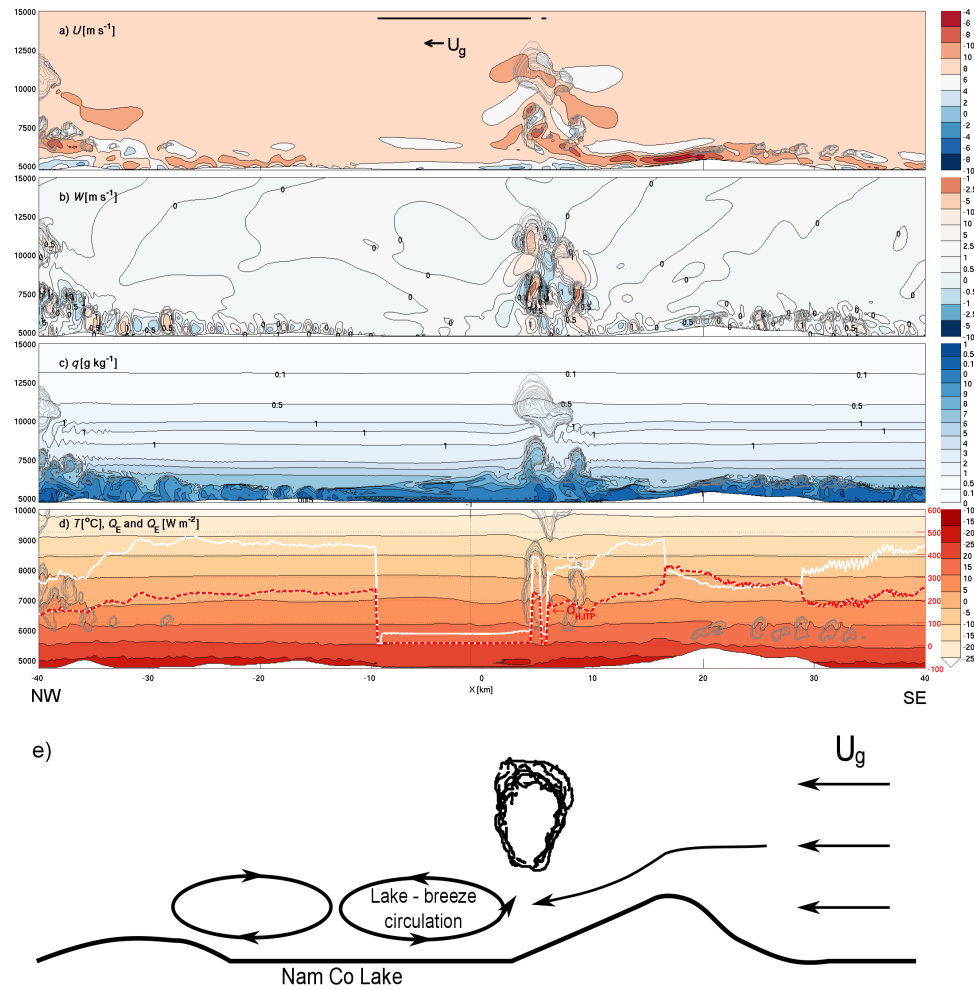


Figure 3.9. As Figure 3.8, but for case U+3.00 and at 13:50 h BST (11:50 LST).
Figure from Gerken et al. (2013a), Appendix C.

Int (ERA) reanalysis data and GFS-FNL (GFS) analysis were used to generate temperature and relative humidity profiles for the initialisation of ATHAM. The wind speed is fixed to 3 m s^{-1} , which was found to produce the most realistic results in the mesoscale circulation study. We present here the results for 18 July 2012, while the full results presented in Gerken et al. (2013b), Appendix C, include both days.

There are large differences in the cloud development, timing of convection and precipitation dynamics between the simulations based on the four different sources of atmospheric profiles. Figure 3.10 shows the temporal development of clouds and precipitation for the five cases. With respect to cloud top and cloud base height as well as the centre of the cloud mass, there is no agreement between the gridded data sets. While the simulation result of NCEP resembles convection development for case StdLev, clouds in ERA are confined to the lowermost 2 km above ground until 10:00 LST. Thereafter, convection of comparable strength develops. GFS in contrast produces fewer clouds and convection and almost no precipitation. The RS case highlights the importance of vertical resolution. Convection is less strong in RS than in StdLev and develops later. This is at least partially explained by an inversion layer in the middle troposphere. Overall, the findings indicate considerable uncertainties in convection development that stem from uncertainties in the vertical profiles, such as differences in stability or systematic biases: GFS for instance is found to be excessively warm in proximity to the surface, while ERA has a tendency to be too cold and too moist (in terms of RH). A potential reason for this is the surface's influence on the lower tropospheric profile.

As the modelling system of this work is set up to have a fully interactive surface, where cloud development influences global radiation and thus turbulent surface fluxes, these differences in convection development have significant impact on the surface energy balance and the total amount of energy that is supplied to the atmosphere (Figure 3.11) As surface heating on the Tibetan Plateau is thought to modify the monsoon system, such uncertainties are not only of importance on the basin scale, but potentially also for large-scale circulation and climate. For the Nam Co basin there are differences in the total integrated turbulent energy fluxes (E) of up to 50% found, which are attributed to the evolution of clouds. On 18 July, StdLev and NCEP have the lowest energy transfer over land with regard to both sensible and latent heat, which is explained by their similar convection dynamics. ERA instead shows the largest energy-flux despite its very moist surface layer, while the contribution of GFS to the latent heat flux within the basin is large compared to its relative contribution in sensible energy.

The profile development on 18 July 2012 highlights some of the merits and weaknesses of the chosen modelling approach. For 17 July, there is a reasonable agreement in convection development and observed weather at Nam Co station,

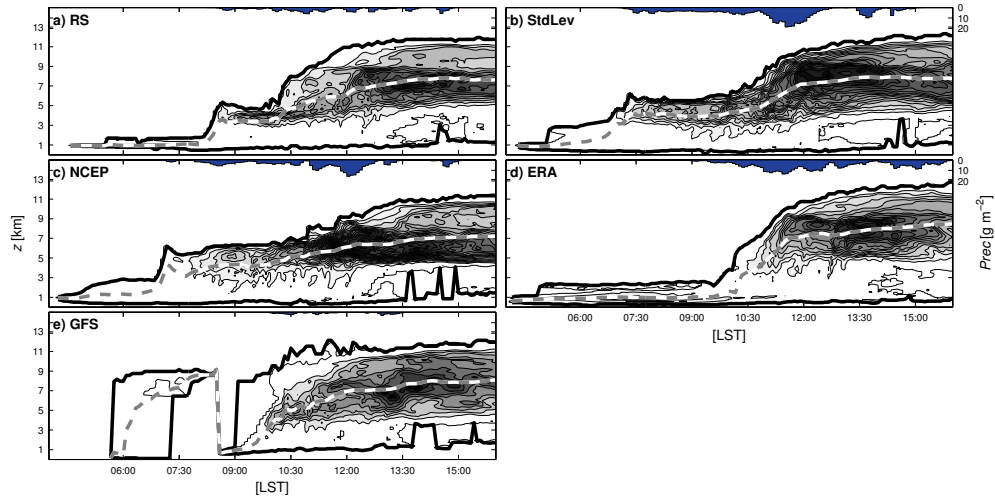


Figure 3.10. Modelled development of convection at Nam Co Lake for cases RS, StdLev, NCEP, ERA and GFS (a–e) on 18 Jul 2012: Contours correspond to mean cloud particle concentrations in the Nam Co Lake basin. Each contour level corresponds to 0.1 g m^{-3} . The dashed line indicates the height of the centre of cloud mass (Z_c) and black lines indicate cloud top and cloud bottom heights. Figure from Gerken et al. (2013b), Appendix D.

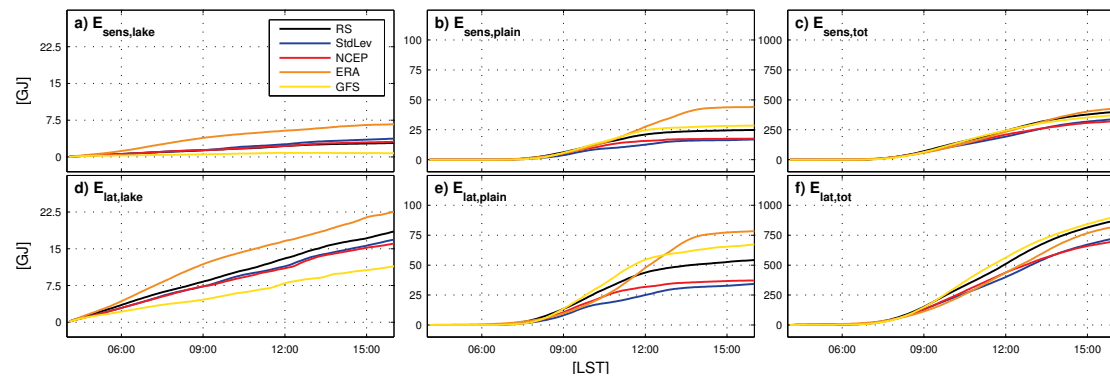


Figure 3.11. Spatially and temporally integrated turbulent energy fluxes (E) at Nam Co Lake for cases RS, StdLev, NCEP, ERA and GFS on 18 Jul 2012: (a+d) Sensible and latent energy over lake, (b+e) over plain adjacent to lake and (c+f) in total domain. Figure from Gerken et al. (2013b), Appendix D.

where a thunderstorm was reported at 11:30 LST. On both days isolated *Cumulonimbus incus* clouds were observed in the basin from 10:00 LST. Additionally, for the lower to middle troposphere there is a good agreement between the radiosonde profile for 6 UTC and the modelled profile at the same time. The 18 July exhibits similar convective development as the previous day. The 2D-approach is likely to overestimate convection due to a lack of entrainment of dry air from the unresolved third dimension (Figure 3.12), causing too much transport of moisture to the upper troposphere above 8 km a.s.l. At the same time, the ATHAM model does not include synoptic effects, so that the moisture contents in the upper layers is predominantly determined by the initialised profile. On 18 July there is clear evidence of upper level drying in the sounding profile, due to either dry air advection or large-scale subsidence as indicated by the NCEP reanalysis data. It should be noted that not all gridded data-sets show this drying in their profiles.

Over the course of the simulation, near surface temperature biases and differences in moisture between the different cases decrease in the lowermost 3 km. This indicates the surface's influence on the boundary layer and lower troposphere and illustrates how the spin-up time can reduce modelling errors.

3.3.4. Precipitation at Nam Co Lake

The surface energy balance is influenced by the development of clouds and convection. Differences in the simulated energy balance, either caused by uncertainties in the profile or by changes in the environmental conditions, are also going to have an impact on modelled precipitation and water resources; a topic of major research interest on the Tibetan Plateau. Locally generated precipitation in the Nam Co region is of special interest due to its location on the northern border of the Indian monsoon's influence. The research in this work indicates that there are major differences in precipitation amounts and dynamics between the different profiles (Table 3.3). Between the driest (GFS on both days) and moistest cases there is approximately one order of magnitude difference in the deposited precipitation. While the 2D-approach, with the Kessler-type microphysics used in this study, is clearly limited in the predictive skill of precipitation in general, it still serves to highlight uncertainties associated with modelling the water cycle. One additional question posed by our research is whether Nam Co Lake is a water source for the region, or whether the basin constitutes a closed water cycle. Evaporation from the lake and evapotranspiration of the vegetated surfaces are advected with the wind and may fall as precipitation on the slopes surrounding the lake basin. About 25–60% of the simulated precipitation on 17 and 18 July 2012 was produced within the Nam Co basin, indicating the lake's importance for the regional water cycle. Another question raised by the investigation of the different convection-triggering mechanisms at Nam Co Lake is the question of representativity of weather sta-

3. Results

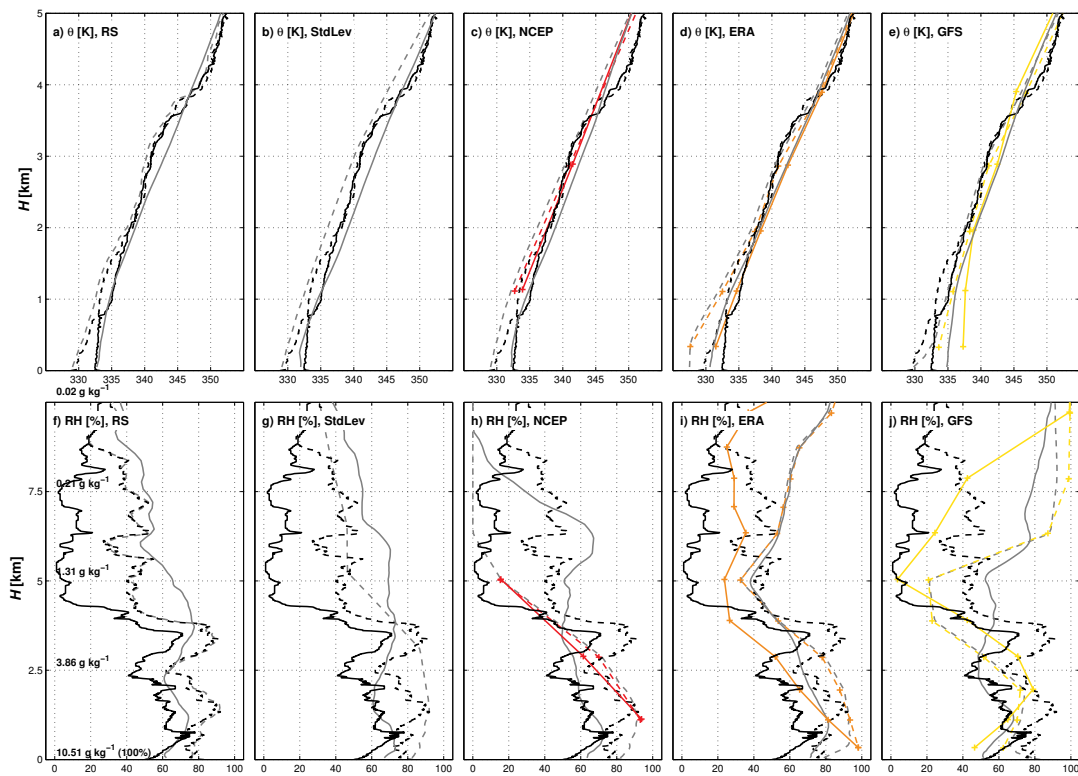


Figure 3.12. Comparison of the mean profiles of the ATHAM simulations initialized with **(a+f)** full radiosonde profile (RS), **(b+g)** radiosonde standard level information only (StdLev), **(c+h)** NCEP-I and **(d+i)** ERA-Int reanalysis and **(e+j)** GFS-FNL products compared to the respective profile data for 18 Jul 2012 00 UTC (dashed) and 06 UTC (solid). The upper panels display potential temperature (θ , [K]) and the lower panels RH [%]. Figure from Gerken et al. (2013b), Appendix D.

tions. Nam Co research station is located close to Nam Co Lake in the centre of the basin. A water body of this size is shown to cause subsidence in summer and enhances snowfall when not yet frozen over in the cold season (Li et al., 2009). Additionally, the Nyenchen Thangla mountain range was determined to be a major trigger of convection (Gerken et al., 2012), Appendix B. Therefore, precipitation measurements at Nam Co Lake are not only not representative for the basin as a whole, but also have systematic errors that change with wind direction and season of the year. Additionally it should be noted that there is a second major source of precipitation within Tibetan mountain valleys (Fujinami et al., 2005; Sato et al., 2007), which occurs in the evenings, when the reversal of the daytime thermal circulation leads to convergence and moist convection in the valley centres (i.e. Ueno et al., 2009). This effect, not included in our studies, would increase the percentage of locally deposited precipitation.

Table 3.3. Deposited precipitation at Nam Co Lake for the model runs on 17 + 18 July 2012 within the Nam Co Basin as defined in the text $Prec_B$ and total domain $Prec_{tot}$. Table from Gerken et al. (2013b), Appendix D.

Run	17 July 2012		18 July 2012	
	$Prec_B$ [m ³]	$Prec_{tot}$ [m ³]	$Prec_B$ [m ³]	$Prec_{tot}$ [m ³]
RS	9.8	17.3	11.6	23.2
StdLev	11.1	28.1	43.4	73.7
NCEP	5.7	18.5	34.2	52.9
ERA	19.4	58.5	19.9	71.3
GFS	3.9	9.5	2.2	6.1

4. Conclusions

The overarching purpose of this work is to develop and adapt a modelling system to conditions on the Tibetan Plateau and then to subsequently investigate surface-atmosphere interactions and environmental processes at Nam Co Lake. It is the goal to gain a better understanding of the system and the physical processes that govern mesoscale circulations and cloud development. Additionally, it is the aim to assess the sensitivities and environmental conditions that impact the lake-land-atmosphere interactions. It is hoped that such studies further our understanding of the surface energy-balance and convection development on the Tibetan Plateau in general and may, thus, be a contribution to the overall effort of a better knowledge of the Earth system and potential effects of changes in it. Therefore, within the framework of the DFG SPP-1372 and through a collaboration between Cambridge and Bayreuth, a modelling framework with an integrated surface and high-resolution atmospheric model has successfully been developed. It has been applied at Nam Co Lake for the modelling of surface fluxes (Gerken et al., 2012, Appendix B), used for the investigation of the lake breeze circulation system and its influencing factors (Gerken et al., 2013a, Appendix C) and for the investigation of some of the uncertainties that are associated with the initial atmospheric profiles (Gerken et al., 2013b, Appendix D). From these efforts it can be concluded:

- i) Data availability and representativity in general are a big issue on the Tibetan Plateau. Especially, the availability of reliable profile information for this remote region has been a major challenge for this work. After exploring the possibility of idealised and synthetic profiles, it was decided to use gridded profile information that was downscaled with the WRF-model. However, as convection development and the surface energy-balance are highly dependent on the initial atmospheric profiles, it was found necessary to obtain direct measurements through radiosoundings conducted in the summer of 2012.
- ii) Substantial improvements have been made to ATHAM, which have removed errors in the code and have led to a more consistent formulation of the upper boundary-condition and the advection of momentum, heat and additional tracers. As a result, the ATHAM model shows improved performance and stability for both convection and volcanic studies.

- iii) The modified soil temperature profile with an extrapolated surface temperature, which was introduced into Hybrid, has decreased the root mean square deviation between modelled and reference surface fluxes by 40–60 %. It has also drastically reduced the time-lag of surface temperature and turbulent fluxes as represented in the cross correlations. Overall, it is demonstrated that a relatively simple change in the surface parameterisation can lead to a substantial improvement in model performance and that the surface model used in the study is principally capable of providing fluxes as a lower boundary condition that reflect the behaviour of the system. This has been tested across variable environmental conditions. Nevertheless, our surface-modelling approach is probably limited by the two-layer surface model as there is still a delay of approximately 1 hour and the skin temperature remains dependent on the layer mean temperature of a relatively thick layer. It was proposed by Liu and Shao (2013) to specifically develop surface models that are capable to react on the time-scale of large-eddies and hence able to resolve the effects of passing cumulus clouds. This would also lead to an improved reaction of the surface model and the fluxes to passing clouds.
- iv) Subsequently, the interactive modelling system has been applied to the Nam Co basin and it is found to adequately model the thermal circulations that are frequently observed during the diurnal cycle at Nam Co station. The lake-breeze reacts as expected to changes in wind direction and strength and collapses at a similar wind speed as measured on 6 August 2009, when no lake breeze was found to form. There is a realistic transition from shallow boundary layer clouds to fully evolved convection in the model.
- v) Depending on wind direction there are two different mechanisms of convection triggering found that are related to interactions of the thermal circulation with topography and with the collision of the lake-breeze front with the geostrophic wind. Hence, the model captures two important components of the lake system, which are shown to have an impact on convection development and are also thought to impact the surface energy balance and the water cycle.
- vi) Compared with other studies, there is no development of a strong cold pool in the onset of deep convection. This is likely due to the heating effect of the mountain. In later stages of the simulation, when the flow field is dominated by convection, there is evidence of cold pool formation. Cold pools and secondary triggering of convection within the lake basin are likely to be of some importance for valleys on the Tibetan Plateau.
- vii) Profiles obtained from a variety of different sources are used to model convection for two days in the summer monsoon season of 2012. These profiles

show considerable variation between each other and consequently in the development of clouds and convection. It is found that the directly measured profiles lead to the most realistic convection development, while the reanalysis products have a low and probably insufficient vertical resolution and are not able to resolve inversion layers and changes in vertical stability and moisture contents that have a large impact on the development of convection.

- viii) While the 2-dimensional modelling approach used at Nam Co Lake is demonstrated to capture the most important features of surface-atmosphere interactions as well as convection development and surface fluxes are realistic, there are some limitations to the approach chosen in this work: Due to a reduced dry air entrainment, modelled convection strength is stronger than observed. Additionally, as complex 3-dimensional flow fields cannot be reproduced due to the lack of a third dimension, cloud shading effects are not realistically represented. The modelling setup is also highly idealised and not capable of reproducing weather effects coming from changes in the synoptic forcing.
- ix) While it is not the objective of this thesis to perform a quality analysis of the available profile information, the comparison of convection evolution with profiles from a variety of sources serves to highlight the importance of vertical information of temperature and moisture and demonstrates the considerable uncertainties that are introduced by the lack of reliable and robust profile information. Convection timing, cloud development and precipitation dynamics vary strongly with the profiles and can be related to differences in atmospheric stability and moisture contents, which show variability on the day to day scale. This results in changes to the surface energy balance and thus to differences in the total amount of energy that is exchanged at the surface.
- x) Nam Co Lake and the surrounding grassland are important for the regional water cycle. Under wet surface conditions, evapotranspiration within the basin is high and substantial amounts of precipitation form. While local recycling of water deposited within the basin and on the mountain slopes makes up a significant part of the precipitation, there is also export of water into the region. As Nam Co Lake is situated at the northern edge of the monsoon's influence, this may be of special importance for regional water supply.
- xi) The role of surface moisture on the convection development at Nam Co Lake has not been assessed within this thesis. As surface moistures vary greatly in the Nam Co Lake area, this would be an important next step for future research in this area.

References

- Albertson, J. D., Kustas, W. P., and Scanlon, T. M.: Large-Eddy Simulation Over Heterogeneous Terrain with Remotely Sensed Land Surface Conditions, *Water Resour. Res.*, 37, 1939–1953, doi:10.1029/2000WR900339, 2001.
- Babel, W.: Site-specific modelling of turbulent fluxes on the Tibetan Plateau, PhD thesis, University of Bayreuth, Bayreuth, URL <http://opus.ub.uni-bayreuth.de/opus4-ubbayreuth/frontdoor/index/index/docId/1254>, 155 p., 2013.
- Banta, R. M. and Barker Schaaf, C.: Thunderstorm Genesis Zones in the Colorado Rocky Mountains as Determined by Traceback of Geosynchronous Satellite Images, *Mon. Wea. Rev.*, 115, 463–476, doi:10.1175/1520-0493(1987)115<0463:TGZITC>2.0.CO;2, 1987.
- Bao, X. and Zhang, F.: Evaluation of NCEP–CFRSR, NCEP–NCAR, ERA-Interim, and ERA-40 Reanalysis Datasets against Independent Sounding Observations over the Tibetan Plateau, *J. Climate*, 26, 206–214, doi:10.1175/JCLI-D-12-00056.1, 2013.
- Batchvarova, E. and Gryning, S.-E.: Applied model for the growth of the daytime mixed layer, *Boundary-Layer Meteorol*, 56, 261–274, doi:10.1007/BF00120423, 1991.
- Beniston, M.: Climatic Change in Mountain Regions: A Review of Possible Impacts, *Climatic Change*, 59, 5–31, doi:10.1023/A:1024458411589, 2003.
- Beniston, M., Diaz, H. F., and Bradley, E. F.: Climatic change at high elevation sites: An overview, *Climatic Change*, 36, 233–251, doi:10.1023/A:1005380714349, 1997.
- Biermann, T., Babel, W., Olesch, J., and Foken, T.: Mesoscale Circulations and Energy and Gas Exchange over the Tibetan Plateau - Documentation of the Micrometeorological Experiment, Nam Tso, Tibet - 25th of June - 08th of August 2009, *Arbeitsergebnisse* 41, University of Bayreuth, Bayreuth, URL <http://opus.ub.uni-bayreuth.de/opus4-ubbayreuth/frontdoor/index/index/docId/626>, ISSN 1614-8916, 37 p., 2009.

- Biermann, T., Babel, W., Ma, W., Chen, X., Thiem, E., MA, Y., and Foken, T.: Turbulent flux observations and modelling over a shallow lake and a wet grassland in the Nam Co basin, Tibetan Plateau, *Theor. Appl. Climatol.*, online first, doi:10.1007/s00704-013-0953-6, 2013.
- Boos, W. R. and Kuang, Z.: Dominant control of the South Asian monsoon by orographic insulation versus plateau heating, *Nature*, 463, 218–222, doi:10.1038/nature08707, 2010.
- Boos, W. R. and Kuang, Z.: Sensitivity of the South Asian monsoon to elevated and non-elevated heating, *Sci. Rep.*, 3, 1192, doi:10.1038/srep01192, 2013.
- Camillo, P. J. and Gurney, R. J.: A resistance parameter for bare-soil evaporation models, *Soil Science*, 141, 95–105, 1986.
- Caplan, P., Derber, J., Gemmill, W., Hong, S.-Y., Pan, H.-L., and Parrish, D.: Changes to the 1995 NCEP Operational Medium-Range Forecast Model Analysis-Forecast System, *Wea. Forecasting*, 12, 581–594, doi:10.1175/1520-0434(1997)012<0581:CTTNOM>2.0.CO;2, 1997.
- Charuchittipan, D., Babel, W., Mauder, M., Leps, J.-P., and Foken, T.: Extension of the averaging time of the eddy-covariance measurement and its effect on the energy balance closure, *submitted to Boundary-Layer Meteorol.*, 2013.
- Chen, B., Xu, X.-D., Yang, S., and Zhang, W.: On the origin and destination of atmospheric moisture and air mass over the Tibetan Plateau, *Theor. Appl. Climatol.*, 110, 423–435, doi:10.1007/s00704-012-0641-y, 2012.
- Chen, S.-H. and Lin, Y.-L.: Effects of Moist Froude Number and CAPE on a Conditionally Unstable Flow over a Mesoscale Mountain Ridge, *J. Atmos. Sci.*, 62, 331–350, doi:10.1175/JAS-3380.1, 2005.
- Chen, X., Añel, J. A., Su, Z., de la Torre, L., Kelder, H., van Peet, J., and Ma, Y.: The Deep Atmospheric Boundary Layer and Its Significance to the Stratosphere and Troposphere Exchange over the Tibetan Plateau, *PLoS ONE*, 8, e56909, doi:10.1371/journal.pone.0056909, 2013.
- Cheng, G. and Wu, T.: Responses of permafrost to climate change and their environmental significance, Qinghai-Tibet Plateau, *J. Geophys. Res.*, 112, F02S03, 2007.
- Chou, M.-D., Suarez, M. J., Liang, X.-Z., and Yan, M. M.: A Thermal Infrared Radiation Parameterization for Atmospheric Studies, *Tech. Rep. 19*, Greenbelt, 2001.

- Chu, C.-M. and Lin, Y.-L.: Effects of Orography on the Generation and Propagation of Mesoscale Convective Systems in a Two-Dimensional Conditionally Unstable Flow, *J. Atmos. Sci.*, 57, 3817–3837, doi:10.1175/1520-0469(2001)057<3817:EOOOTG>2.0.CO;2, 2000.
- Cong, Z., Kang, S., Smirnov, A., and Holben, B.: Aerosol optical properties at Nam Co, a remote site in central Tibetan Plateau, *Atmos. Res.*, 92, 42–48, doi:10.1016/j.atmosres.2008.08.005, 2009.
- Courault, D., Drobinski, P., Brunet, Y., Lacarrere, P., and Talbot, C.: Impact of surface heterogeneity on a buoyancy-driven convective boundary layer in light winds, *Boundary-Layer Meteorol.*, 124, 383–403, doi:10.1007/s10546-007-9172-y, 2007.
- Crosman, E. T. and Horel, J. D.: Sea and Lake Breezes: A Review of Numerical Studies, *Boundary-Layer Meteorol.*, 137, 1–29, doi:10.1007/s10546-010-9517-9, 2010.
- Cui, X. and Graf, H.-F.: Recent land cover changes on the Tibetan Plateau: a review, *Climatic Change*, 94, 47–61, doi:10.1007/s10584-009-9556-8, 2009.
- Cui, X., Graf, H.-F., Langmann, B., Chen, W., and Huang, R.: Climate impacts of anthropogenic land use changes on the Tibetan Plateau, *Glob. Plan. Change*, 54, 33–56, doi:10.1016/j.gloplacha.2005.07.006, 2006.
- Deardorff, J. W.: Dependence of Air-Sea Transfer Coefficients on Bulk Stability, *J. Geophys. Res.*, 73, 2549–2557, 1968.
- Dee, D. P., Uppala, S. M., Simmons, A. J., Berrisford, P., Poli, P., Kobayashi, S., Andrae, U., Balmaseda, M. A., Balsamo, G., Bauer, P., Bechtold, P., Beljaars, A. C. M., van de Berg, L., Bidlot, J., Bormann, N., Delsol, C., Dragani, R., Fuentes, M., Geer, A. J., Haimberger, L., Healy, S. B., Hersbach, H., Hólm, E. V., Isaksen, L., Kållberg, P., Köhler, M., Matricardi, M., McNally, A. P., Monge-Sanz, B. M., Morcrette, J.-J., Park, B.-K., Peubey, C., de Rosnay, P., Tavolato, C., Thépaut, J.-N., and Vitart, F.: The ERA-Interim reanalysis: configuration and performance of the data assimilation system, *Q.J.R. Meteorol. Soc.*, 137, 553–597, doi:10.1002/qj.828, 2011.
- Derbyshire, S. H., Beau, I., Bechtold, P., Grandpeix, J.-Y., Piriou, J.-M., Redelsperger, J.-L., and Soares, P. M. M.: Sensitivity of moist convection to environmental humidity, *Q.J.R. Meteorol. Soc.*, 130, 3055–3079, doi:10.1256/qj.03.130, 2004.

- Fairall, C. W., Bradley, E. F., Godfrey, J. S., Wick, G. A., Edson, J. B., and Young, G. S.: Cool-skin and warm-layer effects on sea surface temperature, *J. Geophys. Res.*, 101, 1295–1308, 1996a.
- Fairall, C. W., Bradley, E. F., Rogers, D. P., Edson, J. B., and Young, G. S.: Bulk parameterization of air-sea fluxes for Tropical Ocean-Global Atmosphere Coupled-Ocean Atmosphere Response Experiment, *J. Geophys. Res.*, 101, 3747–3764, 1996b.
- Flohn, H.: Hochgebirge und allgemeine Zirkulation, *Arch. Met. Geoph. Biokl. A.*, 5, 265–279, doi:10.1007/BF02247771, 1952.
- Foken, T.: *Micrometeorology*, Springer, Berlin and Heidelberg, 308 p., 2008a.
- Foken, T.: The Energy Balance Closure Problem: An Overview, *Ecological Applications*, 18, 1351–1367, URL <http://www.jstor.org/stable/40062260>, 2008b.
- Foken, T. and Falke, H.: Technical Note: Calibration device for the krypton hygrometer KH20, *Atmos. Meas. Tech.*, 5, 1861–1867, doi:10.5194/amt-5-1861-2012, 2012.
- Foken, T., Göckede, M., Mauder, M., Mahrt, L., Amiro, B., and Munger, J.: Post field data quality control, in: *Handbook of Micrometeorology: A guide for surface flux measurements and analysis*, edited by Lee, X., Massmann, W., and Law, B., pp. 181–208, Kluwer, Dordrecht, 2004.
- Foken, T., Aubinet, M., Finnigan, J. J., Leclerc, M. Y., Mauder, M., and Paw U, K. T.: Results Of A Panel Discussion About The Energy Balance Closure Correction For Trace Gases, *Bull. Amer. Meteor. Soc.*, 92, ES13–ES18, doi:10.1175/2011BAMS3130.1, 2011.
- Foken, T., Leuning, R., Oncley, S. R., Mauder, M., and Aubinet, M.: Corrections and Data Quality Control, in: *Eddy Covariance*, edited by Aubinet, M., Vesala, T., and Papale, D., Springer Atmospheric Sciences, pp. 85–131, Springer, Dordrecht, doi:10.1007/978-94-007-2351-1_4, 2012.
- Frauenfeld, O. W., Zhang, T., and Serreze, M. C.: Climate change and variability using European Centre for Medium-Range Weather Forecasts reanalysis (ERA-40) temperatures on the Tibetan Plateau, *J. Geophys. Res.*, 110, D02021, doi:10.1029/2004JD005230, 2005.
- Friend, A. D. and Kiang, N. Y.: Land Surface Model Development for the GISS GCM: Effects of Improved Canopy Physiology on Simulated Climate, *J. Clim.*, 18, 2883–2902, doi:10.1175/JCLI3425.1, 2005.

- Friend, A. D., Stevens, A. K., Knox, R. G., and Cannell, M. G. R.: A process-based, terrestrial biosphere model of ecosystem dynamics (Hybrid v3.0), *Ecological Modelling*, 95, 249–287, doi:10.1016/S0304-3800(96)00034-8, 1997.
- Fuchs, K.: Convective boundary layer structures over the Tibetan Plateau, MSc thesis, University of Bayreuth, Bayreuth, 85 p., 2013.
- Fujinami, H., Nomura, S., and Yasunari, T.: Characteristics of Diurnal Variations in Convection and Precipitation over the Southern Tibetan Plateau during Summer, *SOLA*, 1, 49–52, doi:10.2151/sola.2005-14, 2005.
- Gao, Y.-x., Tang, M.-c., Luo, S.-w., Shen, Z.-b., and Li, C.: Some Aspects of Recent Research on the Qinghai-Xizang Plateau Meteorology, *Bull. Amer. Meteor. Soc.*, 62, 31–35, doi:10.1175/1520-0477(1981)062<0031:SAORRO>2.0.CO;2, 1981.
- Gerken, T., Babel, W., Hoffmann, A., Biermann, T., Herzog, M., Friend, A. D., Li, M., Ma, Y., Foken, T., and Graf, H.-F.: Turbulent flux modelling with a simple 2-layer soil model and extrapolated surface temperature applied at Nam Co Lake basin on the Tibetan Plateau, *Hydrol. Earth Syst. Sci.*, 16, 1095–1110, doi:10.5194/hess-16-1095-2012, see Appendix B, 2012.
- Gerken, T., Biermann, T., Babel, W., Herzog, M., Ma, Y., Foken, T., and Graf, H.-F.: A modelling investigation into lake-breeze development and convection triggering in the Nam Co Lake basin, Tibetan Plateau, *Theor. Appl. Climatol.*, online first, doi:10.1007/s00704-013-0987-9, see Appendix C, 2013a.
- Gerken, T., Babel, W., Sun, F., Herzog, M., Ma, Y., Foken, T., and Graf, H.-F.: Uncertainty in atmospheric profiles and its impact on modeled convection development at Nam Co Lake, Tibetan Plateau, *J. Geophys. Res.*, early view, doi:10.1002/2013JD0206471, see Appendix D, 2013b.
- Gerken, T., Fuchs, K., and Babel, W.: Documentation of the Atmospheric Boundary Layer Experiment, Nam Tso, Tibet 08th of July – 08th of August 2012, *Arbeitsergebnisse* 53, University of Bayreuth, Bayreuth, URL <http://opus.lib.uni-bayreuth.de/opus4-ubbayreuth/frontdoor/index/index/docId/1139>, ISSN 1614-8916, 45 p., 2013c.
- Gochis, D. J., Jimenez, A., Watts, C. J., Garatuza-Payan, J., and Shuttleworth, W. J.: Analysis of 2002 and 2003 Warm-Season Precipitation from the North American Monsoon Experiment Event Rain Gauge Network, *Mon. Wea. Rev.*, 132, 2938–2953, doi:10.1175/MWR2838.1, 2004.

- Göckede, M., Rebmann, C., and Foken, T.: A combination of quality assessment tools for eddy covariance measurements with footprint modelling for the characterisation of complex sites, *Agric. Forest Meteorol.*, 127, 175–188, doi:10.1016/j.agrformet.2004.07.012, 2004.
- Göckede, M., Foken, T., Aubinet, M., Aurela, M., Banza, J., Bernhofer, C., Bonafond, J. M., Brunet, Y., Carrara, A., Clement, R., Dellwik, E., Elbers, J., Eugster, W., Fuhrer, J., Granier, A., Grünwald, T., Heinesch, B., Janssens, I. A., Knohl, A., Koeble, R., Laurila, T., Longdoz, B., Manca, G., Marek, M., Markkanen, T., Mateus, J., Matteucci, G., Mauder, M., Migliavacca, M., Minerbi, S., Moncrieff, J., Montagnani, L., Moors, E., Ourcival, J.-M., Papale, D., Pereira, J., Pilegaard, K., Pita, G., Rambal, S., Rebmann, C., Rodrigues, A., Rotenberg, E., Sanz, M. J., Sedlak, P., Seufert, G., Siebicke, L., Soussana, J. F., Valentini, R., Vesala, T., Verbeeck, H., and Yakir, D.: Quality control of CarboEurope flux data – Part 1: Coupling footprint analyses with flux data quality assessment to evaluate sites in forest ecosystems, *Biogeosciences*, 5, 433–450, doi:10.5194/bg-5-433-2008, 2008.
- Graf, H.-F., Herzog, M., Oberhuber, J. M., and Textor, C.: Effect of environmental conditions on volcanic plume rise, *J. Geophys. Res.*, 104, 24 309–24 320, doi:10.1029/1999JD900498, 1999.
- Guo, H., Penner, J., and Herzog, M.: Comparison of the Vertical Velocity Used to Calculate the Cloud Droplet Number Concentration in a Cloud-Resolving and a Global Climate Model, in: Fourteenth ARM Science Team Meeting Proceedings, edited by Carrothers, D., pp. 1–6, Department of Energy, Boston, 2004.
- Haginoya, S., Fujii, H., Kuwagata, T., Xu, J., Ishigooka, Y., Kang, S., and Zhang, Y.: Air-Lake Interaction Features Found in Heat and Water Exchanges over Nam Co on the Tibetan Plateau, *SOLA*, 5, 172–175, doi:10.2151/sola.2009-044, 2009.
- Hansen, J., Russell, G., Rind, D., Stone, P., Lacis, A., Lebedeff, S., Ruedy, R., and Travis, L.: Efficient Three-Dimensional Global Models for Climate Studies: Models I and II, *Mon. Wea. Rev.*, 111, 609–662, doi:10.1175/1520-0493(1983)111<0609:ETDGMF>2.0.CO;2, 1983.
- Herzog, M.: Simulation der Dynamik eines Multikomponentensystems am Beispiel vulkanischer Eruptionswolken, PhD thesis, University of Hamburg, Hamburg, 168 p., 1998.
- Herzog, M., Graf, H.-F., Textor, C., and Oberhuber, J. M.: The effect of phase changes of water on the development of volcanic plumes, *J. Volc. Geotherm. Res.*, 87, 55–74, doi:10.1016/S0377-0273(98)00100-0, 1998.

- Herzog, M., Oberhuber, J. M., and Graf, H.-F.: A Prognostic Turbulence Scheme for the Nonhydrostatic Plume Model ATHAM, *J. Atmos. Sci.*, 60, 2783–2796, doi:10.1175/1520-0469(2003)060<2783:APTSFT>2.0.CO;2, 2003.
- Huang, H.-Y. and Margulis, S. A.: Evaluation of a fully coupled large-eddy simulation-land surface model and its diagnosis of land-atmosphere feedbacks, *Water Resour. Res.*, 46, W06512, doi:10.1029/2009WR008232, 2010.
- Immerzeel, W. W., van Beek, L. P. H., and Bierkens, M. F. P.: Climate Change Will Affect the Asian Water Towers, *Science*, 328, 1382–1385, doi:10.1126/science.1183188, 2010.
- Kalnay, E., Kanamitsu, M., Kistler, R., Collins, W., Deaven, D., Gandin, L., Iredell, M., Saha, S., White, G., Woollen, J., Zhu, Y., Leetmaa, A., Reynolds, R., Chelliah, M., Ebisuzaki, W., Higgins, W., Janowiak, J., Mo, K. C., Ropelewski, C., Wang, J., Jenne, R., and Joseph, D.: The NCEP/NCAR 40-Year Reanalysis Project, *Bull. Amer. Meteor. Soc.*, 77, 437–471, doi:10.1175/1520-0477(1996)077<0437:TNYRPP>2.0.CO;2, 1996.
- Kanamitsu, M., Alpert, J., Campana, K., Caplan, P., Deaven, D., Iredell, M., Katz, B., Pan, H.-L., Sela, J., and White, G.: Recent Changes Implemented into the Global Forecast System at NMC, *Wea. Forecasting*, 6, 425–435, doi:10.1175/1520-0434(1991)006<0425:RCIITG>2.0.CO;2, 1991.
- Kang, S., Xu, Y., You, Q., Flügel, W.-A., Pepin, N., and Yao, T.: Review of climate and cryospheric change in the Tibetan Plateau, *Environ. Res. Lett.*, 5, 015101, doi:10.1088/1748-9326/5/1/015101, 2010.
- Keil, A., Berking, J., Mügler, I., Schütt, B., Schwalb, A., and Steeb, P.: Hydrological and geomorphological basin and catchment characteristics of Lake Nam Co, South-Central Tibet, *Quart. Int.*, 218, 118–130, doi:10.1016/j.quaint.2009.02.022, 2010.
- Khairoutdinov, M. and Randall, D.: High-Resolution Simulation of Shallow-to-Deep Convection Transition over Land, *J. Atmos. Sci.*, 63, 3421–3436, doi:10.1175/JAS3810.1, 2006.
- Kirshbaum, D. J.: Cloud-Resolving Simulations of Deep Convection over a Heated Mountain, *J. Atmos. Sci.*, 68, 361–378, doi:10.1175/2010JAS3642.1, 2011.
- Kuang, Z. and Bretherton, C. S.: A Mass-Flux Scheme View of a High-Resolution Simulation of a Transition from Shallow to Deep Cumulus Convection, *J. Atmos. Sci.*, 63, 1895–1909, doi:10.1175/JAS3723.1, 2006.

- Kurita, N. and Yamada, H.: The Role of Local Moisture Recycling Evaluated Using Stable Isotope Data from over the Middle of the Tibetan Plateau during the Monsoon Season, *J. Hydrometeor.*, 9, 760–775, doi:10.1175/2007JHM945.1, 2008.
- Kurosaki, Y. and Kimura, F.: Relationship between Topography and Daytime Cloud Activity around Tibetan Plateau, *J. Meteorol. Soc. Jap.*, 80, 1339–1355, 2002.
- Kuwagata, T., Numaguti, A., and Endo, N.: Diurnal Variation of Water Vapor over the Central Tibetan Plateau during Summer, *J. Meteorol. Soc. Jap.*, 79, 401–418, doi:10.2151/jmsj.79.401, 2001.
- Langmann, B., Herzog, M., and Graf, H.-F.: Radiative forcing of climate by sulfate aerosols as determined by a regional circulation chemistry transport model, *Atmos. Environ.*, 32, 2757–2768, doi:10.1016/S1352-2310(98)00028-4, 1998.
- Letzel, M. O. and Raasch, S.: Large Eddy Simulation of Thermally Induced Oscillations in the Convective Boundary Layer, *J. Atmos. Sci.*, 60, 2328–2341, doi:10.1175/1520-0469(2003)060<2328:LESOTI>2.0.CO;2, 2003.
- Li, M., Ma, Y., Hu, Z., Ishikawa, H., and Oku, Y.: Snow distribution over the Namco lake area of the Tibetan Plateau, *Hydrol. Earth Syst. Sci.*, 13, 2023–2030, doi:10.5194/hess-13-2023-2009, 2009.
- Liu, J., Kang, S., Gong, T., and Lu, A.: Growth of a high-elevation large inland lake, associated with climate change and permafrost degradation in Tibet, *Hydrol. Earth Syst. Sci.*, 14, 481–489, doi:10.5194/hess-14-481-2010, 2010.
- Liu, S. and Shao, Y.: Soil-layer configuration requirement for large-eddy atmosphere and land surface coupled modeling, *Atmos. Sci. Lett.*, 14, 112–117, doi:10.1002/asl2.426, 2013.
- Liu, W. T., Katsaros, K. B., and Businger, J. A.: Bulk Parameterization of Air-Sea Exchanges of Heat and Water Vapor Including the Molecular Constraints at the Interface, *J. Atmos. Sci.*, 36, 1722–1735, doi:10.1175/1520-0469(1979)036<1722:BPOASE>2.0.CO;2, 1979.
- Ma, L., Zhang, T., Li, Q., Frauenfeld, O. W., and Qin, D.: Evaluation of ERA-40, NCEP-1, and NCEP-2 reanalysis air temperatures with ground-based measurements in China, *J. Geophys. Res.*, 113, D15115, doi:10.1029/2007JD009549, 2008.

- Ma, L., Zhang, T., Frauenfeld, O. W., Ye, B., Yang, D., and Qin, D.: Evaluation of precipitation from the ERA-40, NCEP-1, and NCEP-2 Reanalyses and CMAP-1, CMAP-2, and GPCP-2 with ground-based measurements in China, *J. Geophys. Res.*, 114, D09105, doi:10.1029/2008JD011178, 2009a.
- Ma, Y., Su, Z., Koike, T., Yao, T., Ishikawa, H., Ueno, K., and Menenti, M.: On measuring and remote sensing surface energy partitioning over the Tibetan Plateau—from GAME/Tibet to CAMP/Tibet, *Physics and Chemistry of the Earth*, 28, 63–74, doi:10.1016/S1474-7065(03)00008-1, 2003.
- Ma, Y., Fan, S., Ishikawa, H., Tsukamoto, O., Yao, T., Koike, T., Zuo, H., Hu, Z., and Su, Z.: Diurnal and inter-monthly variation of land surface heat fluxes over the central Tibetan Plateau area, *Theor. Appl. Climatol.*, 80, 259–273, doi:10.1007/s00704-004-0104-1, 2005.
- Ma, Y., Wang, Y., Wu, R., Hu, Z., Yang, K., Li, M., Ma, W., Zhong, L., Sun, F., Chen, X., Zhu, Z., Wang, S., and Ishikawa, H.: Recent advances on the study of atmosphere-land interaction observations on the Tibetan Plateau, *Hydrol. Earth Syst. Sci.*, 13, 1103–1111, doi:10.5194/hess-13-1103-2009, 2009b.
- Mauder, M. and Foken, T.: Documentation and instruction manual of the eddy covariance software package TK2, *Arbeitsergebnisse 26*, University of Bayreuth, Bayreuth, URL <http://opus.lib.uni-bayreuth.de/opus4-ubbayreuth/frontdoor/index/index/docId/639>, ISSN 1614-8916, 45 p., 2004.
- Mauder, M. and Foken, T.: Documentation and Instruction Manual of the Eddy-Covariance Software Package TK3, *Arbeitsergebnisse 46*, University of Bayreuth, Bayreuth, URL <http://opus.lib.uni-bayreuth.de/opus4-ubbayreuth/frontdoor/index/index/docId/681>, ISSN 1614-8916, 60 p., 2011.
- Maussion, F., Scherer, D., Finkelnburg, R., Richters, J., Yang, W., and Yao, T.: WRF simulation of a precipitation event over the Tibetan Plateau, China — an assessment using remote sensing and ground observations, *Hydrol. Earth Syst. Sci.*, 15, 1795–1817, doi:10.5194/hess-15-1795-2011, 2011.
- Mengelkamp, H.-T., Warrach, K., and Raschke, E.: SEWAB - a parameterization of the Surface Energy and Water Balance for atmospheric and hydrologic models, *Adv. Wat. Resour.*, 23, 165–175, doi:10.1016/S0309-1708(99)00020-2, 1999.
- Mesinger, F. and Arakawa, A.: Numerical methods used in atmospheric models, no. 17 in GARP Publications Series, Global Atmospheric Research Program, 64 p., 1976.

- Metzger, S., Ma, Y., Markkanen, T., Göckede, M., Li, M., and Foken, T.: Quality assessment of Tibetan Plateau Eddy Covariance measurements utilizing Footprint modeling, *Advances in Earth Sciences*, 21, 1260–1267, X–XI, 2006.
- Miehe, G., Miehe, S., Bach, K., Nölling, J., Hanspach, J., Reudenbach, C., Kaiser, K., Wesche, K., Mosbrugger, V., Yang, Y., and Ma, Y.: Plant communities of central Tibetan pastures in the Alpine Steppe/*Kobresia pygmaea* ecotone, 75, 711–723, doi:10.1016/j.jaridenv.2011.03.001, 2011.
- Miglietta, M. M. and Rotunno, R.: Numerical Simulations of Conditionally Unstable Flows over a Mountain Ridge, *J. Atmos. Sci.*, 66, 1865–1885, doi:10.1175/2009JAS2902.1, 2009.
- Mlawer, E. J., Taubman, S. J., Brown, P. D., Iacono, M. J., and Clough, S. A.: Radiative transfer for inhomogeneous atmospheres: RRTM, a validated correlated-k model for the longwave, *J. Geophys. Res.*, 102, 16 663–16 682, doi:10.1029/97JD00237, 1997.
- Molnar, P., Boos, W. R., and Battisti, D. S.: Orographic Controls on Climate and Paleoclimate of Asia: Thermal and Mechanical Roles for the Tibetan Plateau, *The Annual Review of Earth and Planetary Sciences*, 38, 77–102, doi:10.1146/annurev-earth-040809-152456, 2010.
- Mügler, I., Gleixner, G., Günther, F., Mäusbacher, R., Daut, G., Schütt, B., Berking, J., Schwalb, A., Schwark, L., Xu, B., Yao, T., Zhu, L., and Yi, C.: A multi-proxy approach to reconstruct hydrological changes and Holocene climate development of Nam Co, Central Tibet, *J. Paleolimnol.*, 43, 625–648, doi:10.1007/s10933-009-9357-0, 2010.
- Ni, J.: Impacts of climate change on Chinese ecosystems: key vulnerable regions and potential thresholds, *Reg. Environ. Change*, 11, 49–64, doi:10.1007/s10113-010-0170-0, 2011.
- Nishikawa, M., Hiyama, T., Tsuboki, K., and Fukushima, Y.: Numerical Simulations of Local Circulation and Cumulus Generation over the Loess Plateau, China, *J. Appl. Meteor. Climatol.*, 48, 849–862, doi:10.1175/2008JAMC2041.1, 2009.
- Oberhuber, J. M., Herzog, M., Graf, H.-F., and Schwanke, K.: Volcanic plume simulation on large scales, *J. Volc. Geothermal. Res.*, 87, 29–53, doi:10.1016/S0377-0273(98)00099-7, 1998.

- OFCM: Federal Meteorological Handbook No.3 Rawinsonde and Pibal Observations, Tech. rep., US Department of Commerce / National Oceanic and Atmospheric Administration, Washington, DC, 1997.
- Patton, E. G., Sullivan, P. P., and Moeng, C.-H.: The Influence of Idealized Heterogeneity on Wet and Dry Planetary Boundary Layers Coupled to the Land Surface, *J. Atmos. Sci.*, 62, 2078–2097, doi:10.1175/JAS3465.1, 2005.
- Petch, J. C.: The predictability of deep convection in cloud-resolving simulations over land, *Q.J.R. Meteorol. Soc.*, 130, 3173–3187, doi:10.1256/qj.03.107, 2004.
- Petch, J. C.: Sensitivity studies of developing convection in a cloud-resolving model, *Q.J.R. Meteorol. Soc.*, 132, 345–358, doi:10.1256/qj.05.71, 2006.
- Qui, J.: China: The third pole, *Nature*, 454, 393–396, 2008.
- Rannik, U., Aubinet, M., Kurbanmuradov, O., Sabelfeld, K. K., Markkanen, T., and Vesala, T.: Footprint Analysis For Measurements Over A Heterogeneous Forest, *Boundary-Layer Meteorol.*, 97, 137–166, doi:10.1023/A:1002702810929, 2000.
- Rebmann, C., Kolle, O., Heinesch, B., Queck, R., Ibrom, A., and Aubinet, M.: Data Acquisition and Flux Calculations, in: *Eddy Covariance*, edited by Aubinet, M., Vesala, T., and Papale, D., Springer Atmospheric Sciences, pp. 59–83, Springer, Dordrecht, doi:10.1007/978-94-007-2351-1_3, 2012.
- Reeves, H. D. and Lin, Y.-L.: The Effects of a Mountain on the Propagation of a Preexisting Convective System for Blocked and Unblocked Flow Regimes, *J. Atmos. Sci.*, 64, 2401–2421, doi:10.1175/JAS3959.1, 2007.
- Sato, T., Yoshikane, T., Satoh, M., Miura, H., and Fujinami, H.: Resolution Dependency of the Diurnal Cycle of Convective Clouds over the Tibetan Plateau in a Mesoscale Model, *J. Meteorol. Soc. Jap.*, 86A, 17–31, doi:10.2151/jmsj.86A.17, 2008.
- Sato, T., Miura, H., and Satoh, M.: Spring diurnal cycle of clouds over Tibetan Plateau: Global cloud-resolving simulations and satellite observations, *Geophys. Res. Lett.*, 34, L18816, doi:10.1029/2007GL030782, 2007.
- Seibert, P., Beyrich, F., Gryning, S.-E., Joffre, S., Rasmussen, A., and Tercier, P.: Review and intercomparison of operational methods for the determination of the mixing height, *Atmos. Environ.*, 34, 1001–1027, doi:10.1016/S1352-2310(99)00349-0, 2000.

- Sellers, P. J., Mintz, Y., Sud, Y. C., and Dalcher, A.: A Simple Biosphere Model (SIB) for Use within General Circulation Models, *J. Atmos. Sci.*, 43, 505–531, doi:10.1175/1520-0469(1986)043<0505:ASBMFU>2.0.CO;2, 1986.
- Sugimoto, S., Ueno, K., and Sha, W.: Transportation of Water Vapor into the Tibetan Plateau in the Case of a Passing Synoptic-Scale Trough, *J. Meteorol. Soc. Jap.*, 86, 935–949, doi:10.2151/jmsj.86.935, 2008.
- Tanaka, K., Ishikawa, H., Hayashi, T., Tamagawa, I., and Ma, Y.: Surface Energy Budget at Amdo on the Tibetan Plateau using GAME/Tibet IOP98 Data, *J. Meteorol. Soc. Jap.*, 79, 505–517, doi:10.2151/jmsj.79.505, 2001.
- Tanaka, K., Tamagawa, I., Ishikawa, H., Ma, Y., and Hu, Z.: Surface energy budget and closure of the eastern Tibetan Plateau during the GAME-Tibet IOP 1998, *J. Hydrometeor.*, 283, 169–183, doi:10.1016/S0022-1694(03)00243-9, 2003.
- Taniguchi, K. and Koike, T.: Seasonal variation of cloud activity and atmospheric profiles over the eastern part of the Tibetan Plateau, *J. Geophys. Res.*, 113, D10104, doi:10.1029/2007JD009321, 2008.
- Tian, L., Masson-Delmotte, V., Stievenard, M., Yao, T., and Jouzel, J.: Tibetan Plateau summer monsoon northward extent revealed by measurements of water stable isotopes, *J. Geophys. Res.*, 106, 28 081–28 088, doi:10.1029/2001JD900186, 2001a.
- Tian, L., Yao, T., Numaguti, A., and Sun, W.: Stable Isotope Variations in Monsoon Precipitation on the Tibetan Plateau, *J. Meteorol. Soc. Jap.*, 79, 959–966, doi:10.2151/jmsj.79.959, 2001b.
- Tian, L., Yao, T., Schuster, P. F., White, J. W. C., Ichianagi, K., Pendall, E., Pu, J., and Yu, W.: Oxygen-18 concentrations in recent precipitation and ice cores on the Tibetan Plateau, *J. Geophys. Res.*, 108(D9), 4293, doi:10.1029/2002JD002173, 2003.
- Tian, L., Yao, T., MacClune, K., White, J. W. C., Schilla, A., Vaughn, B., Vachon, R., and Ichianagi, K.: Stable isotopic variations in west China: A consideration of moisture sources, *J. Geophys. Res.*, 112, D10112, doi:10.1029/2006JD007718, 2007.
- Trentmann, J., Luderer, G., Winterrath, T., Fromm, M. D., Servranckx, R., Textor, C., Herzog, M., Graf, H.-F., and Andreae, M. O.: Modeling of biomass smoke injection into the lower stratosphere by a large forest fire

- (Part I): reference simulation, *Atmos. Chem. Phys.*, 6, 5247–5260, doi:10.5194/acp-6-5247-2006, 2006.
- Twine, T. E., Kustas, W. P., Norman, J. M., Cook, D. R., Houser, P. R., Meyers, T. P., Prueger, J. H., Starks, P. J., and Wesely, M. L.: Correcting eddy-covariance flux underestimates over a grassland, *Agric. Forest Meteorol.*, 103, 279–300, doi:10.1016/S0168-1923(00)00123-4, 2000.
- Ueno, K.: Characteristics of Plateau-Scale Precipitation in Tibet Estimated by Satellite Data during 1993 Monsoon Season, *J. Meteorol. Soc. Jap.*, 76, 533–548, 1998.
- Ueno, K., Takano, S., and Kusaka, H.: Nighttime Precipitation Induced by a Synoptic-scale Convergence in the Central Tibetan Plateau, *J. Meteorol. Soc. Jap.*, 87A, 459–472, doi:10.2151/jmsj.87.459, 2009.
- Uyeda, H., Yamada, H., Horikomi, J., Shirooka, R., Shimizu, S., Liping, L., Ueno, K., Fujii, H., and Koike, T.: Characteristics of Convective Clouds Observed by a Doppler Radar at Naqu on Tibetan Plateau during the GAME-Tibet IOP, *J. Meteorol. Soc. Jap.*, 79, 463–474, doi:10.2151/jmsj.79.463, 2001.
- Wang, A. and Zeng, X.: Evaluation of multireanalysis products with in situ observations over the Tibetan Plateau, *J. Geophys. Res.*, 117, D05102, doi:10.1029/2011JD016553, 2012.
- Wang, J., Zhu, L., Daut, G., Ju, J., Lin, X., Wang, Y., and Zhen, X.: Investigation of bathymetry and water quality of Lake Nam Co, the largest lake on the central Tibetan Plateau, China, *Limnology*, 10, 149–158, doi:10.1007/s10201-009-0266-8, 2009.
- Wu, C.-M., Stevens, B., and Arakawa, A.: What Controls the Transition from Shallow to Deep Convection?, *J. Atmos. Sci.*, 66, 1793–1806, doi:10.1175/2008JAS2945.1, 2009.
- Xu, X., Lu, C., Shi, X., and Gao, S.: World water tower: An atmospheric perspective, *Geophys. Res. Lett.*, 35, L20815, doi:10.1029/2008GL035867, 2008.
- Xue, Y., Zeng, F. J., and Adam Schlosser, C.: SSiB and its sensitivity to soil properties—a case study using HAPEX-Mobilhy data, *Glob. Plan. Change*, 13, 183–194, doi:10.1016/0921-8181(95)00045-3, 1996.
- Yanai, M., Li, C., and Song, Z.: Seasonal Heating of the Tibetan Plateau and Its Effects on the Evolution of the Asian Summer Monsoon, *J. Meteorol. Soc. Jap.*, 70, 319–351, 1992.

- Yang, K., Koike, T., Fujii, H., Tamura, T., Xu, X., Bian, L., and Zhou, M.: The Daytime Evolution of the Atmospheric Boundary Layer and Convection over the Tibetan Plateau: Observations and Simulations, *J. Meteorol. Soc. Jap.*, 82, 1777–1792, doi:10.2151/jmsj.82.1777, 2004.
- Yang, K., Ye, B., Zhou, D., Wu, B., Foken, T., Qin, J., and Zhou, Z.: Response of hydrological cycle to recent climate changes in the Tibetan Plateau, *Climatic Change*, 109, 517–534, doi:10.1007/s10584-011-0099-4, 2011.
- Yao, T., Pu, J., Lu, A., Wang, Y., and Yu, W.: Recent Glacial Retreat and Its Impact on Hydrological Processes on the Tibetan Plateau, China, and Surrounding Regions, *Arctic, Antarctic, and Alpine Research*, 39, 642–650, doi:10.1657/1523-0430(07-510)[YAO]2.0.CO;2, 2007.
- Yao, T., Thompson, L. G., Mosbrugger, V., Zhang, F., Ma, Y., Luo, T., Xu, B., Yang, X., Joswiak, D. R., Wang, W., Joswiak, M. E., Devkota, L. P., Tayal, S., Jilani, R., and Fayziev, R.: Third Pole Environment (TPE), *Environmental Development*, 3, 52–64, doi:10.1016/j.envdev.2012.04.002, 2012.
- Yatagai, A.: Estimation of Precipitable Water and Relative Humidity over the Tibetan Plateau from GMS-5 Water Vapor Channel Data, *J. Meteorol. Soc. Jap.*, 79, 589–598, doi:10.2151/jmsj.79.589, 2001.
- Yin, Z.-Y., Zhang, X., Liu, X., Colella, M., and Chen, X.: An Assessment of the Biases of Satellite Rainfall Estimates over the Tibetan Plateau and Correction Methods Based on Topographic Analysis, *J. Hydrometeor.*, 9, 301–326, doi:10.1175/2007JHM903.1, 2008.
- You, Q., Kang, S., Li, C. L., Li, M. S., and Liu, J. S.: Features of meteorological parameters at Nam Co station, Tibetan Plateau, in: *Annual Report of Nam Co Monitoring and Research Station for Multisphere Interactions*, edited by Nam Co Monitoring and Research Station for Multisphere Interaction, pp. 1–8, Beijing, (in Chinese), 2006.

A. Individual contributions to the joint publications

This cumulative thesis consists of publications listed hereafter. Other authors contributed to these papers as well. Therefore my own contribution to the individual manuscripts is specified in this section.

Appendix B

Gerken, T., Babel, W., Hoffmann, A., Biermann, T., Herzog, M., Friend, A. D., Li, M., Ma, Y., Foken, T., and Graf, H.-F.: *Turbulent flux modelling with a simple 2-layer soil model and extrapolated surface temperature applied at Nam Co Lake basin on the Tibetan Plateau*, Hydrol. Earth Syst. Sci., 16, 1095–1110, doi:10.5194/hess-16-1095-2012, 2012.

This journal article is based on a modified formulation for the surface temperature within the Hybrid model. The resulting turbulent surface fluxes are compared to fluxes calculated with the original Hybrid. The model is driven with atmospheric measurements gathered during the Nam Co Lake 2009 experiment and evaluated against eddy-covariance measurements and fluxes calculated by SEWAB.

- I developed the idea of the manuscript and the modified surface parameterisation within Hybrid, which I also implemented. I was responsible for the experimental design and the analysis of the modelling results. I coordinated individual contributions by the co-authors and wrote the text of the publication and acted as corresponding author.
- Wolfgang Babel conducted the flux modelling with SEWAB for ITP and UBT surfaces, shared the surface parameters for both surfaces and provided the eddy-covariance flux data from UBT together with Tobias Biermann.
- Alex Hoffmann contributed to the development of Hybrid in the form that was used in this work.
- Michael Herzog provided technical advice on the paper.

- Andrew D. Friend is the original author of Hybrid and provided assistance with the Hybrid modelling.
- Li Maoshan and Ma Yaoming provided data from the ITP station and supported the field measurements.
- Thomas Foken and Hans-F. Graf contributed to the manuscript at various stages with advice and fruitful discussions.

Appendix C

Gerken, T., Biermann, T., Babel, W., Herzog, M., Ma, Y., Foken, T., Graf, H.-F.: *A modelling investigation into lake-breeze development and convection triggering in the Nam Co Lake basin, Tibetan Plateau*, Theor. Appl. Climatol., online first, doi:10.1007/s00704-013-0987-9, 2013a

This study is based on a modelling investigation of the interaction between a lake-land breeze at Nam Co Lake and topography in the triggering of convection.

- I was responsible for the original idea of the manuscript, its experimental design and the analysis of modelling results. Additionally, I coordinated individual contributions by the co-authors and wrote the text of the publication and acted as corresponding author.
- Tobias Biermann and Wolfgang Babel were jointly responsible for the gathering and processing of experimental data from the 2009 Nam Co Lake experiment used in this study.
- Michael Herzog provided technical advice for the ATHAM model and the modelling setup.
- Ma Yaoming provided data from the ITP station and supported the field measurements.
- Thomas Foken and Hans-F. Graf contributed to the manuscript at various stages with advice and fruitful discussions.

Appendix D

Gerken, T., Babel, W., Sun, F., Herzog, M., Ma, Y., Foken, T., Graf, H.-F.: *Uncertainty in atmospheric profiles and the impact on modeled convection development at Nam Co Lake, Tibetan Plateau*, J. Geophys. Res., 118, early view, doi:10.1002/2013JD020647, 2013b

This study assesses the differences in modelled convection development at Nam Co Lake, based on atmospheric profiles from different sources.

- I was responsible for the original idea of the manuscript, its experimental design and the analysis of modelling results. Additionally, I coordinated individual contributions by the co-authors and wrote the text of the publication and acted as corresponding author. The field data, such as radiosondes and eddy-covariance measurements, were collected on the Tibetan Plateau during a field experiment Wolfgang Babel and I were jointly responsible for.
- Wolfgang Babel and I were jointly responsible for the field experiment, during which radiosoundings and eddy-covariance fluxes were obtained.
- Sun Fanglin and Ma Yaoming provided data from the ITP station and supported the field measurements.
- Michael Herzog provided technical advice for the ATHAM model and the modelling setup.
- Thomas Foken and Hans-F. Graf contributed to the manuscript at various stages with advice and fruitful discussions.

B. Gerken et al. (2012)

Gerken, T., Babel, W., Hoffmann, A., Biermann, T., Herzog, M., Friend, A. D., Li, M., Ma, Y., Foken, T., and Graf, H.-F.: *Turbulent flux modelling with a simple 2-layer soil model and extrapolated surface temperature applied at Nam Co Lake basin on the Tibetan Plateau*, Hydrol. Earth Syst. Sci., 16, 1095–1110, doi:10.5194/hess-16-1095-2012, 2012.



Turbulent flux modelling with a simple 2-layer soil model and extrapolated surface temperature applied at Nam Co Lake basin on the Tibetan Plateau

T. Gerken^{1,2}, W. Babel², A. Hoffmann¹, T. Biermann², M. Herzog¹, A. D. Friend³, M. Li⁴, Y. Ma⁵, T. Foken^{2,6}, and H.-F. Graf¹

¹Centre for Atmospheric Science, Department of Geography, University of Cambridge, UK

²Department of Micrometeorology, University of Bayreuth, Germany

³Department of Geography, University of Cambridge, UK

⁴Cold and Arid Region Environmental and Engineering Research Institute, Chinese Academy of Sciences, Lanzhou, China

⁵Institute of Tibetan Plateau Research, Chinese Academy of Sciences, Beijing, China

⁶Member of Bayreuth Center of Ecology and Environmental Research (BayCEER), University of Bayreuth, Germany

Correspondence to: T. Gerken (tobias.gerken@uni-bayreuth.de)

Received: 19 October 2011 – Published in Hydrol. Earth Syst. Sci. Discuss.: 21 November 2011

Revised: 8 March 2012 – Accepted: 27 March 2012 – Published: 3 April 2012

Abstract. This paper introduces a surface model with two soil-layers for use in a high-resolution circulation model that has been modified with an extrapolated surface temperature, to be used for the calculation of turbulent fluxes. A quadratic temperature profile based on the layer mean and base temperature is assumed in each layer and extended to the surface. The model is tested at two sites on the Tibetan Plateau near Nam Co Lake during four days during the 2009 Monsoon season. In comparison to a two-layer model without explicit surface temperature estimate, there is a greatly reduced delay in diurnal flux cycles and the modelled surface temperature is much closer to observations. Comparison with a SVAT model and eddy covariance measurements shows an overall reasonable model performance based on RMSD and cross correlation comparisons between the modified and original model. A potential limitation of the model is the need for careful initialisation of the initial soil temperature profile, that requires field measurements. We show that the modified model is capable of reproducing fluxes of similar magnitudes and dynamics when compared to more complex methods chosen as a reference.

1 Introduction

Turbulent fluxes of momentum, latent heat (Q_E) and sensible heat (Q_H) are some of the most important interactions between land surface and atmosphere. These fluxes are responsible for the development or modification of mesoscale circulations and the generation of clouds feed back on surface fluxes through the modification of solar radiation. The effects of vegetation influencing boundary layer structure and moisture are widely acknowledged (i.e. Freedman et al., 2001; van Heerwaarden et al., 2009), while the feedback from short-lived clouds is less understood, but important. Shallow cumulus-surface interactions were shown in an LES (large eddy simulation) study to impact surface temperature and fluxes on very short time scales (Lohou and Patton, 2011). For improved process understanding, it is necessary to use: (1) atmospheric models with sufficiently high resolution ($\mathcal{O}(100\text{ m})$) to resolve boundary layer processes as well as clouds and (2) surface models capable of reproducing the system's surface flux dynamics.

Our research focuses on surface-atmosphere interactions on the Tibetan Plateau (TP) in the Nam Co Lake region. With more than 4700 m a.s.l., a semi-arid climate and with a highly adapted *Kobresia pygmaea* alpine steppe (Miehe et al., 2011), the TP proves to be a difficult environment for surface models (Yang et al., 2003, 2009). Specific problems

include large temporal and spatial variability in soil moisture (Su et al., 2011), large diurnal variations of surface temperature from surface freezing before sunrise to more than 30 °C at noon. Ma et al. (2009) give an overview about the TP surface-atmosphere processes. On the TP, the fraction of diffuse solar radiation is very small, making cloud feedbacks especially important for the surface-atmosphere system. The model studies with a regional model of Cui et al. (2007) imply that some of the precipitation events on the TP are predominantly local and therefore not captured by coarser resolution models.

In this paper we present results of a rather simple flux algorithm based on a modified two-layer soil model that is part of a vegetation dynamics and biosphere model Hybrid (Friend et al., 1997; Friend and Kiang, 2005; Friend, 2010). The original model produces a substantial delay in the diurnal turbulent flux cycle due to the low responsiveness of the model's upper soil layer to changes in atmospheric forcing and fails to capture important dynamics. We therefore introduce an extrapolated surface temperature and show that this new approach is capable of reproducing diurnal flux dynamics for two vegetation covered surfaces near Nam Co Lake. These sites are representative for the basin, but show very different dynamics. In our future studies, the same surface-model version will also be coupled to the spatially and temporally high resolution atmospheric model ATHAM (Active Tracer High-resolution Atmospheric Model, Oberhuber et al., 1998; Herzog et al., 1998) including radiation, cloud microphysics and active tracer transport. As simulations of the high-resolution model will be run for approximately 24 h we tested the surface model in column mode forced with standard atmospheric measurements for the same period of time with initialisation at 00:00 h Beijing Standard Time (BST). We acknowledge that this approach is different from most surface model studies that are run for longer periods, but it is necessary for the planned study of the coupled surface-atmosphere system. Such a surface flux algorithm is generally suitable for high-resolution atmospheric modelling studies of different ecosystems as it does not have built in assumptions about horizontal scales.

It is our objective to test the suitability of a simple two-layer soil model with an improved surface or "skin" temperature estimated from the mean temperature of the uppermost layer that shall subsequently be used for driving an atmospheric circulation model for the Nam Co region on the TP. Therefore, fluxes derived from the surface flux algorithm with and without a specific formulation for "skin" temperature are compared to fluxes measured by eddy-covariance technique and to fluxes derived by a more complex Surface-Vegetation-Atmosphere Transfer (SVAT) Model, with five soil layers.

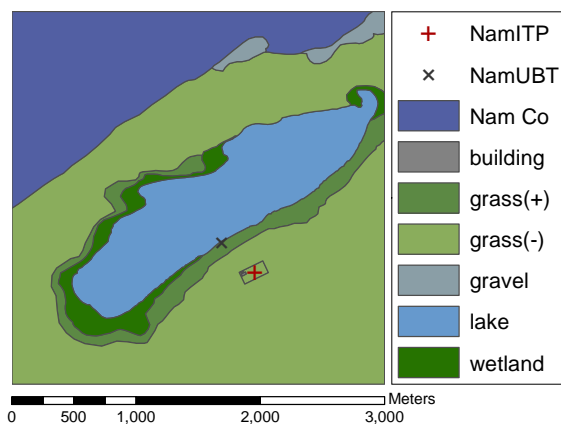


Fig. 1. Landcover map of study area: the black cross indicates the station identified as UBT, close to the small lake with denser surface cover [grass (+)], the red cross shows the station location ITP with sparse surface cover [grass (-)].

2 Site description and model forcing data

From 27 June to 8 August by the University of Bayreuth (UBT) and the Institute of Tibetan Plateau Research, Chinese Academy of Sciences (ITP) conducted a joint field campaign at Nam Co Lake.

2.1 Site description

Nam Co Lake is located on the Tibetan Plateau at approximately 4730 m a.s.l., circa 150 km north of Lhasa. Data from two locations in the vicinity of the lake are used (Fig. 1). Site 1, referred to and operated by UBT, is an eddy-covariance setup on the south shore of a small lake that itself is situated approximately 500 m south of Nam Co lake. UBT has a fairly constant soil moisture below circa 60 cm depth due to the influence of ground water. Additionally, the atmospheric measurements are influenced by a land-lake breeze that originates from Nam Co Lake. Site 2 (operated by and referred to as ITP) is at the Nam Co Station for Multisphere Observation and Research (Li et al., 2009; Cong et al., 2009), approximately 300 m south from both UBT and the direct influence of the small lake with a sandy soil and a very low field capacity ($FC = 5\%$) compared to overall pore volume (39%). The vegetation at both sites is grassland (Metzger et al., 2006) with UBT having a small bare soil fraction (0.1) compared to 0.4 at ITP). Small FC and the generally low volumetric top soil water contents (θ_v) at ITP, lead to large sensible energy fluxes compared to latent heat fluxes ($Q_H \gg Q_E$). After rain events however, θ_v may exceed FC by a factor of up to 3 leading to a similar flux regime at the two stations with $Q_E > Q_H$. Due to the generally drier conditions, reducing soil total heat capacity and the smaller influence of the lake on the temperature cycle at ITP surface temperature

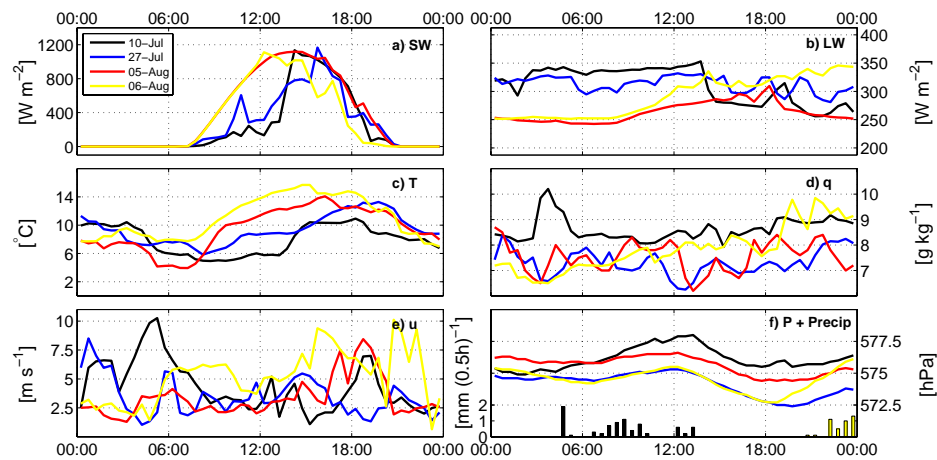


Fig. 2. Forcing data measured at UBT used for model runs: (a) downward shortwave radiation (SW [$W m^{-2}$]); (b) downward longwave radiation (LW [$W m^{-2}$]); (c) air temperature (T [$^{\circ}C$]); (d) water vapour mixing ratio (q [$g kg^{-1}$]); (e) wind speed (U [$m s^{-1}$]); (f) surface pressure (P [hPa]) and precipitation [$mm (0.5h)^{-1}$]). Height c – e is 3 m.

frequently drops below $0^{\circ}C$ in the early morning hours. At UBT there were soil temperature sensors installed at 2.5, 5, 10, 20, 30 and 50 cm depths. At ITP no soil temperatures were available at depths above 20 cm, with data measured at 20, 40, 80 and 160 cm below ground. Comprehensive information of ITP and UBT surface and soil properties, measurement setup and data availability is found in (Biermann et al., 2009) and an overview over the parameters used in the model is presented in Table 1.

2.2 Model forcing data

The data used in the modelling study was selected according to the data quality of turbulence data (Foken et al., 2004) and the wind direction. Finally, we selected four days with high data quality over the whole day encompassing different weather situation. The 24-h model runs are initialised with the soil temperature profile and soil moisture at 00:00 BST ($\sim 22:00$ in local solar time). 10 July was a complex day with rain in the morning and sunshine in the afternoon. 27 July was a cloudy day without rain. 5 August was a radiation day after a period of rain leading to moist conditions and large Q_E at ITP. 6 August was similar to the previous day, but with some of the water drained from the soil at ITP and developing clouds in the afternoon. During 10 July and 5 August, the station close to the lake (UBT) came under the influence of a lake breeze during which the forcing data (except for radiation measurements) correspond rather to the nearby lake than the land surface. Due to the overcast sky on 27 July the lake breeze and thus the influence of the lake surface was severely weakened as described in Zhou et al. (2011), so that there was only limited influence of the lake surface onto the atmospheric measurements.

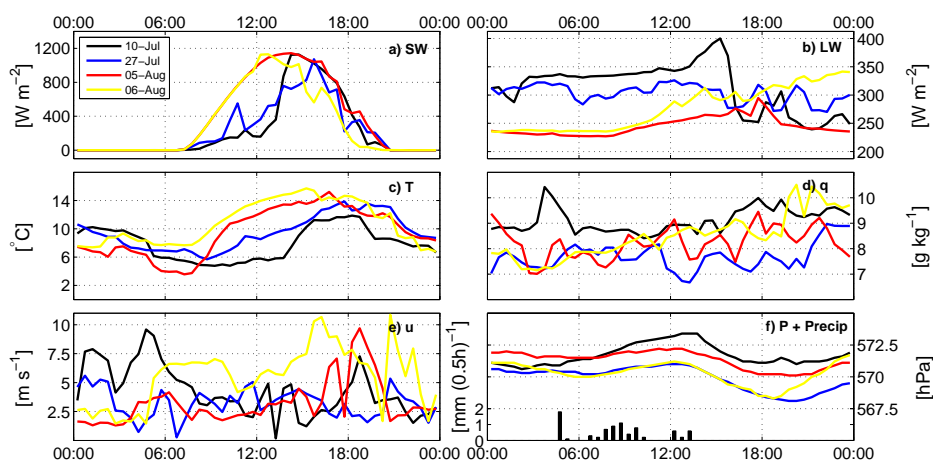
The model is forced with measured atmospheric data from UBT (Fig. 2) and ITP (Fig. 3) providing air temperature, water vapour mixing ratio, wind speed, air pressure, precipitation and downwelling long and shortwave radiation. In general 30-min mean values were linearly interpolated to the surface model time step that was the same as a typical time step of an atmospheric model ($\Delta t = 2.5$ s). The only selected day with precipitation during day-time was 10 July 2009. However, there was also rain recorded at UBT from about 22:00 BST on 6 August 2009, while no precipitation data was available at ITP. Half hourly precipitation was scaled down to the model time step assuming a constant precipitation rate per 30-min interval. There was little difference between the data measured at ITP and UBT, as expected due to the proximity of the sites. However there was an offset of approx. 5 hPa between the recorded pressures, that was not corrected for as this is likely within the uncertainty of the sensors and the model should not be too sensitive to such a pressure difference. Unlike UBT where rain 30-min precipitation was available, there were only daily sums recorded for ITP, which had to be downscaled to 30-min values by scaling them linearly with UBT observations.

3 Modelling approach

The surface model Hybrid (Friend et al., 1997; Friend and Kiang, 2005) is currently coupled to the high-resolution Active Tracer High-resolution Atmospheric Model (ATHAM) by Oberhuber et al. (1998) and Herzog et al. (1998) for the investigation of feedbacks between atmospheric processes and surface fluxes.

Table 1. Description of the two sites (UBT and ITP) near Nam Co lake and the parameters used the model setup (Biermann et al., 2009).

Parameter	UBT	ITP
Coordinates	30°46.50' N 90°57.61' E	30°46.44' N 90°57.72' E
Soil	sandy-loamy	sandy
Porosity	0.63	0.393
Field capacity [$\text{m}^3 \text{m}^{-3}$]	0.184	0.05
Wilting point [$\text{m}^3 \text{m}^{-3}$]	0.115	0.02
Heat capacity of dry soil ($c_{p,d}$) [$\text{Jm}^{-3} \text{K}^{-1}$]	2.5×10^6	2.2×10^6
Thermal conductivity [$\text{Wm}^{-1} \text{K}^{-1}$]	0.53	0.20
Surface albedo (α)	0.20	0.20
Surface emissivity (ϵ)	0.97	0.97
Vegetated fraction	0.9	0.6
LAI [$\text{m}^2 \text{m}^{-2}$] (estim. from: Hu et al., 2009)	0.9	0.6
Vegetation height [m]	0.07	0.15

**Fig. 3.** Same as Fig. 2, but with forcing data measured at ITP. Precipitation at ITP was measured daily and for the purpose of this study distributed to 30 minute intervals according to the recorded rain fall at UBT.

Our high-resolution modelling approach aims at a spatial and temporal resolution in the order of 500 m and 2.5 s, respectively. As our focus is on diurnal surface-atmosphere interactions, the surface model must capture the magnitude of the fluxes and must be able to react quickly to changes in atmospheric forcing. Therefore, a surface model that is capable of reproducing realistic turbulent energy and water vapour fluxes at a sufficiently high temporal resolution and at reasonable computational costs is needed. We decided against a model with more than two soil-layers due to higher computational cost and instead modified the original Hybrid model to meet these requirements.

3.1 The surface model

The modified version of Hybrid which is a process based terrestrial ecosystem and surface model, incorporates a simple two-layer representation of the soil and uses the turbulent transfer parameterisations taken from the GISS model II (Hansen et al., 1983). The transfer equations in Hybrid are described in Friend and Kiang (2005). Bare soil parameterisation follows the approach of SSiB (Xue et al., 1996) that is based on Camillo and Gurney (1986) and Sellers et al. (1986). Turbulent fluxes are calculated using a bulk approach for the sensible heat flux:

$$Q_H = c_p \rho C_H u(z) (T_0 - T(z)) \quad (1)$$

with air specific heat capacity (c_p [$\text{Jkg}^{-1} \text{K}^{-1}$]), the Stanton number (C_H) which is calculated as a function of roughness

length (z_0) and Bulk Richardson Number, air density (ρ [kg m^{-3}]), measured wind speed ($u(z)$ [ms^{-1}]), air temperature ($T(z)$) at measurement height (z [m]) and surface temperature (T_0). All temperatures used are in K. The latent heat flux is derived in a more complex manner from bulk soil evaporation (EV) and a canopy resistance approach estimating plant transpiration (TR), with $Q_E = \text{EV} + \text{TR}$:

$$\text{EV} = \left(\rho \frac{f_h q_s - q_a}{r_s + r_a} \right) \times \exp(-0.7\text{LAI}) \quad (2)$$

$$\text{TR} = \frac{\rho \Delta q_a}{r_c + r_a}, \quad (3)$$

with the relative humidity of soil air (f_h), saturation water mixing ratio at surface temperature (q_s), atmospheric water vapour mixing ratio (q_a), soil and aerodynamic resistance (r_s , r_a), leaf area index (LAI) and canopy resistance (r_c) calculated by the vegetation model component. Transfer coefficients are modified from Deardorff (1968). Plant physiology and stomatal conductance are included via generalised plant types (GPT). As an ecosystem model Hybrid is designed to work on hourly to climate scales (Friend, 2010) and should therefore be capable of reproducing diurnal flux cycles as well as ecosystem changes on climate scales. It was originally developed as a biosphere-surface component for the GISS GCM. A “thin” upper layer of 10 cm thickness follows the daily cycle of surface temperatures, whereas a lower layer with 4 m thickness acts as the memory for the annual cycle in both model versions. However, an upper layer of such thickness imposes a substantial dampening on the diurnal temperature cycle and will effectively act as a low-pass filter for events of short durations such as cloud shading that, especially under the conditions found at the TP, has a substantial immediate impact on surface temperatures and on fluxes as well. This can be seen in Fig. 12 of Hansen et al. (1983), where a time delay of approximately 2 h is visible for surface temperature in the diurnal cycle. A similar behaviour of the original Hybrid is discussed in Sect. 5.4. Shortcomings with the representation of diurnal cycles may also impact on longer term studies as the model drifts away from a realistic state. As we plan to apply the coupled model for high-resolution simulations with a time step in the order of seconds, we focus in this work on the accuracy of the diurnal flux cycles that can be achieved with such a model.

3.2 The modified soil model in Hybrid

In order to improve the delay in diurnal flux evolution and the weak responsiveness of sudden short-term changes in atmospheric forcing, new simulation approaches for surface temperature and heat diffusion were introduced in Hybrid.

3.2.1 Diagnostic surface temperature

An extrapolated surface temperature (T_0) is being introduced that is then subsequently used for the calculation of atmo-

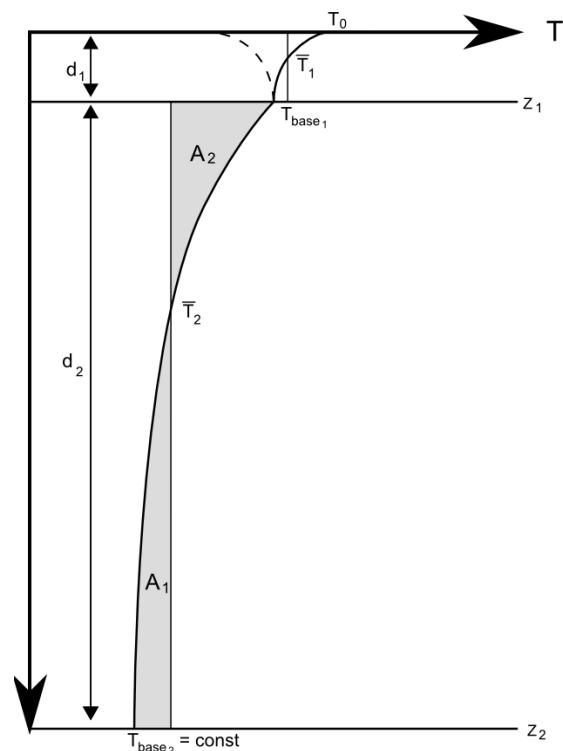


Fig. 4. Conceptual drawing of the assumed quadratic subgrid soil temperature profile and the associated parameters. In order to derive T_1 and T_2 geometrically the areas A_1 and A_2 must be equal.

spheric stability through the Bulk Richardson number as well as for Q_H and Q_E . This approach is somewhat similar to the “force-restore method” (Blackadar, 1979) that also aims at providing a realistic surface temperature imitating the behaviour of real soils. However, while “force-restore” uses an oscillating heat source as forcing term and a heat flux into the ground as restoring term (Yee, 1988), our method is not dependent on a periodic heating function and uses the concept of layer heat storage. T_0 is derived from a set of assumptions that were already included in Hybrid going back to Hansen et al. (1983). For both layers denoted with the subscripts 1 and 2 from the model top, we assume a quadratic temperature profile ($T(z)$) (Fig. 4):

$$T_{1,2}(z_{\text{rel}}) = a_{1,2} (z_{\text{rel}} - d_{1,2})^2 + T_{\text{base}_{1,2}} \quad (4)$$

with a constant (a [K m^{-2}]), the depth below the top of the layer (z_{rel} [m]), the layer thickness (d [m]) and the temperature at the lower boundary of the respective layer (T_{base}). There is assumed to be no transfer of heat through the lower model boundary i.e. T_{base_2} is constant and equal to the annual mean temperature of 0°C (You et al., 2006, recited from Keil et al., 2010). We are aware of this being a simplification.

However, the annual temperature cycle at 4 m is expected to be small and the rate of change as well as the diurnal temperature cycle is too small to have an impact on the day scale. For future research the seasonal mean temperature could be used in order to remove this potential source of error. The relationship between layer heat content E [J] and temperature profile is given by:

$$E = c_{p_s} \int_{z_L}^{z_U} T(z) dz \quad (5)$$

where z_L and z_U are the lower and upper boundaries of the layer and c_{p_s} [$\text{J m}^{-3} \text{K}^{-1}$] is the total soil heat capacity. Hence, with a known heat content for each layer it is possible to solve for

$$a_2 = \frac{\frac{E_2}{c_{p_s,2}} - d_2 T_{\text{base}_2}}{\frac{d_2^3}{3}}, \quad (6)$$

by integrating Eq. (5) with Eq. (4) from $z_L = 0$ to $z_U = d_2$ and solving for a_2 . The base temperature of the first layer is related to T_{base_2} through

$$T_{\text{base}_1} = T_{\text{base}_2} + a_2 d_2^2. \quad (7)$$

In a similar fashion a_1 and T_0 can be approximated:

$$a_1 = \frac{\frac{E_1}{c_{p_s,1}} - d_1 T_{\text{base}_1}}{\frac{-z_1^3}{3}} \quad (8)$$

and

$$T_0 = T_{\text{base}_1} + a_1 d_1^2. \quad (9)$$

As T_{base_1} is a parameter of both Eqs. (7) and (9) and $a_{1,2}$ are of crucial importance to the initialisation of $E_{1,2}$, special care has to be taken, when assigning initial conditions (see discussion in Sect. 3.3).

3.2.2 Heat diffusion estimation

The soil heat flux is derived from the residual of the surface energy balance. In the original heat diffusion algorithm of Hybrid (Hansen et al., 1983), the heat flux from the first to the second soil layer $F(z)$ is dependent on the difference between mean surface layer temperatures (\bar{T}), the soil heat flux calculated as residual of turbulent and radiation fluxes ($F(0)$), layer thickness and thermal resistances r ,

$$F(z) = \frac{3\bar{T}_1 - 3\bar{T}_2 - 0.5F(0)r_1}{r_1 + r_2} \times \Delta t, \quad (10)$$

where Δt is model time-step. This leads to unrealistic modelled heat fluxes $F(z)$ as $F(z)$ is largely dominated by $F(0)$, which is positive during nighttime and negative during daytime, thus leading to a net transfer of heat from a cold to

a warm layer. With the assumption of a subgrid temperature profile the heat flux between the two layers Eq. (10) was modified with a heat diffusion approach and integration of

$$\frac{\partial T}{\partial t} = D \frac{\partial^2 T}{\partial z^2} \approx D \Delta t \frac{T(z_1 + \Delta z) - 2T(z_1) + T(z_1 - \Delta z)}{2\Delta z} \quad (11)$$

with D being a soil moisture dependent diffusion constant for heat. We assume ∂_z to be approximated by the diffusion length $L = 2\sqrt{\Delta t D} = \Delta z$ and the temperatures are taken from the assumed profile. As the model is run with the short time-step of the atmospheric model, such a formulation becomes valid. A rough calculation for L with $D = 10^{-6} \text{ m}^2 \text{ s}^{-1}$, which is close to the determined value, and $\Delta t = 30 \text{ min}$ gives $L = 0.08 \text{ m}$, which is close to d_1 , posing an upper limit on Δt for this method.

3.3 Surface temperature profile initialisation

Due to the quadratic nature of the soil layer temperature profiles and their potential kink at the layer interface (see Fig. 4), the modified model depends on careful initialisation that fulfills two requirements: (1) a realistic estimate of surface temperature and (2) an appropriate estimate of ground heat storage (E) allowing the upper layer to react in a realistic way. In this study soil temperature measurements at several depths were used in order to accomplish both requirements. Surface temperature was estimated from upwelling longwave radiation according to the Stefan-Boltzmann law with a longwave emissivity of $\epsilon = 0.97$. We initialised E_2 by setting T_{base_1} to the measured 10 cm temperature and then subsequently fitted the temperature curve for the first model layer by minimising the squared mean error with regard to measured soil temperatures. Due to the lacking 10 cm temperature at ITP, this temperature had to be estimated from the 20 cm measurement and T_0 was approximated in order to estimate the initial E_1 . It should be noted that the assumed quadratic temperature profile in the lower soil layer clearly underestimated the vertical temperature gradient in the soil as estimated UBT temperatures at 50 cm were always higher than measured temperatures. This difference is reduced from July to August as the summer warming reaches lower layers. This is a limitation due to fixed layer depths.

Table 2 shows the initial temperatures for each day. From the span of layer temperatures \bar{T}_1 and \bar{T}_2 , the theoretical parameter space of T_0 for a constant T_{base_2} (Fig. 5) can be derived. While Fig. 5a and b show the individual dependence of temperature variables on each other as expressed in the respective Eqs. (7) and (9), Fig. 5c shows the combined effect of parameter variation. A random combination of the initial temperatures given in Table 2 would yield T_0 in the range of -10 to 30°C . In contrast, the actual model layer temperatures, indicated by the crosses in Fig. 5c, occupy a much smaller area and are, with the exception of one day, clustered closely. This highlights the importance of a careful initialisation of the soil temperature profile requiring knowledge

Table 2. Initial soil temperatures used in this study (\bar{T}_2 and \bar{T}_1 are estimated from the respective base and top temperatures of the layer according to a quadratic temperature profile), change of layer 1 mean temperature ($\Delta\bar{T}_1$) over the modified Hybrid run, soil moisture content of layer 1 at beginning of the modified model run ($\theta_{1,obs}$) and at the end of the simulation ($\theta_{1,end}$). The values in parenthesis are expressed as θ_1/FC [-].

Site	Date	\bar{T}_2 [°C]	$T_{1,base}$ [°C]	\bar{T}_1 [°C]	T_0 [°C]	$\Delta\bar{T}_1$ [°C]	$\theta_{1,obs}$ [%]	$\theta_{1,end}$ [%]
UBT	10 July	3.9	11.8	10.9	9.3	-1.6	26.9 (1.47)	41.1(2.24)
	27 July	4.5	13.4	12.5	10.6	-1.6	20.8 (1.14)	17.0 (0.92)
	5 August	4.8	14.4	13.4	11.2	-3.0	26.9 (1.47)	19.1 (1.04)
	6 August	4.75	14.3	12.8	9.8	-1.4	25.4 (1.39)	34.0 (1.85)
ITP	10 July	5.4	16.2	13.2	7.2	-1.2	6.0 (1.1)	25.1 (5.02)
	27 July	7.2	21.6	17.8	10.2	-1.7	3.0 (0.6)	1.6 (0.32)
	5 August	5.7	17.1	11.1	-0.8	0.2	11.0 (2.2)	4.3 (0.86)
	6 August	5.6	16.8	11.6	1.1	1.9	9.0 (1.8)	3.7 (0.73)

about subsurface temperatures that are difficult to estimate without field measurements.

4 Flux comparison

Surface fluxes derived with any method contain inaccuracies such as measurement errors or theoretical limitations. Therefore we are not comparing our modelling results to the absolute truth, but to two flux references.

4.1 EC and SEWAB reference fluxes

Fluxes estimated by both versions of Hybrid are compared with observed fluxes derived by eddy covariance (EC) method and fluxes modelled by the SVAT model SEWAB (Surface Energy and Water Balance model – Mengelkamp et al., 1999), which has been configured for the two sites for gap-filling and up-scaling of flux measurements. Both flux references yield fluxes averaged over 30-min intervals. Unlike many SVAT models that derive the soil heat flux from the flux residual, SEWAB is solving the surface energy balance equation ($Q_E + Q_H + Q_{Rad} + Q_{Soil} = 0$) iteratively for T_0 by Brent's method (Mengelkamp et al., 1999), hence closing the energy balance locally (Kracher et al., 2009). In contrast, the surface energy balance closure derived by EC is only in the order of 0.7 at Nam Co Lake (Zhou et al., 2011). Consequently, 30% of the net radiation is not captured by surface flux measurements. However, energy balance closure must not be used as a quality measure for flux measurements (Aubinet et al., 1999) as surface heterogeneity leads to organised low frequency structures and mesoscale circulations (Panin et al., 1998; Kanda et al., 2004) that are mainly responsible for the lack of closure (Foken, 2008). The energy balance problem for eddy-covariance measurements is summarized in Foken et al. (2011). Additionally, in sea (lake) breeze systems a significant portion of the energy fluxes is transported horizontally (Kuwagata et al., 1994). Therefore,

SEWAB (and Hybrid) fluxes are comparatively larger than the measured ones. When the energy balance is closed artificially by redistributing the residual to fluxes according to the Bowen ratio (Twine et al., 2000), the resulting fluxes are in much better agreement with SEWAB (not shown). Therefore energy balance corrected fluxes are used whenever possible ($Q_{EC,EBC}$ and $Q_{HEC,EBC}$). Artificial energy balance closure is only possible, when the Bowen ratio can be determined from flux measurements and when data about the available energy is measured. EC data were collected at 3 m height and calculated using the TK3 package (Mauder et al., 2008; Mauder and Foken, 2011). Quality checks were performed according to Foken et al. (2004). A detailed description of the instrumentation can be found in Biermann et al. (2009). The rain event of 10 July leads to the exclusion of fluxes due to quality concerns. Both Hybrid and SEWAB produce fluxes during rain, but their quality is unknown as they cannot be compared to measurements.

Measuring in close proximity to the lake also means that depending on wind direction the fluxes measured at UBT are originating from land, water or a mixture of both as the footprint of the EC system and thus also of the forcing data is located upwind of the site. This leads to problems in the energy balance closure and the integration of fluxes. The development of a lake breeze system at Nam Co means that during most days there are no flux measurements available from the late morning or early afternoon until the lake breeze ceases. The days of 27 July and 6 August are the only days during which the field campaign provides data that do not have a full lake breeze influence at UBT. Therefore it is beneficial to compare not only to measured fluxes, but also to SEWAB ($Q_{E,SEWAB}$ and $Q_{H,SEWAB}$).

For completeness, fluxes over the lake calculated by the TOGA-COARE algorithm (Fairall et al., 1996a,b) that is also part of the coupled surface-atmosphere model are given during lake breeze events.

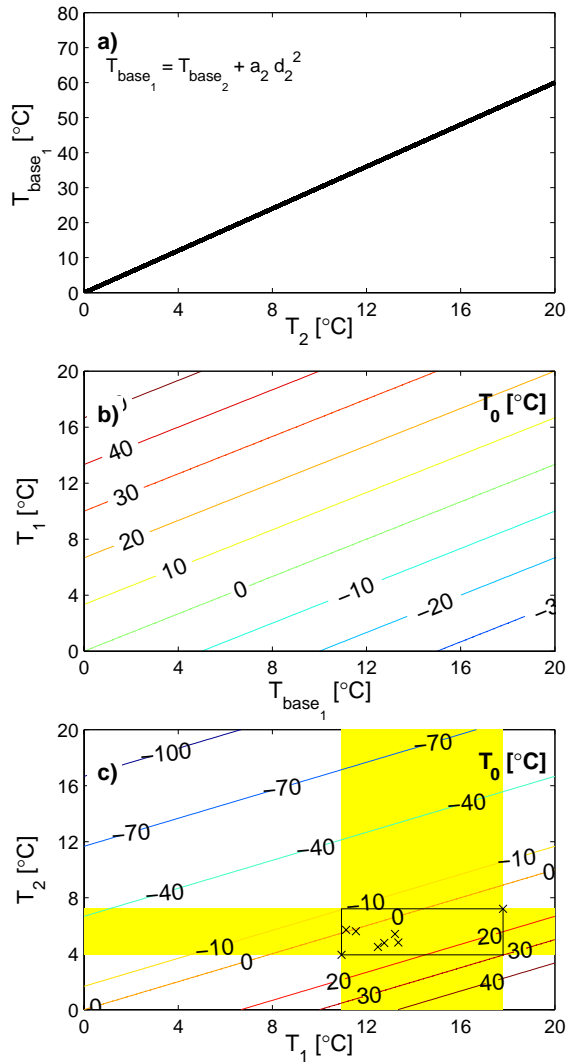


Fig. 5. Dependency of soil temperature parameters: (a) relationship between mean temperature of layer 2 (\bar{T}_2) and bottom temperature of layer 1 [T_{base_1} , Eq. (7)] – a_2 is calculated according to Eq. (6); (b) surface temperature (T_0) contour plot as function of T_{base_1} and layer 1 mean temperature (\bar{T}_1) and (c) contours of (T_0) as function of \bar{T}_2 and \bar{T}_1 . The black rectangle at the intersection of the layer temperature ranges (yellow) indicates the theoretical parameter space given by the temperature values used in this study and the black crosses mark the actual configurations.

4.2 Statistical evaluation measures

Model quality was assessed by Root Mean Square Deviation (RMSD)

$$\text{RMSD} = \sqrt{\frac{1}{N} \sum_{i=1}^N (P_p - P_r)_i^2} \quad (12)$$

and Cross Correlation according to the coefficient of determination (R^2):

$$R^2(j) = \left(\frac{\text{cov}(P_p(1+j:N), P_r(1:N-j))}{\sigma_{P_p(1+j:N)} \sigma_{P_r(1:N-j)}} \right)^2 \quad (13)$$

with $R^2(j)$ being the coefficients of determination for the predicted (P_p) and reference (P_r) flux time series shifted by j elements, the total number of elements in each time series (N) and σ as their respective standard deviations. Both SEWAB and EC measurements produce 30-min flux averages, whereas Hybrid was set to 10-min averaged fluxes. Therefore the reference fluxes were linearly interpolated to Hybrid's output times before statistical evaluation. Periods when no energy balance corrected EC measurements were available (see Figs. 6 and 7 for details) were excluded from the calculation of the statistical measures.

5 Results and discussion

The following section presents and discusses the improvements that are achieved for a simple two-layer model when a new algorithm for the surface temperature was implemented.

The original two-layer model Hybrid fails to reproduce the diurnal dynamics observed at UBT (Figs. 6 and 7) due to the thermal inertia of the top-layer. The delayed response in surface temperature leads to a shift in the resulting turbulent surface fluxes. This causes an underestimation of Q_E and Q_H until $\sim 18:00$ BST and later to an overestimation due to delayed surface cooling. The improvement of the modified Hybrid over the original formulation is discussed in more detail in Sects. 5.1 and 5.4.

The latent (Fig. 6 – left column) and sensible heat fluxes (right column) estimated with the modified Hybrid model are generally in good agreement with the reference fluxes derived by EC and SEWAB. The diagnostic surface temperature (right column) also shows a close agreement. In some instances there remains a small shift in fluxes compared to the reference values, but this has been greatly improved compared to the original Hybrid. The surface temperatures are also in good agreement after sunrise, despite the fact that during the clear sky days in August excessive night-time surface cooling is simulated. This is less of an issue during the overcast nights.

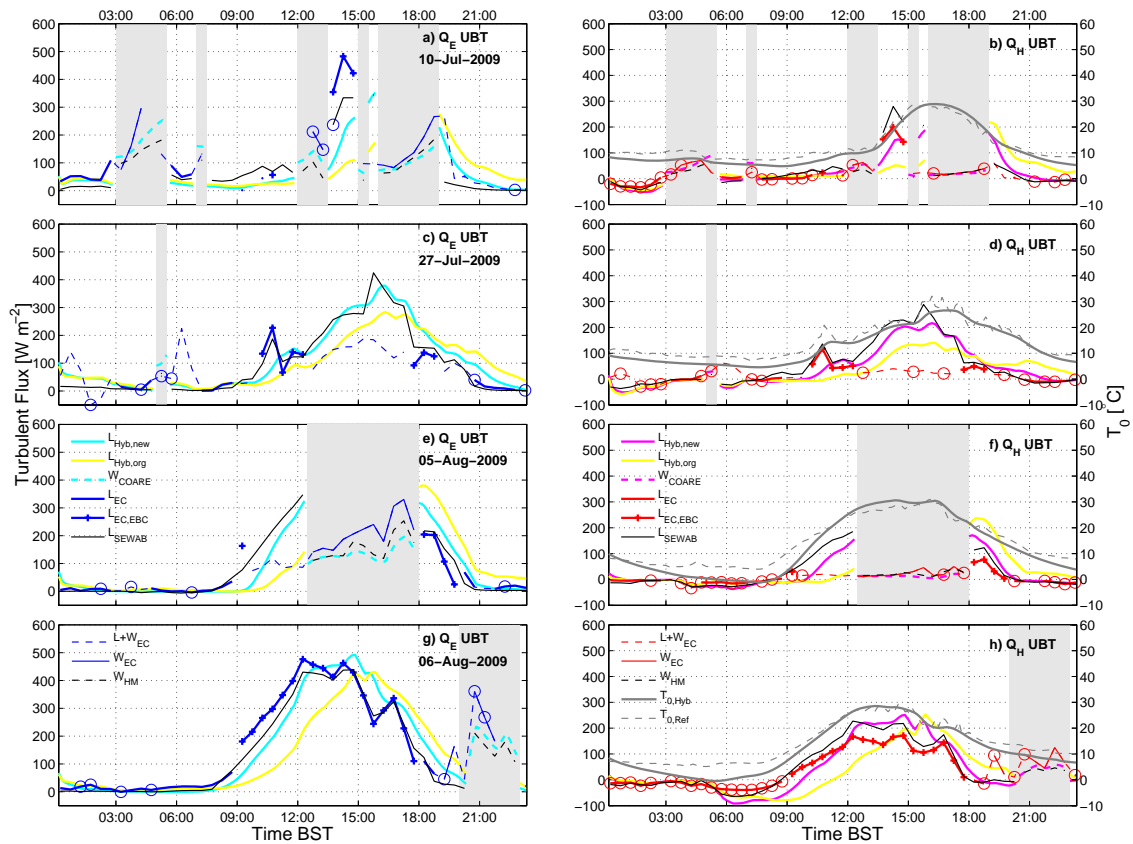


Fig. 6. Model results for the modified Hybrid at UBT for 10 July 2009 (a–b), 27 July 2009 (c–d), 5 August 2009 (e–f) and 6 August 2009 (g–h). Left column: latent heat flux (Q_E); right column: sensible heat flux (Q_H) and surface temperature T_0 [$^{\circ}\text{C}$]. L and W refer to “land” and “water” as origin of the fluxes. $L+W$ is the complete available time series. The subscripts *Hyb,mod* and *Hyb,org* refer to fluxes from the modified and original Hybrid and *COARE* are fluxes from the lake derived by TOGA-COARE whereas *SEWAB* is a SVAT model and *HM* refers to a hydrodynamic multi-layer lake model after Foken (1984) and Panin et al. (2006). *EC* and *EC,EBC* refer to measurements by eddy covariance method where in the latter the energy balance has been closed by distributing the residual according to Bowen-ratio (this requires good data quality and fluxes and can only be done for fluxes that are attributed to land). The circles indicate poor data quality of the EC system according to Foken et al. (2004). Gray shading indicates times where the flux footprint of UBT was over the lake.

The situation at ITP is quite similar to UBT. The modified model agrees well with the EC and SEWAB reference data. On 5 August the turbulent flux dynamics, but not the magnitude of the fluxes, match the EC measurements closely (Fig. 7), while the original Hybrid showed a strong delay in the flux response as the soil remained frozen during the morning. While the magnitude of the latent heat flux is close to EC measurements, Q_H produced by Hybrid are of a similar magnitude as Q_H from SEWAB. These are considerably larger than the fluxes measured by EC and corrected for energy balance closure. For 6 August the modelled maximum of Q_E is larger than the maximum $Q_{EC,EBC}$ and much greater throughout most of the day compared to SEWAB. Q_H in contrast shows similar diurnal dynamics as $Q_{HEC,EBC}$, but with its

magnitude between the sensible heat flux derived by SEWAB and $Q_{HEC,EBC}$. Around 18:00 h the Q_H -fluxes from the different methods become more similar. A large negative Q_H -flux in the morning hours is apparent but greatly improved compared to the unmodified Hybrid version. Figure 6a and b also highlights some limitations of ecosystem research as a large portion of the data had to be rejected due to limitations described in Sect. 4.1.

During lake breeze events the surface fluxes over water derived from TOGA-COARE are displayed. Sensible heat fluxes are in close agreement with EC data and fluxes derived by a hydrodynamic multi-layer lake model (Foken, 1984; Panin et al., 2006). Latent heat fluxes show a similar behaviour and are of similar magnitude on 10 July

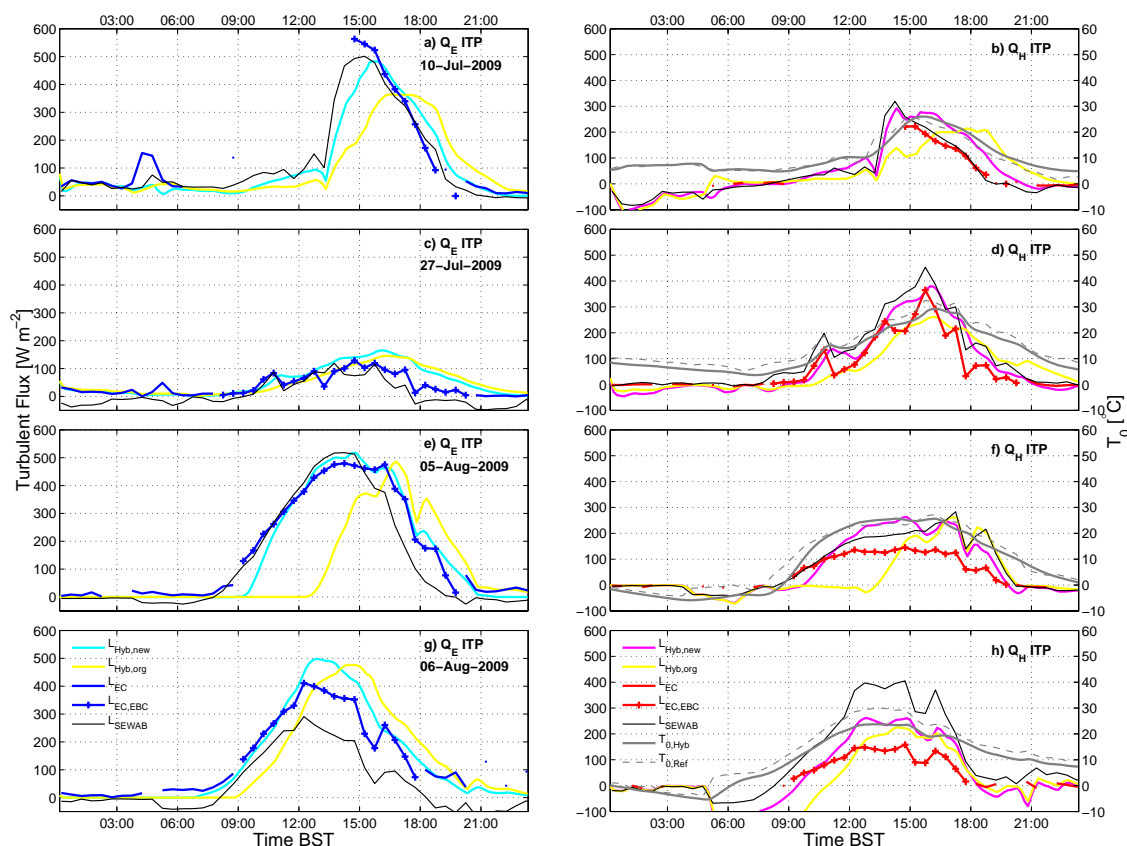


Fig. 7. Same as Fig. 6, but for ITP. There are no contributions from the lake.

and 6 August. On 5 August there is at least a qualitative agreement between COARE and EC measurements.

5.1 Discussion of turbulent fluxes

The original two layer model reacts only slowly to the atmospheric forcing, delaying the fluxes' response. Such a time lag leads to a shift in the diurnal cycle and is problematic for the coupling to atmospheric models since surface fluxes are one of the main drivers of regional and local circulation as well as cloud development. These will certainly be affected by erroneous surface flux dynamics. In our specific case, the dampening of the diurnal temperature cycle and the delay in surface fluxes may reduce the intensity of the land-lake breeze or may delay its development through a reduction of differential heating between land and lake surface. However, there is still a minor delay visible in the modified Hybrid as the surface temperature is purely diagnostic and dependent on \bar{T}_1 . This is discussed in more detail in Sect. 5.4.

Table 3 shows the results of the RMSD between the modelled results and the reference quantities. With the modified

Hybrid model there is a 40–60 % improvement in the RMSDs compared to the original Hybrid, when both are compared against SEWAB. The only notable exception for this is 6 August at ITP, where a strong deviation of turbulent fluxes derived by SEWAB and measured fluxes was encountered. This is due to an underestimation of soil water content by SEWAB as 6 August falls into a dry interval between rainy periods, where SEWAB underestimates the soil water content. The picture is more diverse for the comparison between the energy balance corrected EC fluxes and Hybrid. There is a reduction in the error for all cases, except Q_H on 6 August at ITP, but the reductions cover a much larger range from less than 1 to 80 %. Due to data quality concerns the number of comparable elements is much lower (N given in Table 3) and probably too small for meaningful statistics in case of UBT. This is especially true as the daytime lake breeze influence coincides with the times with periods of usually higher quality of EC fluxes. As flux qualities are usually lower during conditions with limited vertical exchange (stable stratification), EC fluxes at ITP mainly reflect the daytime model performance whereas the comparison with SEWAB also takes

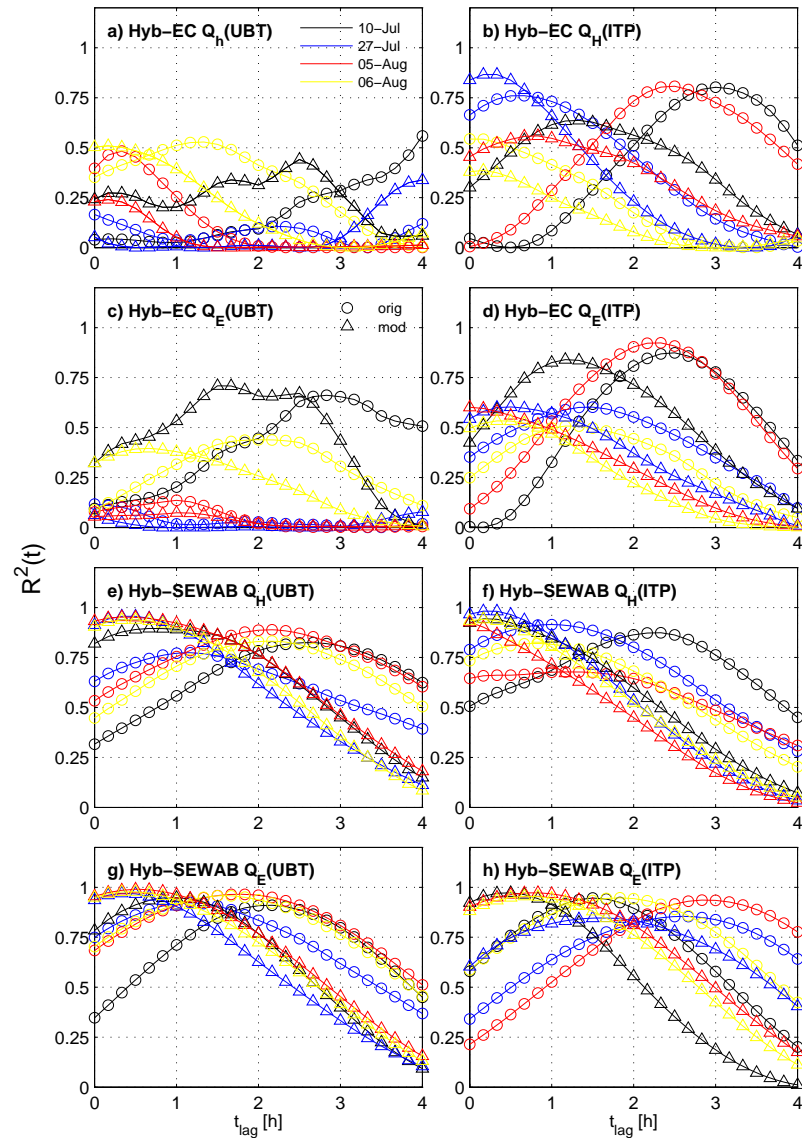


Fig. 8. Cross correlation $R^2(t)$ of simulated fluxes against flux reference shifted by t_{lag} as multiples of 10 minutes for each of the four days simulated with the original and modified Hybrid. The maximum number of elements used in the calculation of R^2 for each curve can be taken from Table 3.

into account the night-time, where fluxes and therefore absolute differences are smaller. The small improvement of RMSD of Q_H and $Q_{H_{EC,EBC}}$ at ITP can be explained by the fact that the modified Hybrid follows the dynamics of EC, but flux estimates are larger and of the same magnitude as fluxes calculated by SEWAB. Mauder et al. (2006) have estimated the error or EC measurements to be 5 % or $<10 \text{ W m}^2$ for Q_H and 15 % or $<30 \text{ W m}^2$ for Q_E . Additional uncertainty

is added to the measured fluxes by the lack in energy balance closure. When this is taken into account there is a significant difference between the $Q_{H_{Hybrid}}$ and $Q_{H_{EC,EBC}}$ for ITP on 6 August. On 5 August (ITP) and 6 August (UBT) the deviation of fluxes may still be explained by measurement errors and by shortcomings in the energy balance closure scheme. Indeed, there is no indication to assume scalar similarity between temperature and moisture transport (Ruppert et al.,

Table 3. Root mean square deviation (RMSD) between the modelled quantities of the original and modified Hybrid and reference values. The reference quantities used are either measured by EC and corrected for energy balance closure (EC,EBC) or modelled with SEWAB for fluxes or taken from longwave outgoing radiation for T_0 . The values in parenthesis (N) correspond to the number of elements used for calculation of RMSD and $R^2(l=0)$ in Fig. 8.

Site	Date	Run	RMSD				
			Q_E EC,EBC [$W m^{-2}$]	Q_H	Q_E SEWAB [$W m^{-2}$]	Q_H	T_0 [$^{\circ}C$]
UBT	10 July	orig	318	117 (8)	94	74 (94)	4.3 (139)
	27 July		97	58 (19)	60	59 (139)	4.5 (143)
	5 August		168	139 (11)	90	64 (110)	4.3 (143)
	6 August		159	84 (52)	87	71 (128)	3.7 (143)
ITP	10 July	orig	182	93 (25)	97	69 (143)	3.7 (143)
	27 July		43	64 (72)	58	75 (143)	3.8 (143)
	5 August		224	103 (64)	179	68 (143)	8.3 (143)
	6 August		118	80 (52)	130	119 (143)	5.1 (143)
UBT	10 July	mod	214	43 (8)	51	36 (94)	2.3 (139)
	27 July		79	44 (19)	32	28 (139)	2.9 (143)
	5 August		93	62 (11)	36	26 (110)	3.4 (143)
	6 August		78	57 (52)	39	32 (128)	3.2 (143)
ITP	10 July	mod	74	73 (25)	42	32 (143)	1.6 (143)
	27 July		42	58 (72)	55	36 (143)	2.6 (143)
	5 August		44	80 (64)	64	30 (143)	2.6 (143)
	6 August		68	82 (52)	113	77 (143)	3.5 (143)
UBT	all	orig	170	92 (90)	83	67 (471)	4.2 (568)
		mod	100	54 (90)	39	31 (471)	3.0 (568)
ITP	all	orig	152	84 (213)	125	86 (572)	5.6 (572)
		mod	54	73 (213)	74	48 (572)	2.7 (572)

2006; Mauder et al., 2007). Therefore, additional research, such as high-resolution atmospheric modelling studies, need to be carried out in order to determine the contributions of Q_H and Q_E to the “missing” energy. It should be noted that all modelled fluxes and measurements have errors, so that there is no absolute way of knowing which method produces the best flux estimates. The incorporation of surface fluxes into a regional circulation model may give some insight into whether modelled surface atmosphere interactions lead to realistic atmospheric flow patterns.

The large negative and potentially unreasonable night-time Q_H -fluxes that are modelled for ITP on 6 August are owed to a frozen soil and strong surface winds that lead to an overestimation of the temperature gradient, delayed reaction of the surface model and resulted in a potential underestimation of modelled surface temperatures and thus surface fluxes.

5.2 Discussion of surface temperature

For surface temperature there is a notable decrease in RMSD for all cases. Additionally, the source of the error changes. In the original model the error in T_0 was mainly due to the time-lag and a general underestimation of daytime maximum

surface temperatures. In the new model daytime T_0 matches a lot better with observations except for ITP 6 August, where evaporative cooling due to excessive evapotranspiration contributes to too small warming rates. In return, the cooling during the nighttime is overestimated. This may either be due to errors in soil moisture, surface emissivity (ϵ) or due to the surface temperature extrapolation function used in this work.

5.3 Soil moisture variation and evapotranspiration

After a 24 h run the moisture content of the first model layer (last two columns of Table 2) is smaller than measurements suggest. For UBT, measured soil moisture content does hardly vary on a day to day scale and is kept well above FC due to groundwater influence. This is not reflected by the model as it lacks the capability to include groundwater tables. The true soil moisture at ITP has a much larger variation due to its low FC and comparatively large pore volume. During the dry day of 27 July the upper soil layer loses 1.5 mm of water whereas during the moist days of August there is a total loss from layer one of 6.7 and 5.3 $mm d^{-1}$, respectively. Comparing $\theta_{1, \text{end}}$ of 5 August with $\theta_{1, \text{obs}}$ of the next day shows that the model would perform considerably worse

if it were not restarted every day. This is caused by a very limited soil hydrology included in Hybrid. Hu et al. (2008) have estimated the summer evapotranspiration on a central Tibetan grassland site to be in the order of $4\text{--}6\text{ mm d}^{-1}$. An experiment conducted within the framework of TiP has estimated bare soil evaporation and evapotranspiration of a very dry soil at Kema in 2010 ($\sim 150\text{ km}$ northeast of Nam Co Lake) at 2 mm d^{-1} rising to at least 6 mm d^{-1} and possibly more for a vegetated *Kobresia* pasture during an irrigation experiment (H. Coners – University of Göttingen, personal communication, 27 June 2011). Even though the soils are not directly comparable this suggests similar dynamics in Q_E to the ITP site. One factor likely to play a role in the local water cycle that is not included is dew fall in the early morning hours. Direct absorption of atmospheric moisture on bare soil (Agam (Ninari) and Berliner, 2004) and dew fall are often considered a significant moisture input for semi-arid environments (Agam and Berliner, 2006). Heavy dewfall in the vicinity of Nam Co Lake is frequently observed, but has, at least to our knowledge, never been quantified. This additional source of water and the associated local recycling of water may account for a significant fraction of the missing water. In addition to this, the too simplistic representation of soil hydrology is very likely responsible for the remaining water deficit in the upper layer of the soil model.

5.4 Cross correlation of turbulent fluxes

A different way of looking at the model performance is cross correlation of the modelled surface fluxes against EC measurements and SEWAB (Fig. 8). These measures give an insight into the reasons for the delayed response of the surface model and the amount of flux-variance explained, but does not yield information whether the model and the reference fluxes show a true one-to-one correlation. As with RMSD the quality of the analysis is limited by the number of data points that can be correlated, which is comparatively small for the energy balance corrected EC measurements at ITP and even smaller at UBT due to lake breeze influences (Fig. 8a–e). Hence, it is very difficult to interpret the cross correlations for EC. It is probably fair to say that there is a tendency for smaller time lags during the time series with higher number of elements, notably UBT 6 August and all days of ITP and that the total explained variances are at the same level of determination, when comparing the maximum $R^2(j)$. A notable exception is ITP 5 August.

For the comparison with SEWAB (Fig. 8f–h), it becomes notable that for many cases the maximum $R^2(j)$ of the modified Hybrid approach $R^2 \rightarrow 1$ and that their maxima are usually found at lags of $10\text{--}30\text{ min}$ ($j = 1\text{--}3$). Solar radiation rapidly modifies the skin temperature that is governing turbulent fluxes. As SEWAB has an instantaneous surface temperature solver for each model time step, one would expect a direct response of SEWAB to changes in solar radiation. This may even be faster than in reality, especially for Q_E flux that

is not only dependent on the actual skin temperature, but also on the vegetation's response. Including negative values of j into Fig. 8 would show a gradual decrease of correlations with decreasing j , showing that the flux dynamics of Hybrid never precede EC measurements or SEWAB.

5.5 Natural variability of fluxes

Atmospheric quantities and turbulent surface fluxes have a large natural variability that is difficult to measure or to model. The EC approach is dependent on averaging procedures and most standard measurements will yield mean values. In order to use high-frequency measurements for flux estimation, less common techniques such as conditional sampling or wavelet-spectra have to be used. Even if models are capable of reproducing variability on realistic scales it is difficult to supply forcing data with similar resolution. The forcing data used in this study, sampled and averaged 10 or 30 min means, are used for SEWAB. Running Hybrid at time steps comparable to a high-resolution mesoscale model requires interpolation of the forcing data and therefore potentially causes a smoothing of the model's response compared to the actual weather forcing as it would be provided by a coupled model. As surface models share a similar approach to the parameterisation of surface fluxes and close the surface energy balance locally, SEWAB and Hybrid fluxes are more similar to each other than they are to field measurements.

6 Conclusions

The accurate generation of surface fluxes is a necessary prerequisite for studies of surface-atmosphere interactions and local to mesoscale circulations. In order to gain a better process understanding of the interaction between atmospheric circulation, clouds, radiation and surface fluxes, the generated diurnal flux cycles have to be of realistic magnitude and without temporal shift. The original two-layer surface model without a specific formulation for T_0 produced both a considerable time lag and failed to capture the full diurnal dynamics due to its unresponsiveness.

We have demonstrated that the introduction of an extrapolated surface temperature enables even a quite simplistic soil model to realistically simulate skin temperatures and thus to generate more realistic surface fluxes. The delay of fluxes during the daily cycle was greatly reduced, making the model usable for diurnal process studies. The total magnitude of fluxes is also much improved, when few and computationally cheap additional physically based processes are introduced. Comparing SEWAB with Hybrid, the RMSD for both fluxes and surface temperature is decreased by generally $40\text{--}60\%$. The improvement in quality was somewhat more varied in comparison to EC measurements, as comparison of models and measurements is not straight forward. The improved $R^2(j)$ for smaller values of j shows that temporal shifts of

the flux time series have been greatly reduced and the overall correlations are high. As with any natural system it is impossible to obtain complete data sets that capture the full amount of natural variability. However, the modified model has been tested for a larger spectrum of environmental conditions on the TP and produced reasonable results for both dry and moist conditions.

We have shown that a rather simple soil surface model can efficiently calculate turbulent fluxes at a high temporal resolution when driven by realistic atmospheric conditions. Nevertheless, it is quite clear that such an approach with extrapolated surface temperature needs careful model initialisation. The initial soil heat contents and therefore knowledge of soil temperature profiles is necessary. Due to the fact that the surface temperature in this study is a purely diagnostic quantity, there may still be some limitations such as a delayed or smoothed response to atmospheric forcing on very short timescales, such as the feedback between passing boundary-layer clouds and the surface fluxes. The influence of surface fluxes and their dynamics to regional circulation will be investigated in a future study.

Acknowledgements. This research was funded by the German Research Foundation (DFG) Priority Programme 1372 “Tibetan Plateau: Formation, Climate, Ecosystems” as part of the Atmosphere – Ecology – Glaciology Cluster (TIP-AEG). ITP data was provided through CEOP-AEGIS, which is a EU-FP7 Collaborative Project/ Small or medium-scale focused research project – Specific International Co-operation Action coordinated by the University of Strasbourg, France under the call ENV.2007.4.1.4.2: “Improving observing systems for water resource management.” The authors would like to thank everyone who has contributed to the collection of field data in one of the world’s most remote regions. ADF acknowledges support from the European Community’s Seventh Framework Programme (FP7/2007–2013) under grant agreement no. 238366. AH acknowledges funding by the Fonds National de la Recherche (FNR-Luxembourg), under the grant BFR07-089 and support by the Cambridge European Trust (CET-UK).

Edited by: C. de Michele

References

- Agam (Ninari), N. and Berliner, P. R.: Diurnal Water Content Changes in the Bare soil of a coastal desert, *J. Hydrometeorol.*, 5, 922–933, doi:10.1175/1525-7541(2004)005<0922:DWCCIT>2.0.CO;2, 2004.
- Agam, N. and Berliner, P. R.: Dew formation and water vapor adsorption in semi-arid environments – A review, *J. Arid Environ.*, 65, 572–590, doi:10.1016/j.jaridenv.2005.09.004, 2006.
- Aubinet, M., Grelle, A., Ibrom, A., Rannik, U., Moncrieff, J., Foken, T., Kowalski, A., Martin, P., Berbigier, P., Bernhofer, C., Clement, R., Elbers, J., Granier, A., Grünwald, T., Morgenstern, K., Pilegaard, K., Rebmann, C., Snijders, W., Valentini, R., Vesala, T., Fitter, A., and Raffaelli, D.: Estimates of the annual net carbon and water exchange of forests: The EUROFLUX Methodology, *Adv. Ecol. Res.*, 30, 113–175, doi:10.1016/S0065-2504(08)60018-5, 1999.
- Biermann, T., Babel, W., Olesch, J., and Foken, T.: Mesoscale circulations and energy and gas exchange over the Tibetan Plateau – Documentation of the micrometeorological experiment, Nam Tso, Tibet – 25 June–8 August 2009, *Arbeitsergebnisse 41*, University of Bayreuth, ISSN 1614-8616, Bayreuth, 2009.
- Blackadar, A.: High resolution models of the planetary boundary layer, in: *Advances in Environmental Science and Engineering*, edited by: Pfafflin, J. and Ziegler, E., Vol. 1, 50–85, Gordon and Breach, New York, 1979.
- Camillo, P. J. and Gurney, R. J.: A resistance parameter for bare-soil evaporation models, *Soil Sci.*, 141, 95–105, 1986.
- Cong, Z., Kang, S., Smirnov, A., and Holben, B.: Aerosol optical properties at Nam Co, a remote site in central Tibetan Plateau, *Atmos. Res.*, 92, 42–48, doi:10.1016/j.atmosres.2008.08.005, 2009.
- Cui, X., Langmann, B., and Graf, H.: Summer monsoonal rainfall simulation on the Tibetan Plateau with a regional climate model using a one-way double-nesting system, *SOLA*, 3, 49–52, 2007.
- Deardorff, J. W.: Dependence of air-sea transfer coefficients on bulk stability, *J. Geophys. Res.*, 73, 2549–2557, 1968.
- Fairall, C. W., Bradley, E. F., Godfrey, J. S., Wick, G. A., Edson, J. B., and Young, G. S.: Cool-skin and warm-layer effects on sea surface temperature, *J. Geophys. Res.*, 101, 1295–1308, 1996a.
- Fairall, C. W., Bradley, E. F., Rogers, D. P., Edson, J. B., and Young, G. S.: Bulk parameterization of air-sea fluxes for Tropical Ocean-Global Atmosphere Coupled-Ocean Atmosphere Response Experiment, *J. Geophys. Res.*, 101, 3747–3764, 1996b.
- Foken, T.: The parameterisation of the energy exchange across the air-sea interface, *Dynam. Atmos. Ocean*, 8, 297–305, doi:10.1016/0377-0265(84)90014-9, 1984.
- Foken, T.: The energy balance closure problem: An overview, *Ecol. Appl.*, 18, 1351–1367, 2008.
- Foken, T., Göckede, M., Mauder, M., Mahrt, L., Amiro, B., and Munger, J.: Post field data quality control, in: *Handbook of Micrometeorology: A guide for surface flux measurements and analysis*, edited by: Lee, X., Massman, W., and Law, B., 181–208, Kluwer, Dordrecht, 2004.
- Foken, T., Aubinet, M., Finnigan, J. J., Leclerc, M. Y., Mauder, M., and Paw U, K. T.: Results Of A Panel Discussion About The Energy Balance Closure Correction For Trace Gases, *B. Am. Meteorol. Soc.*, 92, ES13–ES18, doi:10.1175/2011BAMS3130.1, 2011.
- Freedman, J. M., Fitzjarrald, D. R., Moore, K. E., and Sakai, R. K.: Boundary layer clouds and vegetation-atmosphere feedbacks, *J. Climate*, 14, 180–197, doi:10.1175/1520-0442(2001)013<0180:BLCAVA>2.0.CO;2, 2001.
- Friend, A. D.: Terrestrial plant production and climate change, *J. Exp. Bot.*, 61, 1293–1309, doi:10.1093/jxb/erq019, 2010.
- Friend, A. D. and Kiang, N. Y.: Land surface model development for the GISS GCM: effects of improved canopy physiology on simulated climate, *J. Climate*, 18, 2883–2902, 2005.
- Friend, A. D., Stevens, A. K., Knox, R. G., and Cannell, M. G. R.: A process-based, terrestrial biosphere model of ecosystem dynamics (Hybrid v3.0), *Ecol. Model.*, 95, 249–287, 1997.
- Hansen, J., Russell, G., Rind, D., Stone, P., Lacis, A., Lebedeff, S., Ruedy, R., and Travis, L.: Efficient three-dimensional global models for climate studies: Models I and II, *Mon. Weather Rev.*,

- 111, 609–662, 1983.
- Herzog, M., Graf, H., Textor, C., and Oberhuber, J. M.: The effect of phase changes of water on the development of volcanic plumes, *J. Volcanol. Geoth. Res.*, 87, 55–74, doi:10.1016/S0377-0273(98)00100-0, 1998.
- Hu, Z., Yu, G., Fu, Y., Sun, X., Li, Y., Shi, P., Wang, Y., and Zheng, Z.: Effects of vegetation control on ecosystem water use efficiency within and among four grassland ecosystems in China, *Glob. Change Biol.*, 14, 1609–1619, doi:10.1111/j.1365-2486.2008.01582.x, 2008.
- Hu, Z., Yu, G., Zhou, Y., Sun, X., Li, Y., Shi, P., Wang, Y., Song, X., Zheng, Z., Zhang, L., and Li, S.: Partitioning of evapotranspiration and its controls in four grassland ecosystems: Application of a two-source model, *Agric. For. Meteorol.*, 149, 1410–1420, doi:10.1016/j.agrformet.2009.03.014, 2009.
- Kanda, M., Inagaki, A., Letzel, M. O., Raasch, S., and Watanabe, T.: LES Study of the energy imbalance problem with eddy covariance fluxes, *Bound.-Lay. Meteorol.*, 110, 381–404, doi:10.1023/B:BOUN.0000007225.45548.7a, 2004.
- Keil, A., Berking, J., Mügler, I., Schütt, B., Schwab, A., and Steeb, P.: Hydrological and geomorphological basin and catchment characteristics of Lake Nam Co, South-Central Tibet, *Quart. Int.*, 218, 118–130, 2010.
- Kracher, D., Mengelkamp, H., and Foken, T.: The residual of the energy balance closure and its influence on the results of three SVAT models, *Meteorologische Z.*, 18, 647–661, doi:10.1127/0941-2948/2009/0412, 2009.
- Kuwagata, T., Kondo, J., and Sumioka, M.: Thermal effect of the sea breeze on the structure of the boundary layer and the heat budget over land, *Bound.-Lay. Meteorol.*, 67, 119–144, doi:10.1007/BF00705510, 1994.
- Li, M., Ma, Y., Hu, Z., Ishikawa, H., and Oku, Y.: Snow distribution over the Namco lake area of the Tibetan Plateau, *Hydrol. Earth Syst. Sci.*, 13, 2023–2030, doi:10.5194/hess-13-2023-2009, 2009.
- Lohou, F. and Patton, E. G.: Land-surface response to shallow cumulus, EGU General Assembly, Vienna, Austria, 3–8 April 2011, EGU2011-10280-1, 2011.
- Ma, Y., Wang, Y., Wu, R., Hu, Z., Yang, K., Li, M., Ma, W., Zhong, L., Sun, F., Chen, X., Zhu, Z., Wang, S., and Ishikawa, H.: Recent advances on the study of atmosphere-land interaction observations on the Tibetan Plateau, *Hydrol. Earth Syst. Sci.*, 13, 1103–1111, doi:10.5194/hess-13-1103-2009, 2009.
- Mauder, M. and Foken, T.: Documentation and instruction manual of the eddy covariance software package TK3, *Arbeitsergebnisse* 46, University of Bayreuth, ISSN 1614-8916, Bayreuth, 2011.
- Mauder, M., Oncley, S. P., Vogt, R., Weidinger, T., Ribeiro, L., Bernhofer, C., Foken, T., Kohsiek, W., Bruin, H. A. R., and Liu, H.: The energy balance experiment EBEX-2000. Part II: Intercomparison of eddy-covariance sensors and post-field data processing methods, *Bound.-Lay. Meteorol.*, 123, 29–54, doi:10.1007/s10546-006-9139-4, 2006.
- Mauder, M., Desjardins, R. L., and MacPherson, I.: Scale analysis of airborne flux measurements over heterogeneous terrain in a boreal ecosystem, *J. Geophys. Res.*, 112, D13112, doi:10.1029/2006JD008133, 2007.
- Mauder, M., Foken, T., Clement, R., Elbers, J. A., Eugster, W., Grünwald, T., Heusinkveld, B., and Kolle, O.: Quality control of CarboEurope flux data – Part 2: Inter-comparison of eddy-covariance software, *Biogeosciences*, 5, 451–462, doi:10.5194/bg-5-451-2008, 2008.
- Mengelkamp, H., Warrach, K., and Raschke, E.: SEWAB – a parameterization of the surface energy and water balance for atmospheric and hydrologic models, *Adv. Wat. Resour.*, 23, 165–175, doi:10.1016/S0309-1708(99)00020-2, 1999.
- Metzger, S., Ma, Y., Markkanen, T., Göckede, M., Li, M., and Foken, T.: Quality assessment of Tibetan Plateau Eddy covariance measurements utilizing footprint modeling, *Adv. Earth Sci.*, 21, 1260–1267, 2006.
- Miehe, G., Miehe, S., Bach, K., Nölling, J., Hanspach, J., Reudenbach, C., Kaiser, K., Wesche, K., Mosbrugger, V., Yang, Y., and Ma, Y.: Plant communities of central Tibetan pastures in the Alpine Steppe/Kobresia pygmaea ecotone, *J. Arid Environ.*, 75, 711–723, doi:10.1016/j.jaridenv.2011.03.001, 2011.
- Oberhuber, J. M., Herzog, M., Graf, H., and Schwanke, K.: Volcanic plume simulation on large scales, *J. Volcanol. Geoth. Res.*, 87, 29–53, doi:10.1016/S0377-0273(98)00099-7, 1998.
- Panin, G. N., Tetzlaff, G., and Raabe, A.: Inhomogeneity of the land surface and problems in the parameterization of surface fluxes in natural conditions, *Theor. Appl. Climatol.*, 60, 163–178, doi:10.1007/s007040050041, 1998.
- Panin, G. N., Nasonov, A. E., and Foken, T.: Evaporation and heat exchange of a body of water with the atmosphere in a shallow zone, *Izvestiya, Atmos. Ocean. Phys.*, 42, 337–352, doi:10.1134/S0001433806030078, 2006.
- Ruppert, J., Thomas, C., and Foken, T.: Scalar similarity for relaxed eddy accumulation methods, *Bound.-Lay. Meteorol.*, 120, 39–63, doi:10.1007/s10546-005-9043-3, 2006.
- Sellers, P. J., Mintz, Y., Sud, Y. C., and Dalcher, A.: A Simple Biosphere Model (SIB) for use within general circulation models, *J. Atmos. Sci.*, 43, 505–531, 1986.
- Su, Z., Wen, J., Dente, L., van der Velde, R., Wang, L., Ma, Y., Yang, K., and Hu, Z.: The Tibetan Plateau observatory of plateau scale soil moisture and soil temperature (Tibet-Obs) for quantifying uncertainties in coarse resolution satellite and model products, *Hydrol. Earth Syst. Sci.*, 15, 2303–2316, doi:10.5194/hess-15-2303-2011, 2011.
- Twine, T. E., Kustas, W. P., Norman, J. M., Cook, D. R., Houser, P. R., Meyers, T. P., Prueger, J. H., Starks, P. J., and Wesely, M. L.: Correcting eddy-covariance flux underestimates over a grassland, *Agric. For. Meteorol.*, 103, 279–300, doi:10.1016/S0168-1923(00)00123-4, 2000.
- van Heerwaarden, C. C., de Arellano, J. V., Moene, A. F., and Holtslag, A. A. M.: Interactions between dry-air entrainment, surface evaporation and convective boundary-layer development, *Q. J. Roy. Meteorol. Soc.*, 135, 1277–1291, doi:10.1002/qj.431, 2009.
- Xue, Y., Zeng, F. J., and Schlosser, C. A.: SSiB and its sensitivity to soil properties – a case study using HAPEX-Mobilhy data, *Glob. Planet. Change*, 13, 183–194, doi:10.1016/0921-8181(95)00045-3, 1996.
- Yang, K., Koike, T., and Yang, D.: Surface flux parameterization in the Tibetan Plateau, *Bound.-Lay. Meteorol.*, 106, 245–262, doi:10.1023/A:1021152407334, 2003.
- Yang, K., Chen, Y.-Y., and Qin, J.: Some practical notes on the land surface modeling in the Tibetan Plateau, *Hydrol. Earth Syst. Sci.*, 13, 687–701, doi:10.5194/hess-13-687-2009, 2009.

- Yee, S. Y. K.: The force-restore method revisited, *Bound.-Lay. Meteorol.*, 43, 85–90, doi:10.1007/BF00153970, 1988.
- You, Q. L., Kang, S. C., Li, C. L., Li, M. S., and Liu, J. S.: Features of meteorological parameters at Nam Co station, Tibetan Plateau, in: *Annual Report of Nam Co Monitoring and Research Station for Multisphere Interactions*, edited by: Nam Co Monitoring and Research Station for Multisphere Interaction, 1–8, Chinese Academy of Sciences, Beijing, 2006 (in Chinese with English abstract).
- Zhou, D., Eigenmann, R., Babel, W., Foken, T., and Ma, Y.: The study of near-ground free convection conditions at Nam Co station on the Tibetan Plateau, *Theor. Appl. Climatol.*, 105, 217–228, doi:10.1007/s00704-010-0393-5, 2011.

C. Gerken et al. (2013a)

Gerken, T., Biermann, T., Babel, W., Herzog, M., Ma, Y., Foken, T., Graf, H.-F.: *A modelling investigation into lake-breeze development and convection triggering in the Nam Co Lake basin, Tibetan Plateau*, Theor. Appl. Climatol., online first, doi:10.1007/s00704-013-0987-9, 2013a

A modelling investigation into lake-breeze development and convection triggering in the Nam Co Lake basin, Tibetan Plateau

Tobias Gerken · Tobias Biermann · Wolfgang Babel · Michael Herzog ·
Yaoming Ma · Thomas Foken · Hans-F. Graf

Received: 03 April 2013 / Accepted: 26 July 2013 / Published online: 25 August 2013

Citation: Gerken, T., Biermann, T., Babel, W., Herzog, M., Ma, Y., Foken, T., Graf, H.-F.: *A modelling investigation into lake-breeze development and convection triggering in the Nam Co Lake basin, Tibetan Plateau*, *Theor. Appl. Climatol.*, doi: 10.1007/s00704-013-0987-9, 2013

The final publication is available at link.springer.com © Springer

Abstract This paper uses the cloud resolving Active Tracer High-resolution Atmospheric Model coupled to the interactive surface model Hybrid in order to investigate the diurnal development of a lake-breeze system at Nam Co Lake on the Tibetan Plateau. Simulations with several background wind speeds are conducted and the interaction of the lake-breeze with topography and background wind in triggering moist and deep convection is studied. The model is able to adequately simulate the systems most important dynamical features such as turbulent surface fluxes and the development of a lake-breeze for the different wind conditions. We identify two different mechanisms for convection triggering that are dependent on the direction of the background wind: Triggering over topography, when the

background wind and the lake-breeze have the same flow direction and triggering due to convergence between the lake-breeze front and the background wind. Our research also suggests that precipitation measurements at the centre of basins on the Tibetan Plateau are not representative for the basin as a whole as precipitation is expected to occur mainly in the vicinity of topography.

Keywords Clouds · Surface-fluxes · Thermal Circulation · Tibetan Plateau

1 Introduction

The Tibetan Plateau (TP) and its role within the Asian Monsoon system have recently come into focus of atmospheric research. Land-use change, pasture degradation (Cui and Graf, 2009) and a changing climate have an impact on regional circulation, precipitation patterns, cloud cover and hydrological resources (i.e. Cui et al, 2007a,b, 2006; Immerzeel et al, 2010; Yang et al, 2011). Subsequently, these changes will also be seen on the local scale. While temperatures rise on the whole TP, changes in precipitation are more complex and may be a key for understanding future climate changes. Precipitation is a relatively small scale process, that is strongly influenced by topography and there are diverging trends for precipitation on TP (Xu et al, 2008) with an increase in precipitation in the eastern and a decrease on western TP. At the same time there are no permanent weather stations on the TP above 4800m (Maussion et al, 2011) and gridded

T. Gerken (✉) · T. Biermann · W. Babel · T. Foken
University of Bayreuth, Department of Micrometeorology,
95440 Bayreuth, Germany
E-mail: tobias.gerken@uni-bayreuth.de

T. Gerken · M. Herzog · H.-F. Graf
Department of Geography, Centre for Atmospheric Science,
University of Cambridge, CB2 3EN Cambridge, UK

Ma Y.
Key Laboratory of Tibetan Environment Changes and Land Surface Processes, Institute of Tibetan Plateau Research, Chinese Academy of Sciences, Beijing 100101, China

T. Foken
Member of Bayreuth Center of Ecology and Environment Research (BayCEER)

precipitation products such as TRMM (Tropical Rainfall Measuring Mission) or reanalysis data sets have large errors due to terrain effects (i.e. Yin et al, 2008; Ma et al, 2008). Gaining a better understanding of the interactions and feedbacks in TP's circulation system is crucial and we believe that modelling studies will be an important part of this effort. This includes the modelling of the interactions between the surface, complex topography and the atmosphere in generation of mesoscale circulation systems, the organisation of cloud cover and the surface energy balance.

Due to the high elevation of the Tibetan Plateau and its low pressure environment the surface receives strong solar radiation input and surface heating leads to large diurnal surface temperature cycles (Gao et al, 1981). The fraction of diffuse to total radiation is very small so that clouds and shadows blocking out direct radiation have a profound impact on surface temperatures. This is illustrated by previously unpublished downward shortwave radiation measurements conducted in 1996 (Fig. 1 a; 10 August 1996 Sereng Co Lake). Surface-atmosphere interactions through turbulent latent and sensible heat fluxes (Q_E and Q_H , respectively) as well as the complex topography of the plateau are of great importance, but not fully understood (e.g. Ma et al, 2009; Tanaka et al, 2003). Deep convection triggered by topography is a major source of precipitation in semi-arid mountainous environments (e.g Banta and Barker Schaaf, 1987; Gochis et al, 2004). In the context of TP thermal valley-circulation systems are an important factor in the diurnal organisation of cloud development and convection (Yatagai, 2001; Kuwagata et al, 2001; Kurosaki and Kimura, 2002). Valley scales of 160–240 km were determined to be most effective for this process through modelling (Kuwagata et al, 2001) and satellite observations (Yatagai, 2001). Similarly Yang et al (2004) have investigated secondary triggering of convection within Tibetan valleys as a result of cold-pool fronts caused by convective events that were triggered over the mountains.

Isotopic analysis of precipitation conducted by Tian et al (2001a,b) show the influence of the monsoon as a water source declining as one proceeds north, with a strong monsoonal influence on the central TP, while a more recent analysis by Kurita and Yamada (2008) for the central TP highlights the importance of local moisture recycling: More than half of the rain events in their 14-day study period were locally generated and a large fraction of the total precipitation was water recycled from the region. An important factor in the development of deep convection on TP is the availability of moisture. During the monsoon season a condition-

ally unstable atmosphere is prevalent over central TP and precipitation events are facilitated by atmospheric moisture contents (Taniguchi and Koike, 2008). The two potential sources are local moisture from evapotranspiration or mid-tropospheric water vapour advection associated with monsoonal fronts. It is very perceivable that the initial moistening of the profile occurs through monsoonal transport and that subsequently the convective system remains active through local recycling. Therefore, the transport of moisture and the generation of convection that leads to recycling of water are important processes in the surface-atmosphere system, yet remain poorly understood.

Lake breezes are a subcategory of sea-breeze systems and form due to the thermal contrast between land and water surfaces. Two recent reviews have summarised the current state of research on sea-breeze structure (Miller et al, 2003) and their numerical modelling (Crosman and Horel, 2010): The role of topography onto sea-breeze development is highly dependent on the slope of terrain. Steep slopes act as an obstacle to flow, while thermal hill-valley circulations can assist in the development of mesoscale circulation system. The onset of sea breezes has been studied by Antonelli and Rotunno (2007). Additionally, the role of mountains in thermal circulations is discussed in Rampanelli et al (2004). The work described here work investigates the combination of both mesoscale processes. Kuwagata et al (1994) have found that a substantial amount of energy relative to turbulent fluxes is advected within sea breezes. Additionally, daytime convergence on mountain tops results in the transport of air to the free troposphere (e.g. Banta, 1990).

Our research focuses on surface-atmosphere interactions, the development of mesoscale circulations such as a lake-breeze system and its interaction with local topography in the development of moist convection in the Nam Co Lake basin. In Gerken et al (2012) we stated that such research needs both (1) a surface model that can reproduce the system's turbulent flux dynamics and (2) an atmospheric model with a resolution, high enough to resolve the scales that are significant for boundary-layer processes and convection. Typical resolutions of mesoscale models are on the kilometre scale, whereas the triggering of single convective plumes, simulation of local circulations driven by surface features and the surface shadowing of clouds require high-resolution approaches with resolutions in the order of 200 m assumed to be sufficient Petch (2004, 2006). As convection development is highly dependent on moisture it is of large importance for any modelling approach to get a good estimate of the initial atmospheric moisture contents.

The sparseness of observations in remote regions, the coarse representation of topography as well as the limited number of model levels, prevent the availability of good quality atmospheric profiles on TP, a problem we address here by using a Global Forecasting System – Final analysis (GFS-FNL) profile downscaled after Maussion et al (2011) using the Weather Research and Forecasting model (WRF).

The simulations conducted in this study are designed to explore the interaction between the lake breeze system, the background wind and topography on the development of moist convection. We show that (1) the model is able to simulate the development of the characteristic land-lake circulation system, (2) investigate the sensitivity of the system to different wind speeds and (3) show that the interaction of the lake-breeze, topography and background wind leads to the triggering of deep convection at Nam Co Lake.

2 Model setup and methodology

The non-hydrostatic, cloud resolving Active Tracer High-resolution Atmospheric Model (ATHAM) (Oberhuber et al, 1998; Herzog et al, 2003) was first developed for the study of volcanic plume development (Graf et al, 1999) and then subsequently extended for biomass-burning plumes (e.g. Trentmann et al, 2006) and cloud studies (Guo et al, 2004). ATHAM consists of a dynamic core solving the Navier-Stokes equations in two or three dimensions with an implicit time stepping scheme on a Cartesian grid with a z -vertical coordinate. Incorporated tracers are active in the sense that they influence heat capacity and density of the mixture at each gridpoint (Oberhuber et al, 1998). In the present study all classes of hydrometeors are treated as active tracers. The turbulence scheme is based on a 1.5-order turbulence closure predicting horizontal and vertical turbulent kinetic energy as well as turbulent length scale (Herzog et al, 2003). ATHAM's modular structure allows for the incorporation of several physical processes. In this study short- and long-wave radiation (Langmann et al, 1998; Mlawer et al, 1997), bulk-microphysics (treating the conversion between water vapour, cloud water, cloud ice, graupel and rain, Herzog et al, 1998), a land surface (Friend et al, 1997; Friend and Kiang, 2005) and a water surface (Fairall et al, 1996a,b) scheme supplying turbulent energy fluxes are used. The process based terrestrial ecosystem model Hybrid (v6) (Friend et al, 1997; Friend and Kiang, 2005) was modified for the use on the TP and was able to capture flux dynamics at Nam Co lake for observed forcing data (Gerken et al, 2012). The Coupled Ocean-Atmosphere Response Experi-

ment (COARE) - algorithm v2 (Fairall et al, 1996a,b) is a bulk flux algorithm based on the framework of Liu et al (1979). As Nam Co Lake is a large water body with a mean depth of more than 50 m (Wang et al, 2009), offline simulated lake fluxes compare reasonably well to observations (Gerken et al, 2012).

2.1 Field measurements

In this work, we conduct 2D simulations of a cross section through the Nam Co basin (Fig. 1 b) using realistic topography, in order to gain a better understanding of the physical processes involved in the generation of mesoscale circulations and convection. We apply the interactive surface model shown to work in Gerken et al (2012) and make use of data collected during a field campaign conducted between 26 June and 9 Aug 2009 by the University of Bayreuth in cooperation with the Institute of Tibetan Plateau Research, Chinese Academy of Sciences (Biermann et al, 2013). In this period eddy-covariance and standard atmospheric measurements were carried out at two locations close to the lake, but due to logistical reasons (power supply) not close to the mountains. The measurements of both eddy-covariance stations were post-processed using the TK2/3 software package (Mauder and Foken, 2004, 2011), applying all necessary flux corrections and post-processing steps for turbulence measurements as recommended in Foken et al (2012) and Rebmann et al (2012). On the vast majority of days a lake breeze developed, which could be observed at the Nam Co research station (30°46.44' N; 90°57.72' E), located about 300m from the shore-line of a small lake next to Nam Co Lake at around 10:00h Beijing Standard Time (BST). It should be noted that local solar time is approximately 2h earlier than BST. Lake-breezes developed frequently between 9:00 and 12:00h BST (Biermann et al, 2013). When the system was not observed it was most likely due to closed cloud cover and lack of terrestrial surface heating or due to synoptic scale offshore winds. While measured turbulent surface fluxes were similar on 5 and 6 August, a lake breeze failed to develop in the morning of 6 August, when the offshore component of the measured surface wind exceeded 6 m s^{-1} . On 5 August in contrast, the initial offshore wind component of 2.3 m s^{-1} at 8:15h changes to an onshore wind of 1.6 m s^{-1} at 12:15 (Tab. 1). The change in direction occurred around 10:45h, indicating the lake-breeze onset. Starting from approximately 12:00h BST, deep convection was frequently observed over the mountains during the field campaign.

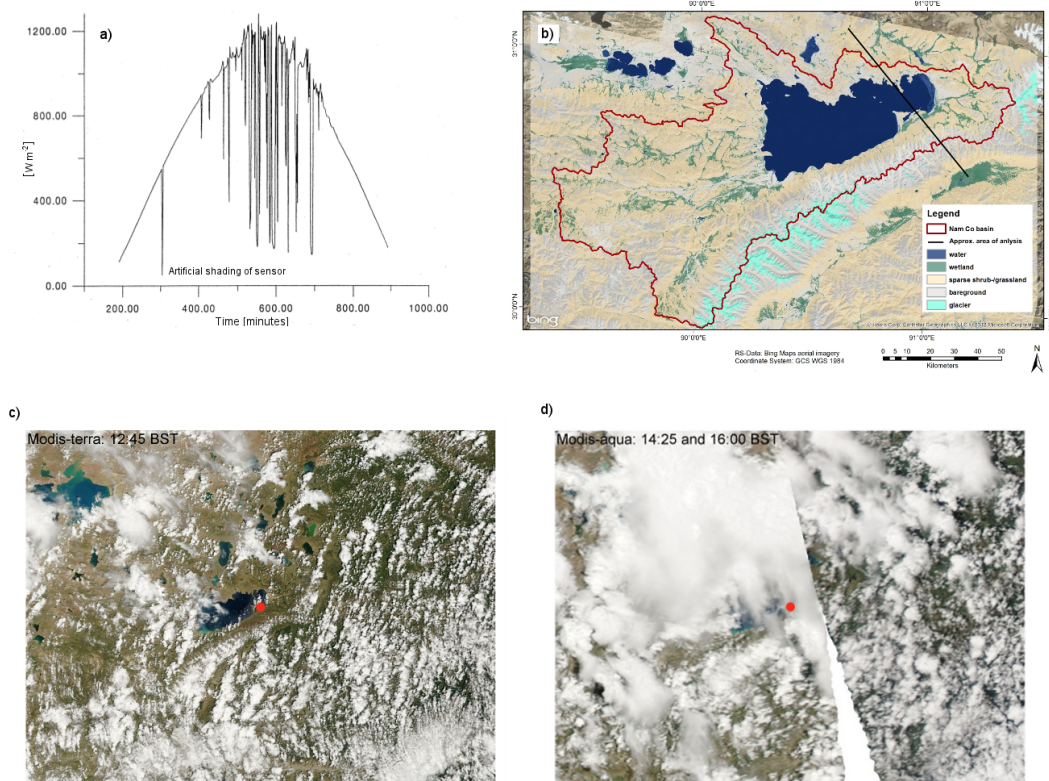


Fig. 1 a) Downwelling solar radiation (SWD , [$W m^{-2}$]) measured with high temporal resolution on the Tibetan Plateau at Sereng Co Lake on 10 Aug 1996. At approx. 300 minutes the radiation sensor was artificially shaded in order to show the strong difference between total and diffuse radiation. Later decreases in radiation are due to passing boundary-layer clouds. b) Land-use map of Nam Co Lake basin created from Landsat data; c) Modis-terra composite of Nam Co Lake captured at 12:45 h BST on 6 Aug 2009; d) Modis-aqua composite for the same day and region as panel c), but at 14:20 and 16:00 h BST. The red circles indicate the location of the Nam Co Lake research station. Microsoft Bing map used with permission from Microsoft Corporation. ©2012 The Microsoft Corporation ©Harris Corp, Earthstar Geographics LLC.

2.2 Simulation setup

ATHAM is run in Cartesian 2D mode, with the horizontal coordinate oriented perpendicular to the lake-land boundary and Nyenchen Thanglha mountain chain, which is situated approx. 10km south of Nam Co Lake. Both the lake shore and the mountains are almost parallel to each other and extend over more than 100km. In the absence of largescale forcings, the circulation in the basin is primarily driven by a lake breeze and a thermal mountain circulation. Hence, a 2D cross-section is capable of reproducing the system's most important dynamical features. We chose a cut across the eastern part of the lake, passing through the Nam Co Lake research station and a comparatively low section of the Nyenchen Thanglha mountain chain. The main reasons are the availability of observations

and the fact that 2D simulations have a tendency to overestimation the influence of topography. The domain size is 150 km with a constant grid spacing of 200 m resolving the central 80km, which includes the lake and the mountains to the south and north of the lake as indicated in Fig. 1 b). Outside the basin horizontal grid stretching is applied to achieve a resolution of approx. 1300m near the lateral boundaries and giving a total number of gridpoints of $n_x=486$. The lateral boundary conditions are cyclic, but hydrometeors and water vapour exceeding the initial moisture profile are removed at the lateral boundaries, without adding a density perturbation. We use 150 layers, starting at 25 m vertical resolution for the first 30 layers, then stretching to a maximum vertical resolution of approx. 300m at the model top 15km above ground level (a.g.l.). The model topography is taken from the

ASTER-DEM with 90 m resolution and was smoothed with a 2 km moving window in order to remove large vertical cliffs and single grid point depressions. Additionally, topography outside the Nam Co basin is set to the lake level and turbulent surface fluxes are gradually reduced to zero near the lateral boundary. This is justified as our area of interest is within the Nam Co Lake basin. The simulation is integrated from 06:00 h BST (approx. 1.25 h before sunrise) to 18:00 h BST. We acknowledge that 2D simulations have a simplified wind field, where clouds can only move along one horizontal direction. Consequently, the surface may experience artificially high shading, which can lead to a potential underestimation of turbulent latent (Q_E) and sensible heat fluxes (Q_H), as soon as large clouds are present. Hence, we limit our analysis to the time before and immediately after the triggering of deep convection.

2.2.1 Test cases

We selected as a base-case for this work 6 August 2009, a radiation day at the centre of the basin, with sudden triggering of deep convection in the afternoon as seen by the MODIS satellites (Fig. 1 c+d). The soil model is initialised in a similar way as the previous study (Gerken et al, 2012), when surface fluxes were already modelled, assuming homogeneous soil properties (Tab. 2). The soil model was initialised with $T_1=9.4$ and $T_2=3.7$ °C as mean layer temperatures, corresponding to a surface temperature $T_0=5.8$ °C for the land surface, while the lake temperature was set to 15.0 °C. A random perturbation in the surface cover of ± 5 % was added in order to account for variations of surface cover. Additionally, the initial volumetric moisture in the model's surface layer (SM_0 , [%]) was set to $1.4 \times$ field capacity and is scaled with height according to

$$SM_0 = SM_0 - (SM_0 - SM_{PWP}) \times h/h_{max} \quad (1)$$

with SM_{PWP} as the soil moisture at permanent wilting point, h the terrain height and h_{max} as the maximum terrain height in the domain.

The atmosphere is initialised from GFS-FNL downscaled to the Nam Co basin (Maussion et al, 2011). The profile on 6 August (Fig. 2) is relatively

Table 1 Mean cross-shore wind component measured at Nam Co Lake 3 m above ground on 5 and 6 Aug 2009. The averaging interval is 30 minutes centred around the given time. Positive values indicate offshore flow.

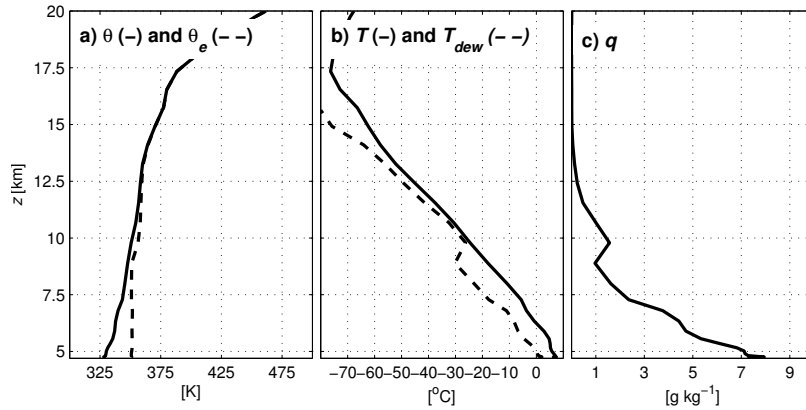
Time [BST]	08:15 [ms ⁻¹]	09:15 [ms ⁻¹]	11:15 [ms ⁻¹]	11:45 [ms ⁻¹]	12:15 [ms ⁻¹]
5 Aug 2009	2.3	1.5	-1.1	-1.5	-1.6
6 Aug 2009	6.1	6.1	5.3	3.9	3.7

dry for the lowermost 5 km a.g.l. with relative humidities between 60-70 % and a moist layer above, which is also seen in the 00-UTC Nagqu radiosounding (not shown, approx. 150 km to the northeast) indicating southerly upper level winds. The equivalent potential temperature (θ_e) indicates conditional instability in the profile as is commonly encountered in summer atmospheric profiles on TP. While there is no CAPE in the initial profile, it is easily built up by surface heating and lower tropospheric moistening. The wind coordinate in our experiments is defined with positive values for winds coming from the Nyenchen Thanglha mountains (southerly winds). For our experiment we chose to initialize our model with constant wind speeds of -3.0, -1.5, 0.0, +1.5, +3.0 and +6.0 m s⁻¹ throughout the model domain. In line with the meteorological convention, where a flow from the south to the north is positive, we define flows from the southeast towards the northwest as positive. The flow direction is indicated in the figures used in this work. We denote the simulations by the initial wind speed (e.g. U+0.00 for the case with no initial wind). The cases were chosen to analyse the development of a lake-breeze and to investigate the sensitivity of convection on changing wind speed. These wind speeds reflect a realistic low level flow, with U+6.00, being close to the observed wind velocity on 6 August, but are comparatively weak for the upper atmosphere. Nevertheless, this allows for the forcing of the surface model with a realistic wind, while not having to deal with impacts of wind shear that are not the object of this study and are poorly represented in 2D-simulations (i.e. Kirshbaum and Durran, 2004). In order to drive the coupled surface model, specifically for the case of no initial wind, a cross-directional wind component of 1 m s⁻¹ was added to all

Table 2 Description of the soil and surface parameters determined for Nam Co Lake (N 30°46.50'; E 90°57.61') in summer 2009.

Parameter	
Soil	sandy-loamy
Porosity	0.63
Field Capacity	0.184
Wilting Point	0.115
Heat capacity (c_p) [J m ⁻³ K ⁻¹]	2.5×10^6
Thermal	
Conductivity [W m ⁻¹ K ⁻¹]	0.53
Surface Albedo (α)	0.2
Surface Emissivity (ϵ)	0.97
Vegetated Fraction	0.9
LAI [m ² m ⁻²]	0.9
Vegetation height [m]	0.07

Fig. 2 Initial profile for Nam Co Lake 6. Aug 2009 06:00 BST used in the model simulations. Derived from GFS-FNL with WRF according to Maussion et al (2011). a) Potential (θ) and equivalent potential temperature (θ_e); b) Temperature (T) and dew-point temperature (T_{dew}) and c) Mixing Ratio (q).



simulations, which is only seen by the surface model. It should be noted that the wind speed is not continuously forced in the simulations so that topography and surface friction lead to an equilibrium wind speed that differs from the initialised flow speed.

Even though the cases U+6.00 and U+3.00 correspond roughly to measured surface conditions on 5 and 6 of August 2009, these sensitivity simulations are not intended to reproduce the atmospheric processes as they took place in the Nam Co basin on a specific day, as this could only be achieved with a 3D simulation that takes into account a full realistic topography and synoptic forcing. Instead we investigate the interactions between the lake, topography and atmosphere to investigate the triggering of convection under different wind conditions, in order to develop a better process understanding.

3 Results

3.1 Development of a lake-breeze system

A fundamental basis for the examination of convection triggering in the Nam Co Lake basin is the question whether ATHAM is capable producing realistic lake-breeze circulations. Figures 3 + 4 display the horizontal wind speed at 11:00 and 12:00h BST. According to theory a symmetrical and pronounced lake breeze should develop in the simulation without background wind, but due to asymmetric topography we expect some deviations. Additionally, we expect interaction of the lake-breeze with the topography. Depending on the slope angle, a mountain can either act as an obstacle to flow (Ookouchi et al, 1978) or can contribute to the lake-breeze development as it may reinforce the thermal circulation (i.e. Miao et al, 2003). With a cross-section of Nam Co Lake in the order of 10km

used in this study there is little found in the literature about lake-breeze behaviour of “small” lakes and how their thermal circulation system interacts with the background wind. For onshore geostrophic winds (U_g) a landward shift of the lake breeze is expected. The reverse effect is expected for offshore flow. Additionally the timing of sea-breezes is affected. For oceanic settings sea breezes with offshore $U_g > 4-8 \text{ m s}^{-1}$ are expected to stall at the land-lake boundary. For onshore $U_g > 3-5 \text{ m s}^{-1}$ sea breezes become indistinguishable from the background flow. For lakes these values are thought to be smaller (Crosman and Horel, 2010). In our simulation setup, the thermal circulation forced by the Nyenchen Thanglha mountains on the south-east shore and the lake-breeze seem to create a single mesoscale circulation system for the case U+0.00. Strong winds delay the formation of a lake-breeze front or it may not be detectable in a stronger off-shore background wind (Crosman and Horel, 2010). As we expect from both theory and observation at Nam Co lake, there is no lake-breeze developing for case U+6.00 (Fig. 4 k+l). In contrast a lake breeze is clearly visible by 12:00h BST in the simulations U+3.00 and U+1.50 (Fig. 4 g-j) on the southeastern shore of the lake, while the lake-breeze is standing out less against the background flow on the northwest shore. The reverse is true for the simulations with $U < 0 \text{ m s}^{-1}$ (Fig. 4 a-d). In accordance with theory the lake breeze front penetrates less onto the lake shore in stronger winds. As the lake-breeze regime usually develops between 9:00 and 12:00h BST, we conclude that our simulations are capable of reproducing the characteristic lake-breeze development at Nam Co Lake, with wind speeds differences in the order of a few meters per second as expected.

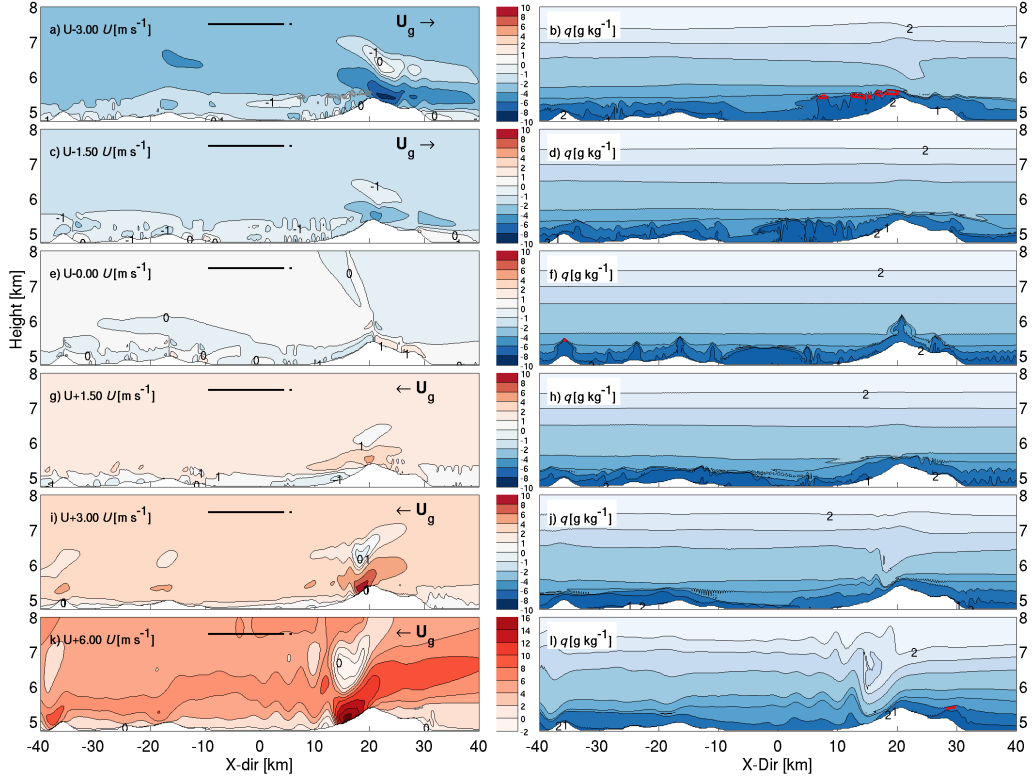


Fig. 3 Horizontal wind speed in the Nam Co Lake basin at 11:00h BST for model runs with initial wind speeds of -6.00 -3.00, -1.50, 0.00, 1.50 and 3.00 m s^{-1} (left column). A positive wind speed indicates southerly winds and flow from left to right in the panel. The black line shows the position of the lake. Right column: Corresponding water vapour mixing ratio (q , [g kg^{-1}]) with contour interval of 1 g kg^{-1} . The grey and red contour lines overlaid indicate the position and extent of clouds.

3.2 Convection development

From late morning onwards clouds begin to form in the Nam Co basin. In our simulations clouds are defined as grid cells in which the total content of condensed ice and water exceeds $q_t > 10^{-3} \text{ g kg}^{-1}$. After sunrise and with a growing boundary-layer, shallow clouds start to appear in the model domain. These clouds grow over time and eventually lead to the triggering of deep convection and precipitation. Fig. 5 displays the domain averaged q_t in the Nam Co basin. A deep convective regime is reached in all simulations. As expected, stronger and earlier convection develops in the scenarios with weaker initial winds. For these, there is little turbulent and advective transport or dispersion of heat and no wind shear to prevent the triggering of convection. As a consequence, developing local vertical instabilities are readily released. Additionally, there is reduced entrainment of dry air into thermals due to lack of turbulence. For low wind speeds there is a relatively fast transition between shallow and deep con-

vection as characterised by a relatively short time interval between the onset of shallow cumulus (t_{cl}), activation time of cumulus clouds (t_*) and the time when the cloud top height reaches the 13 km level (t_{13} ; Table 3). For simulations $U \pm 3.00$ and $U + 6.00$ this takes substantially longer. The transitions for all cases occur between 11:40 and 12:30h, except for $U + 6.00$, where the definition of t_* is not applicable due to a stationary cloud over the large mountain (Fig. 5 e). The transition time t_* is defined as the time when the centre of cloud mass (Z_c) starts to ascend at an increasing speed (Wu et al, 2009).

$$Z_c = \frac{\int \int q_t z dx dz}{\int \int q_t dx dz}, \quad (2)$$

with z as the vertical coordinate and $dx dz$ as the area element to be integrated over. Z_c is assumed to initially grow at a constant rate so that a linear regression is fitted through Z_c for the first 30 minutes after clouds appear in the simulations. t_* is defined as the time, when the Z_c exceeds a band around the regression (Z_{cr}). Wu et al (2009) have proposed $Z_c > 1.15 Z_{cr}$,

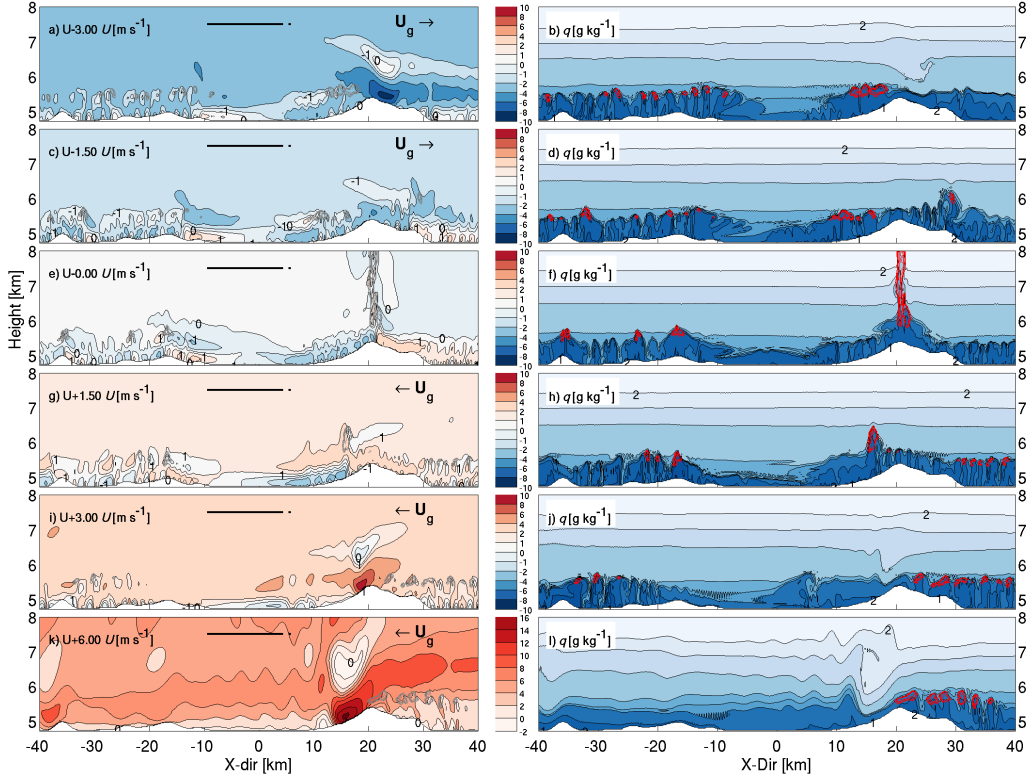


Fig. 4 As Fig. 3, but for 12:00h BST.

which proved to be a robust measure and is also applied in this work. t_* practically marks a change in the regime of cloud development: Clouds that form from the mixing of air into the boundary layer become buoyant as free convection starts. The main reason for the virtually non-existing transition time in case U+0.00 is that the initial cloud forms at the top of the heated mountain and grow immediately into the level of free convection. However, for all other simulations t_* corresponds to the first visible change in the slope (Fig. 5). The fast transition from shallow to deep convection is caused by the conditional instability of our initial atmospheric profile. It should be noted here that both Wu et al (2009) and Kirshbaum (2011) use profiles with idealised stability, while our profile is derived from GFS analysis data, which was downscaled with WRF to reflect local conditions. It is characteristic for the atmosphere above the TP to be conditionally unstable (as indicated by vertically constant values of θ_c) and we can indeed see from observations at Nam Co that convective systems develop rapidly (Fig. 1 c+d). Additionally, Wu et al (2009) and Kirshbaum (2011) use a uniform surface initialisation with prescribed fluxes and in the case of Wu et al (2009) no initial wind. Calculation of Con-

vective Available Potential Energy (CAPE; Emanuel, 1994) reveals that even though there is virtually no CAPE in the initial profile, it is rapidly built up for all cases by both surface warming and boundary-layer moistening. There is little difference in absolute CAPE values between the runs, but a general tendency to generate CAPE exceeding 1000 J kg^{-1} until solar noon and a subsequent release of CAPE in the afternoon. While CAPE behaves similarly over areas classified as mountains and the basin, CAPE values over the water build up much slower, remain lower and show hardly any tendency to be released within the time frame of this investigation. This provides first evidence for the role of land-cover and topography. The mechanism of convection triggering and the role of topography will be discussed in section 3.4. The height of Z_c reaches approx. 12 km in all cases, which corresponds to the level of neutral buoyancy. It should be highlighted that triggering of deep convection may occur too early in the model as the downscaled atmospheric profiles do not contain inversion layers that need to be overcome as would potentially be the case in directly measured profiles. As there are not directly measured radiosonde profiles available for the summer of 2009 at Nam Co,

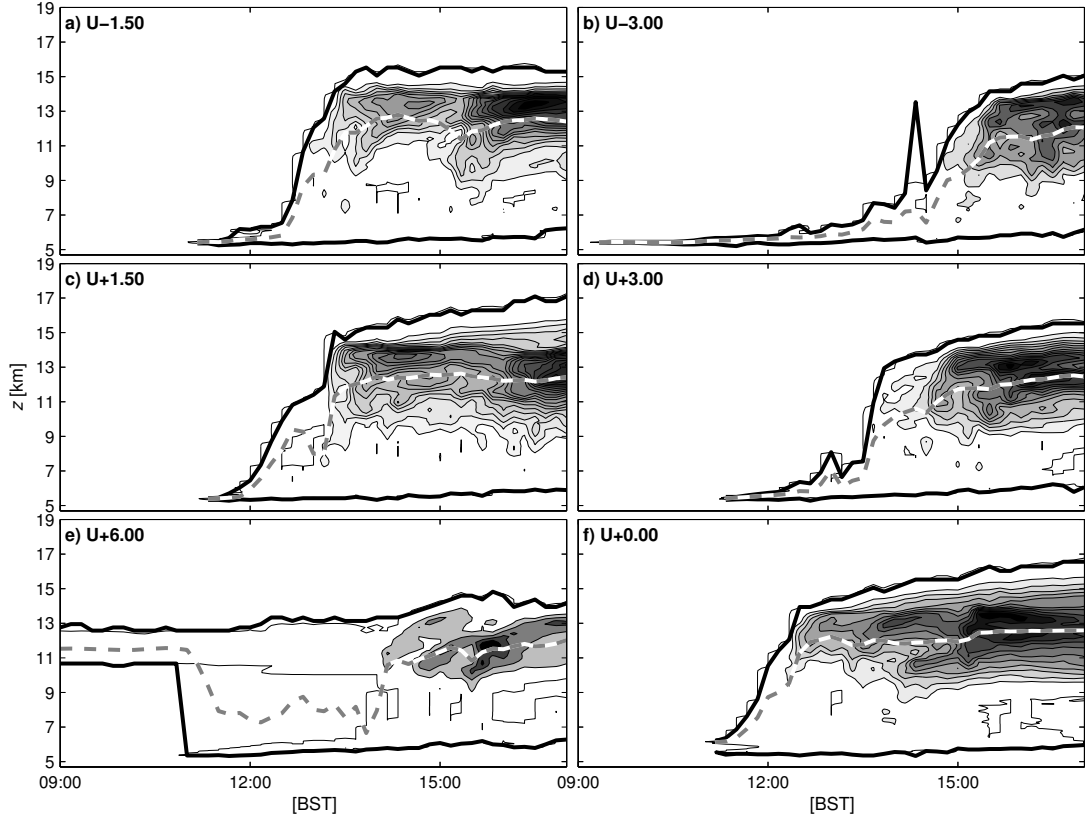


Fig. 5 Development of convection at Nam Co Lake for model runs with initial wind of 1.50, 3.00, -1.50, -3.00 and 0.00 m s^{-1} , a-e) respectively; Contours correspond to mean cloud particle concentrations in the Nam Co Lake basin. Each contour level corresponds to 0.1 g m^{-3} . The dashed line indicates the height of the centre of cloud mass (Z_c) and black lines indicate cloud top and cloud bottom heights.

Table 3 Timing of convection in hours BST. t_{cl} is the time when first boundary layer clouds appear in the model; t_* corresponds to the triggering of moist convection after Wu et al (2009) and t_{13} is the time when convection reaches 13 km a.s.l. t_* for U-6.00 was not calculated due to the occurrence of a high cloud over the mountain chain, rendering the calculation of the centre of the cloud mass Z_c unapplicable.

Run	t_{cl}	t_*	t_{13}
U-3.00	09:20	11:40	14:20
U-1.50	11:10	11:40	13:20
U+0.00	11:10	11:50	12:30
U+1.50	11:20	12:00	13:20
U+3.00	11:20	12:50	14:00
U+6.00	11:40	N/A	N/A

we have decided to limit the scope of this investigation to the influence of the background wind.

3.3 Modelled turbulent surface fluxes

We compare the surface fluxes generated by ATHAM with fluxes measured by eddy covariance (EC). ATHAM's surface model is fully coupled and produces fluxes through bulk transfer relationships, which take into account wind speed, temperature and moisture gradients between the surface and the air above, atmospheric stability, clouds and the net-radiation. Each grid cell is treated independently. EC measurements are direct, high frequency measurements of an atmospheric scalar and the vertical wind speed from which a vertical flux can be calculated (i.e. Foken, 2008b). While the horizontal grid resolution corresponds roughly to the footprint of the eddy covariance measurements they are not directly comparable as surface models will close the surface energy balance by distributing the available net radiation (R_{net}) between Q_E , Q_H and the ground heat flux Q_G . During the campaign an energy balance closure for the EC measure-

ments of about 70% R_{net} was observed Biermann et al (2013). This is due to the inherently unclosed energy balance of EC measurements (i.e. Foken, 2008a; Foken et al, 2011). Particularly under the influence of stationary secondary circulations, like sea-breezes, a substantial amount of energy is exchanged without being measured by EC. Therefore, before comparing measured and modelled fluxes, EC fluxes are corrected according to the Bowen ratio (Twine et al, 2000).

The behaviour of the simulated fluxes in all cases is initially very similar and corresponds to the warming of the surface as part of the diurnal cycle. Due to the high soil moisture, we encounter Bowen ratios of approximately 1/2. Since the model is initialised with nearly homogeneous surface conditions, there is little spatial variation of turbulent fluxes as long as clouds remain absent. After sunrise Q_E and Q_H rise in a sinusoidal manner. From 12:00h BST the occurrence of clouds begins to reduce the downwelling shortwave radiation, which is first seen in a drop in the lower quartile and then in the median radiative flux. As a consequence turbulent fluxes drop and have a larger spatial variation. Fig. 6 a–f) display the median turbulent fluxes and downwelling shortwave radiation within the area of analysis for the six model runs. Fig. 6 g) shows the measured data from two EC complexes. While the magnitudes of simulated and measured fluxes closely resembles each other, modelled fluxes lag behind measurements in the order of 1 h, which is most likely due to the formulation of the surface model, containing a 10cm thick soil layer with an extrapolated surface temperature. In reality skin temperatures react almost instantaneously to changes in energy input, while both our model and integrated EC measurements react more slowly. As boundary layer clouds and later deep convection develop, the spatial variability of surface fluxes increases. In the measured data this is represented in a higher temporal variability of R_{net} . Triggering of deep convection leads to a strong decrease in the median downwelling shortwave radiation, followed by a decrease in turbulent fluxes. Due to the 2D nature of our simulations we limited our analysis to the time before the simulation becomes dominated by clouds, which happens between 14:00 and 16:00h BST in all cases. It should be noted that the flux development of the case $U-3.00\text{m s}^{-1}$ (Fig. 6 b) is most similar to the measured fluxes and agrees reasonably well. A likely reason for this is the fact that the comparatively high wind speeds dissipate enough energy to delay the triggering of convection to a realistic time. $U+6.00$, which corresponds to the observed initial wind speed, has too high fluxes in the afternoon, because too few clouds are produced that reduce solar radiation input. The observed time

lag in the surface model, which is already described in Gerken et al (2012), may be the cause of a relatively late, yet still reasonable, development of lake-breeze system in our simulations.

3.4 Triggering of deep convection

Starting from the initial hypothesis that deep convection is triggered by the interaction of locally generated mesoscale circulations, we analyse the interaction of the background flow with the lake breeze and the mountains found in the domain. The role of the atmospheric vertical profiles is beyond the scope of this work, but strong conditionally instability (i.e. Yanai et al, 1992) as encountered in the profile used in this work is a general feature of the atmosphere on TP during the summer monsoon. Figures 7 + 8 display the spatial development of surface fluxes and the development of clouds for the cases $U+3.00$ and $U-3.00$. Both the lake and the mountains are visible from the change in surface fluxes. Later in the day the reaction of Q_E and Q_H to reduced shortwave radiation can be seen. The diagonal cloud patterns in the c)-panel of both figures show the movement of clouds with the background wind. The first clouds tend to form over land and upwind of topography. In addition to the boundary-layer clouds that form at the top of local updrafts, some clouds form on the windward side of topography, where air is forced upward.

From Fig. 7 it becomes apparent that clouds are organised and form along bands. Before the development of deep convection, which occurs in both simulations around 15:00h and manifests itself in a large cloud liquid water path (q_{liq}) and dark colours in the plot, there is a period from about 12:00h onwards, when clouds form and dissolve. This starts with a sequence of boundary layer clouds, which become larger over time and then finally deep convection is triggered. These clouds do not seem to be generated randomly, but as the diagonal pattern indicates are linked by the “successive thermal mechanism” (Kirshbaum, 2011). After thermals have become activated ($t > t_*$), they penetrate into dryer layers of the atmosphere, entrain dry air and thus dissolve. As thermals are organised and only occupy a small area of the domain, this corresponds to a selective moistening, which is translated with the background wind. Consequently, thermals entering premoistened areas are less subject to mixing with dry air and thus retain their buoyancy. This leads to preferential cloud development downwind of the precursor thermals. Since we have chosen a lake basin, with topography to the sides, some of the triggered convection is immediately transported out of the area

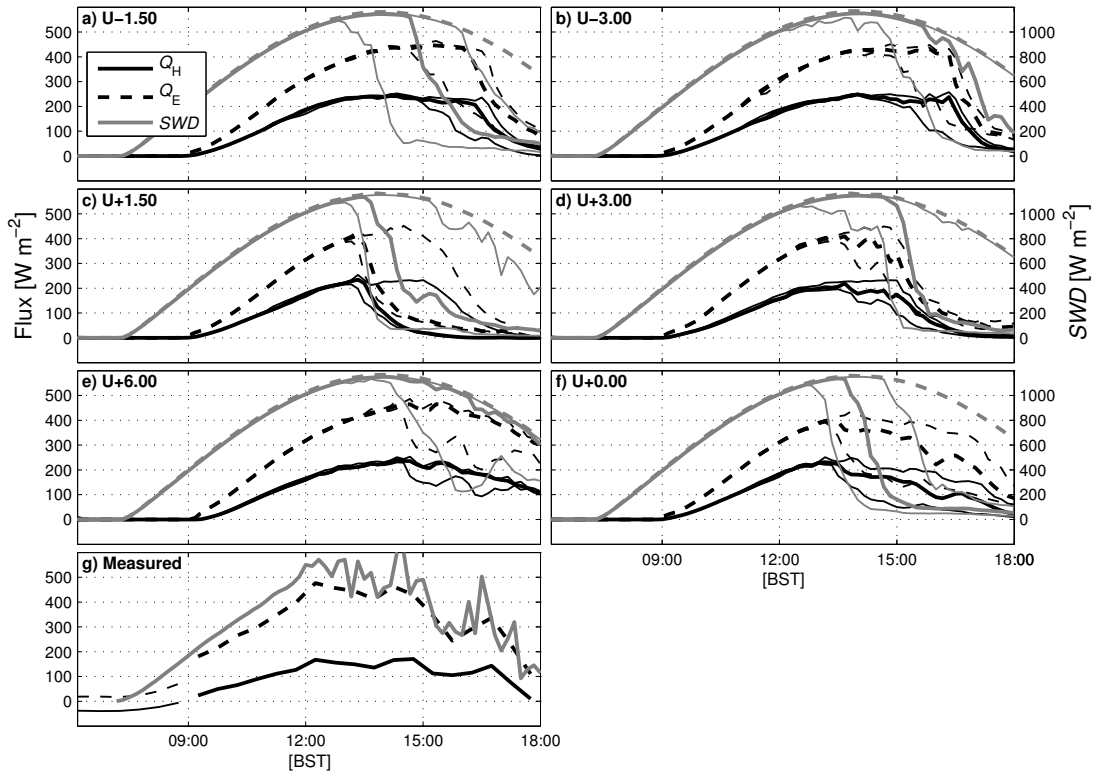


Fig. 6 Development of turbulent surface fluxes in the Nam Co Lake basin for model runs with initial wind of 1.50, 3.00, -1.50, -3.00 and 0.00 ms^{-1} , a–f) respectively (Q_H —; Q_E - -; downwelling shortwave radiation (SWD) grey). Thick black lines correspond to median flux over land. Thin lines are upper and lower quartiles of fluxes. The dashed grey line is clear sky SWD; g) measured turbulent fluxes near Nam Co research station. Thin lines correspond to directly measured EC fluxes on 6 Aug 2009. Thick lines are energy-balance corrected fluxes according to Twine et al (2000).

of analysis. This is especially true for case U–3.00, where deep convection is frequently triggered by the Nyenchen Thanglha. It should also be noted that the relatively slow wind speeds in the upper troposphere reduce wind shear, the entrainment of dry air and the dispersal of moisture, but also lead to a reduction in surface fluxes and thermal activity later in the day.

3.5 Influence of background wind speed and direction on convection triggering

As discussed in section 3.1, the development of the lake-breeze circulation depends on the background wind. The occurrence of boundary-layer clouds within the lake basin depends on the wind direction, and therefore on the result of the interaction between U_g and the sea breeze. Downslope winds lead to adiabatic warming and hence inhibit cloud formation and growth by reducing relative humidity. Air masses ascending on slopes have the opposite effect. This explains why

the cases U–3.00 and U–1.50 have an earlier onset of boundary-layer clouds: As the mountain range located on the southeastern shore is higher than the mountains in the northwest, more clouds are generated there when moist air is forced upward. During the constant growth phase of the boundary layer clouds, characterised by simultaneous increase in cloud top and cloud bottom heights, convective triggering occurs when saturated air masses reach the level of free convection, which develops around 2 km a.g.l., which can be reached by boundary layer growth. We here present two examples of convection triggering, which we suggest to be representative for the triggering of convection in Nam Co region in general. Fig. 9 shows the case U–1.50: Here the background wind and the thermal circulation have both the same sign and transport moist air towards the southeast and over the mountain chain. With the mountain as a trigger, thermals are repeatedly triggered in similar locations, leading to a sequence of convective clouds downstream of the mountain.

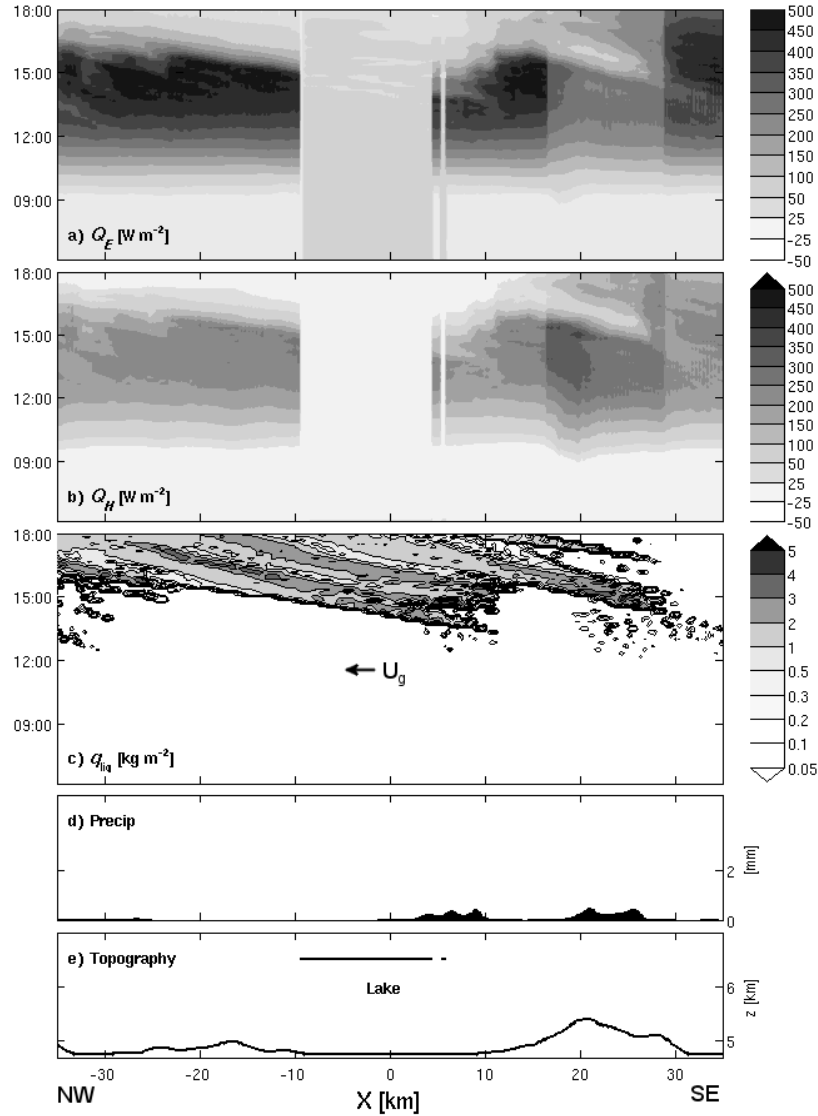


Fig. 7 Hovmöller plot of time [BST] versus horizontal extent of the Nam Co Lake basin for case U+3.00: a) Q_E and b) Q_H [$W m^{-2}$]; c) Total cloud liquid water path q_{liq} [$g kg^{-2}$]; d) Total accumulated precipitation [mm]; and e) Topographic height z and the extent of the lake.

In the second case (U+3.00; Fig. 10), the lake-breeze circulation penetrates into the basin and displaces the warm and moist basin air upwards. This is most pronounced during offshore winds, when the lake-breeze front collides with the background wind. Consequently, convective thermals and eventually deep convection are triggered. In general, frontal collision and the resulting convergence seems to be an important mechanism. Yang et al (2004) described the triggering of secondary convection in Tibetan valleys as gust fronts generated by convective downdrafts causing renewed triggering of convection within the basin.

Similarly, Reeves and Lin (2007) and Miglietta and Rotunno (2009) have studied the propagation of convective systems in mountain flows with respect to the Froude number for highly idealised modelling setups. For low flow speeds ($U < 10 ms^{-1}$) the system was found to be in a blocked state, with a density current travelling against the flow causing precipitation upstream of the topography. These and previous works (Chu and Lin, 2000; Chen and Lin, 2005) highlight the importance of cold pool formation for blocked flows. Low wind speeds are associated with strong cold pools, while at higher wind speeds the advection of heat re-

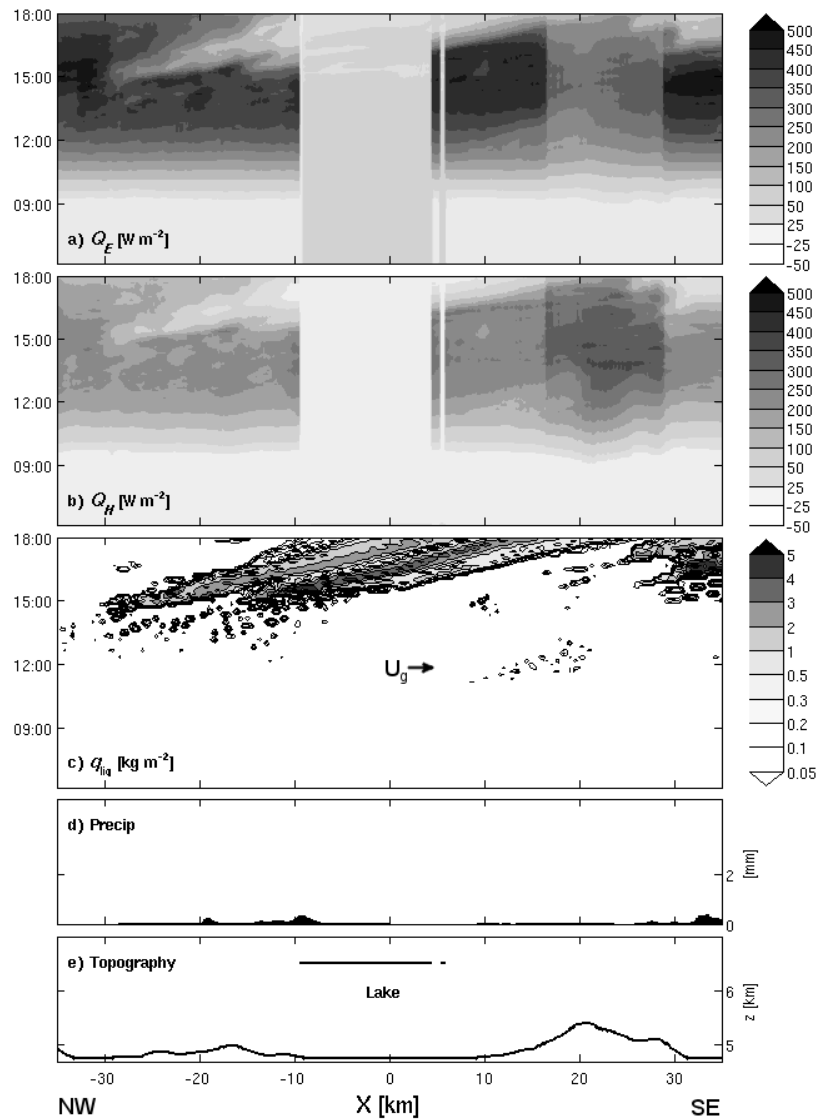


Fig. 8 As Fig. 7, but for case U-3.00.

duces the strength of the cold pool. In this work, the lake breeze and the heated mountain both contribute to the development of a thermal circulation, so that near surface wind speeds are larger than the initialised U_g . Additionally, surface heating through sensible heat fluxes reduces cold pool development and Fig. 9 does not show the development of a strong cold pool. Despite these differences, we see evidence for similar processes during later stages our simulations, where we indeed find the development of a cold pool, as soon as cloud cover results in a decrease of surface heating (not shown).

3.6 Moisture transport and the water cycle

The Nam Co Lake basin is located at the northern fringe of the area influenced by monsoonal circulations during the summer. While the monsoon supplies some water to the area, local recycling of water and the contribution of surface evapotranspiration to the water cycle may be important. For the following analysis we define two control volumes as seen in the sketch of Fig. 11 e): Control volume A corresponds to the boundary layer and lower troposphere in the Nam Co Lake basin and extends to 3km a.g.l. Control volume B is located above A) and extends up to 10km a.g.l. We es-

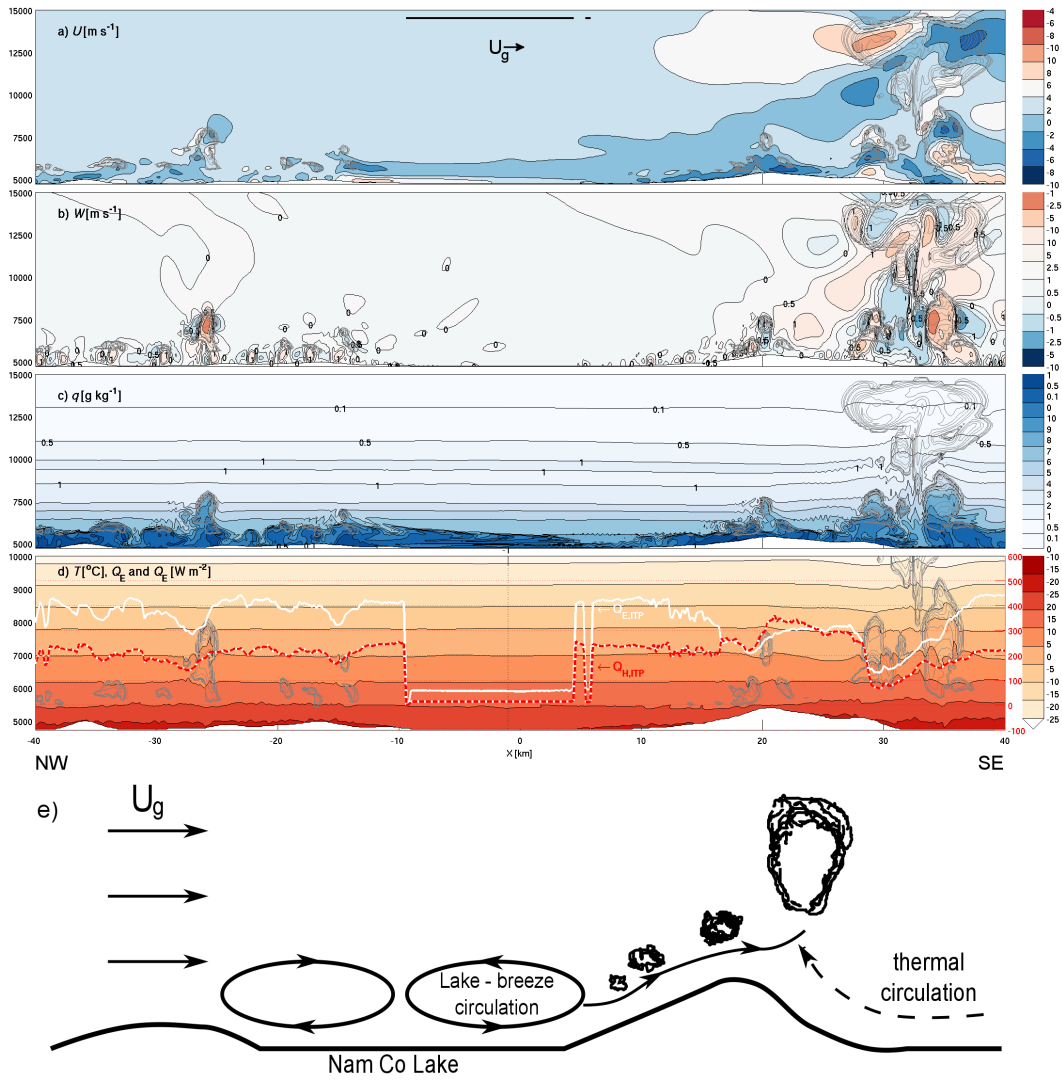


Fig. 9 Modelled a) U [m s^{-1}]; b) W [m s^{-1}]; c) q [g kg^{-1}] and d) T [$^{\circ}\text{C}$] in the Nam Co Lake basin for case U-1.50 at 13:30h BST. Grey contours indicate clouds. The red and white lines indicate Q_H and Q_E with the arrows indicating the magnitude of the measured EC fluxes. The position of the lake is indicated by the black line. Plot e) is a sketch of the mechanism.

timate the transport of moisture, defined as the sum of all water species, across the boundaries of the control volumes as well as evapotranspiration and precipitation as sources and sinks, in order to develop a better understanding of the importance of Nam Co Lake basin for the regional water cycle. The left column of Fig. 11 shows the instantaneous moisture flux for control volume A), while the right column displays the same for volume B) for simulations U-3.00 and U+3.00. The full integrated moisture budget for all simulations is given in Tab. 4.

We find a moistening of the boundary-layer and the lower troposphere and a net export of moisture to the mid troposphere in all cases. The vertical moisture transport from volume A to B is organised into a small number of distinctive events, corresponding to individual convective events carrying water into the mid troposphere. Evapotranspiration, in contrast, is a small continuous flux into Nam Co basin that integrated over the day ($F_{q,ET}$) becomes relatively large and was in most cases approximately twice as large as the flux from volume A to B ($F_{q,3}$). $F_{q,3}$ varied from $0.14 F_{q,ET}$ for U+1.50 to $2.67 F_{q,ET}$ for U-1.50. The transport of

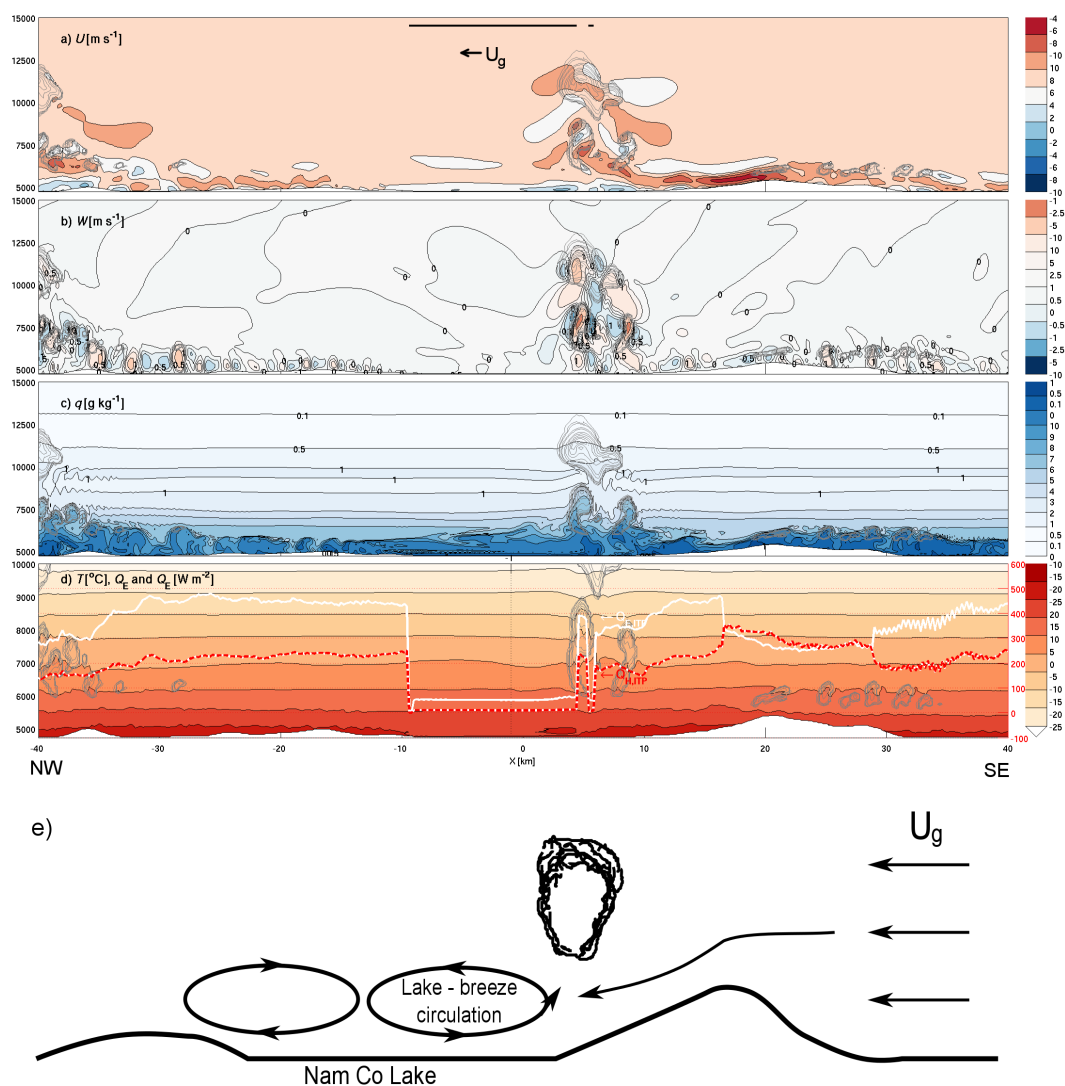


Fig. 10 As Fig. 9, but for case U+3.00 and at 13:50h BST.

moisture above 10km is negligible in terms of the water balance of Nam Co basin. In general we found that the Nam Co Lake basin served as a significant source of moisture to the upper troposphere, where it becomes subject to both transport away from Nam Co Lake and to local recycling through precipitation. Unfortunately, the integration time of our study does not allow us to trace the fate of this moisture during the night, which needs to be done in longer simulations over a larger domain. This study did also not take into account temporal or spatial variation in surface moisture. We started our simulations with a comparatively high surface moisture throughout the domain as the 6 August 2009 was after a period of rain. As a result sim-

ulated and measured Q_E of the land were much larger than the flux from the lake. It is very likely that the importance of the lake as a regional source of moisture becomes more important during drier periods, with large surface heating, such as the pre-monsoon season. As the triggering of moist convection is catalysed by topography, most of the precipitation is also formed over the mountains. Consequently and as many studies show, precipitation is higher over and, in the case of deep convection, on the leeward side of mountains. The Nam Co Lake basin is surrounded by mountain chains and the predominant wind direction is from the northwest, so that we expect precipitation triggered by the Nyenchen Thanglha mountains to occur mainly over

Fig. 11 Instantaneous moisture flux f_q [$\text{kg m}^{-1} \text{s}^{-1}$] for Nam Co Lake basin. a+c) Moisture transport into control volume A, as indicated in panel e) of this figure, representing the Nam Co basin up to 3 km a.g.l.: evapotranspiration (blue); net horizontal flux (—); net vertical flux (---) and resulting total flux (grey). The precipitation flux is not displayed as it is of negligible magnitude. b+d) Transport into the mid-tropospheric control volume B with the same horizontal extent and from 3 to 10 km vertical extent. e) is a schematic drawing of the control volumes.

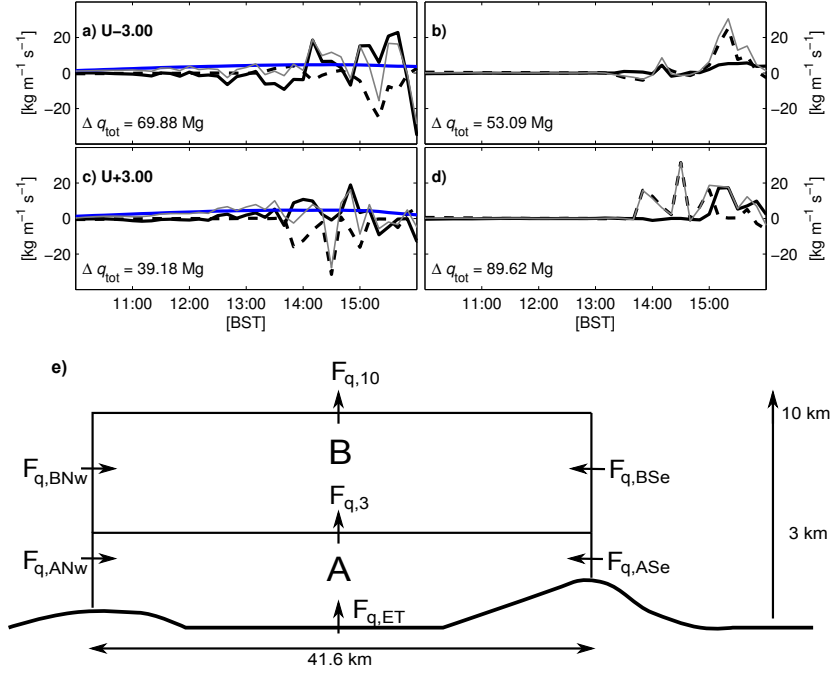


Table 4 Total integrated moisture flux (F_q) into Nam Co Lake basin between 6:00 and 16:00h BST. The control volumes denoted with subscripts *A* and *B* are indicated in Fig. 11 e). The subscripts *Nw*, *Se* for the northwest and southeast boundaries. Positive fluxes across the lateral boundaries indicate flux into the volume. *ET* and *P* are the evapotranspiration and precipitation flux. 3 and 10 indicate the vertical boundaries of the control volumes, with a negative sign for upward flux. Δq_{tot} is the total net moisture flux for a volume.

Case	Volume A				Volume B				$\Delta q_{\text{tot,A}}$ [Mg]	$\Delta q_{\text{tot,B}}$ [Mg]
	$F_{q,\text{ANw}}$	$F_{q,\text{ASe}}$ [Mg]	$F_{q,\text{ET}}$	$F_{q,\text{P}}$	$F_{q,3}$	$F_{q,10}$	$F_{q,\text{BNw}}$	$F_{q,\text{BSe}}$		
U-3.00	825.27	-805.21	86.47	-1.30	-35.35	-0.02	207.30	-189.53	69.88	53.09
U-1.50	385.19	-413.81	85.67	-0.56	-11.83	-0.02	123.07	-103.34	44.66	31.54
U+0.00	-10.65	-15.96	66.32	-1.94	-24.77	-2.10	7.14	18.96	12.99	48.77
U+1.50	-403.60	451.99	73.94	-4.17	-198.10	-1.93	-93.39	109.66	20.06	112.44
U+3.00	-786.45	798.74	85.35	-1.89	-56.56	-0.11	-193.87	225.05	39.18	89.62
U+6.00	-1613.71	1593.66	90.70	-0.49	-45.27	-0.05	-405.13	353.97	24.89	-5.94

the mountain range itself and outside of the basin. Precipitation triggered by the northern mountains likely occurs over the northwest shore or the lake itself. This is also seen in the simulations, where little rain falls over the lake or in close proximity to the shore.

4 Conclusions

This work investigates the development of a lake-breeze system at Nam Co Lake and its interaction with topography and background wind through an idealised modelling study, which did not consider large-scale forcings. We have demonstrated in this setting that 2D

simulations conducted with ATHAM are able to reproduce the system's most important dynamical features, such as the development of a lake-breeze and the transition from shallow boundary-layer clouds to moist convection, reasonably well. While we do acknowledge the limitations of this approach like an unrealistic wind field or overestimation of updraft strength, we think that a better understanding of the system can still be gained from these investigations. Modelled surface fluxes are of realistic magnitude and lead to a realistic timing of the lake breeze providing a triggering mechanism for convection, which is in turn dependent on wind direction and speed. Stronger winds postpone the triggering of convection. An important factor gov-

erning boundary-layer cloud development in the basin is adiabatic warming or cooling as air is transported over topography. This is dependent on wind direction. The interaction or collision of the lake-breeze front with winds coming from the mountain, either as U_g or gust fronts, leads to convergence in the model and subsequently triggering of convection. Additionally, the heated mountains act as a trigger for convection as they represent a heated elevated surface transporting air parcels to the level of free convection. It should be noted though that the effect of albedo change through snow and ice is not considered in this study. This potentially limits the warming effect. Precipitation in the lake basin is mainly generated above the mountains. Therefore stations that are located in the valley have a dry bias and are not representative for the region. This effect is exacerbated by subsidence in the basin caused by the lake. In our future work we will look at the importance of the vertical atmospheric profiles of temperature and moisture and especially stability and smoothness of profiles. Another area of future investigations will also be at the influence of the surface configuration, such as soil moisture or land-use, on turbulent surface fluxes and convection development.

Acknowledgements This research was funded by the German Research Foundation (DFG) Priority Programme 1372 “Tibetan Plateau: Formation, Climate, Ecosystems” as part of the Atmosphere - Ecology - Glaciology - Cluster (TiP-AEG): FO 226/18-1,2. The work described in this publication has been supported by the European Commission (Call FP7-ENV-2007-1 Grant nr. 212921) as part of the CEOP-AEGIS project (<http://www.ceop-aegis.org/>) coordinated by the University of Strasbourg.” The authors wish to acknowledge esri ArcGIS, the Microsoft Corporation and Harris Corp, Earthstar Geographics LLC for the provision of map data of Nam Co Lake. The landcover map was produced by Sophie Biskop and Jan Kropacek within the framework of DFG-TiP. MODIS images were provided through AERONET and we thank the MODIS team for their work. GFS-FNL data was produced by the National Center for Environmental Prediction (NCEP).

References

- Antonelli M, Rotunno R (2007) Large-eddy simulation of the onset of the sea breeze. *J Atmos Sci* 64(12):4445–4457, DOI 10.1175/2007JAS2261.1
- Banta RM (1990) The role of mountain flows in making clouds. In: Blumen W (ed) *Atmospheric Processes over Complex Terrain*, no. 23 in *Meteorological Monographs*, American Meteorological Society, Boston, pp 229–283
- Banta RM, Barker Schaaf C (1987) Thunderstorm genesis zones in the Colorado Rocky Mountains as determined by traceback of geosynchronous satellite images. *Mon Wea Rev* 115(2):463–476, DOI 10.1175/1520-0493(1987)115<0463:TGZITC>2.0.CO;2
- Biermann T, Babel W, Ma W, Chen X, Thiem E, Ma Y, Foken T (2013) Turbulent flux observations and modelling over a shallow lake and a wet grassland in the Nam Co basin, Tibetan Plateau. *Theor Appl Climatol* DOI 10.1007/s00704-013-0953-6
- Chen SH, Lin YL (2005) Effects of moist froude number and CAPE on a conditionally unstable flow over a mesoscale mountain ridge. *J Atmos Sci* 62(2):331–350, DOI 10.1175/JAS-3380.1
- Chu CM, Lin YL (2000) Effects of orography on the generation and propagation of mesoscale convective systems in a two-dimensional conditionally unstable flow. *J Atmos Sci* 57(23):3817–3837, DOI 10.1175/1520-0469(2001)057<3817:E000TG>2.0.CO;2
- Crosman ET, Horel JD (2010) Sea and lake breezes: A review of numerical studies. *Boundary-Layer Meteorol* 137(1):1–29, DOI 10.1007/s10546-010-9517-9
- Cui X, Graf HF (2009) Recent land cover changes on the Tibetan Plateau: a review. *Climatic Change* 94(1):47–61, DOI 10.1007/s10584-009-9556-8
- Cui X, Graf HF, Langmann B, Chen W, Huang R (2006) Climate impacts of anthropogenic land use changes on the Tibetan Plateau. *Glob Plan Change* 54(1-2):33–56, DOI 10.1016/j.gloplacha.2005.07.006
- Cui X, Graf HF, Langmann B, Chen W, Huang R (2007a) Hydrological impacts of deforestation on the Southeast Tibetan Plateau. *Earth Interactions* 11(15):1–18, DOI 10.1175/EI223.1
- Cui X, Langmann B, Graf HF (2007b) Summer monsoonal rainfall simulation on the Tibetan Plateau with a regional climate model using a one-way double-nesting system. *SOLA* 3:49–52
- Emanuel KA (1994) *Atmospheric Convection*. Oxford University Press USA, New York, Oxford
- Fairall CW, Bradley EF, Godfrey JS, Wick GA, Edson JB, Young GS (1996a) Cool-skin and warm-layer effects on sea surface temperature. *J Geophys Res* 101(C1):1295–1308
- Fairall CW, Bradley EF, Rogers DP, Edson JB, Young GS (1996b) Bulk parameterization of air-sea fluxes for Tropical Ocean-Global Atmosphere Coupled-Ocean Atmosphere Response Experiment. *J Geophys Res* 101(C2):3747–3764
- Foken T (2008a) The energy balance closure problem: An overview. *Ecological Applications* 18:1351–1367
- Foken T (2008b) *Micrometeorology*. Springer, Berlin, Heidelberg
- Foken T, Aubinet M, Finnigan JJ, Leclerc MY, Mauder M, Paw U KT (2011) Results of a panel discussion about the energy balance closure correction for trace gases. *Bull Amer Meteor Soc* 92(4):ES13–ES18, DOI 10.1175/2011BAMS3130.1
- Foken T, Leuning R, Oncley SR, Mauder M, Aubinet M (2012) Corrections and data quality control. In: Aubinet M, Vesala T, Papale D (eds) *Eddy Covariance: A practical guide to measurement and data analysis*, Springer Netherlands, Dordrecht, pp 85–131, DOI 10.1007/978-94-007-2351-1_4
- Friend AD, Kiang NY (2005) Land surface model development for the GISS GCM: effects of improved canopy physiology on simulated climate. *J Clim* 18(15):2883–2902, DOI 10.1175/JCLI3425.1
- Friend AD, Stevens AK, Knox RG, Cannell MGR (1997) A process-based, terrestrial biosphere model of ecosystem dynamics (Hybrid v3.0). *Ecological Modelling* 95(2-3):249–287, DOI 10.1016/S0304-3800(96)00034-8
- Gao Y, Tang M, Luo S, Shen Z, Li C (1981) Some aspects of recent research on the Qinghai-Xizang Plateau meteorology. *Bull Amer Meteor Soc* 62(1):31–35, DOI 10.1175/1520-0477(1981)062<0031:SAORRO>2.0.CO;2
- Gerken T, Babel W, Hoffmann A, Biermann T, Herzog M, Friend AD, Li M, Ma Y, Foken T, Graf HF (2012) Turbulent flux modelling with a simple 2-layer soil model and extrapolated

- surface temperature applied at Nam Co Lake basin on the Tibetan Plateau. *Hydrol Earth Syst Sci* 16(4):1095–1110, DOI 10.5194/hess-16-1095-2012
- Gochis DJ, Jimenez A, Watts CJ, Garatuza-Payan J, Shuttleworth WJ (2004) Analysis of 2002 and 2003 warm-season precipitation from the North American Monsoon Experiment Event Rain Gauge Network. *Mon Wea Rev* 132(12):2938–2953, DOI 10.1175/MWR2838.1
- Graf HF, Herzog M, Oberhuber JM, Textor C (1999) Effect of environmental conditions on volcanic plume rise. *J Geophys Res* 104(D20):24,309–24,320, DOI 10.1029/1999JD900498
- Guo H, Penner J, Herzog M (2004) Comparison of the vertical velocity used to calculate the cloud droplet number concentration in a cloud-resolving and a global climate model. In: Carrothers D (ed) Fourteenth ARM Science Team Meeting Proceedings, Department of Energy, Boston, pp 1–6
- Herzog M, Graf HF, Textor C, Oberhuber JM (1998) The effect of phase changes of water on the development of volcanic plumes. *J Volc Geotherm Res* 87(1–4):55–74, DOI 10.1016/S0377-0273(98)00100-0
- Herzog M, Oberhuber JM, Graf HF (2003) A prognostic turbulence scheme for the nonhydrostatic plume model ATHAM. *J Atmos Sci* 60(22):2783–2796, DOI 10.1175/1520-0469(2003)060<2783:APTSFT>2.0.CO;2
- Immerzeel WW, van Beek LPH, Bierkens MFP (2010) Climate change will affect the Asian water towers. *Science* 328(5984):1382–1385, DOI 10.1126/science.1183188
- Kirshbaum DJ (2011) Cloud-resolving simulations of deep convection over a heated mountain. *J Atmos Sci* 68(2):361–378, DOI 10.1175/2010JAS3642.1
- Kirshbaum DJ, Durran DR (2004) Factors governing cellular convection in orographic precipitation. *J Atmos Sci* 61(6):682–698, DOI 10.1175/1520-0469(2004)061<0682:FGCCIO>2.0.CO;2
- Kurita N, Yamada H (2008) The role of local moisture recycling evaluated using stable isotope data from over the middle of the Tibetan Plateau during the monsoon season. *J Hydrometeorol* 9(4):760–775, DOI 10.1175/2007JHM945.1
- Kurosaki Y, Kimura F (2002) Relationship between topography and daytime cloud activity around Tibetan Plateau. *J Meteorol Soc Jap* 80(6):1339–1355
- Kuwagata T, Kondo J, Sumioka M (1994) Thermal effect of the sea breeze on the structure of the boundary layer and the heat budget over land. *Boundary-Layer Meteorol* 67(1–2):119–144, DOI 10.1007/BF00705510
- Kuwagata T, Numaguti A, Endo N (2001) Diurnal variation of water vapor over the central Tibetan Plateau during summer. *J Meteorol Soc Jap* 79(1B):401–418, DOI 10.2151/jmsj.79.401
- Langmann B, Herzog M, Graf HF (1998) Radiative forcing of climate by sulfate aerosols as determined by a regional circulation chemistry transport model. *Atmos Environ* 32(16):2757–2768, DOI 10.1016/S1352-2310(98)00028-4
- Liu WT, Katsaros KB, Businger JA (1979) Bulk parameterization of air-sea exchanges of heat and water vapor including the molecular constraints at the interface. *J Atmos Sci* 36(9):1722–1735, DOI 10.1175/1520-0469(1979)036<1722:BPOASE>2.0.CO;2
- Ma L, Zhang T, Li Q, Frauenfeld OW, Qin D (2008) Evaluation of ERA-40, NCEP-1, and NCEP-2 reanalysis air temperatures with ground-based measurements in China. *J Geophys Res* 113:D15, DOI 10.1029/2007JD009549
- Ma Y, Wang Y, Wu R, Hu Z, Yang K, Li M, Ma W, Zhong L, Sun F, Chen X, et al (2009) Recent advances on the study of atmosphere-land interaction observations on the Tibetan Plateau. *Hydrol Earth Syst Sci* 13(7):1103–1111, DOI 10.5194/hess-13-1103-2009
- Mauder M, Foken T (2004) Documentation and instruction manual of the Eddy-Covariance software package TK2. *Arbeitsergebnisse* 26, University of Bayreuth, Bayreuth, URL <http://opus.ub.uni-bayreuth.de/opus4-ubbayreuth/frontdoor/index/index/docId/639>
- Mauder M, Foken T (2011) Documentation and instruction manual of the Eddy-Covariance software package TK3. *Arbeitsergebnisse* 46, University of Bayreuth, Bayreuth, URL <http://opus.ub.uni-bayreuth.de/opus4-ubbayreuth/frontdoor/index/index/docId/681>
- Masson F, Scherer D, Finkelnburg R, Richters J, Yang W, Yao T (2011) WRF simulation of a precipitation event over the Tibetan Plateau, China – an assessment using remote sensing and ground observations. *Hydrol Earth Syst Sci* 15(6):1795–1817
- Miao JF, Kroon LJM, Vila-Guerau de Arellano J, Holtlag AAM (2003) Impacts of topography and land degradation on the sea breeze over eastern Spain. *Meteorol Atmos Phys* 84(3–4):157–170, DOI 10.1007/s00703-002-0579-1
- Miglietta MM, Rotunno R (2009) Numerical simulations of conditionally unstable flows over a mountain ridge. *J Atmos Sci* 66(7):1865–1885, DOI 10.1175/2009JAS2902.1
- Miller STK, Keim BD, Talbot RW, Mao H (2003) Sea breeze: Structure, forecasting and impacts. *Reviews of Geophysics* 41(3):1011, DOI 10.1029/2003RG000124
- Mlawer EJ, Taubman SJ, Brown PD, Iacono MJ, Clough SA (1997) Radiative transfer for inhomogeneous atmospheres: RRTM, a validated correlated-k model for the longwave. *J Geophys Res* 102(D14):16,663–16,682
- Oberhuber JM, Herzog M, Graf HF, Schwanke K (1998) Volcanic plume simulation on large scales. *J Volc Geotherm Res* 87(1–4):29–53, DOI 10.1016/S0377-0273(98)00099-7
- Ookouchi Y, Uryu M, Sawada R (1978) A numerical study on the effects of a mountain on the land and sea breezes. *J Meteorol Soc Jap* 56:368–386
- Petch JC (2004) The predictability of deep convection in cloud-resolving simulations over land. *QJR Meteorol Soc* 130(604):3173–3187, DOI 10.1256/qj.03.107
- Petch JC (2006) Sensitivity studies of developing convection in a cloud-resolving model. *QJR Meteorol Soc* 132(615):345–358, DOI 10.1256/qj.05.71
- Rampanelli G, Zardi D, Rotunno R (2004) Mechanisms of up-valley winds. *J Atmos Sci* 61(24):3097–3111, DOI 10.1175/JAS-3354.1
- Rebmann C, Kolle O, Heinesch B, Queck R, Ibrom A, Aubinet M (2012) Data acquisition and flux calculations. In: Aubinet M, Vesala T, Papale D (eds) *Eddy Covariance: A practical guide to measurement and data analysis*, Springer Netherlands, Dordrecht, pp 59–83, DOI 10.1007/978-94-007-2351-1_3
- Reeves HD, Lin YL (2007) The effects of a mountain on the propagation of a preexisting convective system for blocked and unblocked flow regimes. *J Atmos Sci* 64(7):2401–2421, DOI 10.1175/JAS3959.1
- Tanaka K, Tamagawa I, Ishikawa H, Ma Y, Hu Z (2003) Surface energy budget and closure of the eastern Tibetan Plateau during the GAME-Tibet IOP 1998. *J Hydrometeorol* 283(1–4):169–183, DOI 10.1016/S0022-1694(03)00243-9
- Taniguchi K, Koike T (2008) Seasonal variation of cloud activity and atmospheric profiles over the eastern part of the Tibetan Plateau. *J Geophys Res* 113(D10):D10,104, DOI 10.1029/2007JD009321
- Tian L, Masson-Delmotte V, Stievenard M, Yao T, Jouzel J (2001a) Tibetan Plateau summer monsoon northward extent revealed by measurements of water stable isotopes. *J Geophys*

- Res 106(D22):28,081–28,088, DOI 10.1029/2001JD900186
- Tian L, Yao T, Numaguti A, Sun W (2001b) Stable isotope variations in monsoon precipitation on the Tibetan Plateau. *J Meteorol Soc Jap* 79(5):959–966, DOI 10.2151/jmsj.79.959
- Trentmann J, Luderer G, Winterrath T, Fromm MD, Servranckx R, Textor C, Herzog M, Graf HF, Andreae MO (2006) Modeling of biomass smoke injection into the lower stratosphere by a large forest fire (Part I): reference simulation. *Atmos Chem Phys* 6(12):5247–5260
- Twine TE, Kustas WP, Norman JM, Cook DR, Houser PR, Meyers TP, Prueger JH, Starks PJ, Wesely ML (2000) Correcting eddy-covariance flux underestimates over a grassland. *Agric Forest Meteorol* 103(3):279–300, DOI 10.1016/S0168-1923(00)00123-4
- Wang J, Zhu L, Daut G, Ju J, Lin X, Wang Y, Zhen X (2009) Investigation of bathymetry and water quality of Lake Nam Co, the largest lake on the central Tibetan Plateau, China. *Limnology* 10(2):149–158, DOI 10.1007/s10201-009-0266-8
- Wu CM, Stevens B, Arakawa A (2009) What controls the transition from shallow to deep convection? *J Atmos Sci* 66(6):1793–1806, DOI 10.1175/2008JAS2945.1
- Xu ZX, Gong TL, Li JY (2008) Decadal trend of climate in the Tibetan Plateau – regional temperature and precipitation. *Hydrological Processes* 22(16):3056–3065, DOI 10.1002/hyp.6892
- Yanai M, Li C, Song Z (1992) Seasonal heating of the Tibetan Plateau and its effects on the evolution of the Asian Summer Monsoon. *J Meteorol Soc Jap* 70(1B):319–351
- Yang K, Koike T, Fujii H, Tamura T, Xu X, Bian L, Zhou M (2004) The daytime evolution of the atmospheric boundary layer and convection over the Tibetan Plateau: Observations and simulations. *J Meteorol Soc Jap* 82(6):1777–1792, DOI 10.2151/jmsj.82.1777
- Yang K, Ye B, Zhou D, Wu B, Foken T, Qin J, Zhou Z (2011) Response of hydrological cycle to recent climate changes in the tibetan plateau. *Climatic Change* 109(3-4):517–534, DOI 10.1007/s10584-011-0099-4
- Yatagai A (2001) Estimation of precipitable water and relative humidity over the Tibetan Plateau from GMS-5 water vapor channel data. *J Meteorol Soc Jap* 79(1B):589–598
- Yin ZY, Zhang X, Liu X, Colella M, Chen X (2008) An assessment of the biases of satellite rainfall estimates over the Tibetan Plateau and correction methods based on topographic analysis. *J Hydrometeor* 9(3):301–326, DOI 10.1175/2007JHM903.1

D. Gerken et al. (2013b)

Gerken, T., Babel, W., Sun, F., Herzog, M., Ma, Y., Foken, T., Graf, H.-F.: *Uncertainty in atmospheric profiles and the impact on modeled convection development at Nam Co Lake, Tibetan Plateau*, J. Geophys. Res., 118, early view, doi:10.1002/2013JD020647, 2013b

Uncertainty in atmospheric profiles and its impact on modeled convection development at Nam Co Lake, Tibetan Plateau

Tobias Gerken,^{1,2} Wolfgang Babel,¹ Fanglin Sun,³ Michael Herzog², Yaoming Ma⁴, Thomas Foken^{1,5} and Hans-F. Graf²

Abstract. This work investigates the influence of atmospheric temperature and relative humidity profiles obtained from radio soundings, NCEP-I and ERA-INT reanalysis and GFS-FNL analysis data on the simulated evolution of clouds and convection at Nam Co Lake on the Tibetan Plateau. In addition to differences in moisture, the initial atmospheric profiles exhibit considerable differences in near-surface temperatures that affect vertical stability. Our analysis is carried out during 2 days in summer 2012 using a 2-D high-resolution modeling approach with a fully interactive surface model so that surface fluxes react to changes in cloud cover. Modeled convection for the radio-sounding profile compares reasonably well with weather observations for the first day, but less well for the second day, when large-scale synoptic effects, not included in the model, become more important. The choice of vertical profile information leads to strongly differing convection development, translating into modifications of the surface energy balance and of the energy and water cycle for the basin. There are strong differences spanning one order of magnitude in the generated precipitation between the model simulations driven by different vertical profiles. This highlights the importance of correct and high-resolution vertical profiles for model initialization.

An edited version of this paper was published by AGU. Copyright 2013 American Geophysical Union.

Citation: Gerken, T, W. Babel, F. Sun, M. Herzog, Y. Ma, T. Foken and H-F. Graf, (2013): Uncertainty in atmospheric profiles and its impact on modeled convection development at Nam Co Lake, Tibetan Plateau, *J. Geoph. Res.*, DOI: 10.1002/2013JD020647.

To view the published open abstract, go to <http://dx.doi.org> and enter the DOI.

Received 30 July 2013; revised 10 October 2013; accepted 23 October 2013.

1. Introduction

The Tibetan Plateau is the largest mountain highland in the world and has an average elevation of more than 4500 m above sea level (asl). As a summer heat source, it acts to modify the monsoon circulation and influences precipitation patterns downstream in Eastern Asia [i.e. Gao et al., 2006; Xu et al., 2008; Chen et al., 2012]. A changing climate and socioeconomic factors contribute to land-use change and pasture degradation [Cui and Graf, 2009], which have an impact on regional circulation, precipitation, cloud cover and hydrological resources [i.e. Cui et al., 2007a, b, 2006; Immerzeel et al., 2010; Yang et al., 2011], and may adversely affect livelihoods.

On the Tibetan Plateau, observations are sparse and there are no permanent weather stations above 4800 m [Maussion et al., 2011], leading to a bias toward lower altitudes. At the same time, reanalysis data sets and gridded precipitation products such as TRMM (Tropical Rainfall Measuring Mission) have large errors due to terrain effects [Frauenfeld et al., 2005; Yin et al., 2008; Ma et al., 2008]. Differences between terrain height and surface levels in global models range from several hundred to almost 2000 m [Wang and Zeng, 2012]. While most comparison studies between observations and reanalysis data focus on ground-based data [Frauenfeld et al., 2005; Ma et al., 2008, 2009; Wang and Zeng, 2012], where systematic biases in elevation can, with some effort, be accounted for, there is to our knowledge only one study, addressing errors in vertical atmospheric profiles of temperature, humidity, and wind speed [Bao and Zhang, 2013]. They compare temperature, moisture, and wind at standard pressure levels, obtained from the GAME-Tibet (Global Energy and Water Exchanges [GEWEX] Asia Monsoon Experiment, 1998) radio soundings with commonly used reanalysis data and find relatively small biases for wind speed and temperature in the averaged data, but considerable biases for relative humidity (RH): Below 200 hPa, ERA-Int (European Centre for Medium-Range Weather Forecasts Interim reanalysis, [Dee et al., 2011]) has a positive bias of approximately 10% RH , while the RH -bias in NCEP/NCAR RA-I (National Centers for Environmental Prediction/National Center for Atmospheric Research Reanalysis-I, [Kalnay et al., 1996]) decreases from +10% close to the surface to -5% at 300 hPa. There was a generally negative temperature bias

¹Department of Micrometeorology, University of Bayreuth, Bayreuth, GERMANY

²Department of Geography, Centre for Atmospheric Science, University of Cambridge, Cambridge, UK

³Cold and Arid Regions Environmental and Engineering Research Institute, Chinese Academy of Sciences, Lanzhou, CHINA

⁴Key Laboratory of Tibetan Environment Changes and Land Surface Processes, Institute of Tibetan Plateau Research, Chinese Academy of Sciences, Beijing, CHINA

⁵Member of Bayreuth Center of Ecology and Environment Research, Bayreuth, GERMANY

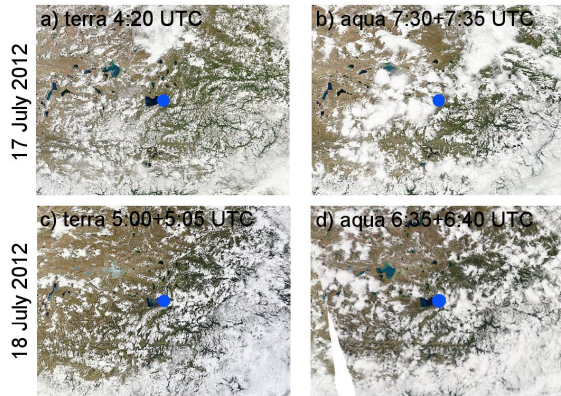


Figure 1. Modis visible composite pictures for 17 and 18 July 2012. Nam Co station (N 30°46.44'; E 90°57.72', 4730 m asl) is indicated by a blue circle.

for both products below 200 hPa (-0.5°C increasing to -2°C with height for ERA-Int and -1.5°C close to the surface decreasing to -0.5°C). There was also a temporal pattern in the discovered biases with the smallest values during the daytime. It should be noted, however, that such a comparison of the mean over a large number of profiles does not address the quality of individual profiles nor the nature of observed profiles between standard pressure levels, which is important for the evolution of convection.

With increasing horizontal and vertical model resolutions, the quality of atmospheric profiles becomes more important as regional weather models start to resolve convection directly. This requires the atmospheric profiles to reflect local conditions and to be of sufficient vertical resolution to adequately model convection.

The total amount of precipitable water in the atmospheric column increases from approximately 5 mm to >15 mm be-

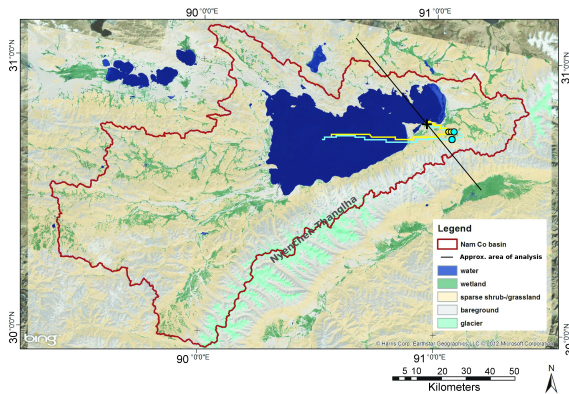


Figure 2. Land-use map of Nam Co Lake created from Landsat data. The yellow and cyan lines indicate the path of radiosonde ascents on 17 and 18 July 2012. The markers (yellow and cyan circles) indicate 10 km above ground level (agl) and the cold point heights. The black cross indicates the location of Nam Co station ©2012 The Microsoft Corporation ©Harris Corp, Earthstar Geographics LLC.

Table 1. Description of the Soil and Surface Parameters Determined for Nam Co Station (N 30°46.44'; E 90°57.72') in Summer 2009 as Well as Leaf Area Index and Vegetation Height Estimated for July 2012.

Parameter	
Texture	sandy
Porosity	0.39
Field capacity	0.05
Wilting point	0.02
Heat capacity (c_p) ($\text{J m}^{-3} \text{K}^{-1}$)	2.2×10^6
Thermal conductivity ($\text{W m}^{-2} \text{K}^{-1}$)	0.20
Surface albedo (α)	0.2
Surface emissivity (ϵ)	0.97
Vegetated fraction	0.6
Leaf area index ($\text{m}^2 \text{m}^{-2}$)	0.6
Vegetation height [m]	0.07

tween premonsoon and monsoon seasons [Taniguchi and Koike, 2008]. Stable isotope investigations indicate that the importance of the Bay of Bengal and the Arabian Sea as a water source for summer precipitation decreases northward on the Tibetan Plateau [Tian et al., 2001, 2003, 2007] as the influence of the monsoon becomes weaker. Isotope measurements at high temporal resolutions show a complex pattern of synoptic, monsoonal precipitation and subsequent water recycling through locally generated precipitation [Kurita and Yamada, 2008].

Atmospheric and ecosystem modeling provide important tools to investigate these developments if they (1) include the relevant processes in their model physics and parameterizations, (2) can be applied on relevant spatial and temporal scales, and (3) can be supplied with initial conditions that reflect the state of the system to be modeled. In Gerken et al. [2012, 2013a] we have demonstrated the first two assertions and will discuss here the third point with respect to atmospheric profiles of temperature and moisture. Five different atmospheric profiles from 17 and 18 July 2012 are combined with field measurements for high-resolution studies of convection development at Nam Co Lake.

During the monsoon season, there is frequent development of deep convection at Nam Co Lake, starting with shallow boundary layer clouds in the morning, which then develop into moist convection. This is partially caused by the interactions between the lake and the complex topography. Scenes taken from MODIS-terra/aqua, which show the development of locally triggered convection at Nam Co Lake, illustrate this development (Figure 1).

The simulations conducted in this study are designed to investigate the impact of different vertical profiles on the simulated convection development at Nam Co Lake. We (1) show that the model is able to reproduce realistic convection development for the local radiosonde profile, (2) investigate the impact of other profiles on simulated convective activity, and (3) discuss its impact by investigations of the energy and water cycle.

These simulations provide valuable information about the impact of uncertainties in atmospheric profiles for the estimation of surface-atmosphere interactions and the surface energy balance in general and specifically for remote and data-sparse regions.

2. Materials and Methods

In this work we conduct 2-D simulations with the ATHAM (Active Tracer High-Resolution Atmospheric Model) model for a cross section through the Nam Co basin (Figure 2). We use realistic topography and a fully interactive surface model in order to gain a better understanding of physical processes involved in the development of convection at the lake. This work uses a similar setup as tested and applied in the 2009 summer monsoon season [Gerken et al.,

2012, 2013a], but uses directly measured profiles and reanalysis data in order to investigate the influence of atmospheric profiles on convection evolution.

2.1. Site Description

From 6 July to 6 August 2012 a field experiment was conducted by the University of Bayreuth in cooperation with the Institute of Tibetan Plateau Research, Chinese Academy of Sciences at the Nam Co Lake Monitoring and Research Station for Multisphere Interactions (N 30°46.44'; E 90°57.72', 4730 m asl) located approximately 300 m from a small lake, which is directly adjacent to the southeast shore of Nam Co Lake (Experiment documentation in Gerken et al. [2013b]). During this period, radiosondes were launched on 8 days for 00, 06, and 12 UTC between 17 and 29 July, while eddy covariance, soil, and standard atmospheric measurements were carried out continuously. The eddy-covariance measurements were post-processed using the TK2/3 software package [Mauder and Foken, 2004, 2011], applying all flux corrections and post-processing steps for turbulence measurements recommended in Foken et al. [2012] and Rebmann et al. [2012]. A portable Vaisala radio-sounding system was deployed, using RS92-SGP sondes, Totex-TA600 balloons, mobile GPS antenna, and processed with SPS-220 and DigiCora III MW21 (v3.2.1). The error of the *RH* measurements is given as < 5% by the manufacturer.

Local solar time (LST) is assumed to be UTC+6, which is in almost perfect agreement with the times of sunrise, noon, and sunset at 23:05, 06:02, and 13:00 UTC as given by the National Oceanic and Atmospheric Administration Sunrise/Sunset Calculator for 17 July. Hence, the soundings correspond to 1 h after sunrise, solar noon and 1 h before sunset.

Soil parameters at the station were measured in 2009 [Biermann et al., 2009], and vegetation parameters were reassessed in 2012 (Table 1). The area around the station is sandy, rather sparsely vegetated, and the soil has little water retention capacity. Gerken et al. [2012] showed that the Bowen ratio at Nam Co station varied considerably from 3 to 0.5 depending on the soil moisture.

2.2. Model Description

We use the non hydrostatic, cloud resolving ATHAM-model [Oberhuber et al., 1998; Herzog et al., 2003], which was designed for the study of volcanic plumes [Graf et al., 1999] and then further developed for biomass-burning plumes [e.g. Trentmann et al., 2006] and clouds [Guo et al., 2004]. ATHAM's dynamic core is capable of solving the Navier-Stokes equations in two or three dimensions, and transported tracers such as all hydrometeors are active in the sense that they influence heat capacity and density of the mixture at each grid point [Oberhuber et al., 1998].

The physical processes included in the model for this work are as follows: 1.5-order turbulence closure predicting horizontal and vertical turbulent kinetic energy as well as turbulent length scale [Herzog et al., 2003], short- and long-wave radiation [Langmann et al., 1998; Mlawer et al., 1997], bulk-microphysics [Herzog et al., 1998], the modified Hybrid (v6) land surface model [Friend et al., 1997; Friend and Kiang, 2005; Gerken et al., 2012] and the Coupled Ocean-Atmosphere Response Experiment (COARE) - algorithm v2 [Fairall et al., 1996a, b] water surface scheme for turbulent energy fluxes above land and Nam Co Lake, which has a mean depth of >50 m [Wang et al., 2009]. The surface models were demonstrated to perform well at this site in Gerken et al. [2012].

2.3. Model Setup and Cases

Both the lake shore and the Nyenchen Thanglha mountain chain are oriented almost parallel to each other so that a

2-D cross section is capable of simulating the most important dynamical features of the lake-mountain system. The mountain chain is located approximately 10 km south of Nam Co Lake. In the absence of large-scale forcings, the circulation in the basin is primarily driven by a lake breeze and a thermal mountain circulation, which was successfully simulated in 2-D [Gerken et al., 2013a]. The horizontal domain cuts across Nam Co Lake research station, where our measurements were situated, and through a relatively low section of the mountain chain. As 2-D simulations have a tendency to overestimate the influence of topography, we deem this acceptable. The domain size is 153.6 km using 200 m horizontal resolution, which gives a total number of horizontal grid points of $nx = 770$. The lateral boundary conditions are cyclic for momentum, but hydrometeors and water vapor in excess of the initial profile are removed without perturbing density. There are 175 layers, starting at 50 m vertical resolution for the first 50 layers, then stretching to a constant vertical resolution of 200 m for the last 50 layers below the model top, set to 17.5 km above ground level (agl). The model topography uses the ASTER-DEM (Advanced Spaceborne Thermal Emission and Reflection Radiometer-Digital Elevation Model) with 90 m resolution smoothed with a 2 km moving window, removing vertical cliffs and single grid point depressions. A sensitivity study into the effects of topographic smoothing on our results showed, that smoothing windows ≤ 2 km only have a small influence on the shape of topography and the maximum elevation of the relief. The variation in generated precipitation was considerably smaller than the variation between the cases chosen in this work (see supporting information for details). As we are interested in the Nam Co basin, the topography outside is set to the lake level and turbulent surface fluxes are gradually reduced to zero near the lateral boundary. The simulations are integrated from the initial profile for 12 h with a timestep of 2.5 s from 04:00 LST to 16:00 LST. No synoptic effects or external changes to the profile are included in the model, so that large-scale weather developments cannot be reproduced.

We acknowledge the limitations of our approach, which arise from the lack of a third dimension and thus result in a simplified flow field and reduced entrainment of dry air into convective updrafts, potentially leading to an overestimation of convective activity. But as the focus of this work is on the comparison of the convection development between profiles rather than attempting to simulate specific days, we believe that the chosen approach yields valuable information about the interaction of processes during convection evolution and about the impact of uncertainty in atmospheric profiles on convection. Additionally, we lack distributed observations that would be required to validate the results of 3-D simulations.

This work investigates the development of moist convection on 17 and 18 July 2012 using five different vertical atmospheric profiles of temperature (T) and relative humidity (RH). The cases denoted RS use the original measured radiosonde profile. StdLev uses standard pressure levels (500, 400, 300, 250, 200, 150, 100, 70, and 50 hPa) extracted from RS, NCEP uses the NCEP/NCAR Reanalysis-I

Table 2. Soil Model Initialization for Temperature and Upper-Layer Soil Moisture: T_0 , \bar{T}_1 , and \bar{T}_2 Correspond to “Skin” Temperature and Mean Layer Temperatures for the First and Second Model Layer (0.1 and 4 m Layer Depth)^a.

Date	T_0 (°C)	\bar{T}_1 (°C)	\bar{T}_2 (°C)	SM_0 (-)
17 July	4.5	6.8	2.6	2.0
18 July	7.1	9.0	3.3	2.0

^a SM_0 is upper-layer soil moisture expressed in terms of field-capacity. The model initialization procedure follows Gerken et al. [2012] using soil data measured at Nam Co station.

[Kalnay et al., 1996], ERA uses the ERA-Interim reanalysis [Dee et al., 2011] and GFS uses the Global Forecasting System’s final analysis product (GFS-FNL) [Kanamitsu et al., 1991; Caplan et al., 1997]. For model initialization the initial RH is reduced to a maximum of 90% in order to prevent cloud formation at the start of the integration time.

In this work the focus was placed on the impacts of T and RH , so that the initial geostrophic wind speed was uniformly set to 3 m s^{-1} , which produced most realistic convection in Gerken et al. [2013a]. This also addresses that the 2-D simulations are highly sensitive to wind shear [i.e. Kirshbaum and Durran, 2004].

The surface configuration for both days is presented in Table 2. The lake surface temperature is initialized with 10°C , which corresponds to the mean temperature of Nam Co Lake in July and August for 2006–2008 [Haginoya et al., 2009].

2.4. Atmospheric Profiles

Both days selected for our analysis show a development from fair weather cumulus in early morning to observed *Cumulonimbus* activity from the midmorning onward (10:00 and 9:00 LST for 17 and 18 July), as is frequently observed in the Nam Co Lake basin. Figure 3 displays the vertical profiles for temperature, relative humidity, and wind speeds for these 2 days at 00 UTC (6:00 LST). The radiosondes launched at Nam Co show that both measured profiles have inversion layers of more than 0.5 K temperature increase in the mid-troposphere. These are most likely the result of large-scale subsidence. While there is little synoptic activity on 17 July, the NCEP-I reanalysis and the decrease in relative humidity indicate that the Nam Co region becomes influenced by large-scale subsidence on the following day. The cold point in the profiles is approximately at 85 hPa or 13 km agl (not shown). For T , there is little difference between the sounding and the gridded products above 300 hPa, whereas differences of several K are found below. In both days, ERA underestimates temperatures close to the surface, while GFS overestimates them considerably. In terms of RH , there are much greater differences between the profiles. The gridded data sets reflect less the observations from radiosondes. For 17 July, there is a good agreement between RH at Nam Co and Nagqu, a permanent sounding station located 2° to the East and 0.75° to the North, while the Lhasa sounding station (1° to the South) shows a different profile. This indicates that moisture fields are not purely determined by local conditions but are also dependent on air masses and their advection. There is little agreement between gridded products. GFS and NCEP agree reasonably well with the sounding in the lower troposphere, but there is no RH data available above 300 hPa for NCEP. ERA-Int and GFS are excessively moist aloft, with ERA-Int being generally too moist, despite being the highest spatial resolution data set. The sounding of 18 July is overall moister than the day before. Interestingly, NCEP closely reflects the Lhasa sounding for both days, which is assimilated into the reanalysis. The gridded products show little variability between each other and between days, while the soundings are noisier and deviate at some altitudes where high wind speeds are found.

3. Results

Our simulations show the development of clouds, which are defined for the purpose of this work as grid cells with a total content of condensed ice and water of $q_t > 10^{-3} \text{ g kg}^{-1}$, and convection within the Nam Co basin. Shortly after the start of the simulations, shallow boundary layer clouds form, which subsequently grow deeper with moist and deep convection developing later in the day. As in Gerken et al. [2013a], we use the center of the cloud mass (Z_c) as a diagnostic for the activation of clouds [Wu et al., 2009], which

will develop into moist convection:

$$Z_c = \frac{\int \int q_t z dx dz}{\int \int q_t dx dz}, \quad (1)$$

with z as the vertical coordinate and $dx dz$ as the area element to be integrated over.

For both days it is apparent that simulations initialized with atmospheric profiles from different sources lead to big differences in convective development. Convection occurs in several phases with all simulations reaching similar cloud morphology, but showing differences in timing that are related to feedbacks between vertical profiles, surface fluxes, and cloud microphysical structure (Figure 4 and 5).

On 17 July for RS, there are shallow boundary layer clouds until 7:00 LST, and then there is a transitional period with activated clouds that form and dissolve, while at the same time the cloud top height and the center of the cloud mass increase in height. At approximately 10:30 LST simulated convection suddenly becomes deep and substantial rain is generated. The weather observations for Nam Co station for 17 July show the first *Cu congestus* clouds at 8:00 LST and a heavy thunderstorm was recorded over the plain south of Nam Co station at 11:30 LST, which dissolved after approximately 30 min. More *Cumulonimbus* clouds were observed during the afternoon. This illustrates the rapid convection development in the Nam Co basin. Compared to RS, StdLev shows a more continuous convection development with time, which only accelerates in the afternoon. The convection development in RS on the other hand is characterized by sudden increases in the center of the cloud mass. This is likely to be associated with layers of high stability at 1.5, 3, and 5 km agl found in the sounding (Figure 6). Convection development in NCEP appears to be an intermediate between RS and StdLev both in terms of Z_c and mean cloud concentrations, which is not surprising given the close similarity of NCEP to the sounding at the standard pressure levels. ERA, the moistest case, has the fastest development of convection and produces the largest amount of clouds and precipitation. GFS in contrast shows the longest delay between the activation of clouds, which is followed by a relatively fast growth in convective height after 10:00 LST. It also produces by far the least amount of rain and has lower cloud concentrations, than RS.

On 18 July there are similar differences in precipitation and convection development between the cases: RS shows a step-pattern in the development of convection that is associated with a strong inversion layer at around 4 km agl. After the first activation of boundary layer clouds, clouds are confined below the inversion until deep convection develops at approximately 10:30 LST. StdLev, in contrast, develops both faster and stronger resulting in maximum precipitation rates comparable to the much moister ERA case. Convection in ERA develops later with all clouds confined to the first 2 km above ground until 10:00 LST. The NCEP run appears to be comparable to StdLev for cloud concentration, convection development, and precipitation timing although the amount of precipitation is smaller than StdLev. As on the previous day, the GFS case develops late and produces little precipitation. GFS’s high cloud top height in the morning is not caused by convection, but results from mountain waves leading to condensation and a layer that is considerably moister than the day before.

The following sections discuss the generation of precipitation (section. 3.1), the influence of vertical stability (section. 3.2) and the impact of convection on the surface energy budget (section 3.3). Sections 3.4 and 3.5 discuss the profile evolution and feedbacks between clouds and the surface.

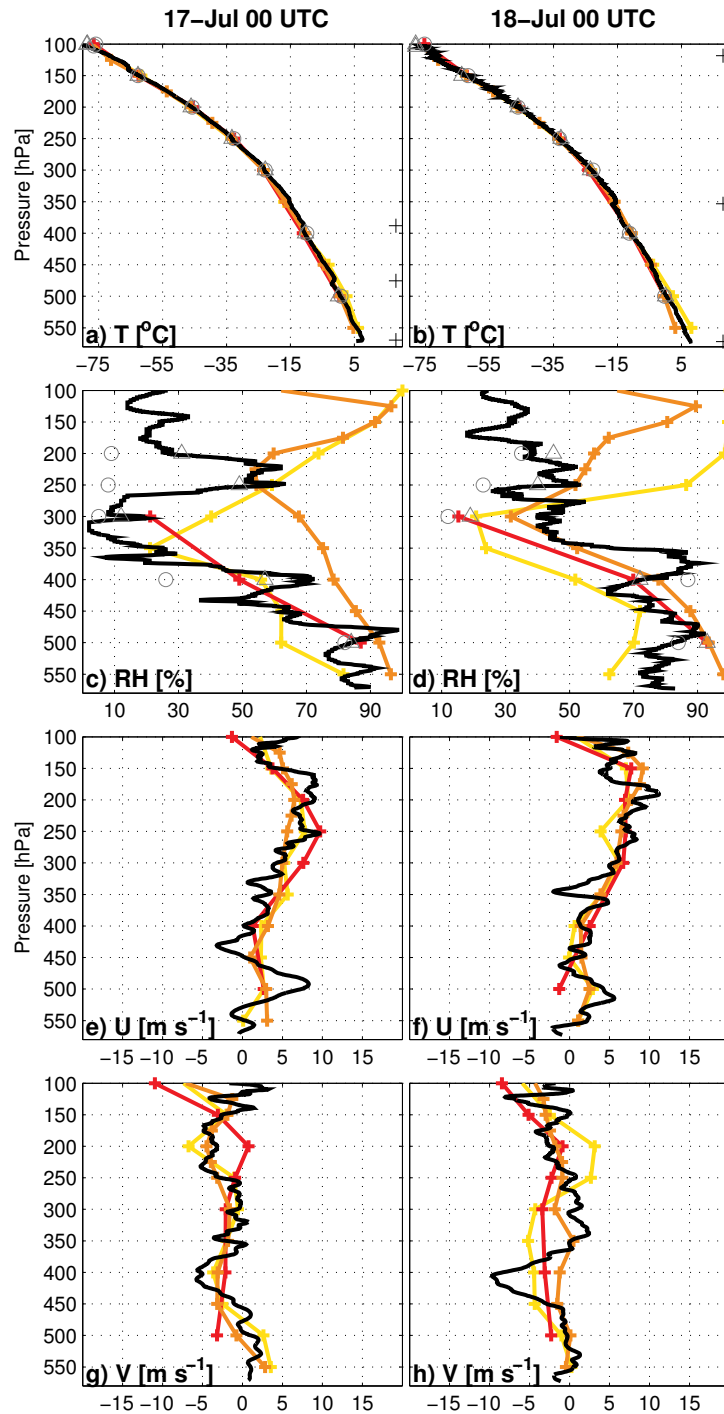


Figure 3. Vertical profiles for 17 and 18 July 2012 00 UTC (6:00 h Local time) at Nam Co station (N30°46.44'; E90°57.72') as determined by radiosonde ascent (black), NCEP reanalysis (red), ERA-Interim (orange), and GFS-FNL analysis (yellow). The gray circles and triangles indicate the radiosonde measurement at Nagqu (N31°28.8'; E92°03.6', circle) and Lhasa (N29°39.6'; E91°07.8', triangle): (a, b) T [°C]; (c, d) RH [%]; (e, f) U [m s^{-1}] and (g, h) V [m s^{-1}]. The black crosses indicate the height of inversion layers with more than 0.5 K increase in temperature. Gridded products are bilinearly interpolated to the station location.

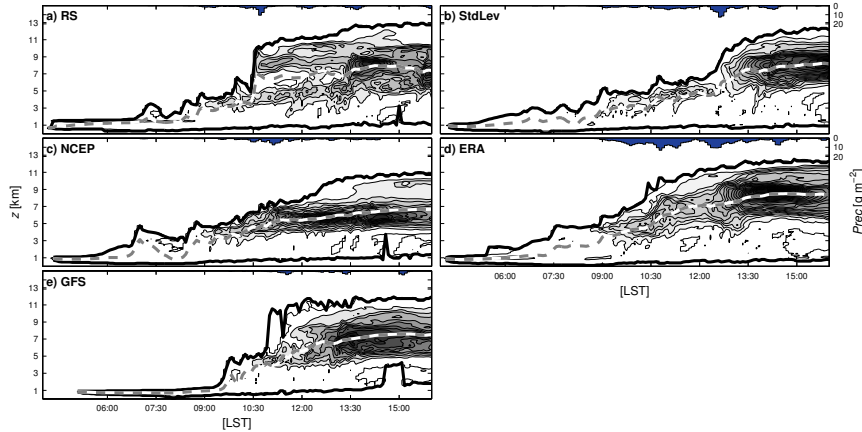


Figure 4. Modeled development of convection at Nam Co Lake for cases (a) RS, (b) StdLev, (c) NCEP, (d) ERA, (e) and GFS on 17 July 2012: Contours correspond to mean cloud particle concentrations in the Nam Co Lake basin. Each contour level corresponds to 0.1 g m^{-3} . The dashed line indicates the height of the center of cloud mass (Z_c), and black lines indicate cloud top and cloud bottom heights. The blue shaded area shows the accumulated precipitation.

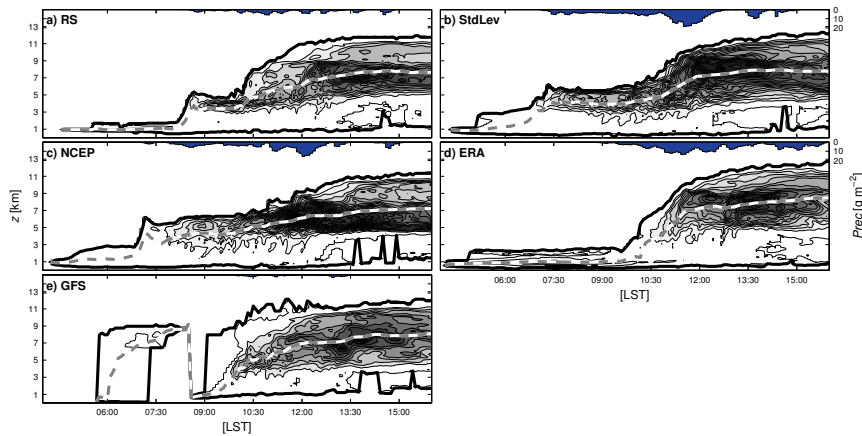


Figure 5. As in Figure 4, but for 18 July 2012.

3.1. Precipitation

A key variable governing environmental processes on the Tibetan Plateau is precipitation. There is a large difference in the dynamics and total amount of simulated precipitation between the cases. Atmospheric stability and surface flux dynamics impact the development of convection and thus of precipitation. The microphysics used in this work includes graupel and rain. Snow is not represented separately. We are more interested in the comparison between the different cases than in the absolute values. The 18 July produces a larger amount of simulated precipitation than 17 July for all cases except GFS, which is related to the moister initial profiles. In reality though, this day was influenced by upper level drying, a synoptic effect not included in our simulations, suppressing convection. There is approximately one order of magnitude difference in the deposited precipitation between the driest case (GFS) and StdLev or ERA, which are the wettest (Table 3). When distinguishing between precipitation that falls within the basin ($Prec_B$) and the total precipitation ($Prec_{tot}$), we find that a substantial fraction (25–60%) of the simulated precipitation occurs within the Nam Co basin, which is defined here as the area between the

Table 3. Deposited Total Precipitation at Nam Co Lake for the Model Runs on 17 and 18 July 2012 within the Nam Co Basin as Defined in the Text $Prec_B$ and Entire Domain $Prec_{tot}$.

Run	17 July 2012		18 July 2012	
	$Prec_B$ [m^3]	$Prec_{tot}$ [m^3]	$Prec_B$ [m^3]	$Prec_{tot}$ [m^3]
RS	9.8	17.3	11.6	23.2
StdLev	11.1	28.1	43.4	73.7
NCEP	5.7	18.5	34.2	52.9
ERA	19.4	58.5	19.9	71.3
GFS	3.9	9.5	2.2	6.1

lake and the top of the Nyenchen Thanglha mountain chain in the south and an equal area north of Nam Co Lake. Nam Co Lake is situated at the northern edge of the area influenced by the monsoonal circulation. The lake itself may be a water source for the region through the export of moisture from the basin, especially during breaks in the monsoon. A competing hypothesis to this is that Nam Co Lake mainly constitutes a closed water cycle, where the evaporated water is deposited as precipitation on the surrounding mountain slopes and thus remains within the catchment.

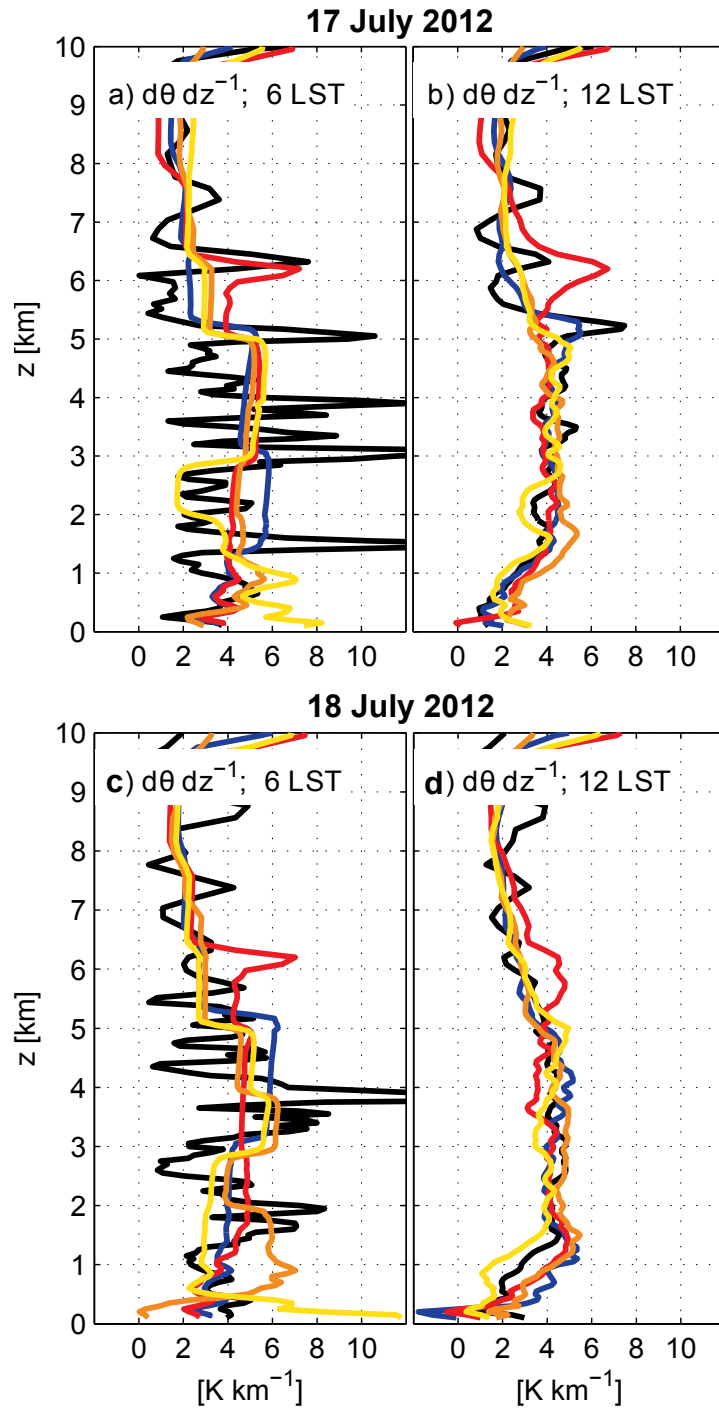


Figure 6. Atmospheric lapse rate ($d\theta dz^{-1}$, K km^{-1}) for simulations of 17 July 2012 at 6:00 and 12:00 LST (a, b) and 18 July 2012 (c, d) for profiles from cases RS (black), StdLev (blue), NCEP (red), ERA (orange), and GFS (yellow).

The precipitation simulated in this work is consistent with locally generated cumulus convection frequently observed on the Tibetan Plateau [i.e. *Uyeda et al.*, 2001], which is controlled by the surface and triggered over mountain ranges [*Gerken et al.*, 2013a]. According to *Fujinami et al.* [2005] and *Sato et al.* [2007], there is a second major source of precipitation within Tibetan mountain valleys, occurring in the evenings, when the reversal of the daytime thermal circulation leads to convergence and moist convection in the valley centers. This effect, not included in our studies, would increase the percentage of locally deposited precipitation. Overall, recycling of locally generated precipitation is likely to be an important part of the water cycle at Nam Co Lake. Our findings also highlight the importance of initialized profiles for the generation of precipitation and show that the considerable uncertainty in *RH* and surface effects, impacting stability, lead to large uncertainties in precipitation.

3.2. Influence of Atmospheric Stability

We expect atmospheric stability to play an important part in controlling convective evolution at Nam Co Lake. Additionally, vertical profile resolution and inversion layers matter. For 17 July (Figures 6a and 6b) there is direct evidence from the step-wise increase in cloud heights as displayed in Figure 4 that the stable inversion layers in the radiosonde below 4 km agl profile have a delaying effect on convection development and precipitation generation. Until 7:00 LST, clouds remain below the inversion layer at 1 km agl and later the center of the cloud mass is confined to altitudes below the higher stable layers until after 10:00 LST, when the inversion layers of the initial profile have been eroded. While the potential temperature gradient ($d\theta/dz$) of StdLev is close to the mean gradient of RS, there is a more gradual development of convection in the absence of distinct inversion layers. In general, the stability of all profiles in the middle troposphere is comparable, but there are differences below 3 km agl that influence cloud development: GFS is the most stable profile near the surface and the least stable for higher altitudes. Hence, the late activation of clouds is followed by rapid growth in cloud height around 10:00 LST. There is some convergence between the profiles of different sources for 12:00 LST that highlight the influence of surface heating. However, especially for GFS and RS, some features of the initial profile remain distinguishable. The development of the stable layer in NCEP is associated with the absence of moisture in the initial profile above 300 hPa, which causes instability in the atmospheric profile initialized by ATHAM.

There is a similar situation for 18 July (Figures 6c and 6d), where the layer of high stability below 4 km agl in the RS case coincides with a plateau in the convection development between 9:00 and 10:30 LST. However, StdLev has a similar plateau but no inversion layers or particularly high stability below 6 km agl. We suspect two reasons for the effect. First, the stability of StdLev is highest of all profiles at this altitude and, second, the feedback between cloud cover and surface fluxes leads to a reduction of surface fluxes and thus of convective activity. This is further discussed in the next section. ERA is the least stable profile in proximity to the surface and then most stable below 2 km agl, explaining the late activation of clouds and the fact that moist convection does not occur before 10:00 LST.

3.3. Energy Transfer to the Atmosphere

The surface energy-balance of the Tibetan Plateau is a key factor to understand regional climate. This section discusses the impact of different profiles for the simulated surface energy-balance. The ATHAM modeling system is set up with an interactive surface. Clouds modify the available radiation and thus have direct impact on the surface energy-balance and consequently on turbulent energy fluxes. Due to

the remoteness and thus low aerosol loading on the Tibetan Plateau [*Cong et al.*, 2009] and its high elevation, there is little indirect shortwave radiation, so that cloud shading effects are stronger compared to other regions. The surface and its reaction to shading impact the development of convection by controlling sensible heat and water vapor fluxes. As a consequence, and unlike simulations with prescribed idealized fluxes as are commonly used in high-resolution simulations, we expect feedbacks between convection development and the total energy exchanged through turbulent surface fluxes. One measure of these interactions are the spatially and temporally integrated turbulent surface fluxes. Despite the removal of condensate at the lateral boundary, which reduces cloud cover and increases insolation near the boundary, simulations are comparable to each other and we believe that the comparison of the runs in terms of relative values yields more information than the total amount of energy that is supplied to the atmosphere.

Figures 7 and 8 show the integrated turbulent surface fluxes separated for the lake surface, the land area adjacent to the lake (called plain), and the total domain. The plain is defined as the area between the lake and the Nyenchen Thanglha mountain chain plus an equal area to the north of the lake. Sensible heat fluxes from the lake, both simulated and measured [*Biermann et al.*, 2013], are small compared to the land surface, so that the variations' influence on the total energy balance are negligible. For latent heat, where the lake does have a significant contribution to the total energy and water vapor that is supplied within the basin, there are differences of up to 50% between runs.

On 17 July (Figure 7), there is little variation in the sensible and latent energy contributions between the simulated cases. For the basin fluxes ($E_{\text{sens,plain}}$ and $E_{\text{lat,plain}}$) StdLev is approximately 30% larger than the rest of the fluxes. The simulations using GFS, which has the latest triggering convection, do not have a higher energy contribution than the rest of the simulations due to strong modeled convection after 11:00 LST, leading to reduced energy input during the time of strongest solar radiation. For the whole domain there are two groups with NCEP and ERA having smaller $E_{\text{sens,plain}}$ and $E_{\text{lat,plain}}$ than the other simulations. This is despite the substantially differing initialization profiles and differences in simulated convection. However, as discussed in the next section, in both cases, the model has developed similar atmospheric profiles of T and RH in the middle troposphere at 12:00 LST.

For 18 July (Figure 8) there is a larger scatter in surface heat fluxes than during the previous day, and there are different evolutions for the latent and sensible heat fluxes. For both $E_{\text{sens,plain}}$ and $E_{\text{lat,plain}}$ StdLev and NCEP have the lowest energy transfer, which is explained by their similar convection dynamics and early triggering, while ERA has the largest energy flux despite being the moistest close to the surface. GFS has a large contribution to the latent heat flux over land, but not for sensible heat. Interestingly, for GFS, lake fluxes behave differently to land fluxes, which is due to higher water vapor mixing ratios over water for GFS.

In general, there is considerable variation in the total amount of energy that is transferred from the surface to the atmosphere ranging up to 50% between the cases. The absolute variation is larger for latent than for sensible heat but is comparable when normalized with the magnitude of the fluxes.

3.4. Profile Development

The above analysis is dependent on reasonable model performance. We, therefore, compare the development of the vertical profiles in the simulated cases with respect to the radio sounding and reanalysis data. As previously mentioned,

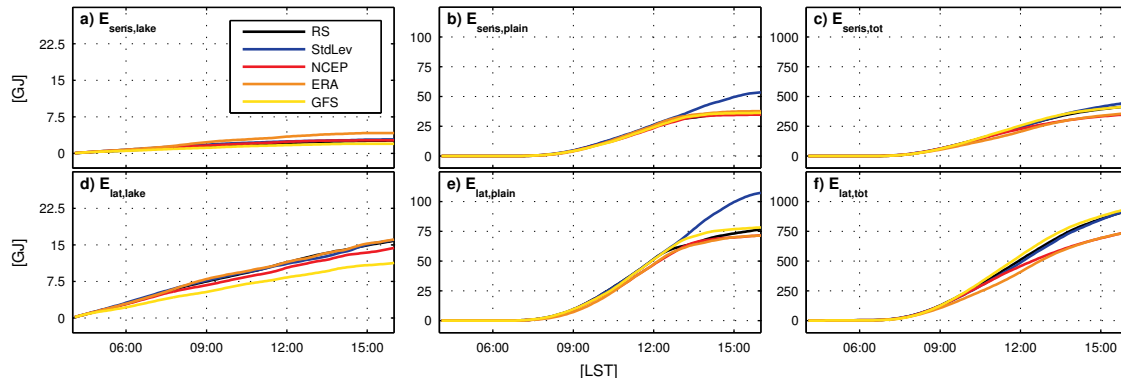


Figure 7. Spatially and temporally integrated turbulent energy fluxes (E) at Nam Co Lake for cases RS, StdLev, NCEP, ERA and GFS on 17 July 2012: a+d) Sensible and latent energy over lake, b+e) over plain adjacent to lake and c+f) in total domain.

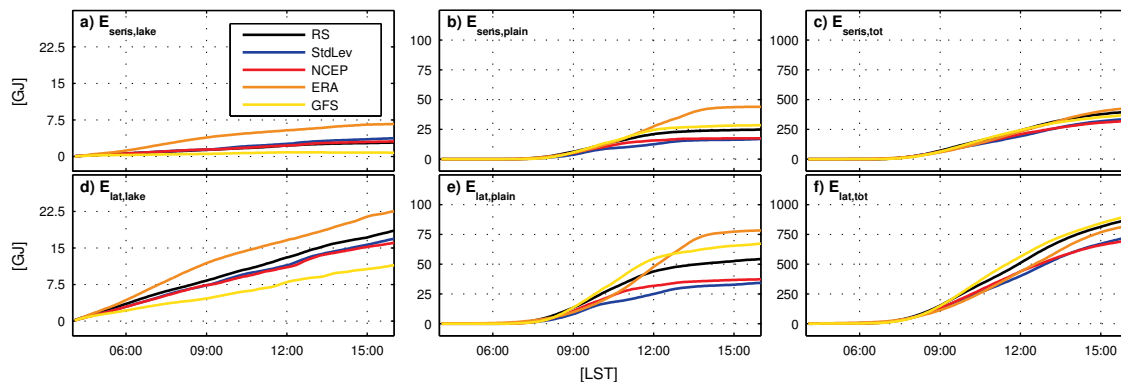


Figure 8. As in Figure 7, but for 18 July 2012.

we chose 4:00 LST as start time of the simulations, which corresponds to 1 h before sunrise, while the atmospheric data is from 6:00 LST or 1 h after sunrise. We assume that there is little change in the profile over this 2 h period, which is confirmed for all cases, because modeled and observed surface fluxes are small, so that little heat is transferred from the surface to the atmosphere.

Figures 9 and 10 show the modeled atmospheric profiles compared to the radio soundings and reference profiles at 6:00 LST and 12:00 LST (00 UTC; 06 UTC). On the first day (Figure 9) the simulated temperature profile in the RS case (Figure 9a) closely resembles the sounding profile for 12:00 LST, except that the inversion layer at 3.7 km agl has eroded. StdLev is very similar to RS. For RH , the situation is different: Up to 3 km agl, the mean RS humidity profile matches the sounding, but between 3 and 5 km agl and above the height of the initial inversion layer, there is substantially more moisture in the case RS than in the observed profile. This is due to simulated convection. While there is some increase of moisture in the 06 UTC sounding above 3 km and weather observations report the occurrence of *Cb incus* clouds from 10:00 LST as well as a thunderstorm at 11:30 LST, the convective transport of moisture is overestimated in the RS simulation. This is likely to be attributed to the 2-D approach, which underestimates entrainment of dry air into thermals. Above 5 km, the 06 UTC sounding profile has dried considerably compared to the 00 UTC sounding, which is not reproduced in the simulations due to the exclusion of synoptic effects.

For the cases initialized with gridded products, it clearly shows that the simulations and their RH profiles are dom-

inated by the initialized water vapor contents. Cases ERA and GFS are much too moist above 3 km compared to the observed 06 UTC data. In general, the differences in temperature and RH between the different simulations for the lowermost 3 km have decreased, which indicates the influence of the surface on both the boundary layer (approximately 2 km high) and the lower troposphere in general.

All simulations are moister than the measured profile in close proximity to the surface, which might be due to the fact that the mean profile also contains lake cells, whereas the radiosonde was launched in several hundred meters distance to water bodies.

For the second day (Figure 10), the situation is different. With respect to temperature, there is still a reasonable agreement between the simulated and measured temperature profiles, but for RH they show little agreement. While one could argue that boundary layer moisture profiles are reasonably close to the observed sounding data and the gridded products, the 06 UTC radio sounding is very dry above 4 km agl and is substantially drier throughout the entire column. As RH is influenced by both absolute water contents and temperature, the drier boundary layer can be explained by the higher temperatures, but above that there is no indication of a substantially warmer profile. However, the NCEP reanalysis shows the region to be in subsidence, which would lead to a reduction in RH and, in addition, advection of dry air under the prevailing west-wind conditions might be responsible. Nevertheless, there were *Cb incus* clouds observed in the Nam Co basin during the afternoon of 18 July, showing that convection was indeed taking place.

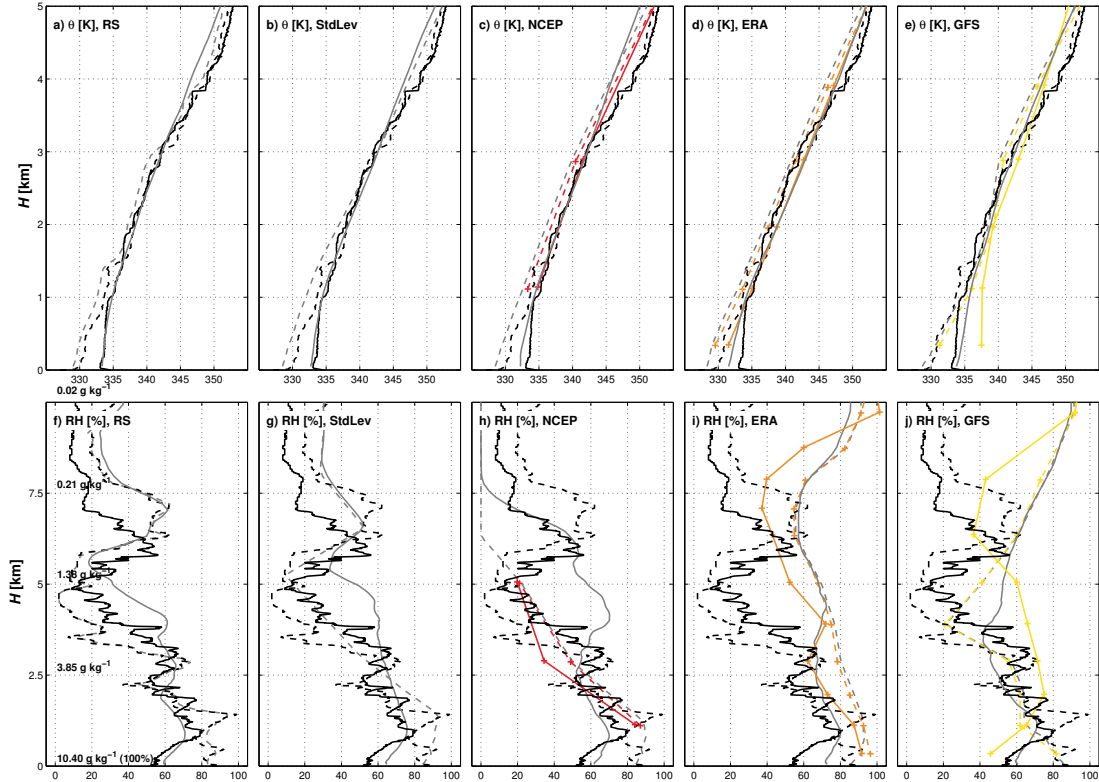


Figure 9. Comparison of the mean profiles of the ATHAM simulations initialized with (a) full radiosonde profile (RS, black lines); (b) radiosonde standard level information only (StdLev); (c) NCEP-I (red); (d) ERA-Int (orange) reanalysis, and (e) GFS-FNL (yellow) products compared to the respective profile data for 17 July 2012 00 UTC (dashed, 6:00 LST) and 06 UTC (solid, 12:00 LST). The gray lines are the simulated profiles for each case.

Overall the development of profiles shows that the 2-D model somewhat overestimates convective evolution, as expected, but also that the profile evolution is in good agreement with the initial conditions.

3.5. Cloud — Surface Flux Interactions

Feedbacks between the highly variable cloud cover and surface fluxes are of importance for the surface energy balance. This section investigates the interactions between cloud development and surface fluxes. Due to space constraints we focus on 17 July, but 18 July exhibits similar behavior. Figure 11 shows the temporal development of the sensible and latent heat fluxes (Q_H and Q_E) for the five simulations and fluxes measured at Nam Co station. For the simulated fluxes, the me-

dian of the fluxes is given together with the upper and lower quartiles of shortwave radiation and latent heat flux as a measure of variability. The energy balance of the measured eddy-covariance fluxes was closed according to the Bowen ratio [Twine *et al.*, 2000], assuming a ground heat flux corresponding to 10% of the net radiation. Even though it is difficult to compare the spatially averaged simulated fluxes with measurements that have the footprint of approximately 1 grid cell, it is apparent that both have similar Bowen ratios ($Bo \approx 0.5$) and flux evolution. For all cases except StdLev, both Q_H and Q_E increase gradually during the morning hours and then decrease sharply in the afternoon due to cloud cover reducing incoming shortwave radiation (SWD). StdLev and measured fluxes show a more gradual decrease and higher SWD. As previously discussed, 2-D simulations tend to overestimate convection so that simulated fluxes

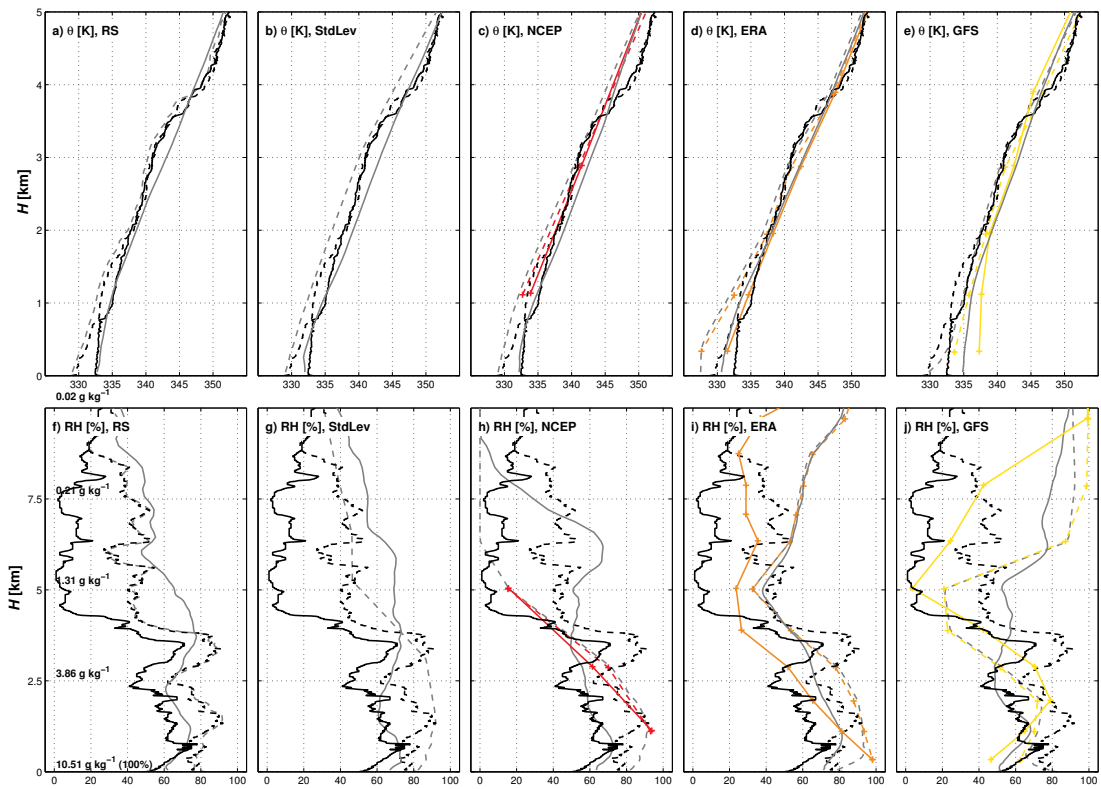


Figure 10. As in Figure 9, but for 18 July 2012.

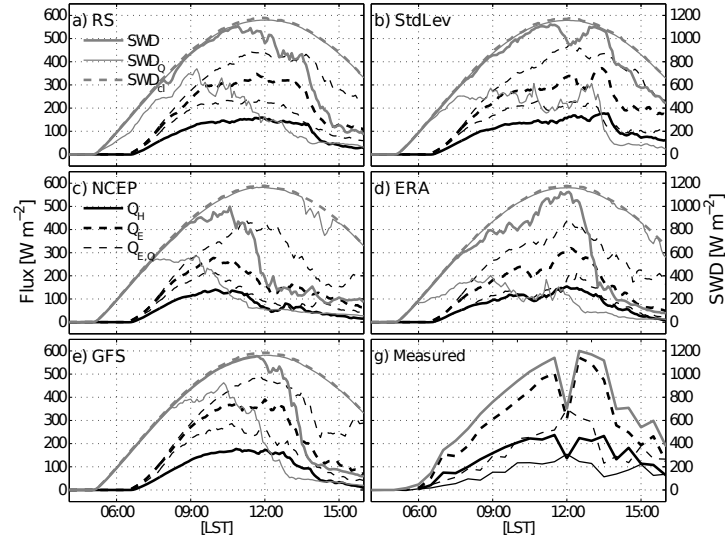


Figure 11. Development of turbulent surface fluxes in the Nam Co Lake basin for cases (a) RS, (b) StdLev, (c) NCEP, (d) ERA, and (e) GFS on 17 July 2012, respectively (Q_H —; Q_E --; down-welling shortwave radiation (SWD) gray). Thick black lines correspond to the median flux over land. SWD_Q and $Q_{E,Q}$ are upper and lower quartiles of SWD and Q_E , giving a measure of spatial flux variation. SWD_{cl} is clear sky SWD; (f) measured turbulent fluxes near Nam Co research station. Thin lines correspond to directly measured eddy-covariance fluxes. Thick lines are energy-balance corrected fluxes according to *Twine et al.* [2000].

may be excessively low due to cloud shading. On the other hand, the flux measurements were carried out in close proximity to the lake, which induces subsidence and thus are not entirely representative for the basin. Hence, we cannot determine which of these processes is responsible for the difference.

We generally find strong evidence for a positive correlation between surface fluxes and SWD ($p < 0.05$, not shown). There is, however, considerable scatter and generally only 15 to 50% of the variance is explained by changes in shortwave solar radiation as determined by orthogonal regression. This highlights the importance of additional factors affecting surface-exchange processes. One possible approach to analyze the relative importance of SWD flux interactions is to estimate the ratio of the standard deviation of the flux and its spatially averaged value ($\sigma_{Flux} / \langle Flux \rangle$, Figure 12). For this we only consider grid cells at the altitude of the lake in order to eliminate the influence of topography on fluxes. In the diurnal cycle of this quantity, there is a minimum in the morning hours, when shallow cumulus dominates. Earlier in the morning, the variation of fluxes is higher reaching a maximum around 7:00 LST, when the simulated surface fluxes start to increase. This occurs approximately 1 h later than observed, indicating some inertia in the surface model. With the development of moist convection later in the day, the spatial variation of fluxes increases and becomes as big as the mean value of the fluxes. This is both due to the decreasing magnitude of fluxes and in-

creased differences in solar shading. When comparing the variances of fluxes between shaded and unshaded areas, it becomes apparent that the shaded areas show the larger variance, sometimes exceeding the mean flux, while $\sigma_{Flux} / \langle Flux \rangle$ in un-shaded areas remains below a maximum of 50%, and below 30% except during times with large liquid water paths (lwp). This variation must be attributed to other processes than cloud-surface feedbacks. At higher lwp shaded and unshaded areas show different behavior. The variation of the shaded areas increases with lwp (mature convection), while unshaded areas have a maximum flux variation with intermediate lwp (developing convection). A possible explanation for this is the development of cold pools and fronts and their influence on surface wind speeds and turbulent exchange. In general the variation of sensible heat fluxes is larger than the variation of evapotranspiration, which is expected, because Q_H depends directly on skin temperature, while Q_E is dependent on more variables in both the surface model [*Gerken et al.*, 2012] and reality.

4. Discussion and Conclusions

In this work we use a coupled high-resolution atmospheric and surface model to perform 2-D simulations of daily cycles, especially of the evolution from shallow cumulus to deep, precipitating convection at the Nam Co Lake basin on the Tibetan Plateau, which is frequently observed during the summer monsoon. We investigate the influence of different atmospheric profiles. The aim of this work is less to quantitatively sim-

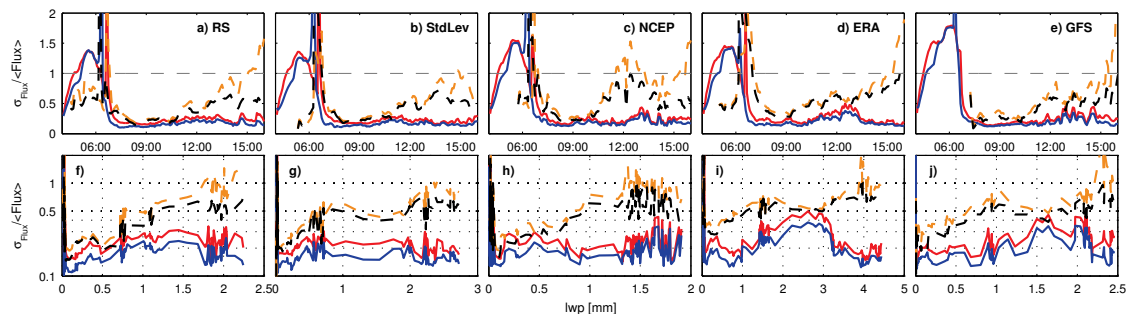


Figure 12. Normalized standard deviation of turbulent surface fluxes at lake level on 17 July ($\sigma_{\text{Flux}} / \langle \text{Flux} \rangle$) for cases (a) RS, (b) StdLev, (c) NCEP, (d) ERA, and (e) GFS diurnal development; (f–j) with respect to domain-averaged liquid water path (lwp, [mm]). Unshaded areas: Q_H (red), Q_E (blue); shaded areas: Q_H (orange), and Q_E (black).

ulate the convection development of specific days, but rather to qualitatively investigate the atmospheric profiles’ influence on simulated convection. This is then used to evaluate the impact of profile choice on surface-atmosphere-interactions and energy exchange. Due to the sparseness of observations, there are considerable uncertainties in the initial atmospheric profiles. While gridded atmospheric products, such as reanalysis data, are readily available, the available vertical resolution is coarse and grid cells may not accurately reflect local conditions.

As reported by *Bao and Zhang* [2013], we found gridded atmospheric products at Nam Co Lake to have a reasonable quality for temperature, but show larger biases with respect to moisture. Furthermore, their lack of vertical resolution leads to the omission of inversion layers and abrupt changes of water vapor, which also have an impact on convection development. For both these limitations there is presently no feasible approach for correction, highlighting the importance of direct measurements through atmospheric soundings.

Radio soundings on the other hand, are cost-intensive and difficult to conduct in remote areas. Additionally, they give very local and temporal “snapshots,” which may not be representative of the entire area. This work shows that the uncertainties in vertical profiles are important for modeling studies both for the development of convection and impact both the surface energy balance and the generation of precipitation on the basin scale. Hence, careful choice and evaluation of profiles is needed.

ATHAM is generally able to adequately simulate the convection development and its dynamics at Nam Co Lake. There are limitations to the 2-D approach such as a likely overestimation of convective activity and cloud cover. We find that differences in stability and relative humidity in the initial profiles are consistent with differences in convective activity and generated precipitation. Our simulations match weather observations at Nam Co Lake quite well for 17 July, a day with negligible contribution from large-scale advection. As our model does

not include synoptic-scale forcings, the 18 July matches less well observations and later soundings, which is due to the selected case and not to problems with the applied model.

Local water recycling of locally generated convection is an important part of the regional water cycle. With the choice of profile having a large impact on deposited precipitation, accurate profiles of temperature and moisture are crucial for modeling of the water cycle.

From the integrated energy fluxes, we see that, depending on the profile used, there are considerable differences in the amount of water vapor and sensible heat that are transferred from the surface to the atmosphere. One of the main causes for this are changes in cloud cover and thus net radiation. This highlights the importance of the vertical profiles for the surface energy balance. Potentially, also studies of climate change with common coarse-grid numerical models will be affected by these processes. Overall, due to the uncertainties in the gridded profile information, users of such data should be aware of the potential impacts of their choice with respect to the surface energy balance and convection development. Ideally, the robustness of modeling results should be tested by using input and validation data from several independent sources.

Feedbacks between cloud shading and surface fluxes are likely to play a significant role and need to be investigated. We investigated some of the connections between radiation input and surface fluxes and find that modeled and observed fluxes are comparable. Simulations utilizing StdLev profiles have the best agreement, while the other profiles produce too strong reduction of fluxes in the afternoon. Differences in radiation input are the main contributing factor to spatially and temporally varying fluxes, but additional effects, such as the generation of fronts or cold pools associated with deep convection, are also important as shown by the dependency of the flux variance to liquid water path. The soil model used in this work is able to capture the fundamental dynamics of fluxes. For the future, we believe that specifically adapted surface models that react

on the timescales of large eddies as presented in *Liu and Shao* [2013] would further increase the value of our approach.

Acknowledgments. This research was funded by the German Research Foundation (DFG) Priority Programme 1372 “Tibetan Plateau: Formation, Climate, Ecosystems” as part of the Atmosphere - Ecology - Glaciology - Cluster (TiP-AEG): FO 226/18-1,2. The work described in this publication has been supported by the European Commission (Call FP7-ENV-2007-1 grant 212921) as part of the CEOP-AEGIS project (<http://www.ceop-aegis.org/>) coordinated by the University of Strasbourg. We thank Kathrin Fuchs for her help during the radiosonde measurement. The map of Nam Co was produced by Sophie Biskop and Jan Kropacek within DFG-TiP and Phil Stickler of the Cambridge Geography Department. MODIS images were provided through AERONET, and we thank the MODIS team for their work. GFS-FNL data were produced by the National Center for Environmental Prediction (NCEP). NCEP Reanalysis data provided by the NOAA/OAR/ESRL PSD, Boulder, Colorado, USA, from their Web site at <http://www.esrl.noaa.gov/psd/>. ERA-Int reanalysis were downloaded from <http://data-portal.ecmwf.in>. Sounding data for Nagqu and Lhasa were obtained through the University of Wyoming’s Atmospheric Sounding Portal (<http://weather.uwyo.edu>).

References

- Bao, X., and F. Zhang (2013), Evaluation of NCEP-CFSR, NCEP-NCAR, ERA-Interim, and ERA-40 reanalysis datasets against independent sounding observations over the Tibetan Plateau, *J. Clim.*, *26*(1), 206–214, doi:10.1175/JCLI-D-12-00056.1.
- Biermann, T., W. Babel, J. Olesch, and T. Foken (2009), Mesoscale Circulations and Energy and Gas Exchange over the Tibetan Plateau - Documentation of the Micrometeorological Experiment, Nam Tso, Tibet - 25th of June - 08th of August 2009, *Arbeitsergebnisse 41*, University of Bayreuth, Bayreuth, ISSN 1614-8916, 37 pp.
- Biermann, T., W. Babel, W. Ma, X. Chen, E. Thiem, Y. Ma, and T. Foken (2013), Turbulent flux observations and modelling over a shallow lake and a wet grassland in the Nam Co basin, Tibetan Plateau, *Theor. Appl. Climatol.*, online first, doi:10.1007/s00704-013-0953-6.
- Caplan, P., J. Derber, W. Gemmill, S.-Y. Hong, H.-L. Pan, and D. Parrish (1997), Changes to the 1995 NCEP operational medium-range forecast model Analysis-Forecast system, *Wea. Forecasting*, *12*(3), 581–594, doi:10.1175/1520-0434(1997)012<0581:C'TTNOM>2.0.CO;2.
- Chen, B., X.-D. Xu, S. Yang, and W. Zhang (2012), On the origin and destination of atmospheric moisture and air mass over the Tibetan Plateau, *Theor. Appl. Climatol.*, *110*(3), 423–435, doi:10.1007/s00704-012-0641-y.
- Cong, Z., S. Kang, A. Smirnov, and B. Holben (2009), Aerosol optical properties at Nam Co, a remote site in central Tibetan Plateau, *Atmospheric Research*, *92*(1), 42–48, doi:10.1016/j.atmosres.2008.08.005.
- Cui, X., and H.-F. Graf (2009), Recent land cover changes on the Tibetan Plateau: a review, *Climatic Change*, *94*(1), 47–61, doi:10.1007/s10584-009-9556-8.
- Cui, X., H.-F. Graf, B. Langmann, W. Chen, and R. Huang (2006), Climate impacts of anthropogenic land use changes on the Tibetan Plateau, *Glob. Plan. Change*, *54*(1-2), 33–56, doi:10.1016/j.gloplacha.2005.07.006.
- Cui, X., H.-F. Graf, B. Langmann, W. Chen, and R. Huang (2007a), Hydrological impacts of deforestation on the Southeast Tibetan Plateau, *Earth Interactions*, *11*(15), 1–18, doi:10.1175/EI223.1.
- Cui, X., B. Langmann, and H.-F. Graf (2007b), Summer monsoonal rainfall simulation on the Tibetan Plateau with a regional climate model using a one-way double-nesting system, *SOLA*, *3*, 49–52, doi:10.2151/sola.2007-013.
- Dee, D. P., S. M. Uppala, A. J. Simmons, P. Berrisford, P. Poli, S. Kobayashi, U. Andrae, M. A. Balmaseda, G. Balsamo, P. Bauer, P. Bechtold, A. C. M. Beljaars, L. van de Berg, J. Bidlot, N. Bormann, C. Delsol, R. Dragani, M. Fuentes, A. J. Geer, L. Haimberger, S. B. Healy, H. Hersbach, E. V. Hólm, L. Isaksen, P. Kållberg, M. Köhler, M. Matricardi, A. P. McNally, B. M. Monge-Sanz, J.-J. Morcrette, B.-K. Park, C. Peubey, P. de Rosnay, C. Tavolato, J.-N. Thépaut, and F. Vitart (2011), The ERA-Interim reanalysis: configuration and performance of the data assimilation system, *Q.J.R. Meteorol. Soc.*, *137*(656), 553–597, doi:10.1002/qj.828.
- Fairall, C. W., E. F. Bradley, J. S. Godfrey, G. A. Wick, J. B. Edson, and G. S. Young (1996a), Cool-skin and warm-layer effects on sea surface temperature, *J. Geophys. Res.*, *101*(C1), 1295–1308.
- Fairall, C. W., E. F. Bradley, D. P. Rogers, J. B. Edson, and G. S. Young (1996b), Bulk parameterization of air-sea fluxes for Tropical Ocean-Global Atmosphere Coupled-Ocean Atmosphere Response Experiment, *J. Geophys. Res.*, *101*(C2), 3747–3764.
- Foken, T., R. Leuning, S. R. Oncley, M. Mauder, and M. Aubinet (2012), Corrections and data quality control, in *Eddy Covariance: A practical guide to measurement and data analysis*, edited by M. Aubinet, T. Vesala, and D. Papale, pp. 85–131, Springer, Dordrecht, doi:10.1007/978-94-007-2351-1.4.
- Frauenfeld, O. W., T. Zhang, and M. C. Serreze (2005), Climate change and variability using European Centre for Medium-Range Weather Forecasts reanalysis (ERA-40) temperatures on the Tibetan Plateau, *J. Geophys. Res.*, *110*, D02021, doi:10.1029/2004JD005230.
- Friend, A. D., and N. Y. Kiang (2005), Land surface model development for the GISS GCM: effects of improved canopy physiology on simulated climate, *J. Clim.*, *18*(15), 2883–2902, doi:10.1175/JCLI3425.1.
- Friend, A. D., A. K. Stevens, R. G. Knox, and M. G. R. Cannell (1997), A process-based, terrestrial biosphere model of ecosystem dynamics (Hybrid v3.0), *Ecological Modelling*, *95*(2-3), 249–287, doi:10.1016/S0304-3800(96)00034-8.
- Fujinami, H., S. Nomura, and T. Yasunari (2005), Characteristics of diurnal variations in convection and precipitation over the southern Tibetan Plateau during summer, *SOLA*, *1*, 49–52, doi:10.2151/sola.2005-14.
- Gao, X., Y. Xu, Z. Zhao, J. S. Pal, and F. Giorgi (2006), On the role of resolution and topography in the simulation of East Asia precipitation, *Theor. Appl. Climatol.*, *86*(1), 173–185, doi:10.1007/s00704-005-0214-4.
- Gerken, T., W. Babel, A. Hoffmann, T. Biermann, M. Herzog, A. D. Friend, M. Li, Y. Ma, T. Foken, and H.-F. Graf (2012), Turbulent flux modelling with a simple 2-layer soil model and extrapolated surface temperature applied at Nam Co Lake basin on the Tibetan Plateau, *Hydrol. Earth Syst. Sci.*, *16*(4), 1095–1110, doi:10.5194/hess-16-1095-2012.
- Gerken, T., T. Biermann, W. Babel, M. Herzog, Y. Ma, T. Foken, and H.-F. Graf (2013a), A modelling investigation into lake-breeze development and convection triggering in the Nam Co Lake basin, Tibetan Plateau, *Theor. Appl. Climatol.*, online first, doi:10.1007/s00704-013-0987-9.
- Gerken, T., K. Fuchs, and W. Babel (2013b), Documentation of the atmospheric boundary layer experiment, Nam Tso, Tibet 08th of July – 08th of August 2012, *Arbeitsergebnisse 53*, University of Bayreuth, Bayreuth, ISSN 1614-8916, 48 pp.
- Graf, H.-F., M. Herzog, J. M. Oberhuber, and C. Textor (1999), Effect of environmental conditions on volcanic plume rise, *J. Geophys. Res.*, *104*(D20), 24,309–24,320, doi:10.1029/1999JD900498.
- Guo, H., J. Penner, and M. Herzog (2004), Comparison of the vertical velocity used to calculate the cloud droplet number concentration in a cloud-resolving and a global climate model, in *Fourteenth ARM Science Team Meeting Proceedings*, edited by D. Carrothers, pp. 1–6, Department of Energy, Boston.
- Haginoya, S., H. Fujii, T. Kuwagata, J. Xu, Y. Ishigooka, S. Kang, and Y. Zhang (2009), Air-lake interaction features found in heat and water exchanges over Nam Co on the Tibetan Plateau, *SOLA*, *5*, 172–175, doi:10.2151/sola.2009-044.
- Herzog, M., H.-F. Graf, C. Textor, and J. M. Oberhuber (1998), The effect of phase changes of water on the development of volcanic plumes, *J. Volc. Geotherm. Res.*, *87*(1-4), 55–74, doi:10.1016/S0377-0273(98)00100-0.
- Herzog, M., J. M. Oberhuber, and H.-F. Graf (2003), A prognostic turbulence scheme for the nonhydrostatic plume model ATHAM, *J. Atmos. Sci.*, *60*(22), 2783–2796, doi:10.1175/1520-0469(2003)060<2783:APTSFT>2.0.CO;2.

- Immerzeel, W. W., L. P. H. van Beek, and M. F. P. Bierkens (2010), Climate change will affect the Asian water towers, *Science*, *328*(5984), 1382–1385, doi:10.1126/science.1183188.
- Kalnay, E., M. Kanamitsu, R. Kistler, W. Collins, D. Deaven, L. Gandin, M. Iredell, S. Saha, G. White, J. Woollen, Y. Zhu, A. Leetmaa, R. Reynolds, M. Chelliah, W. Ebisuzaki, W. Higgins, J. Janowiak, K. C. Mo, C. Ropelewski, J. Wang, R. Jenne, and D. Joseph (1996), The NCEP/NCAR 40-year reanalysis project, *Bull. Amer. Meteor. Soc.*, *77*(3), 437–471, doi:10.1175/1520-0477(1996)077<0437:TNYRP>2.0.CO;2.
- Kanamitsu, M., J. Alpert, K. Campana, P. Caplan, D. Deaven, M. Iredell, B. Katz, H.-L. Pan, J. Sela, and G. White (1991), Recent changes implemented into the Global Forecast System at NMC, *Wea. Forecasting*, *6*(3), 425–435, doi:10.1175/1520-0434(1991)006<0425:RCITG>2.0.CO;2.
- Kirshbaum, D. J., and D. R. Durran (2004), Factors governing cellular convection in orographic precipitation, *J. Atmos. Sci.*, *61*(6), 682–698, doi:10.1175/1520-0469(2004)061<0682:FGCCIO>2.0.CO;2.
- Kurita, N., and H. Yamada (2008), The role of local moisture recycling evaluated using stable isotope data from over the middle of the Tibetan Plateau during the monsoon season, *J. Hydrometeorol.*, *9*(4), 760–775, doi:10.1175/2007JHM945.1.
- Langmann, B., M. Herzog, and H.-F. Graf (1998), Radiative forcing of climate by sulfate aerosols as determined by a regional circulation chemistry transport model, *Atmos. Environ.*, *32*(16), 2757–2768, doi:10.1016/S1352-2310(98)00028-4.
- Liu, S., and Y. Shao (2013), Soil-layer configuration requirement for large-eddy atmosphere and land surface coupled modeling, *Atmos. Sci. Lett.*, *14*(2), 112–117, doi:10.1002/asl2.426.
- Ma, L., T. Zhang, Q. Li, O. W. Frauenfeld, and D. Qin (2008), Evaluation of ERA-40, NCEP-1, and NCEP-2 reanalysis air temperatures with ground-based measurements in China, *J. Geophys. Res.*, *113*, D15115, doi:10.1029/2007JD009549.
- Ma, L., T. Zhang, O. W. Frauenfeld, B. Ye, D. Yang, and D. Qin (2009), Evaluation of precipitation from the ERA-40, NCEP-1, and NCEP-2 reanalyses and CMAP-1, CMAP-2, and GPCP-2 with ground-based measurements in China, *J. Geophys. Res.*, *114*, D09105, doi:10.1029/2008JD011178.
- Mauder, M., and T. Foken (2004), Documentation and instruction manual of the Eddy-Covariance software package TK2, *Arbeitsergebnisse 26*, University of Bayreuth, Bayreuth, ISSN 1614-8916, 45 p.
- Mauder, M., and T. Foken (2011), Documentation and instruction manual of the Eddy-Covariance software package TK3, *Arbeitsergebnisse 46*, University of Bayreuth, Bayreuth, ISSN 1614-8916, 60 p.
- Maussion, F., D. Scherer, R. Finkelnburg, J. Richters, W. Yang, and T. Yao (2011), WRF simulation of a precipitation event over the Tibetan Plateau, China – an assessment using remote sensing and ground observations, *Hydrol. Earth Syst. Sci.*, *15*(6), 1795–1817.
- Mlawer, E. J., S. J. Taubman, P. D. Brown, M. J. Iacono, and S. A. Clough (1997), Radiative transfer for inhomogeneous atmospheres: RRTM, a validated correlated-k model for the longwave, *J. Geophys. Res.*, *102*(D14), 16,663–16,682.
- Oberhuber, J. M., M. Herzog, H.-F. Graf, and K. Schwanke (1998), Volcanic plume simulation on large scales, *J. Volc. Geothermal. Res.*, *87*(1-4), 29–53, doi:10.1016/S0377-0273(98)00099-7.
- Rebmann, C., O. Kolle, B. Heinesch, R. Queck, A. Ibrom, and M. Aubinet (2012), Data acquisition and flux calculations, in *Eddy Covariance: A practical guide to measurement and data analysis*, edited by M. Aubinet, T. Vesala, and D. Papale, pp. 59–83, Springer, Dordrecht, doi:10.1007/978-94-007-2351-1_3.
- Sato, T., H. Miura, and M. Satoh (2007), Spring diurnal cycle of clouds over Tibetan Plateau: Global cloud-resolving simulations and satellite observations, *Geophys. Res. Lett.*, *34*, L18816, doi:10.1029/2007GL030782.
- Taniguchi, K., and T. Koike (2008), Seasonal variation of cloud activity and atmospheric profiles over the eastern part of the Tibetan Plateau, *J. Geophys. Res.*, *113*, D10104, doi:10.1029/2007JD009321.
- Tian, L., V. Masson-Delmotte, M. Stievenard, T. Yao, and J. Jouzel (2001), Tibetan plateau summer monsoon northward extent revealed by measurements of water stable isotopes, *J. Geophys. Res.*, *106*(D22), 28,081–28,088, doi:10.1029/2001JD900186.
- Tian, L., T. Yao, P. F. Schuster, J. W. C. White, K. Ichiyanagi, E. Pendall, J. Pu, and W. Yu (2003), Oxygen-18 concentrations in recent precipitation and ice cores on the Tibetan Plateau, *J. Geophys. Res.*, *108*(D9), 4293, doi:10.1029/2002JD002173.
- Tian, L., T. Yao, K. MacClune, J. W. C. White, A. Schilla, B. Vaughn, R. Vachon, and K. Ichiyanagi (2007), Stable isotopic variations in west China: A consideration of moisture sources, *J. Geophys. Res.*, *112*, D10112, doi:10.1029/2006JD007718.
- Trentmann, J., G. Luderer, T. Winterrath, M. D. Fromm, R. Servranckx, C. Textor, M. Herzog, H.-F. Graf, and M. O. Andreae (2006), Modeling of biomass smoke injection into the lower stratosphere by a large forest fire (Part I): reference simulation, *Atmos. Chem. Phys.*, *6*(12), 5247–5260.
- Twine, T. E., W. P. Kustas, J. M. Norman, D. R. Cook, P. R. Houser, T. P. Meyers, J. H. Prueger, P. J. Starks, and M. L. Wesely (2000), Correcting eddy-covariance flux underestimates over a grassland, *Agric. Forest Meteorol.*, *103*(3), 279–300, doi:10.1016/S0168-1923(00)00123-4.
- Uyeda, H., H. Yamada, J. Horikomi, R. Shirooka, S. Shimizu, L. Liping, K. Ueno, H. Fujii, and T. Koike (2001), Characteristics of convective clouds observed by a doppler radar at Naqu on Tibetan Plateau during the GAME-Tibet IOP, *J. Meteorol. Soc. Jap.*, *79*(1B), 463–474, doi:10.2151/jmsj.79.463.
- Wang, A., and X. Zeng (2012), Evaluation of multireanalysis products with in situ observations over the Tibetan Plateau, *J. Geophys. Res.*, *117*, D05102, doi:10.1029/2011JD016553.
- Wang, J., L. Zhu, G. Daut, J. Ju, X. Lin, Y. Wang, and X. Zhen (2009), Investigation of bathymetry and water quality of Lake Nam Co, the largest lake on the central Tibetan Plateau, China, *Limnology*, *10*(2), 149–158, doi:10.1007/s10201-009-0266-8.
- Wu, C.-M., B. Stevens, and A. Arakawa (2009), What controls the transition from shallow to deep convection?, *J. Atmos. Sci.*, *66*(6), 1793–1806, doi:10.1175/2008JAS2945.1.
- Xu, Z. X., T. L. Gong, and J. Y. Li (2008), Decadal trend of climate in the Tibetan Plateau – regional temperature and precipitation, *Hydrological Processes*, *22*(16), 3056–3065, doi:10.1002/hyp.6892.
- Yang, K., B. Ye, D. Zhou, B. Wu, T. Foken, J. Qin, and Z. Zhou (2011), Response of hydrological cycle to recent climate changes in the Tibetan Plateau, *Climatic Change*, *109*(3-4), 517–534, doi:10.1007/s10584-011-0099-4.
- Yin, Z.-Y., X. Zhang, X. Liu, M. Colella, and X. Chen (2008), An assessment of the biases of satellite rainfall estimates over the Tibetan Plateau and correction methods based on topographic analysis, *J. Hydrometeorol.*, *9*(3), 301–326, doi:10.1175/2007JHM903.1.

Corresponding author: T. Gerken, Department of Micrometeorology, University of Bayreuth, 95440 Bayreuth, GERMANY. (tobias.gerken@uni-bayreuth.de)

Erklärung

Hiermit erkläre ich, dass ich diese Arbeit selbständig verfasst habe und keine anderen als die angegebenen Quellen und Hilfsmittel verwendet habe.

Ferner erkläre ich, dass ich nicht anderweitig mit oder ohne Erfolg versucht habe, eine Dissertation einzureichen oder mich einer Doktorprüfung zu unterziehen.

Bayreuth, den

Tobias Gerken